



**HAL**  
open science

# Structure and assembly of bacterial microbiomes in the *Emiliana huxleyi* phycosphere

Mariana Câmara Dos Reis

► **To cite this version:**

Mariana Câmara Dos Reis. Structure and assembly of bacterial microbiomes in the *Emiliana huxleyi* phycosphere. Biodiversity and Ecology. Sorbonne Université, 2021. English. NNT : 2021SORUS077 . tel-03642323

**HAL Id: tel-03642323**

**<https://theses.hal.science/tel-03642323>**

Submitted on 15 Apr 2022

**HAL** is a multi-disciplinary open access archive for the deposit and dissemination of scientific research documents, whether they are published or not. The documents may come from teaching and research institutions in France or abroad, or from public or private research centers.

L'archive ouverte pluridisciplinaire **HAL**, est destinée au dépôt et à la diffusion de documents scientifiques de niveau recherche, publiés ou non, émanant des établissements d'enseignement et de recherche français ou étrangers, des laboratoires publics ou privés.

# Sorbonne Université

École doctorale 227 « Sciences de la Nature et de l'Homme : Évolution et Écologie »  
*Station Biologique de Roscoff / Adaptation et Diversité en Milieu Marin, UMR7144*

## **Structure and assembly of bacterial microbiomes in the *Emiliana huxleyi* phycosphere**

Par Mariana Câmara dos Reis

Thèse de doctorat en Écologie Microbienne Marine

Dirigée par Christian Jeanthon et Colomban de Vargas

Présentée et soutenue publiquement le 13 Avril 2021

Devant un jury composé de :

**Rebecca Case, Rapportrice**

Associate Professor, Nanyang Technological University, Singapore.

**Hans-Peter Grossart, Rapporteur**

Professor, Leibniz Institute of Freshwater Ecology and Fisheries and University of Potsdam, Germany.

**Catherine Leblanc, Examinatrice**

Senior Researcher, UMR8227 Sorbonne Université-CNRS, Integrative Biology of Marine Models. Station Biologique de Roscoff, France.

**Hélène Agogué, Examinatrice**

CNRS Researcher, UMR7266 La Rochelle Université-CNRS, Littoral Environnement et Sociétés, France.

**Christian Jeanthon, Directeur de Thèse**

Research Director, UMR7144 Sorbonne Université-CNRS, Adaptation and Diversity in the Marine Environment. Station Biologique de Roscoff, France.

**Colomban de Vargas, Co-Directeur de Thèse**

Research Director, UMR7144 Sorbonne Université-CNRS, Adaptation and Diversity in the Marine Environment. FR2022, Global Ocean Systems Ecology & Evolution. Station Biologique de Roscoff and Paris Michel-Ange, France.

Je tiens à remercier la région Bretagne (COH17019) et Sorbonne Université (C17/1508 and C20/1269) pour avoir financé ce travail de thèse.



*To my parents,*

*Aos meus pais,*

# Acknowledgements

I would like first to acknowledge my advisors, Christian and Colombar, for giving me the opportunity to work on this project. Thank you for your advices and for the enriching discussions. Thank you for stimulating me to think 'out of the box'. Having done this PhD is one of the greatest experiences of my life, and for sure the most intense. Really thank you for this opportunity to come in France! It was an honor to work with you both.

I would like to thank also to my thesis committee which followed me over this journey. Thank you to Samuel Chaffron, Simon Dittami, Frédérique Viard and Georg Pohnert for your valuable feedback on the project.

I'm very grateful to Catherine Leblanc, H  l  ne Agogu  , Rebecca Case and Hans-Peter Grossart for accepting to review and examine my work. It's an honor for me to have you as part of my jury.

A special thanks to my unofficial advisors Domi, Sarah, Florence and Nico. Thank you for sharing your knowledge with me, for being always kind and most importantly thank you for your patience!! Thank you to Christophe Six for all the help with the PAM.

Of course, thank you to the ECOMAP team! I'll miss very much the coffee breaks and all the good moments that I had with you all.

Thank you to the RCC members for all the help (and all the strains :D) that you gave me. A special thanks to the coccolovers Ian and Mahdi, I've learned a lot with you about all the ehux morphotypes/groups/species?

I'm extremely thankful to the friends that I have done in Roscoff. For sure you were very important during this time. Thanks to Lydia, Valeria, Catherine, Adriana, Peche, Mariarita, Laure, Emilie, Nico, Louison, Yasmine, Lisa, Marie and Ewen. It makes me happy to know that I've met such great people and I hope to always have contact with you.

Thank you, Jeremy, for everything. Thank you for being there all this time, for being you. For sure a great part of this work was possible because of your support and I'm very grateful to that.

Thank you also to the Szymczak family for your kindness and for adopting me.

Last, but not least, obrigada    minha fam  lia, a base de tudo. Obrigada por apoiarem as minhas decis  es e por estarem comigo mesmo com a dist  ncia. Voc  s s  o incr  veis.

Muito obrigada!



# Contents

Acknowledgements.....	5
Contents .....	7
Preamble .....	11
Introduction.....	13
1) The ecological relevance of phytoplankton-bacteria interactions in the oceans .....	13
1.1) The classical view of marine phytoplankton .....	13
1.2) Marine heterotrophic bacteria.....	18
1.3) The phycosphere: Where phytoplankton and bacteria interact.....	21
1.4) Large scale impacts of phytoplankton-bacteria interactions .....	32
2) <i>Emiliana huxleyi</i> : a model organism to study phytoplankton-bacteria interactions.....	34
2.2) Morphology and phylogenomics .....	35
2.3) Life cycle .....	42
2.4) Interactions with bacteria.....	44
Main PhD objectives.....	47
Chapter 1 .....	51
The microbiome of the cosmopolitan coccolithophore <i>Emiliana huxleyi</i> .....	53
Chapter 2.....	109
Microbiome assembly in phytoplankton cultures is partially driven by deterministic processes .....	111
Chapter 3.....	151
Microbiome assembly in axenic <i>Emiliana huxleyi</i> cultures is influenced by the source community composition and is resilient to disturbance.....	153
References.....	225
Annexes.....	247
Résumé.....	253
Abstract.....	254



---

# INTRODUCTION

---



## Preamble

The term microbiome nowadays incorporates all the microbial communities (microbiota) associated with an environment and their ‘theatre of activity’ (structural elements, metabolites/signal molecules, and the surrounding environmental biotic and abiotic conditions) (Whipps *et al.*, 1988; Berg *et al.*, 2020). This term has evolved together with the microbiome research in order to fit all the elements involved in the interactions between hosts and associated microbial communities (Berg *et al.*, 2020). Although the first microbes’ observations are dated from the 17th century by Antonie van Leeuwenhoek of what he called ‘animalcules’, the onset of microbiome research started approximately 20 years ago with the first ‘next-generation’ sequencing technologies (Berg *et al.*, 2020). Notably, the microbiome research became popular at both the scientific community and general public levels with the Human Microbiome Project which started in 2007. It is common to hear that the human microbiome is an additional organ which impacts our health and emotions (Baquero and Nombela, 2012). Nowadays, microbiome studies are revolutionizing the way that we understand interactions, functions, and traits between visible and invisible organisms.

Along the decades of microbiome studies much has been discovered about the microbiomes of different taxa, including marine microorganisms such as phytoplankton. These are the central topics of this thesis. Here, I focus on the heterotrophic bacterial communities associated with *Emiliana huxleyi*, a cosmopolitan coccolithophore species. In the introduction of this manuscript the reader is guided through the main concepts and the state of the art in phytoplankton microbiome research, which are necessary for understanding the following chapters. Three chapters then present my experimental research regarding the microbiome of *E. huxleyi* and other phytoplankton species. Finally, a general discussion synthesizes all the contributions of this thesis work into the current state of the art and proposes new perspectives for a better understanding of phytoplankton microbiomes.



# Introduction

## 1) The ecological relevance of phytoplankton-bacteria interactions in the oceans

### 1.1) The classical view of marine phytoplankton

The term “phytoplankton” (from the Greek terms “phyton” or plant and “planktos” or wanderer) was first used in 1897 to describe unicellular photosynthetic organisms that drift on the sunlit layer of the oceans and fresh waters (Falkowski and Raven, 1997; Falkowski *et al.*, 2004). The phytoplankton comprise organisms from 0.2 to > 200  $\mu\text{m}$  that capture the energy from sunlight and transform carbon dioxide ( $\text{CO}_2$ ) into organic matter (*i.e.*, primary production) (Figure 1, step 1) (Field *et al.*, 1998). This organic matter can be dissolved (DOM; < 0.45  $\mu\text{m}$ ) or particulate (POM; > 0.45  $\mu\text{m}$ ) and is defined into carbon, nitrogen and phosphorus partitions (Figure 1, step 2). In addition to organic matter, the primary production results in the release of oxygen produced from water. Together, the marine phytoplankton contribute to about 50% of the global net primary production (Field *et al.*, 1998).

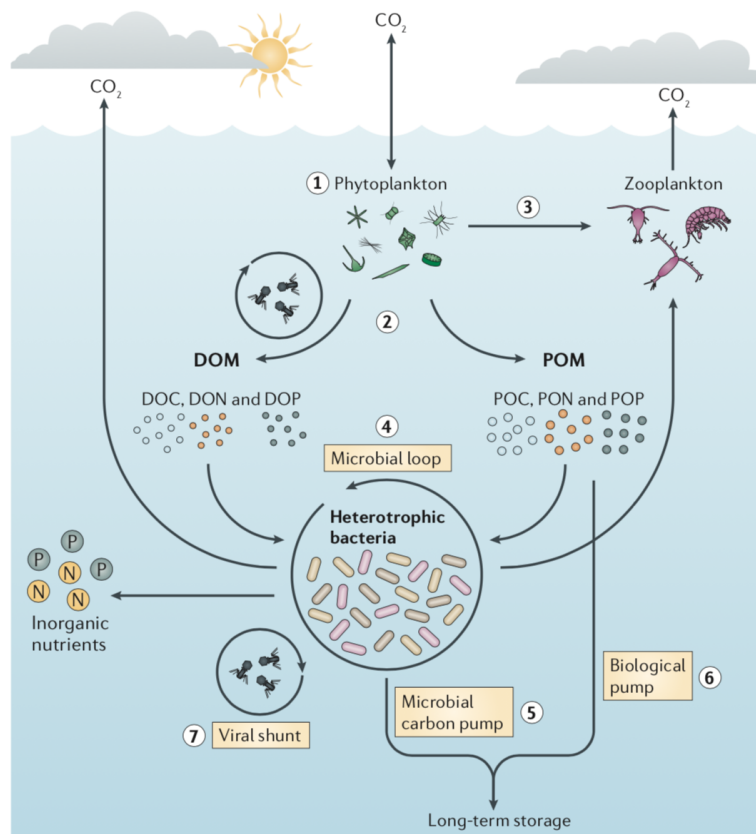


**Figure 1.** Classical view of marine microorganisms' participation in the carbon cycle. Figure and legend (adapted) from Buchan *et al.*, (2014). Key processes of the marine carbon cycle include the conversion of inorganic carbon (such as  $\text{CO}_2$ ) to organic carbon by photosynthetic phytoplankton species (step 1); the release of both dissolved organic matter and particulate organic matter which contain various proportions of carbon, nitrogen and phosphorus (step 2); the consumption of phytoplankton biomass by zooplankton grazers (step 3) and the mineralization (that is the release of inorganic compounds and  $\text{CO}_2$  via respiration during the catabolism of organic matter) and recycling of organic matter by diverse heterotrophic bacteria (known as the microbial loop) (step 4). A fraction of the heterotrophic bacteria is consumed by zooplankton, and the carbon is further transferred up the food web. Heterotrophic bacteria also contribute to the remineralization of organic nutrients, which are then available for use by phytoplankton. The microbial carbon pump (step 5) refers to the transformation of organic carbon into recalcitrant DOM that resists further degradation and is sequestered in the ocean for thousands of years. The biological pump (step 6) refers to the export of phytoplankton-derived POM from the surface oceans to deeper depths via sinking. Finally, the viral shunt (step 7) describes the contributions of viral-mediated cell lysis to the release of dissolved and particulate matter from both the phytoplankton and bacterial pools.

The organic matter released by phytoplankton sustains the aquatic food webs. Part of it can be respired, by grazers (Figure 1 – step 3) and bacteria (Figure 1- step 4). In addition, a portion of the organic matter can sink to the deep oceans as sinking biogenic particles or dissolved organic matter, a process named the biological carbon pump, which is responsible for export and accumulation of organic carbon from photosynthetic CO<sub>2</sub> fixation in deep layers of the ocean down to the sediments (Figure 1 – step 6) (Ducklow *et al.*, 2001). Besides being key actors in the carbon cycle, the phytoplankton functional groups are also actively involved in the other major biogeochemical cycles such as nitrogen, phosphorus and silica (Litchman *et al.*, 2015).

The phytoplankton is formed by a tremendous taxonomic diversity of prokaryotes and eukaryotes displaying a wide range of sizes, shapes, and structures. The prokaryotic phytoplankton belongs to the phylum Cyanobacteria, a group previously known as blue-green algae (Garcia-Pichel *et al.*, 2020) capable of performing oxygenic photosynthesis. Cyanobacteria have played a central role in the primary oxygenation of the Earth's atmosphere about 2.4 billion years ago (Bekker *et al.*, 2004; Whitton, 2012). The main marine cyanobacterial groups are the dominant *Prochlorococcus* and *Synechococcus* in addition of the nitrogen fixers *Trichodesmium*, *Crocosphaera* and *Richelia* which form symbioses with diatoms and other protists (Foster *et al.*, 2011; Karlusich *et al.*, 2020). *Prochlorococcus* and *Synechococcus* are considered the most abundant photosynthetic organisms on Earth (Partensky *et al.*, 1999) and important primary producers (Garcia-Pichel *et al.*, 2009).

Among the eukaryotic phytoplankton, the most diverse and ecologically relevant groups are the prasinophytes, diatoms, dinoflagellates and haptophytes (Not *et al.*, 2012) (Figure 2). Evolution of photosynthetic eukaryotes started at the Proterozoic oceans about 1.5 billion years ago (Falkowski *et al.*, 2004; Karlusich *et al.*, 2020). Thanks to at least one endosymbiotic event when a cyanobacterium-like organism was engulfed by a heterotrophic eukaryote two main lineages of plastids evolved (primary endosymbiosis) (Hackett *et al.*, 2007; Leliaert *et al.*, 2011). The first one, characterized by the presence of chlorophyll b, is dominated by the green algae prasinophytes (Chlorophyta) while the second lineage, the “red lineage”, is characterized by the presence of chlorophyll a + c, and eventually gave rise, through secondary endosymbiosis, to the diatoms, haptophytes and dinoflagellates (Falkowski *et al.*, 2004).

The prasinophytes appear to be the prevalent eukaryotic phytoplankton in the Paleozoic era before the rising of the red lineages when they were largely displaced (Falkowski *et al.*,

2004; Leliaert *et al.*, 2011). Even though, this group still encompasses a large diversity of taxa, body forms, life cycle and ecophysiological traits (see Leliaert *et al.*, 2011) and references therein). They are particularly abundant and diverse in the picoplankton (0.8-2  $\mu\text{m}$ ) (Not *et al.*, 2012), and the most known genera are *Ostreococcus*, *Micromonas*, *Bathycoccus*, which can form blooms in coastal waters (Not *et al.*, 2004; Engelen *et al.*, 2015). Another important group is Chloropicophyceae, which has been found as the main green algae in oceanic waters (Lopes dos Santos, Gourvil, *et al.*, 2017; Lopes dos Santos, Pollina, *et al.*, 2017).



**Figure 2.** Eukaryotic tree of life with the main phytoplanktonic groups highlighted (purple stars). This schematic tree represents a synthesis of information on morphologic, phylogenetic (based on a few genes from a large diversity of organisms) and phylogenomic analyses (based on many genes from representatives of major lineages). The phytoplankton diversity is distributed in many branches of this tree, mainly Alveolates, Stramenopiles and Archaeplastids. Note that the Haptophyte lineage does not belong to any of the seven major eukaryotic supergroups. Adapted from Worden *et al.*, (2015).

Another important phytoplankton group emerged at a time when phytoplankton diversity consisted mainly of cyanobacteria and green algae, the diatoms (Falkowski *et al.*, 2004). Diatoms are ubiquitous photosynthetic unicellular eukaryotes surrounded by porous silica shells called frustules. The name of this group is derived from the Greek *diatomos* which means “cut in half” in reference to their cell wall divided in two parts (Armbrust, 2009). Thanks to the frustules, diatoms are very well conserved in the fossil record, which allows to estimate their origin and diversity over the geological time (Armbrust, 2009). Their first appearance in the fossil record is dated at about 190 Myr ago in the Jurassic (Sims *et al.*, 2006). Diatoms cells can be solitary or colonial and vary in size from a few micrometers to a few millimeters. Due to their high sinking rates, caused by the frustules, diatoms are a major driver of the biological pump, carrying photosynthetically fixed carbon to the deep ocean. It has been estimated that they are responsible for about 20% of the primary production on Earth (Nelson *et al.*, 1995; Field *et al.*, 1998).

Together with diatoms, the dinoflagellates diversified in the Mesozoic era, with a major radiation in the early Jurassic (Falkowski *et al.*, 2004). This major group of protists has diversified into a tremendous morphological and trophic complexity comprising phototrophic organisms, predators, mixotrophs, symbionts and parasites (Gomez, 2012). Roughly, about 50% of the dinoflagellates are considered photosynthetic, harboring different types of plastids although mixotrophy is very common (Taylor *et al.*, 2007). Members of this group are well known as harmful algal blooms forming species of global importance. About 70-80% of the toxic eukaryotic phytoplankton species are dinoflagellates (Janouskovec *et al.*, 2017). Dinoflagellates can cover their cell with cellulose-like polysaccharide plates forming together an organic theca (Not *et al.*, 2012). Remarkably, their nucleus contains permanently condensed chromosomes (dinokaryon), and their cells are moved by two flagella, a ribbon-like flagellum with multiple waves situated in a transverse groove (cingulum) and another one emerging from the ventral furrow (sulcus) (Not *et al.*, 2012). They are typically dominant biota in pelagic marine and freshwater ecosystems where they can form large blooms at optimal conditions (Taylor *et al.*, 2007; Gomez, 2012).

Last but not least, the haptophytes form a monophyletic widespread group of marine phytoplankton characterized by the presence of an organelle called haptonema which harbors similarities with a flagellum but differs in the arrangement of its microtubules (Parke *et al.*, 1955). The haptonema can be used to capture preys, to attach to substrates and as sensory

structures (de Vargas *et al.*, 2007). However, in some groups the haptonema is only reduced to a vestigial structure (de Vargas *et al.*, 2007). The haptophytes are found everywhere in aquatic environments, mainly in marine, and can be found as solitary free-living cells but also as colonial and as symbionts of foraminifera and radiolarians (Jordan and Chamberlain, 1997). Coccolithophores are one of the most abundant and widespread groups of haptophytes. These organisms form an important part of the oceanic phytoplankton since the Jurassic (de Vargas *et al.*, 2007). The name of the group is attributed to the calcium carbonate scales covering their cells, called coccoliths. Coccolithophores play important roles in the carbon cycle as primary producers and calcifiers and are involved in the control of the alkalinity and carbonate chemistry of the photic zone of the oceans (de Vargas *et al.*, 2007). Besides being involved in the classical organic carbon pump, which fixes CO<sub>2</sub>, they also contribute to the carbonate counter pump, which releases CO<sub>2</sub> to the atmosphere (Rost and Riebesell, 2004). Coccolithophores are responsible for the largest production of calcite on earth (Brownlee and Taylor, 2004). Another important role of coccolithophores in the carbon cycle involves the formation of aggregates of coccoliths and organic matter, which represents an enormous source of carbon that sink to the deep oceans (de Vargas *et al.*, 2007). Additionally, they are important actors in the global sulfur cycle by the production of dimethylsulfoniopropionate (DMSP) and emission of dimethylsulfide (DMS) to the atmosphere (Alcolombri *et al.*, 2015).

### **1.2) Marine heterotrophic bacteria**

Marine heterotrophic bacteria, together with Archaea, can be seen as the engines of Earth's biogeochemical cycles (Falkowski *et al.*, 2008). They are responsible for the remineralization of organic nutrients into inorganic nutrients (mostly nitrogen and phosphorus). They are also involved in reintroduction of phytoplankton released carbon in the food web through the production of biomass, which is consumed by protists, a process named 'microbial loop' (Figure 1- step 4) (Azam *et al.*, 1983; Pomeroy *et al.*, 2007). Moreover, they produce a pool of recalcitrant organic matter that represents a relevant carbon storage pathway, a process named the "microbial carbon pump" (Figure 1 – step 5) (Jiao *et al.*, 2010). It has been estimated that about 50% of the carbon fixed by marine phytoplankton is processed by bacteria (Azam *et al.*, 1983).

In order to survive in the oceans, bacteria compete for nutrients and organic matter to support their growth (Smriga *et al.*, 2016). Over the evolutionary time, bacteria have developed

different strategies to acquire organic matter that are reflected in their genomic content (Lauro *et al.*, 2009). Among these strategies, the oligotrophy and the copiotrophy are two extremes. Oligotrophic bacteria are the ones that thrive in poor nutrients concentrations (Lauro *et al.*, 2009). Considering that the oceans are in majority oligotroph, they are among the most abundant organisms in the world (Giovannoni, Tripp, *et al.*, 2005; Giovannoni, 2017). Some strategies developed by this group to thrive in nutrient-limited environments are their ability to grow slowly and their relatively small cell size (Cavicchioli *et al.*, 2003). The benefits of having small cell sizes can be to avoid predation, to increase the surface/volume ratio which allows efficient nutrient acquisition, and to decrease the replication costs (Cavicchioli *et al.*, 2003). In addition, oligotrophic bacteria present streamlined genomes (Giovannoni *et al.*, 2014), retaining only core metabolic genes, while reducing pseudogenes and intergenic spacers (Giovannoni, Tripp, *et al.*, 2005). The streamlining favors cell architecture that minimizes resources required for replication (Giovannoni, Tripp, *et al.*, 2005; Giovannoni *et al.*, 2014). An example of marine oligotrophic lineages is the ubiquitous SAR11 clade from the Alphaproteobacteria class, the most abundant organisms in the oceans. This clade accounts to about 30% of bacterial abundance in surface oligotrophic waters (Morris *et al.*, 2002; Giovannoni, 2017) and can be found everywhere in the global ocean (Wietz *et al.*, 2010). Other oligotrophic lineages belonging to Gammaproteobacteria are SAR92, OM60/NOR5, OM182, BD1-7, and KI89A, which are all part of the oligotrophic marine gammaproteobacteria (OMG) clade (Giovannoni *et al.*, 2005). Members of this clade are ultrasmall (volume < 0.1  $\mu\text{m}^3$ ), ubiquitous, phylogenetically diverse and seem unable to grow at high nutrient concentrations (> 351 mg of carbon per liter) (see Giovannoni, Tripp, *et al.*, 2005 and references therein).

On the other end of the trophic spectrum, copiotrophs are bacteria that favor nutrient-rich conditions and complex organic matter. In general, copiotrophic bacteria display relatively large genomes sizes (> 4Mb), including a higher genetic potential to rapidly respond to changing environmental conditions (Lauro *et al.*, 2009). They present higher capacity to sense, transduce and integrate extracellular stimuli, and they are also able to activate alternative catabolic pathways when the high energy compounds have been exhausted (Lauro *et al.*, 2009). In addition, these bacteria have a developed chemical sensing and locomotion system (Smriga *et al.*, 2016). This allows them to sense and swim towards hotspots of organic carbon (Stocker and Seymour, 2012). It has been shown that copiotrophs have more than 10% of their genes under transcriptional control, which allow them to respond to environmental stimuli (Cottrell and Kirchman, 2016). Moreover, a high fraction of marine bacteria (from 40% to 70% during

summer) are motile and strongly respond to the chemical stimuli sent by phytoplankton cells and detrital aggregates that serve as organic matter sources (Grossart *et al.*, 2001). Bacterial families that contain mainly copiotrophic members known to thrive in phytoplankton blooms are the *Alteromonadaceae* (López-Pérez and Rodríguez-Valera, 2014), *Marinobacteraceae* (Handley and Lloyd, 2013), *Rhodobacteraceae* and *Flavobacteriaceae* (Buchan *et al.*, 2014; Teeling *et al.*, 2016). (Figure 3 – legend can be found in the next page).

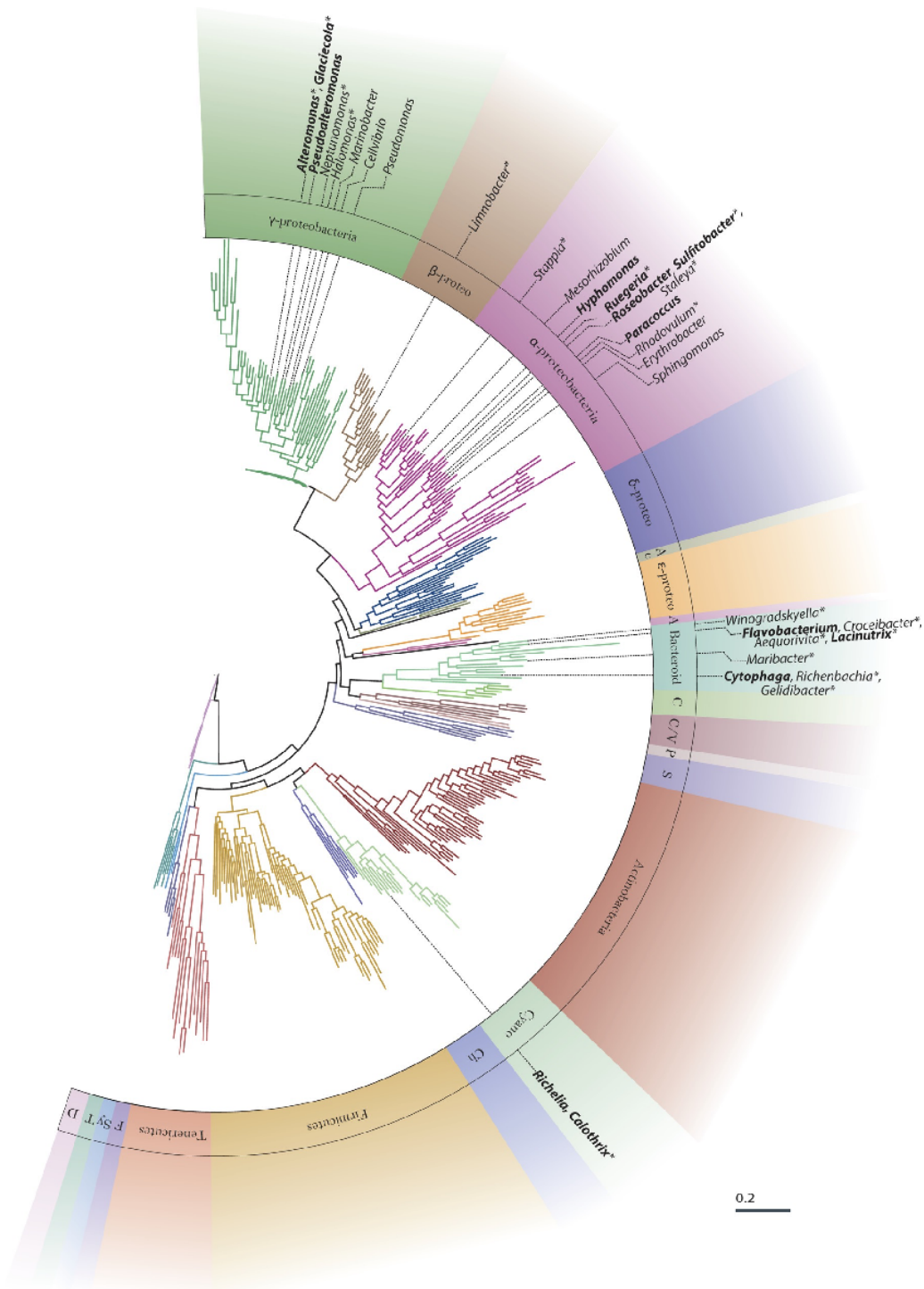


**Figure 3.** Maximum-likelihood phylogenetic tree of the bacterial domain, highlighting heterotrophic taxa most commonly found associated with diatoms. Figure and legend (adapted) from Amin *et al.*, (2012). Also shown are the autotrophic nitrogen-fixing cyanobacteria known to be associated with diatoms. Bacterial phyla are color coded and labeled in the corresponding-colored ring. Taxa reported to be associated with diatoms in culture or field samples are labeled in the outer ring. Boldface genera were reported in two or more independent studies. The tree is based on a concatenated alignment of 31 conserved predicted proteins from 350 bacterial species with whole genome sequences. Asterisks indicate taxonomic positions that are estimated from nearest 16S rRNA neighbor on the tree because they were not included in the original alignment. See Amin *et al.*, (2012) for more details on the figure and phylogeny construction.

These extreme opposite strategies (copiotrophs vs oligotrophs) indicate the ability of bacteria to adapt to their surrounding environment. However, this is a rather simplistic view, and a complex spectrum of eco-evolutionary strategies does exist between these two extremes (Lauro *et al.*, 2009). In the context of this thesis, although simplistic, these concepts help to understand why certain bacterial groups are often found surrounding the phytoplankton cells.

### **1.3) The phycosphere: Where phytoplankton and bacteria interact**

#### **A) The concept of phycosphere**

The phycosphere defines the microenvironment surrounding a phytoplankton cell which is enriched in organic molecules (Seymour *et al.*, 2017). This term was first used by Bell and Mitchell in the 70's as an analogue of the rhizosphere in plants (Bell and Mitchell, 1972). The rhizosphere is the vicinity region around the plant roots which is influenced by the nutrients and oxygen released by the plant (Philippot *et al.*, 2013) (Figure 4). This region is characterized by a gradient of chemical, biological and physical properties that change along the roots (Trivedi *et al.*, 2020). The colonization at the rhizosphere is in majority done by chemotactic bacteria, which are attracted by the plant exudates and able to thrive in these particular conditions (Philippot *et al.*, 2013). In addition, the plants have evolved strategies to avoid the colonization by pathogens and non-desired organisms such as the production of antibiotics and antifungal compounds, and the stimulation of the growth of specific bacterial groups (Trivedi *et al.*, 2020).

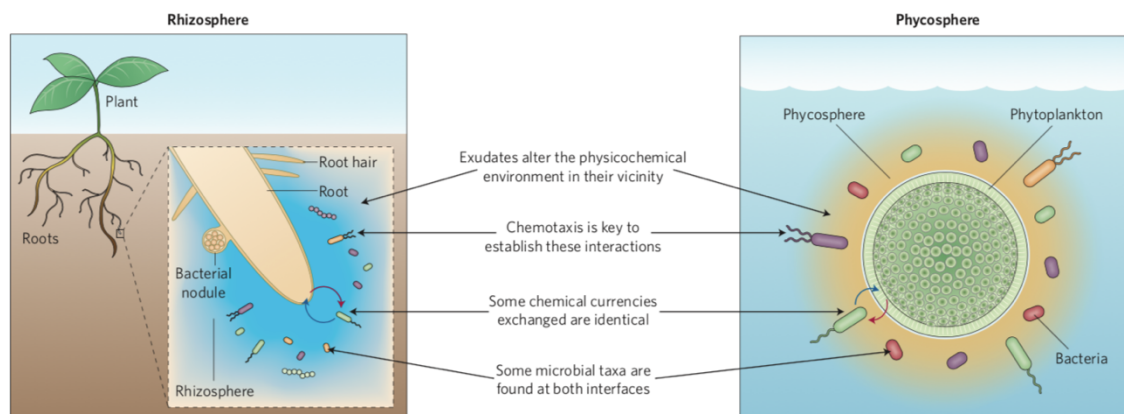


**Figure 4.** The rhizosphere and the phycosphere are analogous microenvironments. The phycosphere defines the region surrounding a phytoplankton cell which is enriched in organic substrates exuded by the cell. The phycosphere is an important microenvironment for planktonic bacteria. Figure and legend (adapted) from Seymour *et al.*, (2017).

Similarly, the phycosphere is also characterized by a gradient of oxygen, pH and organic molecules exuded by the microalgal cell which can attract heterotrophic bacteria (Bell and Mitchell, 1972) (Figure 4). As it will be exposed in the next sections, chemotactic bacteria are amongst the most important colonizers of the phycosphere (Smriga *et al.*, 2016; Seymour *et al.*, 2017). In addition, some chemical currencies are commonly found in both regions, such as sugars, amino acids and sulfur compounds (Durham *et al.*, 2015). Finally, these two regions also share some bacterial groups. This is the case of *Rhizobium* members that are often associated with plant roots and represent important members of the phycosphere of green algae (Ramanan *et al.*, 2015; Seymour *et al.*, 2017; Haberkorn *et al.*, 2020). On the other hand, a remarkable particularity of the phycosphere is that phytoplankton is inserted in a turbulent environment (Seymour *et al.*, 2017). This feature impacts the size and shape of the phycosphere and ultimately the rates to which bacteria encounters the phytoplankton cell (Smriga *et al.*, 2016; Seymour *et al.*, 2017).

In their pioneer work in 1972 Bell and Mitchell stated, “*It would appear that the phycosphere is a region of interactions that have only begun to be evaluated*” (Bell and Mitchell, 1972). Since then, much has been discovered regarding the interactions occurring in the phycosphere and this will be detailed in the next sections.

## **B) The microbiome assembly processes in the phycosphere**

The microalgal microbiome assembly is a result of complex interactions involving the bacterial community, the microalgal host and the environment (Seymour *et al.*, 2017). The most investigated process of assembly in the phycosphere is the traditional niche-based theory, which postulates that specific variables (biotic and abiotic interactions, life history traits) determine how communities are organized (Hutchinson, 1957).

Considering that physical and chemical conditions present in the phycosphere are different from that of the bulk seawater (Seymour *et al.*, 2017), it is expected that the bacteria found in the phycosphere environment are selected by its conditions. Moreover, it is suspected that microalgae can select which bacteria are able to grow in the phycosphere by different mechanisms such as the release of specific organic molecules that will favor specific groups and/or inhibit others (Fu *et al.*, 2020). Many studies investigating the phycosphere of different phytoplankton have found deterministic processes as the main drivers of the bacterial diversity in natural blooms (Landa *et al.*, 2016; Teeling *et al.*, 2016; Hattenrath-Lehmann and Gobler, 2017) and in cultures (Ajani *et al.*, 2018; Behringer *et al.*, 2018; Lawson *et al.*, 2018; Shin *et al.*, 2018; Kimbrel *et al.*, 2019; Sörenson *et al.*, 2019; Sara L Jackrel *et al.*, 2020; Mönnich *et al.*, 2020). The deterministic factors pointed out by these studies were the place/time of isolation (Ajani *et al.*, 2018), the host genotype (Hattenrath-Lehmann and Gobler, 2017; Behringer *et al.*, 2018; Lawson *et al.*, 2018; Shin *et al.*, 2018; Kimbrel *et al.*, 2019; Sörenson *et al.*, 2019; Sara L Jackrel *et al.*, 2020; Mönnich *et al.*, 2020) and the composition of the organic matter released by different phytoplankton species (Teeling *et al.*, 2012; Landa *et al.*, 2016). During a diatom bloom, the bacterial community composition differs drastically from before, during, and at late stages and appear to be strongly controlled by the substrate succession (Teeling *et al.*, 2012). Changes in community composition are mainly associated with the decrease of oligotrophic bacterial clades (such as SAR11 and Actinobacteria) and the increase of copiotrophs (such as Rhodobacteraceae, Alteromonadaceae and Flavobacteriaceae members) (Teeling *et al.*, 2012). Moreover, these patterns are similar among different phytoplankton groups, such as diatoms, dinoflagellates and coccolithophores (Teeling *et al.*, 2012). The bacterial groups of bacteria often found associated to microalgal blooms have been called ‘archetypal phytoplankton-associated taxa’ and are mainly members of Alphaproteobacteria, Flavobacteriia and Gammaproteobacteria (Buchan *et al.*, 2014) (see Figure 3 for details). Not surprisingly, they are also the most dominant groups found in cultures of diatoms (Ajani *et al.*,

2018; Behringer *et al.*, 2018; Crenn *et al.*, 2018; Mönnich *et al.*, 2020), dinoflagellates (Bolch *et al.*, 2017; Lawson *et al.*, 2018; Shin *et al.*, 2018; Sörenson *et al.*, 2019), coccolithophores (Green *et al.*, 2015), green algae (Abby *et al.*, 2014; Geng *et al.*, 2016; Lupette *et al.*, 2016; Jackrel *et al.*, 2019) and cyanobacteria (Dziallas and Grossart, 2011).

Contrary to earlier studies in other marine models, such as macroalgae (Burke, Steinberg, *et al.*, 2011; Burke, Thomas, *et al.*, 2011), microbiomes assembly mechanisms other than the niche-based theory started only recently to be considered in the phycosphere (Kimbrel *et al.*, 2019; Zhou *et al.*, 2019; Mönnich *et al.*, 2020). The absence of consistent microbiomes across individuals of the macroalga *Ulva australis* led the authors to hypothesize that the microbiome assembly is a process rather governed by random selection (Burke, Thomas, *et al.*, 2011). The main theory considering the influence of stochasticity on community structure is the neutral theory of biodiversity (Hubbell, 2001). It postulates that community assembly is largely independent of specific traits of individual species, and mostly influenced by stochastic processes such as births, deaths, immigration, extinction, and speciation (Hubbell, 2001). The broad assumption from the neutral theory that all species are equivalent was not supported by results showing that the bacterial community composition of *U. australis* was significantly different from that of bulk seawater which favored a niche-based selection (Burke, Thomas, *et al.*, 2011). In this context, the competitive lottery which considers both the niche-based theory and random processes seems to better explain the microbiome assembly on *U. australis* (Sale, 1979). In the competitive lottery, a guild of organisms with similar capacity to colonize an empty niche, e. g. bacteria capable of colonizing the *U. australis* surface, will be selected by stochasticity and priority effects (Sale, 1979). Since all organisms of this guild are equally able to colonize the given environment, the one arriving first wins the lottery (Sale, 1979). The competitive lottery differs from neutral theory by considering that the organisms able to colonize that environment belong to a guild with similar functional traits which are not equivalent to all members of the community (Burke, Steinberg, *et al.*, 2011). This model is gaining attention in microalgal microbiome studies because it can justify why bacteria enriched at different phytoplankton blooms and in cultures are often assigned the same taxonomic groups (Rhodobacteraceae, Gammaproteobacteria and Flavobacteriaceae) which are often found in lower abundance in bulk seawater (Buchan *et al.*, 2014). At the same time, this model can also justify why microbiomes of the same phytoplankton species (e. g. the *Leptocylindrus sp.* microbiomes) can differ between strains (stochasticity) (Ajani *et al.*, 2018).

Two recent studies investigating phytoplankton microbiomes discussed the possible participation of the competitive lottery on the assembly of microbiomes in culture (Kimbrel *et al.*, 2019; Mönnich *et al.*, 2020). Kimbrel *et al.*, (2019) studied the assembly of attached and free-living communities associated to the diatom *Phaeodactylum tricornutum* and to the eustigmatophyte *Microchloropsis salina* in outdoor mesocosms and in culture enrichments. In outdoor mesocosms, each microalga harbored taxonomic distinct free-living and alga-associated communities, indicating a niche-based selection (Kimbrel *et al.*, 2019). By inoculating the free-living community from the outdoor mesocosms (one from monoalgal *P. tricornutum* and one from polyalgal *P. tricornutum*/*M. salina*) into axenic *P. tricornutum* cultures, similar communities emerged, demonstrating that the host has also an important role in its microbiome assembly, which also agreed with the niche-based theory (Kimbrel *et al.*, 2019). In another experiment, these authors inoculated the attached bacterial community in axenic *P. tricornutum* and submitted this community to several washings and growth cycles in order to keep only the community attached to the microalga. By sequencing the final established community, they detected random patterns in community composition (Kimbrel *et al.*, 2019). These last results agree with the competitive lottery by showing that the attached community (which was equally able to colonize the surface of *P. tricornutum*) was randomly selected in different *P. tricornutum* axenic cultures (Kimbrel *et al.*, 2019). Recently, Mönnich *et al.*, (2020) investigated how compositionally different bacterial inocula obtained from phytoplankton cultures and from natural seawater were selected by an axenic diatom *Thalassiosira rotula*. These authors found that the different inocula converged to a stable and reproducible core community very similar to the initial microbiome of xenic *T. rotula* pointing out a selective microhabitat filtering and discarding the competitive lottery (Mönnich *et al.*, 2020). The association of deterministic and stochastic processes has been also investigated in a natural bloom of *Scrippsiella trochoidea* (Zhou *et al.*, 2019). Interestingly, the authors found that stochastic and deterministic assembly processes varied depending on the stage of the bloom and between free-living and particle-attached communities (Zhou *et al.*, 2019). For the free-living part of the community, deterministic processes had higher influence at the peak of the bloom, while early and late stages of the bloom were governed mainly by stochasticity (Zhou *et al.*, 2019). The particle-attached community was more influenced by deterministic processes at the pre- and during bloom phases, while the post-bloom phase was more governed by stochasticity (Zhou *et al.*, 2019). Altogether, these studies suggested that complex spatio-temporal processes are involved in microbial community assembly in phycospheres of cultures and natural environments. Further studies involving several phytoplankton models in both

natural and controlled conditions are necessary to further understand how the microbiomes are assembled in the phycosphere.

### **C) Diversity and remarkable traits of phycosphere colonizers**

Although our understanding of the patterns of community assembly in the phycosphere remains limited, valuable information regarding the traits and diversity of the organisms around phytoplankton cells has been obtained over the last decades. Considering that phytoplankton exudates have different diffusion rates and thus will spread more or less around the cells, the chemotaxis and cell motility have important roles in the first steps of phycosphere colonization (Slightom and Buchan, 2009; Seymour *et al.*, 2010; Stocker and Seymour, 2012; Smriga *et al.*, 2016). Other important traits for phycosphere colonizers can be signaling (such as quorum sensing and quorum quenching) and attachment capacities (Slightom and Buchan, 2009; Rolland *et al.*, 2016). Chemotaxis has been shown to be an important mechanism for phycosphere colonization and is widespread among copiotrophic bacteria (Slightom and Buchan, 2009; Smriga *et al.*, 2016). Prokaryotic chemotaxis includes both stimuli recognition and motility towards the stimuli source or away from it and involves sensory pathways such as the histidine-aspartate phosphorelay system (Wadhams and Armitage, 2004). These systems are involved in measuring chemical concentrations around the cells and processing the information, which is then used to tune the motility accordingly (Wadhams and Armitage, 2004; Stocker and Seymour, 2012). Marine bacteria have developed efficient ways to swim faster and precisely which guarantee their fast response to the chemical stimuli (Stocker and Seymour, 2012) and increase the probability that they will reach its source (Johansen *et al.*, 2002). Bacteria with a strong chemotactic ability, such as Proteobacteria (*Vibrio*, *Pseudoalteromonas*, roseobacters, *Caulobacter* and *Marinobacter* members) and Bacteroidetes (*Sphingomonas*, Flavobacteria), are often enriched in the phycosphere of different microalgal groups in natural environments (Gonzalez *et al.*, 2000; Zubkov *et al.*, 2001; Teeling *et al.*, 2012; Zhou *et al.*, 2018, 2019) and cultures (Ramanan *et al.*, 2015; Lupette *et al.*, 2016; Bolch *et al.*, 2017; Krohn-Molt *et al.*, 2017; Ajani *et al.*, 2018; Behringer *et al.*, 2018; Zheng *et al.*, 2018; Lawson *et al.*, 2018; Shin *et al.*, 2018; Sörenson *et al.*, 2019; Kimbrel *et al.*, 2019; Mönnich *et al.*, 2020) (see Figure 3 for more details). The response of *Ruegeria pomeroyi* (Roseobacter clade) to *Alexandrium tamarense* depicted through transcriptomic data showed an increase in the expression of genes related to flagellar motility (Landa *et al.*, 2017). Motile bacteria are estimated to consume up to 5 times more DOM in the phycosphere than non-motile bacteria

(Smriga *et al.*, 2016). Interestingly, the partitioning of DOM in coastal conditions (at usual bacterial and phytoplankton cell concentrations) seems unaffected by motility. However, in nutrient-rich conditions (such as in phytoplankton blooms), chemotaxis play an important role in the fate of DOM, which highlights the important role of chemotaxis on phytoplankton-bacteria interactions (Smriga *et al.*, 2016).

Besides adjusting their swimming speed and trajectory, bacteria need to be able to modulate their cell concentrations and behavior. Quorum sensing is the term used to describe the cell-cell communication system used by bacteria to control their population density and gene expression according to the ambient bacterial density (Fuqua *et al.*, 1994; Rolland *et al.*, 2016). This mechanism is controlled by autoinducers released by bacteria which above a certain threshold triggers the change of bacterial phenotype and behavior from individual to collective (Fuqua *et al.*, 1994). DMSP released by phytoplankton is another signal hypothesized to trigger quorum sensing in bacteria (Johnson *et al.*, 2016). In the phycosphere, quorum sensing is important for the formation of biofilms (Fei *et al.*, 2020), acquisition of nutrients (Van Mooy *et al.*, 2012), regulation of microbial population dynamics (Rolland *et al.*, 2016) and modulating virulence of algicidal bacteria (Harvey *et al.*, 2016; Wang *et al.*, 2016). Quorum-sensing will influence the persistency of the bacteria around the phytoplankton cell and phytoplankton survival. Members of the Roseobacter clade, such as several *Phaeobacter* species, *Ruegeria pomeroyi* (formerly *Silicibacter pomeroyi*), and *Dinoroseobacter shibae* have been shown to produce quorum sensing molecules (Slightom and Buchan, 2009; Seyedsayamdost, Case, *et al.*, 2011; Patzelt *et al.*, 2013; Johnson *et al.*, 2016; Wang *et al.*, 2016; Fei *et al.*, 2020). However, this cell-to-cell signaling mechanism does not seem to be phylogenetically conserved by all Roseobacter clade members (Slightom and Buchan, 2009).

Attachment of bacteria onto the microalgal cell represents an additional important mechanism in microbiome assembly. In the turbulent conditions of the oceans, attachment gives to the bacteria the advantage to stay close to the host, to profit of its exudates, and potentially to influence phytoplankton aggregation (Grossart, Czub, *et al.*, 2006; Fei *et al.*, 2020). Different phytoplankton groups have been shown to harbor a variety of epiphytic bacteria (Gärdes *et al.*, 2012; Sonnenschein *et al.*, 2012; Crenn *et al.*, 2016; Segev, Wyche, *et al.*, 2016; Crenn *et al.*, 2018; Zheng *et al.*, 2018; Zhou *et al.*, 2019; Haberkorn *et al.*, 2020). Alphaproteobacteria (*Algimonas*, *Erythrobacter*, *Paracoccus* and *Silicimonas algicola*), Gammaproteobacteria (*Pseudoalteromonas* and *Marinobacter*) and Flavobacteriia (*Tenacibaculum*) are common

diatom-attached bacteria from cultures and/or from the field (Gärdes *et al.*, 2011; Sonnenschein *et al.*, 2012; Crenn *et al.*, 2016, 2018). The attachment of bacteria is not restricted to diatoms. For example, Zheng *et al.*, (2018) found *Flavobacteriales* attached to *Synechococcus* cells at all growth phases. In addition, bacterial groups such as *Rhodobacterales*, *Vibrionales*, and *Flavobacteriales* dominated in the particle-attached fraction (>3 µm) during a bloom of dinoflagellates (Zhou *et al.*, 2019). During the decline phase of this bloom, other groups such as Gammaproteobacteria (*Vibrionales*, *Oceanospirillales*, *Alteromonadales*, *Thiotrichales*, and *Legionellales*) and Epsilonproteobacteria (*Pseudomonadales* and *Enterobacteriales*) emerged and their abundance increased in the post-bloom phase (Zhou *et al.*, 2019).

Besides facilitating the access of bacteria to phytoplankton exudates, attachment is often used by pathogenic bacteria for infection. Alphaproteobacteria (*Tistrella* sp.) attach to *Chlorella vulgaris* and ultimately kill the microalga (Haberkorn *et al.*, 2020). Another example is *Phaeobacter inhibens* which attach to senescent *E. huxleyi* cells and promote cell lysis by the production of specific compounds (Segev *et al.*, 2016).

The traits presented here are some of the characteristics common among bacteria inhabiting the phycosphere which seems shared between different phytoplankton species. These characteristics are important because they will determine how bacteria encounter the phycosphere, their behavior and their residence time which will ultimately impact phytoplankton-bacteria interactions.

### **D) Metabolic exchanges at the phycosphere: How these organisms interact?**

Phytoplankton-bacteria dynamics have been studied in a large-scale perspective (from meters to kilometers) and across long temporal scales (seasonal to annual) (see Seymour *et al.*, 2017 and references therein). Although large scale investigations are able to show a tight coupling between distribution and seasonal patterns of both partners (Bird and Kalff, 1984), they are not precise enough to explore their interactions. The term ‘interaction’ is related to the influence of one species on the growth rate or metabolism of another; interactions range from negative, neutral to positive (Figure 5) (Faust and Raes, 2012; Tipton *et al.*, 2019). Some authors defend the use of the term ‘symbiosis’ to define all the continuum of interactions between host and microbiome (Tipton *et al.*, 2019). This continuum includes the mutualistic interactions which are beneficial to both partners (Tipton *et al.*, 2019). Other type of interactions

included are parasitism, which is positive for one and negative to the other, and competition, which is negative for both (Figure 5) (Tipton *et al.*, 2019).

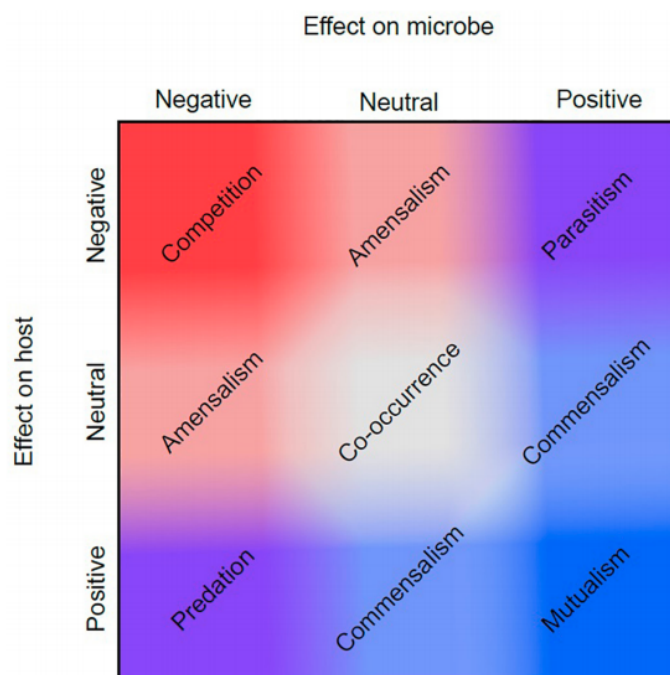


**Figure 5.** The continuum of symbiotic relationships. Symbiotic relationships encompass multiple dimensions of effects represented on two axes. If a symbiosis has a positive (blue) effect for a microbe and a negative (red) effect for the host, this is known as parasitism (top right corner). Some symbioses may have more positive or negative effects for a symbiont or host than others, and these may shift depending upon their environmental context as shown in the figure by the gradation of red and blue values between the two axes. In addition, an interaction that is neutral for both partners is considered simply co-occurrence. Figure and legend (adapted) from Tipton *et al.*, (2019).

To decipher metabolic and molecular mechanisms of phytoplankton-bacteria interactions at larger scales represents a challenge considering that the metabolites exchanged are found in very low concentrations in seawater and many of these molecules are yet not described (Moran *et al.*, 2016). Yet this challenge can be overcome by the association and complementarity of different techniques. In this context, co-culture experiments (where host and bacterial partners can be controlled) associated with the ‘omics’ tools such as genomics, transcriptomics and metabolomics represent a powerful approach, allowing to identify the genes differentially expressed and the metabolites potentially exchanged. These studies provide

key information on specific interaction metabolites that can then be targeted in environmental investigations. For example, co-culture experiments allowed to tease apart the interaction between a *Sulfitobacter* species with the globally distributed diatom *Pseudo-nitzschia multiseries* (Amin *et al.*, 2015). This interaction involves the production and release of the phytohormone indole-3-acetic acid (IAA) by the bacterium using algal released and endogenous tryptophan, which promotes diatom cell division (Amin *et al.*, 2015). Moreover, by targeting the IAA gene expression by metatranscriptomic analysis, the authors found that IAA production by *Sulfitobacter*-related bacteria is widespread in the oceans, particularly in coastal environments, revealing the large-scale relevance of these interactions (Amin *et al.*, 2015).

In the past decades, many studies have expanded the list of molecules involved in phytoplankton-bacteria interactions (Croft *et al.*, 2005; Amin *et al.*, 2009; Seyedsayamdost, Case, *et al.*, 2011; Paul and Pohnert, 2011; Paul *et al.*, 2013; Mausz and Pohnert, 2015; Wang *et al.*, 2016; Durham *et al.*, 2017; Barak-Gavish *et al.*, 2018; Bramucci *et al.*, 2018; Mühlenbruch *et al.*, 2018; Brown *et al.*, 2019; Shibl *et al.*, 2020; Fei *et al.*, 2020). Different molecules are exchanged depending on the nature of the interaction.

Mutualistic phytoplankton-bacteria interactions can involve the exchange of compounds released by bacteria such as vitamins (for example B12) (Croft *et al.*, 2005), iron (Amin *et al.*, 2009), ammonium and growth promoters (Amin *et al.*, 2015). In exchange, bacteria can benefit from organic nitrogen compounds (Amin *et al.*, 2015) and organic sulfur molecules such as DMSP that are released by microalgae. Overall, recent literature reports that these interactions are sophisticated and involve different mechanisms of recognition and control by both microalgae and bacteria (Durham *et al.*, 2017; Shibl *et al.*, 2020). They can involve a cascade of recognition that allows the microalgae to identify the presence of the bacterium partner as shown for *Thalassiosira pseudonana* in the presence of *R. pomeroyi* (Durham *et al.*, 2017). The cascade involved the differential expression of genes responsible in recognition of biotic stimuli (calcium-binding proteins and calcium-dependent protein kinase), transmission of signal, and protein-protein interactions (leucine-rich repeat receptors) analogous to that observed in plants (Durham *et al.*, 2017). Besides recognizing the presence of bacteria, microalgae seem able to control which bacteria will thrive in the phycosphere by the production and release of secondary metabolites (Shibl *et al.*, 2020). One of them, rosmarinic acid, suppresses motility and promotes attachment of beneficial bacteria, while the other, azelaic acid, inhibits the growth of

opportunistic bacteria but stimulates the growth of beneficial ones (Shibl *et al.*, 2020). This sophisticated strategy allows the microalgae to benefit from their microbiome by controlling the most favorable partners (Shibl *et al.*, 2020). Similar results were found in synthetic phycospheres containing common metabolites released by diatoms (xylose, glutamate, glycolate, ectoine, and dihydroxypropanesulfonate) and dinoflagellates (ribose, spermidine, trimethylamine, isethionate, and DMSP) (Fu *et al.*, 2020). By inoculating natural bacterial communities in treatments with single metabolites and with different combinations of them, the authors showed that the final communities were different between the treatments, depending on the metabolites used (Fu *et al.*, 2020). Furthermore, by using modeling approach, the authors were able to predict the community composition of treatments with multiple metabolites based on the community composition of single metabolites treatments (Fu *et al.*, 2020).

Negative phytoplankton-bacteria interactions (parasitism and competition) have been extensively investigated (Mayali and Azam, 2004; Paul and Pohnert, 2011; Seyedsayamdost, Carr, *et al.*, 2011; Seyedsayamdost, Case, *et al.*, 2011; Meyer *et al.*, 2017; Bigalke and Pohnert, 2019). Here, I will focus on some examples of the mechanisms used by parasitic bacteria to interact with phytoplankton (see Mayali and Azam, 2004 and Meyer *et al.*, 2017 for a detailed review on algicidal bacteria). Certain bacteria are capable of releasing compounds that display algicidal activity against different phytoplankton species. Among them, *Kordia algicida* killed the diatoms *Skeletonema costatum*, *Thalassiosira weissflogii* and *Phaeodactylum tricornutum* while *Chaetoceros didymus* was unaffected (Paul and Pohnert, 2011). The mechanisms of the algicidal activity of *K. algicida* do not require direct contact with the microalgae and involve protease activity (Paul and Pohnert, 2011). This protease activity is controlled by the bacterial cell concentration, suggesting a quorum sensing control (Paul and Pohnert, 2011). Further studies revealed that the resistance of *C. didymus* against *K. algicida* was affected when a microalgal competitor (*S. costatum*) was added in the co-cultures (Bigalke and Pohnert, 2019). These interactions are however complex because growth of *C. didymus* was stimulated in the presence of low concentrations of *S. costatum*/*K. algicida* but inhibited when these partners were provided in high concentrations (Bigalke and Pohnert, 2019). Interestingly, the algicidal activity of *K. algicida* was also effective on natural *Chaetoceros socialis* populations collected in the North Sea (Bigalke *et al.*, 2019). Algicidal compounds released by bacteria have been shown to kill different harmful phytoplankton species (Lovejoy *et al.*, 1998; Li *et al.*, 2018). The dominance of Pseudoalteromonadaceae members in a *Prorocentrum donghaiense* coastal bloom was associated with high concentrations of putative algicidal molecules (beta-

glucosidase) which were hypothesized to have important roles in the bloom termination (Li *et al.*, 2018). Algicidal bacteria play an important role in shaping species composition in pelagic environments. Thanks to the decades of intense investigation, their ecological role is not far from being fully understood (Mayali & Azam, 2004; Meyer *et al.*, 2017).

### **1.4) Large scale impacts of phytoplankton-bacteria interactions**

Given the diversity, abundance and global distribution of phytoplankton and bacteria, their interactions are critical for marine ecosystems functions. Although these interactions are restricted to  $\mu\text{m}$ - $\text{mm}$  spatial scales, their impact can scale up to major ecological processes in the oceans (Seymour *et al.*, 2017). Phytoplankton-bacteria interactions can strongly impact carbon and nutrient cycling and the productivity and stability of aquatic food webs (Field *et al.*, 1998). For example, bacteria can sustain phytoplankton growth in areas where the availability of limiting resources, such as nutrients, are scarce (Roth-Rosenberg *et al.*, 2020). It has been shown that the cosmopolitan cyanobacteria *Prochlorococcus* relied on associated bacteria to survive starvation when their nutrient-saving mechanisms are not sufficient (Roth-Rosenberg *et al.*, 2020). This can be related to the recycling of inorganic nutrients by bacteria, as well as the production of organic compounds which contain nutrients such as N and P (Roth-Rosenberg *et al.*, 2020). This might affect the distribution and activity of *Prochlorococcus* on a global scale and may have profound impacts on the overall oceanic productivity and carbon cycling (Roth-Rosenberg *et al.*, 2020). Moreover, microscale phytoplankton-bacteria interactions play an important role in the carbon cycle by facilitating the formation of aggregates (Gärdes *et al.*, 2011). Several studies have shown that bacteria can stimulate the formation of aggregates by phytoplankton, a phenomenon that varies among microalgal species (Grossart, Czub, *et al.*, 2006; Grossart, Kiørboe, *et al.*, 2006; Gärdes *et al.*, 2011; Tran *et al.*, 2020). Such interactions may potentially have important implications for mediating vertical carbon flux in the oceans (Tran *et al.*, 2020) and enhancing the efficiency of the biological carbon pump (Gärdes *et al.*, 2011).

Another large-scale impact of phytoplankton-bacteria interactions is the termination of harmful algal blooms. Harmful algal blooms have considerable economic and ecological impacts (Assmy and Smetacek, 2009). They are responsible for the loss of marine biodiversity and their damage can extend to public health problems. As previously mentioned, algicidal compounds released by bacteria have been shown to kill different harmful phytoplankton

species and are considered as potential controllers of harmful algal blooms (Bates *et al.*, 1995; Lovejoy *et al.*, 1998; Li *et al.*, 2018). Certain bacteria can however stimulate the growth of harmful phytoplankton species (Bolch *et al.*, 2017).

Pathogenic bacteria may also contribute to the regulation of major oceanic cycles. In an experimental approach, a *Sulfitobacter* strain, isolated from an *E. huxleyi* bloom, showed increased virulence against *E. huxleyi* at higher concentrations of DMSP (Barak-Gravish *et al.*, 2018). Although the mechanisms used by the bacterium to kill the microalgae are yet not known, the authors suggest that the bacterial consumption of large amounts of DMSP can reduce the production of DMS by the algal degradation (through DMSP-lyase - Alma1 enzyme) (Barak-Gravish *et al.*, 2018). Since DMS is a volatile gas which accounts for 90% of the sulfur emissions by biological processes (Sievert *et al.*, 2007), these interactions, taking place in the demise phase of *E. huxleyi* blooms, could contribute to the regulation of oceanic sulfur cycling and feedback to the atmosphere (Barak-Gravish *et al.*, 2018).

These few examples do not resume all the large-scale impacts that phytoplankton-bacteria interactions can have in the oceans. However, they exemplify the importance of investigating the phycosphere microbiomes in order to achieve a better understanding of global ocean ecology.

## 2) *Emiliana huxleyi*: a model organism to study phytoplankton-bacteria interactions

*Emiliana huxleyi*, the main phytoplankton taxa used in this work, is a relevant model organism to explore the phytoplankton-bacteria interactions. The next sections will explain its relevance and also present *Gephyrocapsa oceanica*, sister group of *E. huxleyi*, that was used for comparative purposes. The characteristics of *G. oceanica* will be described when they are relevant for the study.

### 2.1) Evolution, ecology and distribution

*Emiliana huxleyi* (Lohmann, 1902; Hay *et al.*, 1967) is the most abundant coccolithophore in modern oceans (Paasche, 2001; Hagino *et al.*, 2011). It belongs to the order Isochrysidales of the Haptophyta phylum. Together with the genus *Gephyrocapsa* and *Reticulofenestra*, they form the family Noelaerhabdaceae (Young *et al.*, 2003). *E. huxleyi* is a relatively recent taxa, with a first appearance in the fossil record well documented at 291,000 years ago (Raffi *et al.*, 2006). Fossil evidence suggests that *E. huxleyi* evolved directly from a *Gephyrocapsa* species (Samtleben, 1980) during glacial periods with low atmospheric CO<sub>2</sub> partial pressure and presumably high oceanic productivity (Paasche, 2001).

Contrary to their close relatives, *E. huxleyi* is globally distributed from tropical to subpolar oceans, from oligotrophic to eutrophic waters and they can form massive annual blooms in high latitudes such as the North Sea, the Western English Channel, the Bay of Biscay and in the North Atlantic (Gonzalez *et al.*, 2000; Zubkov *et al.*, 2001; Tyrrell and Merico, 2004). *Emiliana* blooms can cover areas up to 250,000 km<sup>2</sup> and reach cell concentrations of 10<sup>5</sup> cells/mL (Tyrrell and Merico, 2004). *G. oceanica* (Kamptner, 1943) presents a more restricted distribution, being found mainly in lower latitudes, in tropical and temperate regions, and in eutrophic waters. It is more widespread in the Pacific than Atlantic Oceans (Bollmann, 1997), and can also form large blooms in coastal waters (Blackburn and Cresswell, 1993; Rhodes *et al.*, 1995; Kai *et al.*, 1999).

Both *Emiliana* and *Gephyrocapsa* blooms are characterized by milky-turquoise waters that can be observed by satellite sensors (Figure 6) although *E. huxleyi* blooms are more frequent (Tyrrell and Merico, 2004). The highest reflectance observed are mainly generated by

detached coccoliths that float in surface water at the bloom declining phase (Neukermans and Fournier, 2018) .



**Figure 6.** Coccolithophores bloom in the English Channel (June 24, 2020). Source: [https://eoimages.gsfc.nasa.gov/images/imagerecords/146000/146897/englishchannel\\_tmo\\_2020176\\_lrg.jpg](https://eoimages.gsfc.nasa.gov/images/imagerecords/146000/146897/englishchannel_tmo_2020176_lrg.jpg).

Both taxa are easy to cultivate, comprising most of the coccolithophores diversity in culture collections (Probert and Houdan, 2004) which make them attractive models. *E. huxleyi* is indeed one of the best-studied phytoplankton in many aspects: physiology (Beaufort *et al.*, 2011; Van Oostende *et al.*, 2013; Plummer *et al.*, 2019), ecology (Cook *et al.*, 2011; Seyedsayamdost, Case, *et al.*, 2011; Patil *et al.*, 2017; Poulton *et al.*, 2017), phylogeny and genomics (Read *et al.*, 2013; Bendif *et al.*, 2014, 2015, 2016, 2019), life cycle (Von Dassow *et al.*, 2009; Frada *et al.*, 2012; Mausz and Pohnert, 2015), blooms characteristics (Tyrrell and Merico, 2004; Neukermans and Fournier, 2018) and interactions with viruses (Frada *et al.*, 2008, 2017; Vardi *et al.*, 2012; Lehahn *et al.*, 2014).

## 2.2) Morphology and phylogenomics

*E. huxleyi* and *G. oceanica* presents similar extracellular architecture (Figure 7). The main morphological feature used to differentiate these coccolithophores rely on the coccoliths. Both *E. huxleyi* and *G. oceanica* produce heterococcoliths in their diploid stage. Formed of a radial array of complex crystal-units (Young *et al.*, 2003), the heterococcoliths are produced in

Golgi-derived calcifying vesicles and extruded to the cell surface when fully calcified (Billard and Inouye, 2004; Brownlee and Taylor, 2004). While *Emiliana* can have one or more layers of coccoliths, *Gephyrocapsa* presents only a single layer (Young *et al.*, 2003). The main distinguishing feature among both groups is the absence of the bridge in the central area of *E. huxleyi* cells (Young *et al.*, 2003) (Figure 7).

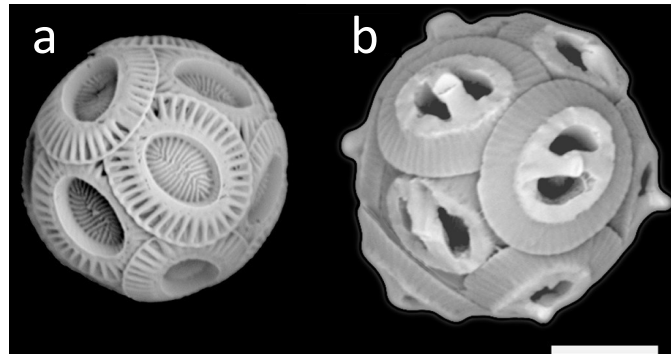


**Figure 7.** Difference in heterococcolith architecture between **a)** *Emiliana huxleyi* and **b)** *Gephyrocapsa oceanica*. *E. huxleyi* lacks the bridge in the central area which is present in *G. oceanica*. Adapted from Bendif *et al.*, (2016). Scale bar = 2 microns.

Beyond morphologic characterization, several studies have used genomic information to unveil the evolutionary history of the *Emiliana/Gephyrocapsa* species complex. The first attempts highlighted the difficulty of using genetic markers to solve such a recent diversification (Bendif *et al.*, 2014). Usual genetic markers used to detect phytoplankton species, such as the ribosomal 18S and 28S, are evolving too slowly to evidence differences between species that diversified relatively recently (Bendif *et al.*, 2014). A recent study applied phylogenomics based on full genome comparisons of different morpho-species of *Gephyrocapsa* (*G. oceanica*, *G. muelleriae*, *G. parvula*, *G. ericsonii*) and *Emiliana* including first appearance dates from the fossil record (Bendif *et al.*, 2019). This approach allowed to solve their phylogenetic relationship and showed that *E. huxleyi* is nested within the *Gephyrocapsa* genus and was thus proposed to be renamed *Gephyrocapsa huxleyi* (Bendif *et al.*, 2019). In addition, the consensus phylogeny reflected well the morphological diversity within the genus, suggesting that they belong indeed to different species (Bendif *et al.*, 2019). Fossil record suggests that these species evolved by repeated species radiation causing pulses

of coccolith size changes (Bendif *et al.*, 2019). Of note, these species appear to have formed in sympatry or parapatry, with occasional gene flow between them (Bendif *et al.*, 2019).

*E. huxleyi* presents different cellular morphotypes. Based on morphological observations it is possible to subdivide *E. huxleyi* morphotypes into two main morphogroups, A and B, (Young and Westbroek, 1991; Hagino *et al.*, 2011) (Table 1). These groups are divided by the coccoliths' profile shapes, the structure of central areas, and the degree of calcification (Young *et al.*, 2003) (Table 1).

**Table 1.** *Emiliana huxleyi* morphotypes characteristics, including coccoliths size, shield elements, central area elements, as well as geographic distribution (Young and Westbrook, 1991; Young *et al.*, 2003).

<i>Group</i>	<i>Morphotype</i>	<i>Liths medium size (<math>\mu\text{m}</math>)</i>	<i>Shield elements</i>	<i>Central area elements</i>	<i>Distribution</i>
<i>A</i>	A	3-4	Distal shield elements robust	Curved	Widespread (Paasche, 2001)
	A overcalcified	3-4	Similar to A	Closed	-
	R	< 4	Similar to type A but with heavily calcified shield elements	Grill	Southwest Pacific (Young <i>et al.</i> , 2003)
	Type Corona	3-4	Distal shield elements robust	Inner tube cycle forming discontinuous elevated crown around central area	-
<i>B</i>	B	3.5-5	Distal shield elements delicate. Proximal shield is often wider than distal shield.	Irregular laths	Primarily North Sea (Hagino <i>et al.</i> , 2011)
	B/C	3-4	Distal shield elements delicate	Similar in morphology to types B and C	Southern Ocean and Subpolar waters (Patil <i>et al.</i> , 2017)
	C	2.5-3.5	Distal shield elements delicate	Open or covered by thin plate	Southern Ocean and Subpolar waters (Patil <i>et al.</i> , 2017)
	O	Varied size	Distal shield elements delicate	Open central area	Northern North Pacific and Southern ocean (Hagino <i>et al.</i> , 2011)

The group A is formed by the typical A morphotype (Young and Westbrook, 1991), besides the morphotype A-overcalcified (Young *et al.*, 2003), the morphotype R (Young *et al.*, 2003), and the corona type (Okada and McIntyre, 1977) (Figure 7). The group B is formed by the morphotype B (Young and Westbrook, 1991), B-C (Young *et al.*, 2003), C (Young and Westbrook, 1991) and the type O (Hagino *et al.*, 2011) (Figure 8).

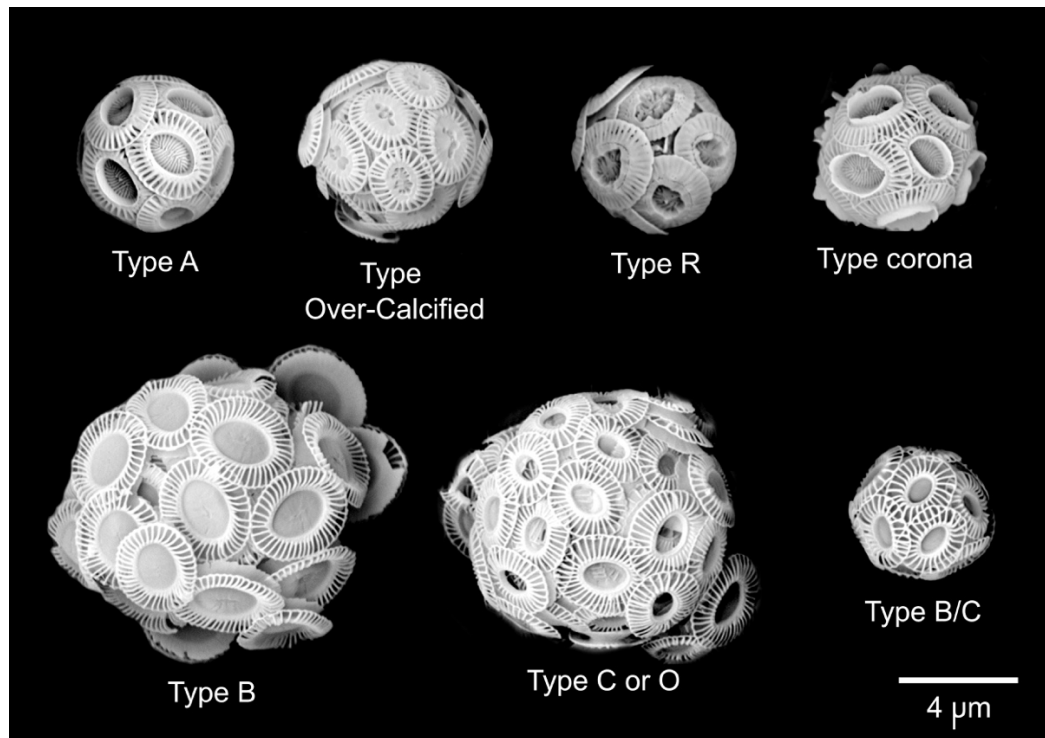


**Figure 8.** Main morphotypes described in *Emiliana huxleyi*. The classification is based on morphometric characteristics of the coccoliths and structural features of the central area (Table 1). Courtesy of El Mahdi Bendif.

The objective here is not to provide a detailed characterization of *Emiliana* morphotypes but rather point out to the morphological diversity inside the taxa. These different morphotypes display biogeographical patterns across the global ocean and thus reflect different niche adaptations. Furthermore, recent investigation evidenced that *Emiliana* morphotypes isolated from different oceanic regions reflect intraspecific differentiation (Figure 9) (Bendif *et al.*, in prep). These differences were evidenced by phylogenomic analysis based on fragments (10,000 bp) of 100 random genes extracted from full *Emiliana* isolates genomes. Results showed that morphological groups A and B represent two different species (Table 1 and Figure 9a). Within group A, two species were identified (A1 and A2). Clades included in A1 group reflect an environmental gradient from low latitudes (A1a - found mainly in Mediterranean Sea

and English Channel) to high latitudes (A1d - Arctic strains) (Figure 9a and b). The sub-clades also represent the morphotypes differentiation. Clade A1a is the classic A morphotype, A1b represents the morphotypes overcalcified A and R and A1c is a hybrid between A1b and A1d (Figure 9a).

Species B incorporates all the morphotypes mentioned for group B (Table 1 and Figure 9a). The traditional morphotype B is common in the North East Atlantic, more specifically in the seas surrounding the United Kingdom (Hagino *et al.*, 2011) (Figure 9b). Morphotypes B/C and C can be found dominating samples from the Polar frontal zone and Indian sector of the Southern Ocean (Patil *et al.*, 2017). Their dominance seems to be associated with high nutrient concentrations and low temperature regions (Patil *et al.*, 2017). More specifically, morphotype C has also been reported from temperate surface waters and lower photic zones of stratified tropical waters and appear to change its depth habitat depending on the levels of stratification, temperature and nutrients (Hagino *et al.*, 2011). Morphotype O is extensively distributed in the Southern Ocean and is a dominant morphotype in the Northern North Pacific (Hagino *et al.*, 2011). In addition, morphotype O seems rare or absent in the Pacific tropical surface waters (Hagino *et al.*, 2011).

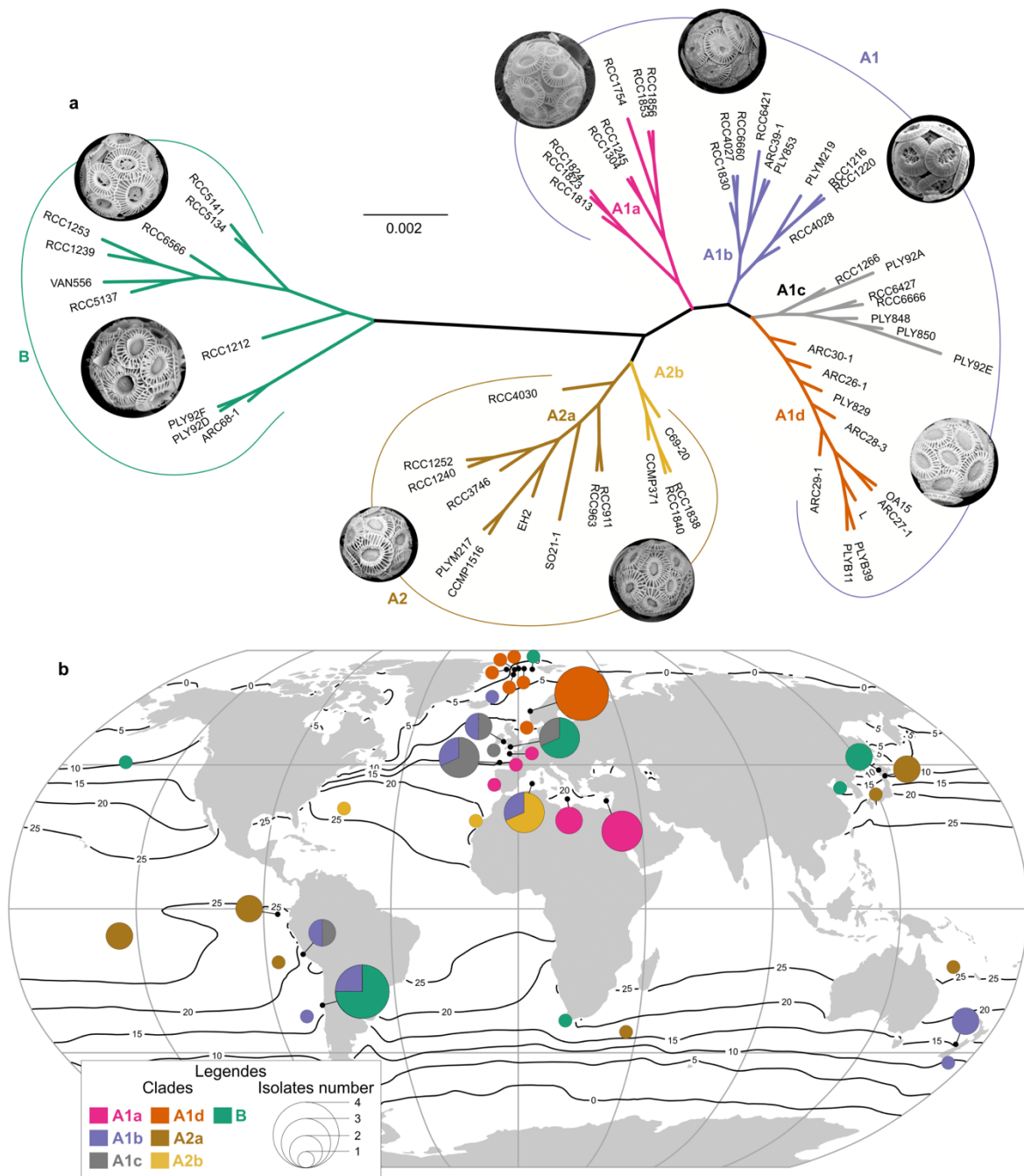


**Figure 9.** Phylogeography of *G. huxleyi* populations (Bendif *et al* in prep). **a.** Phylogenetic tree of 61 isolates based on the concatenation of 1,000 supergenes (10 kbp) randomly selected, forming a matrix of 10 Mbp. The delineation of species A1, A2 and B is congruent with a principal component analysis (PCA) based on wide-genomic single nucleotide polymorphism (~ 2.6 million snps), genetic structure inferred from a discriminant analysis in principal component (DAPC) and coalescent phylogenetic reconstruction. Sub-clades correspond to a mixture of geographical and morphotype delineation. **b.** Biogeography of phylogenetic groups. black continuous lines represent isotherms (Annual SST; Ocean Global Database).

### 2.3) Life cycle

*Emiliana huxleyi* presents a haplodiplontic and heteromorphic life cycle dominated by the coccolith-bearing non-motile diploid phase (Figure 10) (Green *et al.*, 1996). The coccolith bearing phase alternates with a diploid non-calcifying non-motile phase (naked cells) and a motile haploid flagellated phase where the cell is covered by organic scales (Green *et al.*, 1996). These three forms are capable of independent mitotic division producing populations that likely interconnect through sex and meiosis. However, sexual reproduction has never been observed in *E. huxleyi* (Frada *et al.*, 2017). In addition, the factors triggering meiosis division are still intriguing (Frada *et al.*, 2012). Experimental and bloom surveys revealed that meiosis may be induced at the end of exponential and stationary phases as a resistance response to viral infection, a mechanism coined the “Cheshire Cat” (Frada *et al.*, 2008, 2012). In the Cheshire Cat, the haploid cells are not recognized by the viruses and thus are resistant to infection (Frada *et al.*, 2008). This mechanism releases the host from short-term pathogen pressure and might select for a biphasic life-cycle strategy over evolutionary time (Frada *et al.*, 2008). Together with haploid flagellated cells, the naked diploid cells also increase in abundance at the end of blooms (Frada *et al.*, 2012). It has been hypothesized that this increase could be a result of cell-cell signaling among *E. huxleyi* cells mediated by IAA (Labeeuw *et al.*, 2016). Culture experiments showed that calcifying cells are able to produce IAA while the naked cells cannot produce but are sensible to variable concentrations of it, showing changes in growth rates depending on the concentration (Labeeuw *et al.*, 2016). While susceptible to viral infection, these naked cells appear to be resistant against the pathogenic bacteria *Ruegeria* R11 (Mayers *et al.*, 2016). Together, the complex morphogenetic strategy of *E. huxleyi* could guarantee its resistance to different viral and bacterial pathogens and maintain its bloom dynamics over time.

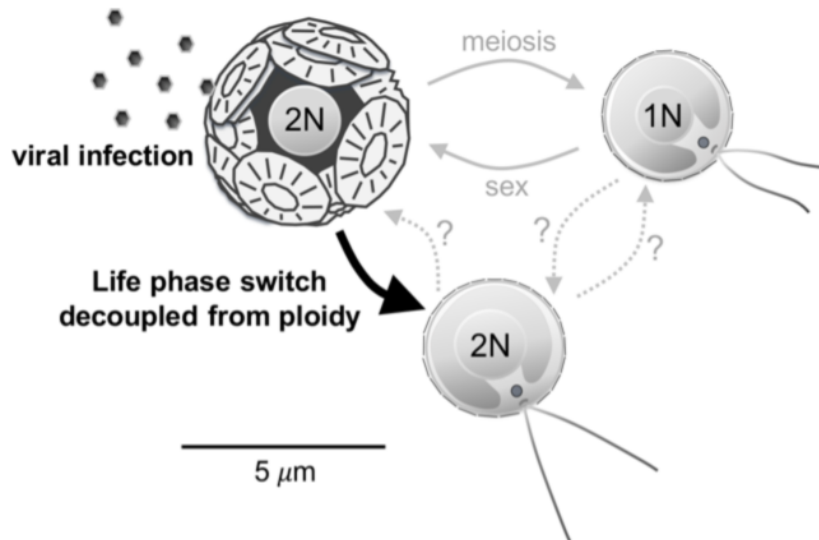


**Figure 10.** Schematic representation of the ‘Cheshire Cat’ mechanism in *E. huxleyi* in response to viral infection. As currently described, the haplodiplontic life cycle of *E. huxleyi* comprises a calcified diploid and noncalcified scale-bearing biflagellate haploid stage that is resistant to specific viruses (EhV). Both diploid and haploid cells likely interconnect through meiosis and syngamy. In a new study, the authors show that in response to infection by EhV, *E. huxleyi* can produce diploid biflagellate and scale-bearing cells that are resistant to infection as indicated by the black arrow. This mechanism seems to be decoupled from the regular sexual cycle and to enable *E. huxleyi* cells to rapidly respond to and escape EhV infection. Figure and legend (adapted) from Frada *et al.*, (2017).

Recently, two new types of cells have been observed in response to viral infection, adding more complexity to *E. huxleyi* life cycle (Frada *et al.*, 2017). The first, produced by coccolith bearing diploid cells, is diploid, biflagellate and covered by organic scales (Figure 9) (Frada *et al.*, 2017). This cellular type was called ‘decoupled’, because it characterizes a morphological switch from diploid coccolith bearing cell to a diploid scale-bearing cell (similar to haploid cells) as a response to escape to viral infection (Frada *et al.*, 2017). Contrary to the haploid cells, the decoupled has not experienced meiosis (Frada *et al.*, 2017). The other type of cells is produced by naked *E. huxleyi* strain and is also diploid and covered by organic scales, however it does not present flagella (Frada *et al.*, 2017). Both new types of cells have lower growth rates compared to their parent strains however they are both resistant to virus and increase in abundance during viral infection (Frada *et al.*, 2017). Although the fate of these

cells is yet not known it is possible that they revert back to the calcified state or undergo meiosis to produce the haploid cells (Frada *et al.*, 2017).

The differences among diploid and haploid cells are not restricted to the cellular architecture but also at the transcript level. Transcriptomes of diploid and haploid cells demonstrated that diploid cells present a richness of transcripts 20% higher than the haploid ones, and just 50% of transcripts were estimated to be shared between both stages (Von Dassow *et al.*, 2009). This suggests that haploid flagellated cells have more streamlined functions in order to adapt to specific niches, while diploid non-motile cells are more versatile being able to explore a wide variety of productive environments (Von Dassow *et al.*, 2009). The major functional categories distinguishing haploid cells were signal transduction and motility genes (Von Dassow *et al.*, 2009). In addition, both life stages differ also in the metabolite production (Mausz and Pohnert, 2015). The main differences are related to the primary metabolites (such as isoleucine, xylose, citric acid, fructose and others) which were enriched in haploid cells (Mausz and Pohnert, 2015).

### **2.4) Interactions with bacteria**

Many characteristics presented above make *E. huxleyi* an interesting model to study phytoplankton-bacteria interactions. Their close phylogenetic relationship with *G. oceanica*, together with their morpho-genomic variants and their different life-cycle stages, allow investigation of both the inter- and intra-specific specificity of the associated bacterial community. In addition, their ecological relevance as primary producers, calcifiers, and main actors in the sulfur cycle, call attention to the possible large-scale impacts that these interactions might have on ocean biogeochemistry. However, the state of the art regarding the bacterial diversity associated with coccolithophore species and the patterns and mechanisms of interactions between coccolithophores and bacteria is much less complete than for other phytoplankton groups such as diatoms (Amin *et al.*, 2012).

The first gap concerns the bacterial diversity associated with these microalgae in cultures and in environmental samples. Two studies have investigated the associations between *E. huxleyi* and bacteria in natural environments (Gonzalez *et al.*, 2000; Zubkov *et al.*, 2001). An investigation of an algal bloom with dominance of *E. huxleyi* cells in the North Atlantic using different approaches (16S rRNA clone libraries, group-specific oligonucleotide probe hybridizations, and terminal restriction fragment length poly-morphism fingerprinting) found

significant contribution of Roseobacter clade members to the bacterial community composition which accounted for 13% of the clones (Gonzalez *et al.*, 2000). Other abundant groups were SAR86 (24%) and SAR11 (11%) phylotypes (Gonzalez *et al.*, 2000). The abundance of *Roseobacter* genus members associated with *E. huxleyi* bloom was also revealed in the North Sea, using a Lagrangian sampling approach (Zubkov *et al.*, 2001). In this study, *Roseobacter*, accounted for 24% of bacterial abundance and more than 50% of the total prokaryotic biomass (Zubkov *et al.*, 2001). When investigated in cultures, the association between coccolithophores (two cultures of *Coccolithus pelagicus f. braarudii* and three of *E. huxleyi*) and bacteria revealed the presence of five phyla: Proteobacteria, Actinobacteria, Acidobacteria, Bacteroidetes and Planctomycetes (Green *et al.*, 2015). Alphaproteobacteria (average 53% of the richness of isolates, mainly from Roseobacter clade), Gammaproteobacteria (average 21%) and Bacteroidetes (average 17%) were present in all cultures (Figure 3). Two genera, *Marinobacter* and *Marivita*, were observed in all coccolithophores cultures which may represent a specific interdependence of bacteria and microalgae (Green *et al.*, 2015). Other groups such as *Acidobacteria*, *Schlegelella*, and *Thermomonas* were reported for the first time associated with microalgal cultures (Green *et al.*, 2015). The acidobacterial strain was closely related to a marine sponge isolate, while *Schlegelella* and *Thermomonas* were observed in marine springs, suggesting that their associations with coccolithophores may be related to their calcification capacity (Green *et al.*, 2015).

Furthermore, the genetic and metabolic features underlying positive *E. huxleyi*-bacteria interactions are poorly known. Co-culture experiments revealed *E. huxleyi*-bacteria interactions that are ultimately pathogenic (Seyedsayamdost, Case, *et al.*, 2011; Harvey *et al.*, 2016; Labeeuw *et al.*, 2016; Mayers *et al.*, 2016; Segev, Wyche, *et al.*, 2016; Barak-Gavish *et al.*, 2018; Bramucci *et al.*, 2018). Although some interactions start as mutualistic, their nature can change depending on the signals released by *E. huxleyi* cells (Seyedsayamdost *et al.*, 2011). Two important released bacterial molecules have been identified with potential to kill *E. huxleyi* cells: roseobactin and IAA. Roseobactin are potent algicidal compounds produced by Roseobacter clade members that are toxic to the algae in nM to  $\mu$ M concentrations (Seyedsayamdost *et al.*, 2011). The role of roseobactin on *E. huxleyi*-bacteria interactions was described for two roseobacters: *Phaeobacter gallaeciensis* and *Phaeobacter inhibens* (Seyedsayamdost, Case, *et al.*, 2011; Seyedsayamdost *et al.*, 2014). These interactions are described in two phases. In a first phase young *E. huxleyi* cells are favored by bacterial tropodithetic acid (TDA), which protects against pathogenic bacteria. In a second phase,

roseobactin production is induced by senescence signals (p-coumaric acid - pCa) released by *E. huxleyi* cells combined with a quorum sensing molecule N-acyl homoserine lactone signal (Seyedsayamdost, Carr, *et al.*, 2011; Seyedsayamdost, Case, *et al.*, 2011; Seyedsayamdost *et al.*, 2014; Wang *et al.*, 2016). Interestingly, a common set of bacterial genes is necessary for the production of antibiotics that protect *E. huxleyi* during the mutualistic phase, and for the production of roseobactin during the pathogenic phase. This allows a fast change from mutualism to parasitism, since the biosynthetic pathway is already active (Wang *et al.*, 2016).

Interactions between *E. huxleyi* and *P. inhibens* can also be controlled by IAA produced by the bacterium. This phytohormone promotes algal growth at low concentrations but is harmful when it accumulates in the culture medium, inducing *E. huxleyi* population decline (Segev, Wyche, *et al.*, 2016). This strategy seems to ensure nutrient supply for the bacterium by promoting the algal growth (Segev *et al.*, 2016). When the host is killed, bacteria utilize the least amount of nutrients released from dead cells before swimming away to attach to younger host cells (Segev *et al.*, 2016). Other chemical compounds involved in *E. huxleyi*-bacteria negative interactions are 2-heptyl-4-quinolone (a quorum sensing molecule produced by bacteria) that reduce *E. huxleyi* growth (Harvey *et al.*, 2016) and DMSP that modulates *Sulfitobacter* D7 virulence against *E. huxleyi* (Barak-Gravish *et al.*, 2018).

The virulence of bacteria against *E. huxleyi* can also be controlled by temperature and strain-specific, as observed for the *Ruegeria* sp. R11 (Mayers *et al.*, 2016). *E. huxleyi* cultures were shown to bleach at 25°C while unaffected at 18°C (Mayers *et al.*, 2016). In addition, while the diploid coccolith bearing cells and haploid flagellate cells were susceptible to R11 infection, the non-calcifying strain showed resistance (Mayers *et al.*, 2016). This change in susceptibility among strains could be related to the cell composition among these strains (*i.e.*, lack of coccolith and organic scales on naked strain, which may change the sensitivity to pathogens) (Mayers *et al.*, 2016). Another possible reason pointed out by the authors is a geographic specificity of R11 (Mayers *et al.*, 2016). While the susceptible strains were isolated from the same geographic region as R11 (Tasman Sea), the resistant strain was isolated from Equator (Mayers *et al.*, 2016). The specific virulence of R11 brings the question whether beneficial bacteria also present strain or life stages specificity when associated to *E. huxleyi* and/or whether they are related to the geographic origin of the host strains.

## Main PhD objectives

Altogether, the relevance of phytoplankton-bacteria interactions, the global abundance and key ecological role of cosmopolitan coccolithophores and the recognized gap regarding their associated bacterial diversity motivated the construction of this thesis.

The main goal of my thesis was to investigate the microbiome diversity associated with coccolithophores (mainly *E. huxleyi*) in cultures and to explore the mechanisms of microbiome selection in the phycosphere.

More specifically, in the first chapter, I aimed to identify how the inter- and intra-specific specificities in the *Emiliana/Gephyrocapsa* species complex would be reflected in the diversity of the microbiomes. Moreover, I also aimed to identify the main drivers of microbiome diversity in cultures. The results of this investigation are incorporated in the **Chapter 1** entitled “The microbiome of the cosmopolitan coccolithophore *Emiliana huxleyi*”.

The second specific goal was to investigate the drivers of microbiome diversity in different phytoplankton cultures that were isolated from the same seawater samples. This work is entitled “Microbiome assembly in phytoplankton cultures is partially driven by deterministic processes” and composes the **Chapter 2** of this thesis.

The final objective was to investigate how bacteria from different inocula are selected by an axenic *E. huxleyi* strain and the compositional changes at short and long-time scales. This work is detailed in the **Chapter 3** with the title “Microbiome assembly in axenic *Emiliana huxleyi* cultures is influenced by the source community composition and is resilient to disturbance”.

The specific objectives and motivation underlying each study will be detailed in the outline before each chapter.



---

# CHAPTER 1

---



# Chapter 1

In this first chapter I report a high-resolution investigation of the microbiomes associated with the coccolithophore *Emiliana huxleyi* and its sister species *Gephyrocapsa oceanica*, for which a large diversity of isolates is available in culture collections. I have tried to answer fundamental questions regarding the diversity, drivers, and short-term stability of the *E. huxleyi*/*G. oceanica* microbiomes in cultures. In total 58 *E. huxleyi* and 15 *G. oceanica* cultures were selected with the main objective to test whether their microbiome diversity was driven by inter-species specificities, ocean origin of isolation, and/or age of the cultures. The *E. huxleyi* isolates selected which contained different morphotypes, that displayed different levels of calcification and niche adaptations, also allowed us to investigate microbiome patterns from inter- to intra-specific levels. The stability of the community composition was tested by sampling the microbiomes over three consecutive serial dilution transfers. We expected to find microbiomes with stable composition over time and differences related to biogeographical patterns and/or host specificities. We also hypothesized that the different levels of calcification in *E. huxleyi* morphospecies could have an impact on the diversity of the microbiomes by changing the pH of the medium.

To decipher the specificities of coccolithophore microbiomes I further compared our data to that from published datasets for cyanobacteria, diatoms and dinoflagellates microbiomes using a home-made standard bioinformatic pipeline. Finally, to expand our knowledge on these associations, I investigated the abundance and distribution of the most abundant coccolithophore-associated bacterial taxa in the datasets from the circum-global *Tara* Oceans and *Malaspina* expeditions.

This chapter resulted in an unprecedented catalogue of bacterial diversity associated with *E. huxleyi* and *G. oceanica* in cultures providing valuable knowledge for further studies. Additionally, this work involved careful selection of strains and morphological identification of *E. huxleyi* by scanning electron microscopy, in collaboration with the Drs. Ian Probert and El Mahdi Bendif. Part of the identification work will be included in a publication entitled “Coccolith morphometrics partially delineate morphotypes in worldwide isolates of *Gephyrocapsa huxleyi*” (Annex 1).



## The microbiome of the cosmopolitan coccolithophore *Emiliana huxleyi*

Mariana Câmara dos Reis<sup>1</sup>, Sarah Romac<sup>1</sup>, Ewen Corre<sup>1</sup>, Erwan Delage<sup>2</sup>, Isabel Sanz Sáez<sup>3</sup>, Silvia G. Acinas<sup>3</sup>, Samuel Chaffron<sup>2</sup>, Nicolas Henry<sup>1,4</sup>, Colomán de Vargas<sup>1,4</sup>, Christian Jeanthon<sup>1,4</sup>

<sup>1</sup> Sorbonne Université & Centre National de la Recherche Scientifique, UMR7144, Adaptation et Diversité en Milieu Marin, Station Biologique de Roscoff, France

<sup>2</sup> Université de Nantes & Centre National de la Recherche Scientifique, UMR6004, LS2N - Laboratoire des Sciences du Numérique de Nantes, France

<sup>3</sup> Department of Marine Biology and Oceanography, Institut de Ciències del Mar (CSIC), Barcelona, Spain

<sup>4</sup> Research Federation for the study of Global Ocean Systems Ecology and Evolution, FR2022/Tara GOSEE, Paris, France

### Abstract

Interactions between phytoplankton and bacteria are fundamental in aquatic ecosystems and emerging evidence indicates that these relationships are often governed by microscale interactions occurring within the phycosphere. Coccolithophores are one of the main phytoplankton groups in modern oceans and *Emiliana huxleyi*, which is present in most oceanic biomes, plays an important role in the marine carbon cycle as both primary and calcite producers. Given its biogeochemical importance, it is surprising that relatively little is known about the bacterial consortia associated with *E. huxleyi*. In this study, we characterized the microbial assemblages associated with a large collection of coccolithophore isolates obtained from different geographical locations, using amplicon sequencing of the 16S rRNA gene. Microbiome composition differed between strains, but there was significant overlap in heterotrophic bacterial community composition across the cultures. The coccolithophore strain-specific microbiomes were stable across consecutive serial dilution transfers. Observed differences in community composition were not associated with coccolithophore inter-species specificities, *E. huxleyi* cellular morphotype, time since isolation, and geographic location of origin. We found that different *Marinobacter* species that dominate coccolithophore microbiomes were responsible for the beta diversity patterns. Finally, the majority of culture associated bacteria are rare in the surface of global oceans but are substantially enriched in large planktonic size fractions and in bathypelagic layers, indicating that coccolithophore-associated copiotrophs are indeed adapted to a particle-associated mode of life in the surface ocean, and may be substantially exported to the bathypelagic environment.

## Introduction

Phytoplankton, including microalgae and cyanobacteria, are responsible for nearly half of photosynthetic carbon fixation on Earth, making them major drivers of global carbon fluxes (Longhurst *et al.*, 1995; Field *et al.*, 1998). Marine heterotrophic bacteria consume a significant fraction of phytoplankton-derived organic matter and thereby heavily influence major biogeochemical cycles (Pomeroy *et al.*, 2007; Falkowski *et al.*, 2008). Microscale interactions between phytoplankton and bacteria are therefore one of the most important interspecies relationships in the oceans and exert an ecosystem-scale influence on fundamental biological and biogeochemical processes (Cole, 1982; Azam and Malfatti, 2007; Seymour *et al.*, 2017).

Obligate relationships between phytoplankton and bacteria are known to be widespread in the marine environment (Foster *et al.*, 2006). By far the most abundant of these symbiotic associations occur in the phycosphere, *i.e.* the region immediately surrounding and influenced by phytoplankton cells (Bell and Mitchell, 1972). Phytoplankton-bacteria associations in the phycosphere are numerous, varied and often complex (Amin *et al.*, 2012). The exchange of metabolites and info-chemicals in the phycosphere governs phytoplankton-bacteria associations, which span the spectrum of ecological relationships from cooperative to antagonistic (Amin *et al.*, 2012).

Several recent studies suggest that diverse phytoplankton taxa harbor unique prokaryotic communities in cultures which are consistently associated with the same host and across temporal scales, suggesting that associated bacteria carry out important and specific functions for the host (Sison-Mangus *et al.*, 2014; Krohn-Molt *et al.*, 2017; Behringer *et al.*, 2018; Lawson *et al.*, 2018; Sörenson *et al.*, 2019). However, although a core microbiome (*i.e.*, stable and consistent members of the microbiome) can be identified for a host species, other factors like the sampling time and location can determine variations in the composition of phytoplankton microbiomes in cultures (Ajani *et al.*, 2018).

Most of our current knowledge of the microbiomes associated with phytoplankton cultures is derived from examining diatoms (Ajani *et al.*, 2018; Behringer *et al.*, 2018), dinoflagellates (Lawson *et al.*, 2018; Shin *et al.*, 2018; Sörenson *et al.*, 2019), cyanobacteria (Zheng *et al.*, 2018; Kearney *et al.*, 2021), and green algae (Abby *et al.*, 2014; Lupette *et al.*, 2016). Remarkably, the bacterial diversity associated with one of the most important groups of marine phytoplankton, the coccolithophores, has been poorly investigated. These widespread

and abundant marine microalgae characterized by their ability to cover their cells with delicate calcite platelets, the coccoliths (Paasche, 2001), are estimated to account for more than 50% of the particulate inorganic carbon produced in the pelagic ocean each year (Taylor *et al.*, 2017). *Emiliana huxleyi* and *Gephyrocapsa oceanica* represent the most abundant extant coccolithophore morphospecies and display different geographic distribution. The ubiquitous *E. huxleyi* frequently forms extensive “milky water” blooms in high latitude ecosystems (Probert and Houdan, 2004; Tyrrell and Merico, 2004). *G. oceanica* is more restricted to tropical and subtropical waters and occasionally forms massive blooms in transitional coastal waters in the Pacific Ocean (Blackburn and Cresswell, 1993). *Gephyrocapsa* and *Emiliana* have distinguished coccolith morphology, *E. huxleyi* lacking the conjunct bridge over the central area found in *Gephyrocapsa* (Young *et al.*, 2003). Variability in the degree of calcification of *E. huxleyi* coccolith elements, their profile shapes and central area characteristics has led to the definition of two main groups A and B (Young and Westbroek, 1991) comprising intermediate (A) and heavily-calcified (A-overcalcified and R) to lightly-calcified (B, B/C, C, and O) morphotypes, respectively. Importantly, some of these morphotypes display specific physiological features and biogeographical patterns (Paasche, 2001; Hagino *et al.*, 2011; Patil *et al.*, 2017). In addition, many strains of *E. huxleyi* that have been maintained in laboratory culture for several years are only partially calcified or have lost the ability to calcify entirely (Paasche, 2001).

In spite of the biogeochemical and ecological importance of coccolithophores and the large amount of data from laboratory, mesocosm and field observations, the prokaryotic diversity associated with coccolithophores is poorly known. This is surprising given the considerable potential for addressing this question by further exploiting existing cultures of coccolithophore species currently maintained in collections around the world. The only study that investigated the microbiome of coccolithophore cultures analyzed a few strains (Green *et al.*, 2015). In this study, bacterial membership of three *E. huxleyi* and two *Coccolithus pelagicus* f. *braarudii* cultures was assessed using bacterial cultivation and cultivation-independent methods. Alphaproteobacteria and Gammaproteobacteria dominated and specific taxa, including *Marinobacter* and *Marivita*, occurred in all cultures (Green *et al.*, 2015).

In order to perform a high-resolution investigation of the microbiome diversity associated with coccolithophores in cultures, we focused on the sister taxa *Emiliana huxleyi* and *Gephyrocapsa oceanica* and selected a large set of strains isolated from the world ocean

and maintained for several years in the Roscoff Culture Collection (RCC), including different *E. huxleyi* morphotypes. Our aim was to evaluate whether the microbiome diversity was stable over time and could be related to the inter and/or intra-species specificities of their hosts, different geographic origins, and time since isolation. To further understand the specificity and ecology of *Emiliania/Gephyrocapsa* microbiomes, we then compared their bacterial composition to that of other phytoplankton cultures and examined how the most abundant associated bacteria were represented in DNA metabarcoding datasets from the global oceans.

## Materials and Methods

### Origin and growth conditions of algal cultures

The 73 non axenic coccolithophore cultures (58 *E. huxleyi* and 15 *G. oceanica* clonal strains) used in this study were obtained from the RCC (<http://roscoff-culture-collection.org/>) and from the National Institute of Environmental studies (NIES) Microbial culture collection (<https://mcc.nies.go.jp/>) (Supplementary Table 1 and Supplementary figure 1). Most of the *E. huxleyi* strains (33 strains) belonged to the morphogroup A (comprising morphotypes A, A overcalcified, or R), while 8 were part of the morphogroup B (morphotypes B and O), 16 were non-calcifying strains, and one was a haploid strain (RCC1217; haploid version of RCC1216). Upon receipt, the cultures were maintained in K/2 medium prepared with natural aged seawater collected at the SOMLIT-ASTAN monitoring site (48°46'18''N-3°58' 6''W) (Brittany, France) (Keller *et al.*, 1987; Probert, 2019). Seawater was first filtered-sterilized (0.2 µm pore size), heated at 100°C for 20 min, cooled, and enhanced to K/2 by adding the nutrients and vitamins. Then, the pH was adjusted to 8.2 and the medium was filtered-sterilized (0.1 µm) (Probert, 2019). Cultures were grown in 50 mL vented tissue culture flasks at their maintenance temperature (Supplementary Table 1) on a 12:12 light:dark cycle under a white light irradiance (Philips Master TL\_D 18W/865) of about 60 µmol photons m<sup>-2</sup> s<sup>-1</sup>. Cultures were acclimated to light, temperature and medium conditions for at least two growth cycles prior to experiments. Biological replication was achieved through time. Briefly, 200 µL of culture from each strain were transferred into a new medium (20 mL) every 2 weeks after sampling to maintain healthy cultures. Replication over time was conducted at two or three consecutive transfers yielding two or three replicates for each of the 73 strains (total n=204).

## Culture monitoring

*Fluorimetry.* Photosystem II fluorescence quantum yield ( $F_v/F_M$ ) was measured using a pulse amplitude-modulated fluorometer (Phyto-PAM II, Walz, Germany). Two mL of each culture was dark-acclimated for 20 min at room temperature prior to analysis. A 5-wavelength (440, 480, 540, 590, 625 nm) low irradiance, modulated light (1 Hz) was applied to measure the mean basal chlorophyll fluorescence ( $F_0$ ). Then, a saturating light pulse (400 ms, 8000  $\mu\text{mol photons m}^{-2} \text{s}^{-1}$ ) was applied, and the mean maximum fluorescence was measured ( $F_M$ ). The PSII quantum yield was calculated as  $F_v/F_M = (F_M - F_0)/F_M$ . Low values of PSII quantum yield result from photoinhibition or down-regulation of PSII, indicative of culture stress. Five days after transfer, the  $F_v/F_M$  ratio was measured from actively growing cultures of each strain. When  $F_v/F_M$  ratios were lower than 0.5, cultures were grown for 24 extra hours.

*Cytometry.* At each time point, 1 mL of culture was fixed using glutaraldehyde 25% (0.125% final concentration) incubated for 20 min in the dark, flash frozen in liquid nitrogen and stored at  $-80^\circ\text{C}$ . A FACSCanto flow cytometer (Becton Dickinson, San Jose, CA, USA) equipped with 488 and 633 nm lasers and standard filter setup was used to enumerate coccolithophores and bacterial cells (Marie *et al.*, 1999). To avoid attachment of coccolithophore cells to the tube wall, Polaxamer 188 solution 10% (Sigma-Aldrich) (0.1% final concentration) was first added to the thawed fixed-frozen samples (Marie *et al.*, 2014). For coccolithophores, data acquisition was triggered on the red fluorescence signal and samples diluted 5- to 10-fold were run for 1 min at medium rate ( $\sim 50 \mu\text{L}/\text{min}$ ). To quantify prokaryotes, samples were diluted 10- to 100-fold in TE (10 mM Tris, 1 mM EDTA [pH 7.5]), stained with SYBR Green-I (1/10,000, final concentration) and incubated for 15 min in the dark. The discriminator was set on green fluorescence, and the samples were analyzed as before.

## DNA extraction, 16S rRNA PCR amplification and sequencing

To examine variability in the coccolithophores microbiome across strains, 2 mL of culture from each strain was centrifuged at 2,000 g for 30 sec to reduce the microalgal load. The supernatants were transferred into new tubes containing 2  $\mu\text{L}$  of Poloxamer 188 solution 10% (Sigma-Aldrich) and centrifuged at 5,600 g for 5 min. Bacterial cell pellets were stored at  $-20^\circ\text{C}$  until DNA extraction. DNA extraction was carried out using NucleoSpin Plant II kit (Macherey Nagel) following the manufacturer protocol. To prevent protein contamination and improve bacterial cell lysis, proteinase K (25  $\mu\text{l}$  of a 20 mg/mL solution) and lysozyme (100

µl of a 20 mg/mL solution) were added to the cell lysis step, respectively. The V4-V5 variable region of the prokaryotic 16S rRNA gene was amplified by PCR, using primers (5'-CTTTCCTACACGACGCTCTTCCGATC-515F-Y) and (5'-GGAGTTCAGACGTGTGCTCTTCCGATCT-926R).

Primers 515F-Y (5'-GTGYCAGCMGCCGCGGTAA-3') and 926R (5'-CCGYCAATTYMTTTRAGTTT-3') were previously described by (Parada *et al.*, 2016). Triplicate PCR reactions (30 µL) contained 10 ng of DNA, 0.625 units of GoTaq G2 Flexi polymerase (Promega), 1X of enzyme buffer, 1.5 mM of MgCl<sub>2</sub>, 0.4 mM of each dNTPs, and 0.32 µM of each primer. Cycling conditions consisted in an initial denaturation step of 10 min at 95°C followed by 32 cycles of 95 °C for 30 s, 50 °C for 1 min, 72 °C for 1 min, and a final extension of 72 °C for 10 min. The pooled PCR products were sent for sequencing at the GeT-PlaGe platform of Genotoul (Toulouse, France). Detailed sequencing procedures are described in the Supplementary Methods.

### Sequence processing and bacterial community analyses

Sequencing reads were processed as outlined in the Supplementary Figure 2 and [https://github.com/mcamarareis/Coccolithophores\\_microbiomes](https://github.com/mcamarareis/Coccolithophores_microbiomes). Briefly, primers were removed from the raw demultiplexed reads with cutadapt (version 2.8.1) using anchored primer removal allowing errors rate of 0.1 (Martin, 2011). Read pairs without primers or shorter than 75 nt were discarded. The resultant reads were processed using DADA2 (version 1.14.0) (Callahan *et al.*, 2016) in R (version 3.6.1) (R Core Team, 2017). Reads were filtered using the function *filterAndTrim* default filtering parameters and truncation according to the quality profile of the sequences. Then, the error models were produced using the function *learnErrors*. Amplicon sequence variants (ASVs) were inferred from forward and reverse reads independently using *dada* function in pooled mode. After merging, chimeras were removed using the function *isBimeraDenovo* method pooled. The taxonomy was assigned using the Silva database v138 (Quast *et al.*, 2013) by both, IDtaxa (using confidence threshold of 50) (Murali *et al.*, 2018) and vsearch global alignment (using id threshold of 0.9) (Rognes *et al.*, 2016). The following analyzes were performed using R software version 4.0.2 in Rstudio (1.1.442) (RStudio Team, 2016; R Core Team, 2017). ASVs shorter than 366 bp and longer than 376 bp, resulting mostly from non-specific priming, were removed. In addition, ASVs assigned to chloroplasts or identified as algal mitochondrial sequences were also removed as

well as ASVs that accounted for less than 0.001% of the total number of reads (corresponding to 52 reads). Abundance filters removed 74% of the ASVs while keeping 99% of the reads.

A Bray-Curtis dissimilarity matrix was produced using relative abundance of ASVs (Bray and Curtis, 1957; Borcard *et al.*, 2011). This matrix was used to test the stability of the microbiomes over time by hierarchical cluster analysis (complete linkage method) (Borcard *et al.*, 2011; Oksanen *et al.*, 2015). The function *meandist* was used to calculate the mean Bray-Curtis dissimilarity among the microbiome samples of the same strain and between strains (Oksanen *et al.*, 2015). Then the independent microbiome replicates samples of each strain were merged for the next analysis by keeping the mean number of reads to avoid large discrepancies. In this case, only ASVs that were present in all the replicates of the same strain were kept.

A Principal Component Analysis using the Hellinger transformed data was performed to identify possible beta-diversity patterns (van den Wollenberg, 1977; Legendre and Gallagher, 2001). A heatmap was constructed using the *pheatmap* function to visualize the dominant ASVs (more than 5% of the reads in each sample) (Kolde, 2015). The clustering of the samples was performed using Euclidean distance and complete linkage method (Borcard *et al.*, 2011). Clusters formed using ASVs with more than 5% of the reads were consistent with PCA grouping. The same clusters were used to plot taxonomic diversity in the cultures. The three most abundant families were displayed at the plot while the others were merged together.

In order to investigate the possible drivers of the groups found in the PCA, a redundancy analysis (RDA) was performed using the function *rda* on the Hellinger transformed data (van den Wollenberg, 1977; Legendre and Gallagher, 2001). We first studied the effect of culture age (years since isolation) and of the place of isolation (latitude and longitude coordinates) and inter-specific differences on the composition of *E. huxleyi* and *G. oceanica* microbiomes. Then, the influence of cellular morphogroups (A, B, and non-calcifying), and culture age, place of isolation on the *E. huxleyi* microbiome composition was further tested. Statistical significance of RDA models was tested using an *anova*-like permutation test with *anova* (1,000 permutations). To test for homogeneity of multivariate dispersions among the hosts and morphogroups, the function *betadisper* was used followed by an *anova*-like permutation test as before (Oksanen *et al.*, 2015).

## **Comparative analysis of coccolithophore and other phytoplankton culture datasets**

We compared 16S rRNA sequences obtained in this study to sequences found in other phytoplankton cultures (Behringer *et al.*, 2018; Sörenson *et al.*, 2019; Kearney *et al.*, 2021). Behringer *et al.* (2018) used the V4 region of the 16S rRNA gene (primers 515F-806R) to investigate the microbiome associated to 19 isolates of two diatoms species, *Asterionellopsis glacialis* and *Nitzschia longissima*. Sörenson *et al.* (2019) on the other hand, analysed the V3-V4 region (primers 341F and 805R) of prokaryotic communities from 26 cultures of different dinoflagellate *Alexandrium* species (*A. tamarense*, *A. minutum* and *A. ostenfeldii*). Finally, Kearney *et al.* (2021) targeted the V4-V5 region (primers 515F and 926R) of heterotrophic prokaryotes associated with 74 *Prochlorococcus* and *Synechococcus* isolates. Considering the different primers and techniques used in each study, we re-processed each dataset independently using DADA2 (Callahan *et al.*, 2016). The details of the informatic steps used for each study are available in the Github repository. Taxonomy was first assigned to ASVs using `vsearch --usearch_global` (90% identity threshold) and Silva database v138 (Quast *et al.*, 2013; Rognes *et al.*, 2016). Then, ASV table of each study was pre-filtered to remove all sequences not classified as prokaryotes. The ASVs with their abundance information were then pooled together and clustered as operational taxonomic units (OTUs) at 97% similarity threshold using `vsearch --cluster_size` (Rognes *et al.*, 2016). The OTU table was produced using `vsearch --usearch_global` at 97% similarity and the flag `--otutabout`. The centroids were used to assign taxonomy as before mentioned (Quast *et al.*, 2013). We performed a second filtering to remove remaining sequences not classified or classified as chloroplasts and mitochondria. In addition, OTUs with less than 0.001% of the total of reads were filtered out. The OTU table was rarefied to the minimum number of reads (2,015) and used to produce the Venn diagram with the function `venn` from the package `gplots` (Warnes *et al.*, 2016).

## **Abundance and distribution of dominant coccolithophore associated ASVs in global ocean DNA metabarcoding datasets**

The 10 most abundant ASVs found in this study were compared to ASVs and denoised zOTUs (zero-radius OTUs, *i.e.* OTUs defined at 100% sequence similarity) (Edgar, 2010) obtained from high-throughput sequencing of the 16S rRNA sequences retrieved from the *Tara Oceans* (*Tara Oceans* 2009-2012 and *Tara Oceans* Polar Circle 2013) and *Malaspina* Expeditions datasets, respectively. Sample collection which covered surface, DCM and mesopelagic layers (*Tara Oceans*), and surface to bathypelagic layers (*Malaspina*), DNA

extraction, sequence processing and data treatment are detailed in Supplementary Methods. For the *Tara* Oceans dataset, raw reads were processed using DADA2 (Callahan *et al.*, 2016). Once the final ASV table was obtained, relative abundance of each ASV was calculated by station, depth and plankton size fraction. For the *Malaspina* dataset, reads were processed to obtain a zOTUs (100% identity OTUs) table using USEARCH v10.0.240 (Edgar, 2010; Sanz-Sáez *et al.*, 2020). Like for *Tara* Oceans data, we calculated the relative abundance of each zOTU by station and depth. To find zOTUs and *Tara* Oceans ASVs corresponding to the ASVs from cultures, we used `vsearch --usearch_global` method and selected zOTU and ASVs with > 97.3 and 100% similarity to the culture ASVs, respectively (Rognes *et al.*, 2016). Finally, the maps and barplots were produced for both datasets using `ggplot2` (Wickham, 2016).

### Phylogenetic placement

For phylogenetic placement *Marinobacter* reference sequences and outgroups of about 1,382 bp were aligned in MAFFT version 7.453 (Katoh and Standley, 2013). Maximum-likelihood phylogenetic trees were calculated using RAxML 8.2.12 (Stamatakis, 2014) with GTRCAT evolution model and 1,000 bootstraps. ASVs sequences were aligned to the reference tree using PaPara software v2 (Berger and Stamatakis, 2012). Phylogenetic placement was produced using EPA-ng (Barbera *et al.*, 2019). Accumulation analysis was performed with GAPPA using a 95% threshold (Czech *et al.*, 2020). The Interactive Tree of Life (iTOL) tool was used for the display and visualization of the trees (Letunic and Bork, 2019).

## Results

### Coccolithophore collection and microbiome stability across time

The 58 *E. huxleyi* and 15 *G. oceanica* clonal strains used in this study (Supplementary Table 1) were derived from water samples collected as part of research cruises in many oceanic and coastal regions of the Pacific, Atlantic, Indian and Arctic Oceans, and the Mediterranean Sea (Supplementary figure 1). The coccolithophores were isolated between 1959 and 2015 and co-cultivated with their associated heterotrophic prokaryotic communities through roughly monthly serial transfer since then. Because of the long-term co-cultivation, it can be assumed that presumably well-adapted microbial communities have been established under these conditions.

To test microbiome stability over culturing time, we first monitored bacterial and microalgal cell populations along 2 to 3 consecutive culture transfers. In the cultures, bacterial cells were on average 111 times more abundant than coccolithophores ( $2.07 \times 10^7 \pm 1.23 \times 10^7$  cells.ml<sup>-1</sup> versus  $2.87 \times 10^5 \pm 2.54 \times 10^5$  cells.ml<sup>-1</sup>) (Supplementary Figures 3 and 4), which is consistent with bacterial communities commonly reported from other microalgal cultures (Amin *et al.*, 2015). Mid to late exponential phase *E. huxleyi* cultures had average fluorescence-based maximum quantum yields for PSII ( $F_v/F_m$ ) of  $0.57 \pm 0.03$  (Supplementary Figure 5) indicating that microbiomes were collected from healthy cultures (Loebl *et al.*, 2010).

A total of 204 samples (3 replicates for 58 strains, and 2 of 3 replicates for 15 strains yielded enough sequences) were analyzed for their prokaryotic community composition. After filtering, 430 ASVs corresponding to 5,158,560 reads were obtained across all the replicate samples and were used to compare them. Although a few exceptions were noticed, clustering analysis (Supplementary Figure 6) and community dissimilarities measured between biological replicates (average Bray-Curtis of 0.12; Supplementary Figure 7) and between coccolithophore strains (0.86) indicated that microbiomes of culture replicates were highly similar, suggesting that the composition of prokaryotic communities associated with *E. huxleyi* and *G. oceanica* cultures is stable across time while differing between coccolithophore strains. A substantial drift was however observed between the microbiomes of the same strain (RCC1844) maintained alive by subculturing and regrown after cryopreservation.

### **Composition and structure of the bacterial communities associated to coccolithophore cultures**

A total of 418 ASVs (1,822,779 reads) were kept after merging replicates of each strain. Prokaryotic reads from *E. huxleyi* and *G. oceanica* cultures were dominated by Proteobacteria (95.7%) with Alpha- and Gammaproteobacteria (21.2% and 74.5%, respectively) as the most abundant classes within the dataset (Figure 1). Among the other phyla, Rhodothermaeota (1.8%) (Munoz *et al.*, 2016) were frequently found and exceptionally dominated (RC3962) while Bdellovibrionata and Actinobacteriota represented each less than 0.4%. Noticeably, sequences belonging to the two later phyla formed however considerable proportions (> 20%) in certain strains (*i.e.* RCC3711 and RCC3985). Only a few reads (0.02% of total sequences) could not be classified at the phylum level. Marinobacteraceae (61% of total sequences) predominated in 71% of the cultures whereas Rhodobacteraceae (19% of total sequences), Alteromonadaceae (8% of total sequences), and Balneolaceae (2% of total sequences) were

also found as prevalent families. Less than 1% of total sequences could not be classified at the family level.

The widespread dominance of Gammaproteobacteria was due to the prevalence of the genus *Marinobacter* (present in all coccolithophore cultures) that also represented the top four most abundant ASVs (ASV2 to 5). In total, we identified 28 ASVs (61% of total sequences) assigned to *Marinobacter*, most of them displaying a prevalence higher than 20%. The most abundant *Marinobacter*-related ASV, ASV2, was found in all cultures and accounted for 28% of the total sequences. ASV3 (19% of total sequences) occurred in all cultures but one, while less prevalent ASV4 and ASV5 (9.92% of the total sequences) were present in 47% and 79% of the cultures, respectively (Supplementary figure 8). Phylogenetic placement of the *Marinobacter* ASVs and 16S rRNA similarities revealed that they represent different species (Supplementary Figure 9). The affiliation of ASV3 and 5 other ASVs within *M. salarius* was highly supported (95% likelihood weight ratio). The short 16S rRNA region we sequenced was not resolute enough (Supplementary Figure 9) to confidently place the ASVs. However, since the relatedness between *Marinobacter* ASVs was in the range of the 16S rRNA similarities that separate validated species of this genus, we assume that they may represent different species. Other abundant genera (>1% of the sequences) included several members of the family Rhodobacteraceae such as an uncultured bacterium (ASV6), *Marivita* (ASV8 and ASV9), *Shimia* (ASV10), *Pseudophaeobacter* (ASV13) and members of the Alteromonadaceae (*Alteromonas*-ASV7) and the Balneolaceae (*Balneola*-ASV11) (Supplementary figure 8). Other prevalent ASVs (> 20% of the samples) belonged to the genera *Hoflea*, *Hyphomonas*, *Pseudomonas*, *Roseovarius*, *Janthinobacterium*, and unclassified Rhodobacteraceae. Among them, those affiliated with *Pseudomonas* and with *Janthinobacterium* exhibited a very high prevalence (99 and 94% of the samples, respectively).

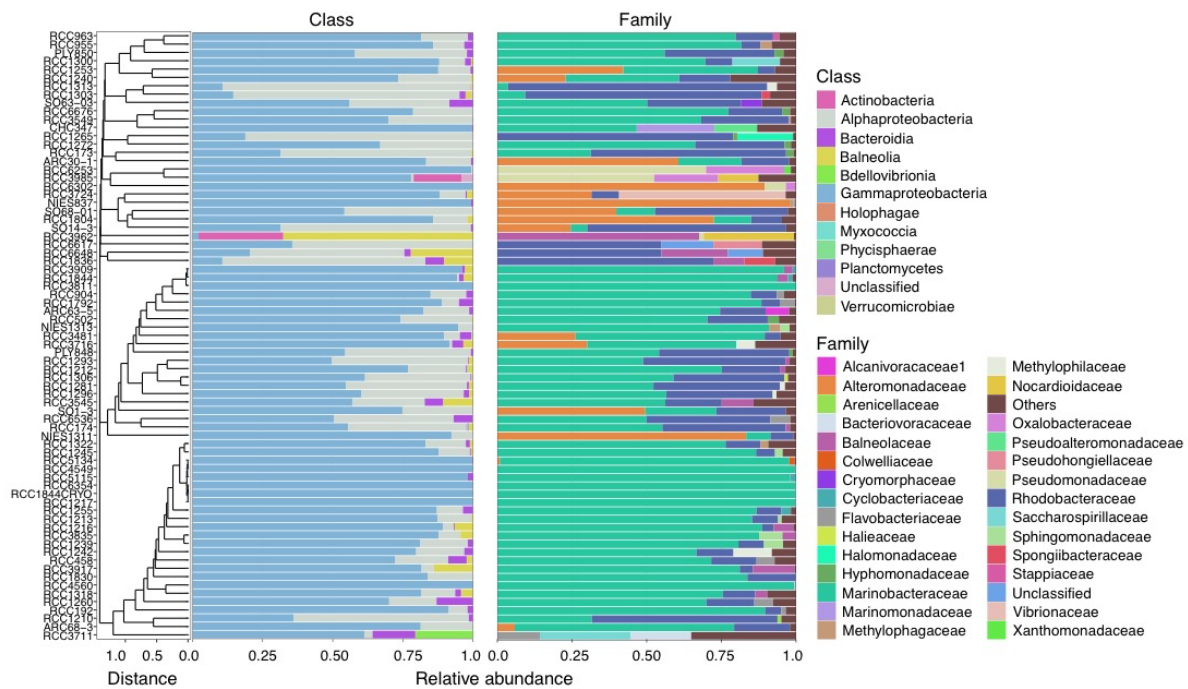


**Figure 1.** Composition of the coccolithophore microbiomes as defined by class and family of ASVs. The bacterial communities are grouped by hierarchical clustering of the ASVs accounting for more than 5% of the reads in each culture. Only the three most abundant families are represented to improve visualization.

A Principal Component Analysis (PCA) of the microbiome composition at the ASV level separated the coccolithophore cultures into 3 main groups (Figure 2), one formed by cultures where *Marinobacter* ASV2 dominated, a second including cultures dominated by *Marinobacter* ASV3, and a third dominated by other ASVs including ASV4, ASV5 and ASV7. A substantial part (36.8%) of the variability in bacterial community composition was explained by differences in the relative abundance of the dominant ASVs (Figure 2A and B). No significant correlations were found between patterns of bacterial community composition and the coccolithophore taxa (*E. huxleyi* and *G. oceanica*), the different *E. huxleyi* morphotypes, the age of the cultures, and the place of their isolation ( $p > 0.05$ , data not shown).

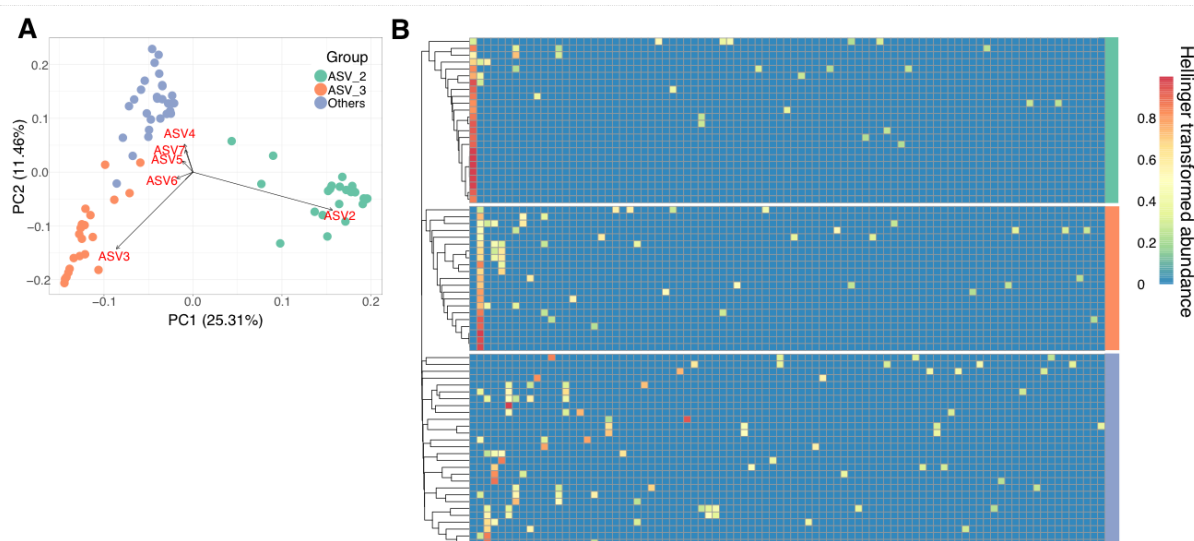


**Figure 2.** A) Principal Component Analysis (PCA) of the microbiome composition including all ASVs. B) Heatmap including the ASVs with more than 5% of the reads in each culture. Colors on the right side of the clusters correspond to the groups formed at the PCA.

### Comparison of coccolithophore microbiome composition with that of other phytoplankton

To assess the similarity of other phytoplankton-associated microbiomes to that of coccolithophores, we combined our dataset with the data from published diatom (Behringer *et al.*, 2018), *Alexandrium* (Sörenson *et al.*, 2019) and *Synechococcus* and *Prochlorococcus*-associated prokaryotic communities (Kearney *et al.*, 2021) (Figure 5). 16S rDNA ASVs were clustered at 97% identity (hereafter, OTUs) due to differences in the generation of the amplicon data in the published studies (see Material and Methods).

Heterotrophic communities in coccolithophore cultures shared about half of their OTUs with those found in cyanobacterial (51%) and *Alexandrium* spp. cultures (40%) (Figure 3), but only 10% (18/172) with those obtained from diatoms. The four groups of phytoplankton shared seven OTUs. The most prevalent (43%) among the total phytoplankton samples was *Alteromonas*, a ubiquitous genus from our study. Other shared OTUs, that comprised alphaproteobacterial genera (*Hyphomonas*, *Roseivirga*, SAR 11 clade 1, and *Nautella*), *Pseudohongiella*, and an unclassified Flavobacteriaceae were not prevalent in coccolithophores. The two most prevalent OTUs that included the two most abundant ASVs

(ASV2 and ASV3) from our study, were shared with other phytoplankton. Interestingly, the OTU that contained *Marinobacter* ASV2 was shared with cyanobacteria only and was present in 53% of cyanobacterial strains (39/74). Other prevalent OTUs shared with cyanobacteria belonged to *Thalassobius* (38/74), *Alcanivorax* (44/74) and to a member of the Rhodobacteraceae (19/74). The OTU that contained ASV3, was shared with cyanobacteria and also *Alexandrium* 49/100 samples. Other coccolithophores OTUs shared with both microalgae were *Hyphomonas*, *Thalassospira*, *Methylophaga*, and *Balneola*. OTUs specific to coccolithophores were mainly members of Gammaproteobacteria (52%, 24/46) and Bacteroidia (28%, 13/46) classes. The most prevalent belong to the genera *Pseudomonas* and *Janthinobacterium* and were found in 81% and 69% of the coccolithophore strains, respectively. One OTU belonging to *Nioella* genus (Rhodobacteraceae) was found in 16 strains and a *Polycyclovorans* (Gutierrez *et al.*, 2013) was present in 10 strains. Other OTUs specific to coccolithophores belong to Cyclobacteriaceae, Flavobacteriaceae, Rhodobacteraceae, Alteromonadaceae, and Cryomorphaceae families.

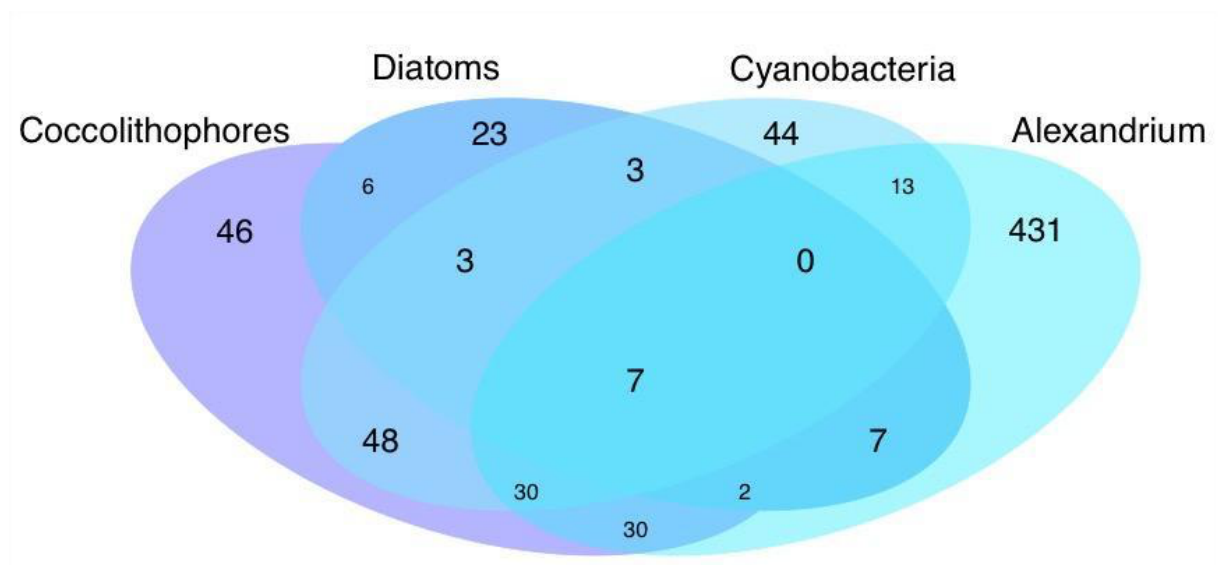


**Figure 3.** Venn diagram showing the number of OTUs shared by coccolithophore microbiomes and that of diatoms (Behringer *et al.*, 2018), *Alexandrium* sp. (Sörenson *et al.*, 2019), and cyanobacteria (Kearney *et al.*, 2021).

## **Relative abundance and distribution of dominant coccolithophore-associated bacteria in the world ocean**

To determine the representation of dominant ASVs from coccolithophore cultures in the global oceans, we used the *Tara Oceans* and *Malaspina* 16S rRNA metabarcoding datasets, which together span 888 samples (723 *Tara Oceans* and 165 *Malaspina*) at multiple depths in locations throughout the globe (see Materials and Methods for details). We found perfect matches of our ASVs in the *Tara Oceans* dataset, while in the *Malaspina* dataset we considered only zOTUs with > 97.3% identity with our ASVs. ASV2 and ASV3, our two most abundant ASVs in cultures, were widely distributed across stations of both global expeditions but not abundant (Figure 4). Interestingly, they were enriched in the larger size fractions (> 3  $\mu\text{m}$ ). Although their relative abundance differed in the upper ocean layers (Figure 4C, H), both were enriched in the bathypelagic samples of *Malaspina* (Figure 4E, J).

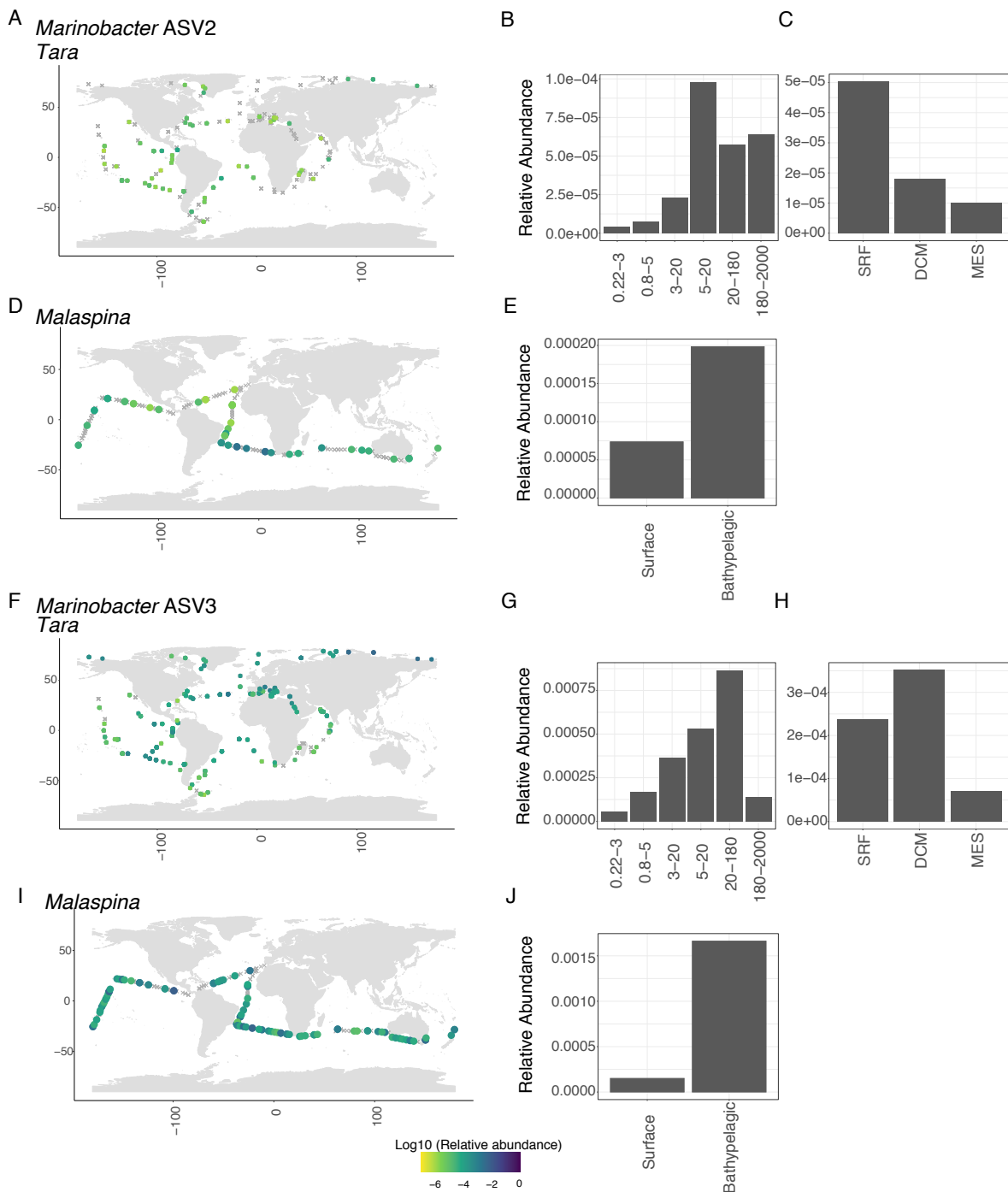


**Figure 4.** Relative abundance (proportion) and distribution of dominant coccolithophores-associated *Marinobacter* ASVs in the *Tara* Oceans and *Malaspina* expeditions. (A) Log<sub>10</sub>-transformed relative abundance of ASV2 in *Tara* Oceans dataset. (B) Relative abundance of ASV2 in *Tara* Oceans dataset by plankton size fraction. (C) by depth. (D) Log<sub>10</sub>-transformed relative abundance of ASV2 in the *Malaspina* dataset. (E) Relative abundance of ASV2 in *Malaspina* dataset by depth. (F) Log<sub>10</sub>-transformed relative abundance of ASV3 in *Tara* Oceans dataset. (G) Relative abundance of ASV3 in *Tara* Oceans dataset by size fraction. (H) by depth. (I) Log<sub>10</sub>-transformed relative abundance of ASV3 in the *Malaspina* dataset. (J) Relative abundance of ASV3 in *Malaspina* dataset by depth. SRF – surface; DCM – deep chlorophyll maximum; MES – mesopelagic. Relative abundance was calculated as the number

of reads of the ASV/zOTU by station/size fraction/depth divided by the total number of reads at the corresponding station/size fraction/depth.

Other *Marinobacter* ASVs highly abundant in coccolithophores (ASV4 and ASV5) showed similar distribution patterns in the wild, and preference for surface, DCM and bathypelagic layers (Supplementary Figure 10). ASV7 (*Alteromonas* spp.) was the only ASV dominating in coccolithophore cultures that was abundant in the global oceans. Poorly found in the 3-20  $\mu\text{m}$  fractions collected during the *Tara* Oceans Polar Circle expedition, ASV7 favored large size fractions of Mediterranean and subtropical waters (Supplementary Figure 11). ASV6, assigned to Rhodobacteraceae unclassified and *Marivita* (ASV8 and ASV9) had more restricted distributions (Supplementary Figures 11 and 12). Contrasting with the above depth profiles, they were mostly found in surface waters, but not enriched in the largest plankton fractions although they populated fractions below 20  $\mu\text{m}$ . *Shimia* (ASV10) did not follow the above patterns; although it was more abundant in size fractions  $> 5 \mu\text{m}$ , it was equally present in surface and bathypelagic layers (Supplementary figure 13).

## Discussion

*E. huxleyi* and *G. oceanica* are the most intensively studied members of the coccolithophorid microalgae because they are common bloom-forming species and are easily cultured (Rhodes *et al.*, 1995; Taylor *et al.*, 2017). Surprisingly, information on the bacterial assemblages associated with coccolithophore blooms and laboratory cultures is currently limited (Gonzalez *et al.*, 2000; Zubkov *et al.*, 2001; Green *et al.*, 2015; Orata *et al.*, 2016; Rosana *et al.*, 2016). Today, the largest body of research on coccolithophores-bacteria interactions is devoted to antagonistic relationships that lead to *E. huxleyi* cell death (Seymour *et al.*, 2010; Seyedsayamdost *et al.*, 2011; Harvey *et al.*, 2016; Mayers *et al.*, 2016; Segev *et al.*, 2016), suggesting that bacteria could participate in bloom demises (Barak-Gavish *et al.*, 2018). We address the paucity of knowledge on the total diversity and variation of bacteria associated with coccolithophores by performing the first high resolution investigation of the bacterial communities associated with a large set of *E. huxleyi* and *G. oceanica* cultures.

Coccolithophore microbiomes were dominated by Gammaproteobacteria followed by Alphaproteobacteria. Both classes are often reported as abundant in microalgal microbiomes however with varying magnitude. Similarly, to our study, Gammaproteobacteria dominated the microbiomes of the green algae *Ostreococcus tauri* and the dinoflagellate *Cochlodinium*

*polykrikoides* (Lupette *et al.*, 2016; Shin *et al.*, 2018). However, a dominance of Alphaproteobacteria is more common in microalgal cultures and it was reported for several species of diatoms (Ajani *et al.*, 2018; Behringer *et al.*, 2018; Chernikova *et al.*, 2020), dinoflagellates (Shin *et al.*, 2018; Sörenson *et al.*, 2019) and the haptophyte *Pavlova lutheri* (Chernikova *et al.*, 2020). Alphaproteobacteria were also found to dominate 16S rRNA gene clone libraries from *E. huxleyi* and *Coccolithus pelagicus* f. *braarudii* cultures (Green *et al.*, 2015), but only a limited number of cultures and clones were analyzed. The reason of differential dominance of Gammaproteobacteria or Alphaproteobacteria in phytoplankton microbiomes is yet unknown because both classes contain *r*-strategists (most copiotrophs that prefer nutrient-rich niches and have a metabolism of low efficiency but high plasticity) and *K*-strategists (most oligotrophs that have long phases of continuous growth characterized by a constant low growth rate). However, the boundary between these two major trophic strategies is sometimes unclear, and representatives belonging to the oligotrophic guild of both classes show an improved growth under nutrient-rich conditions (Luo *et al.*, 2013; Spring and Riedel, 2013). Indeed, the higher proportion of Gammaproteobacteria in coccolithophore cultures could correspond to species with higher versatility and capacity to degrade complex carbohydrates derived from these hosts.

The core microbiome is often defined as the bacteria that are found in all the samples of a given host with a relative abundance higher than 0.0001% (Lawson *et al.*, 2018; Sörenson *et al.*, 2019). The presence of a core microbiome suggests stable and potentially symbiotic interactions (Hernandez-Agreda *et al.*, 2017). Here we identified a *Marinobacter* sp. as the unique core ASV. *Marinobacter* is a very diversified genus (Gauthier *et al.*, 1992; De la Haba *et al.*, 2011) and its phenotypic versatility contributes to its ubiquity and ability to occupy an exceptionally wide range of marine habitats. While *Marinobacter* spp. account numerically for only a small proportion of the total bacteria present in the field (Green *et al.*, 2015), they are often the dominant and/or core genus associated with cultures of cyanobacteria, coccolithophores, dinoflagellates, and a chlorophyte (Green *et al.*, 2015; Lupette *et al.*, 2016; Lawson *et al.*, 2018; Sörenson *et al.*, 2019; Kearney *et al.*, 2021). In terms of functions, the *Marinobacter* symbionts can promote growth of the dinoflagellate *G. catenatum* (Bolch *et al.*, 2011, 2017) and of the cyanobacterium *Prochlorococcus* (Sher *et al.*, 2011). In contrast, *Marinobacter* spp. are much less abundant/prevalent in diatom cultures (Amin *et al.*, 2009; Green *et al.*, 2015). Diatom-bacteria co-culture experiments suggest however their functional importance, either by promoting algal assimilation of iron (Amin *et al.*, 2009), inducing cell

aggregation (Gärdes *et al.*, 2011, 2012), or reducing mating success without affecting growth (Cirri *et al.*, 2018). Negative growth-affecting properties of *Marinobacter* strains have also been demonstrated in co-culturing experiments with diatoms (Wang *et al.*, 2014; Johansson *et al.*, 2019; Stock *et al.*, 2019).

In order to unveil possible drivers of the bacterial composition in coccolithophore cultures, we compared 73 strains from two closely related taxa including all the *E. huxleyi* morphotypes, covering the global ocean and isolated between 61 and 6 years before our experiment. None of the parameters tested could explain the bacterial composition patterns. Recent studies have shown that the microbiome diversity of phytoplankton strains becomes rapidly stable and consistent across time once cultures have been established (Behringer *et al.*, 2018; Sörenson *et al.*, 2019; Kearney *et al.*, 2021). Taken together, our results also show that the microbiomes of coccolithophores are consistent and stable among strains although we identified shifts in relative abundance for some members. This probably explains why no significant differences were found between cultures maintained for up to 61 years and others obtained from more recent cruises. We did not find significant differences either between the microbiomes of *E. huxleyi* and *G. oceanica*, or between the *E. huxleyi* morphotypes whose varying carbonate contents could be putatively influence associated bacterial communities (Green *et al.*, 2015). Similarly, no significant differences were found between the microbiome structure of *Leptocylindrus* species (Ajani *et al.*, 2018). However, place/time from which these diatoms were isolated had a stronger effect on the microbiome selection than host specificity. A similar situation was observed in *Thalassiosira rotula* whose microbiomes differed across seasons (Mönnich *et al.*, 2020).

We found that variability in the bacterial community between cultures was ascribed to differences in relative abundance of the most abundant ASVs. This finding supports previous results showing the influence of certain bacteria on the microbiome assembly in axenic cultures of *Thalassiosira rotula* (Majzoub *et al.*, 2019), and of a *Marinobacter* strain on the microbiome of *Cylindrotheca closterium* (Stock *et al.*, 2019). Interestingly, by comparing coccolithophore-associated bacteria with that of diatoms (Behringer *et al.*, 2018), cyanobacteria (Kearney *et al.*, 2021) and *Alexandrium* spp. (Sörenson *et al.*, 2019), we demonstrated that all the microbiomes dominated by *Marinobacter* shared the highest number of OTUs. A possible explanation is that these hosts may release common specific carbon and nutrient compounds selecting for the associated copiotrophs like Marinobacteraceae and Alteromonadaceae that outcompete other

heterotrophic bacteria. *Marinobacter* and *Alteromonas* can metabolize hydrocarbons and C1 compounds derived from lipid catabolism, suggesting that hydrocarbons might play an important role in their success in phytoplankton cultures (Green *et al.*, 2015). Our results suggest that mechanisms such as bacterial signaling or competition for common resources may be important for determining the overall bacterial community composition and structure in coccolithophore cultures.

The OTUs shared between coccolithophores, cyanobacteria, diatoms and *Alexandrium* spp. belong to archetypal phytoplankton-associated families (Buchan *et al.*, 2014) such as the Rhodobacteraceae, Alteromonadaceae, Flavobacteriaceae and Pseudomonadaceae. The presence of *Alteromonas* sp. among the most shared OTUs is not surprising since these metabolically versatile copiotrophs respond rapidly to increases in dissolved organic matter (Shi *et al.*, 2012; Hogle *et al.*, 2016) including algal exudates (Romera-Castillo *et al.*, 2011) and often dominate in phytoplankton cultures and blooms (Buchan *et al.*, 2014). *Alteromonas* bacteria have previously been shown to interact with individual eukaryotic and prokaryotic phytoplankton species. These interactions range from impairing algal growth (Mayali and Azam, 2004) to effects that are either neutral or beneficial to algal growth in co-culture (Sher *et al.*, 2011; Le Chevanton *et al.*, 2013). Not surprisingly, the *E. huxleyi* ASV7 clustered into *Alteromonas* OTU was the most abundant found in 16S rDNA metabarcoding datasets from the world ocean. Our cross-phytoplankton analysis also allowed identification of OTUs specific to coccolithophores, suggesting some level of selection from or adaptation to the host. The most prevalent coccolithophore-specific OTUs, assigned to *Pseudomonas* sp. and *Janthinobacterium* sp., were not abundant. Like *Marinobacter* sp., members of the genus *Pseudomonas* are r-strategists, generalist bacteria that are typically enriched in the attached communities of microalgal cultures (Kimbrel *et al.*, 2019). They can also exert negative effects on phytoplankton growth performance (Le Chevanton *et al.*, 2013). The presence of the *Janthinobacterium* sp. in marine settings is not well documented. These betaproteobacteria are usually rare members of the bacterioplankton, yet Alonso-Sáez *et al.*, (2014) reported a bloom of a *Janthinobacterium* sp. population in the Arctic Ocean. The genus reached up to 22% of the total of bacteria in the epipelagic zone and remained abundant in the mesopelagic layer. *Janthinobacterium* sp. also displayed high abundance in the particle-attached fractions of mesopelagic and bathypelagic water masses of the bathypelagic Southern Ocean, suggesting an obligate particle-associated lifestyle (Milici *et al.*, 2017). The high prevalence of *Janthinobacterium* sp. in coccolithophores cultures may be due to the exchange of common

goods. Interestingly, an isolate from snowfield, that displayed the capacity to produce siderophores and auxins, significantly enhanced the growth of *Chlorella vulgaris* compared to axenic controls (Krug *et al.*, 2020). Although Bacteroidota are found as substantial components in phytoplankton-associated assemblages (Ajani *et al.*, 2018; Sörenson *et al.*, 2019), they represented low proportions in our cultures. However, about 30% of the coccolithophore-specific OTUs belonged to this phylum. In the environment, low abundance microbes have been proposed to have important ecological roles such as stabilizing ecosystem processes after disturbance or maintaining critical biogeochemical functions (Lynch and Neufeld, 2015). Their role in phytoplankton cultures needs further investigation.

Interestingly, heterotrophic bacteria most prominently enriched in coccolithophore cultures are not very abundant in oceanic waters (Figure 4). *Marinoacteraceae* and other copiotrophs typically occur at a rather low abundance in oligotrophic marine habitats (Eilers *et al.*, 2000) but can grow rapidly in changing environments and dominate. Local variations in nutrient content can occur in the ocean because of physical processes, such as upwelling of nutrient rich deep waters or biological processes such as phytoplankton blooms or aggregation of particulate organic matter (Tada *et al.*, 2011; Teeling *et al.*, 2012, 2016). In cultures, associated bacteria experience nutrient-rich conditions provided by coccolithophore released exudates and from the cultivation medium. Such exudates, mainly polysaccharides (Mühlenbruch *et al.*, 2018), are also likely abundant in nutrient-rich particles, or ephemeral patches of high organic carbon distributed in open ocean waters (Stocker, 2012; Seymour *et al.*, 2017). The distribution patterns in the open ocean of coccolithophore-associated copiotrophs are not well documented. Our analyses demonstrated that they are ubiquitous, most of them being preferably associated with relatively large plankton size fractions, and enriched in bathypelagic waters. These large plankton size fractions contain phytoplankton, heterotrophic protists, and zooplankton, as well as detritus, fecal pellets, and diverse types of marine aggregates. *Marinobacter* sp. and *Alteromonas* sp., the dominant members in our cultures, are good candidates for attachment to macroaggregates (marine snow; 500  $\mu\text{m}$  to centimeters in diameter) and microaggregates (1 to 500 $\mu\text{m}$ ) (Simon *et al.*, 2002), and further sinking to the deep ocean layers and sediments. Indeed, previous studies reported the presence of *Marinobacter* in the particle-attached fraction (Li *et al.*, 2015), their isolation from bathypelagic waters (Kai *et al.*, 2017; Sanz-Sáez *et al.*, 2020), as well as their potential for organic matter degradation (Fontanez *et al.*, 2015) and colonization of the deep ocean (Sebastián *et al.*, 2019). A strain of *M. adherens*, a very close relative of ASV5, was isolated

from marine aggregates and it was found to specifically attach to the surface of the diatom *Thalassiosira weissflogii* grown in culture, inducing exopolymer and aggregate formation and thus generating marine snow particles (Gärdes *et al.*, 2011, 2012). Finally, Alteromonadaceae were recently found being enriched in diatom-produced and natural transparent exopolymer particles (TEP) (Taylor and Cunliffe, 2017; Zäncker *et al.*, 2019), that are ubiquitous microgels formed by the aggregation of biogenic precursors (Passow, 2002). Our findings support the hypothesis that bacteria from the surface thrive at depth and that a strong vertical connectivity via particle sinking exists through the entire water column in the ocean (Mestre *et al.*, 2018). They also suggest that phytoplankton-associated copiotrophs likely contribute to these communities. The demise of *E. huxleyi*'s oceanic blooms is often attributed to coccolithoviruses and the transport of cellular debris and associated particulate organic carbon to depth is facilitated by TEP (Bratbak *et al.*, 1993; Vardi *et al.*, 2012; Laber *et al.*, 2018). However, some coccolithophore-associated ASVs (*Marivita* ASV8 and ASV9) did not follow this prevalent pattern. Indeed, our results also showed that bacteria preferentially associated with smaller particles (0.8-5  $\mu\text{m}$ ) were less abundant in the bathypelagic layers. Although we don't know yet how biological processes control the size and amount of particles produced in the surface ocean, they will differently impact the bathypelagic realm (Ruiz-González *et al.*, 2020). This suggests that the vertical connectivity from surface to depth is highly dependent on bacteria-phytoplankton interactions in sunlit water masses. To confirm our hypothesis in natural populations, future field studies in natural *E. huxleyi* blooms should involve detailed investigations of the relative involvement of bacteria in the production and/or utilization of particles throughout the water column.

## Conclusions

Microbiomes of coccolithophore cultures represent stable communities and their taxonomic composition bore notable similarities to that of other marine phytoplankton. Our study confirms the propensity of *Marinobacter* to colonize the phycosphere in phytoplankton cultures. Although a large number of cultivated representatives and several sequenced genomes exist, the functional breath of *Marinobacter* species remains largely unexplored. The ability to metabolize hydrocarbons has been tested in relatively few species and we know little about the nature and magnitude of their actual function and interactions in phytoplankton cultures and in the field. Stable and specific microbiomes over time imply that abundant associated taxa may have functional importance to their host. To understand the stability of interspecies and interkingdom interactions, we need to test whether the relative taxonomic variability between phytoplankton-associated bacteria is related to functional variations and to which extent specific organisms can affect the cellular physiology of the interacting partners and ultimately the stability of the community. Our current knowledge of microalgae-bacteria interactions is based upon pairwise species interactions. The challenge is now to design approaches involving multispecies interactions, including viruses, that could help to better understand the stability of species interactions and ultimately how the dynamical networks building microbiomes shape community dynamics.

## Acknowledgments

This work was supported by Sorbonne University, the Région Bretagne, the Centre National de la Recherche Scientifique (CNRS, France), and the French Government “Investissements d’Avenir” programmes OCEANOMICS (ANR-11-BTBR-0008). The authors are thankful to Cédric Berney for helping in the improvement of the phylogenetic analysis. We are thankful to the ABiMS bioinformatic platform (<http://abims.sb-roscoff.fr>) for the computational resources and to the RCC and NIES culture collections for the cultures provided. This article is contribution number XX of *Tara* Oceans.

## References

- Abby, S., Touchon, M., de Jode, A., Grimsley, N., and Piganeau, G. (2014) Bacteria in *Ostreococcus tauri* cultures - friends, foes or hitchhikers? *Front Microbiol* 5:.
- Ajani, P.A., Kahlke, T., Siboni, N., Carney, R., Murray, S.A., and Seymour, J.R. (2018) The microbiome of the cosmopolitan diatom *Leptocylindrus* reveals significant spatial and temporal variability. *Front Microbiol* 9: 2758.
- Alonso-Sáez, L., Zeder, M., Harding, T., Pernthaler, J., Lovejoy, C., Bertilsson, S., and Pedrós-Alió, C. (2014) Winter bloom of a rare betaproteobacterium in the Arctic Ocean. *Front Microbiol* 5: 1–9.
- Amin, S.A., Green, D.H., Hart, M.C., Kupper, F.C., Sunda, W.G., and Carrano, C.J. (2009) Photolysis of iron-siderophore chelates promotes bacterial-algal mutualism. *Proc Natl Acad Sci* 106: 17071–17076.
- Amin, S.A., Parker, M.S., and Armbrust, E. V. (2012) Interactions between Diatoms and Bacteria. *Microbiol Mol Biol Rev* 76: 667–684.
- Azam, F. and Malfatti, F. (2007) Microbial structuring of marine ecosystems. *Nat Rev Microbiol* 5: 782–791.
- Barak-Gavish, N., Frada, M.J., Ku, C., Lee, P.A., DiTullio, G.R., Malitsky, S., et al. (2018) Bacterial virulence against an oceanic bloom-forming phytoplankter is mediated by algal DMSP. *Sci Adv* 4: eaau5716.
- Barbera, P., Kozlov, A.M., Czech, L., Morel, B., Darriba, D., Flouri, T., and Stamatakis, A. (2019) EPA-ng: massively parallel evolutionary placement of genetic sequences. *Syst Biol* 68: 365–369.
- Behringer, G., Ochsenkühn, M.A., Fei, C., Fanning, J., Koester, J.A., and Amin, S.A. (2018) Bacterial communities of diatoms display strong conservation across strains and time. *Front Microbiol* 9:.
- Bell, W. and Mitchell, R. (1972) Chemotactic and growth responses of marine bacteria to algal extracellular products. *Biol Bull* 143: 265–277.
- Berger, S.A. and Stamatakis, A. (2012) PaPaRa 2.0: a vectorized algorithm for probabilistic phylogeny-aware alignment extension. *Heidelb Inst Theor Stud*.
- Blackburn, S.I. and Cresswell, G. (1993) A coccolithophorid bloom in Jervis Bay, Australia. *Mar Freshw Res* 44: 253–260.
- Bolch, C.J.S., Bejoy, T.A., and Green, D.H. (2017) Bacterial associates modify growth dynamics of the dinoflagellate *Gymnodinium catenatum*. *Front Microbiol* 8:.

- Bolch, C.J.S., Subramanian, T.A., and Green, D.H. (2011) The toxic dinoflagellate *Gymnodinium catenatum* (Dinophyceae) requires marine bacteria for growth. *J Phycol* 47: 1009–1022.
- Borcard, D., Gillet, F., and Legendre, P. (2011) Numerical Ecology with R, *Springer*.
- Bratbak, G., Egge, J.K., and Haldal, M. (1993) Viral mortality of the marine alga *Emiliania huxleyi* (Haptophyceae) and termination of algal blooms. *Mar Ecol Prog Ser* 93: 39–48.
- Bray, J.R. and Curtis, J.T. (1957) An ordination of the upland forest communities of southern Wisconsin. *Ecol Monogr* 27: 325–349.
- Callahan, B.J., McMurdie, P.J., Rosen, M.J., Han, A.W., Johnson, A.J.A., and Holmes, S.P. (2016) DADA2: High-resolution sample inference from Illumina amplicon data. *Nat Methods* 13: 581.
- Chernikova, T.N., Bargiela, R., Toshchakov, S. V., Shivaraman, V., Lunev, E.A., Yakimov, M.M., et al. (2020) Hydrocarbon-degrading bacteria *Alcanivorax* and *Marinobacter* associated with microalgae *Pavlova lutheri* and *Nannochloropsis oculata*. *Front Microbiol* 11:.
- Le Chevanton, M., Garnier, M., Bougaran, G., Schreiber, N., Lukomska, E., Bérard, J.-B., et al. (2013) Screening and selection of growth-promoting bacteria for *Dunaliella* cultures. *Algal Res* 2: 212–222.
- Cirri, E., Vyverman, W., and Pohnert, G. (2018) Biofilm interactions-bacteria modulate sexual reproduction success of the diatom *Seminavis robusta*. *FEMS Microbiol Ecol* 94: 1–9.
- Cole, J.J. (1982) Interactions between bacteria and algae in aquatic ecosystems. *Annu Rev Ecol Syst* 13: 291–314.
- Czech, L., Barbera, P., and Stamatakis, A. (2020) Genesis and Gappa: processing, analyzing and visualizing phylogenetic (placement) data. *Bioinformatics* 36: 3263–3265.
- Edgar, R.C. (2010) Search and clustering orders of magnitude faster than BLAST. *Bioinformatics* 26: 2460–2461.
- Eilers, H., Pernthaler, J., and Amann, R. (2000) Succession of pelagic marine bacteria during enrichment: A close look at cultivation-induced shifts. *Appl Environ Microbiol* 66: 4634–4640.
- Falkowski, P.G., Fenchel, T., and Delong, E.F. (2008) The microbial engines that drive earth's biogeochemical cycles. *Science* (80- ) 320: 1034–1039.
- Field, C.B., Behrenfeld, M.J., Randerson, J.T., and Falkowski, P. (1998) Primary Production of the Biosphere: Integrating Terrestrial and Oceanic Components. *Science* (80- ) 281: 237 LP – 240.

- Fontanez, K.M., Eppley, J.M., Samo, T.J., Karl, D.M., and DeLong, E.F. (2015) Microbial community structure and function on sinking particles in the North Pacific Subtropical Gyre. *Front Microbiol* 6: 1–14.
- Foster, R.A., Carpenter, E.J., and Bergman, B. (2006) Unicellular cyanobionts in open ocean dinoflagellates, radiolarians, and tintinnids: Ultrastructural characterization and immunolocalization of phycoerythrin and nitrogenase 1. *J Phycol* 42: 453–463.
- Gärdes, A., Iversen, M.H., Grossart, H.P., Passow, U., and Ullrich, M.S. (2011) Diatom-associated bacteria are required for aggregation of *Thalassiosira weissflogii*. *ISME J* 5: 436–445.
- Gärdes, A., Ramaye, Y., Grossart, H.-P., Passow, U., and Ullrich, M.S. (2012) Effects of *Marinobacter adhaerens* HP15 on polymer exudation by *Thalassiosira weissflogii* at different N: P ratios. *Mar Ecol Prog Ser* 461: 1–14.
- Gauthier, M.J., Lafay, B., Christen, R., Fernandez, L., Acquaviva, M., Bonin, P., and Bertrand, J.-C. (1992) *Marinobacter hydrocarbonoclasticus* gen. nov., sp. nov., a new, extremely halotolerant, hydrocarbon-degrading marine bacterium. *Int J Syst Evol Microbiol* 42: 568–576.
- Gonzalez, J.M., Simó, R., Massana, R., Covert, J.S., Casamayor, E.O., Pedrós-Alió, C., and Moran, M.A. (2000) Bacterial community structure associated with a dimethylsulfoniopropionate-producing North Atlantic algal bloom. *Appl Environ Microbiol* 66: 4237–4246.
- Green, D.H., Echavarri-Bravo, V., Brennan, D., and Hart, M.C. (2015) Bacterial diversity associated with the coccolithophorid algae *Emiliana huxleyi* and *Coccolithus pelagicus* f. *braarudii*. *Biomed Res Int* 2015:.
- Gutierrez, T., Green, D.H., Nichols, P.D., Whitman, W.B., Semple, K.T., and Aitken, M.D. (2013) *Polycyclovorans algicola* gen. nov., sp. nov., an aromatic-hydrocarbon-degrading marine bacterium found associated with laboratory cultures of marine phytoplankton. *Appl Environ Microbiol* 79: 205–214.
- Hagino, K., Bendif, E.M., Young, J.R., Kogame, K., Probert, I., Takano, Y., et al. (2011) New evidence for morphological and genetic variation in the cosmopolitan coccolithophore *Emiliana huxleyi* (prymnesiophyceae) from the *cox1b-atp4* genes. *J Phycol* 47: 1164–1176.
- Harvey, E.L., Deering, R.W., Rowley, D.C., Gamal, A. El, Schorn, M., Moore, B.S., et al. (2016) A bacterial quorum-sensing precursor induces mortality in the marine coccolithophore, *Emiliana huxleyi*. *Front Microbiol* 7:.

- Hernandez-Agreda, A., Gates, R.D., and Ainsworth, T.D. (2017) Defining the Core Microbiome in Corals' Microbial Soup. *Trends Microbiol* 25: 125–140.
- Hogle, S.L., Bundy, R.M., Blanton, J.M., Allen, E.E., and Barbeau, K.A. (2016) Copiotrophic marine bacteria are associated with strong iron-binding ligand production during phytoplankton blooms. *Limnol Oceanogr Lett* 1: 36–43.
- Johansson, O.N., Pinder, M.I.M., Ohlsson, F., Egardt, J., Töpel, M., and Clarke, A.K. (2019) Friends With Benefits: Exploring the Phycosphere of the Marine Diatom *Skeletonema marinoi*. *Front Microbiol* 10: 1–11.
- Kai, W., Peisheng, Y., Rui, M., Wenwen, J., and Zongze, S. (2017) Diversity of culturable bacteria in deep-sea water from the South Atlantic Ocean. *Bioengineered* 8: 572–584.
- Katoh, K. and Standley, D.M. (2013) MAFFT Multiple Sequence Alignment Software Version 7: Improvements in Performance and Usability. *Mol Biol Evol* 30: 772–780.
- Kearney, S.M., Thomas, E., Coe, A., and Chisholm, S.W. (2021) Microbial diversity of co-occurring heterotrophs in cultures of marine picocyanobacteria. *Environ Microbiomes* 16: 1–15.
- Keller, M.D., Selvin, R.C., Claus, W., and Guillard, R.R.L. (1987) Media for the culture of oceanic ultraphytoplankton. *J Phycol* 23: 633–638.
- Kolde, R. (2015) Package 'pheatmap.' R Packag 1: 790.
- Krohn-Molt, I., Alawi, M., Förstner, K.U., Wiegandt, A., Burkhardt, L., Indenbirken, D., et al. (2017) Insights into Microalga and bacteria interactions of selected phycosphere biofilms using metagenomic, transcriptomic, and proteomic approaches. *Front Microbiol* 8: 1–14.
- Krug, L., Erlacher, A., Markut, K., Berg, G., and Cernava, T. (2020) The microbiome of alpine snow algae shows a specific inter-kingdom connectivity and algae-bacteria interactions with supportive capacities. *ISME J* 14: 2197–2210.
- De la Haba, R.R., Sánchez-Porro, C., Márquez, M.C., and Ventosa, A. (2011) Taxonomy of halophiles. *Extrem Handb* 1: 255–308.
- Laber, C.P., Hunter, J.E., Carvalho, F., Collins, J.R., Hunter, E.J., Schieler, B.M., et al. (2018) Coccolithovirus facilitation of carbon export in the North Atlantic. *Nat Microbiol* 1–11.
- Lawson, C.A., Raina, J.B., Kahlke, T., Seymour, J.R., and Suggett, D.J. (2018) Defining the core microbiome of the symbiotic dinoflagellate, *Symbiodinium*. *Environ Microbiol Rep* 10: 7–11.
- Legendre, P. and Gallagher, E.D. (2001) Ecologically meaningful transformations for ordination of species data. *Oecologia* 129: 271–280.
- Letunic, I. and Bork, P. (2019) Interactive Tree Of Life (iTOL) v4: recent updates and new

- developments. *Nucleic Acids Res* 47: W256–W259.
- Li, J., Wei, B., Wang, J., Liu, Y., Dasgupta, S., Zhang, L., and Fang, J. (2015) Variation in abundance and community structure of particle-attached and free-living bacteria in the South China Sea. *Deep Sea Res Part II Top Stud Oceanogr* 122: 64–73.
- Loebl, M., Cockshutt, A.M., Campbell, D.A., and Finkel, Z. V. (2010) Physiological basis for high resistance to photoinhibition under nitrogen depletion in *Emiliana huxleyi*. *Limnol Oceanogr* 55: 2150–2160.
- Longhurst, A., Sathyendranath, S., Platt, T., and Caverhill, C. (1995) An estimate of global primary production in the ocean from satellite radiometer data. *J Plankton Res* 17: 1245–1271.
- Luo, H., Csúros, M., Hughes, A.L., and Moran, M.A. (2013) Evolution of divergent life history strategies in marine alphaproteobacteria. *MBio* 4:.
- Lupette, J., Lami, R., Krasovec, M., Grimsley, N., Moreau, H., Piganeau, G., and Sanchez-Ferandin, S. (2016) *Marinobacter* dominates the bacterial community of the *Ostreococcus tauri* phycosphere in culture. *Front Microbiol* 7:.
- Lynch, M.D.J. and Neufeld, J.D. (2015) Ecology and exploration of the rare biosphere. *Nat Rev Microbiol* 13: 217–229.
- Majzoub, M.E., Beyersmann, P.G., Simon, M., Thomas, T., Brinkhoff, T., and Egan, S. (2019) *Phaeobacter inhibens* controls bacterial community assembly on a marine diatom. *FEMS Microbiol Ecol* 95:.
- Marie, D., Brussaard, C.P.D., Partensky, F., and Vaultot, D. (1999) Flow cytometric analysis of phytoplankton, bacteria and viruses. *Curr Protoc Cytom* 11.11: 1–15.
- Marie, D., Rigaut-Jalabert, F., and Vaultot, D. (2014) An improved protocol for flow cytometry analysis of phytoplankton cultures and natural samples. *Cytometry* 85: 962–968.
- Martin, M. (2011) Cutadapt removes adapter sequences from high-throughput sequencing reads. *EMBnet.journal*; Vol 17, No 1 Next Gener Seq Data Anal - 1014806/ej171200.
- Mayali, X. and Azam, F. (2004) Algicidal bacteria in the sea and their impact on algal blooms. *J Eukaryot Microbiol* 51: 139–144.
- Mayers, T.J., Bramucci, A.R., Yakimovich, K.M., and Case, R.J. (2016) A bacterial pathogen displaying temperature-enhanced virulence of the microalga *Emiliana huxleyi*. *Front Microbiol* 7:.
- Mestre, M., Ruiz-González, C., Logares, R., Duarte, C.M., Gasol, J.M., and Sala, M.M. (2018) Sinking particles promote vertical connectivity in the ocean microbiome. *Proc Natl Acad Sci U S A* 115: E6799–E6807.

- Milici, M., Vital, M., Tomasch, J., Badewien, T.H., Giebel, H.A., Plumeier, I., et al. (2017) Diversity and community composition of particle-associated and free-living bacteria in mesopelagic and bathypelagic Southern Ocean water masses: Evidence of dispersal limitation in the Bransfield Strait. *Limnol Oceanogr* 62: 1080–1095.
- Mönnich, J., Tebben, J., Bergemann, Case, R.J., Sylke Wohlrab, and Harder, T. (2020) Niche-based assembly of bacterial consortia on the diatom *Thalassiosira rotula* is stable and reproducible. *ISME J* 14: 1614–1625.
- Mühlenbruch, M., Grossart, H.P., Eigemann, F., and Voss, M. (2018) Mini-review: Phytoplankton-derived polysaccharides in the marine environment and their interactions with heterotrophic bacteria. *Environ Microbiol* 20: 2671–2685.
- Munoz, R., Rosselló-Móra, R., and Amann, R. (2016) Revised phylogeny of Bacteroidetes and proposal of sixteen new taxa and two new combinations including Rhodothermaeota phyl. nov. *Syst Appl Microbiol* 39: 281–296.
- Murali, A., Bhargava, A., and Wright, E.S. (2018) IDTAXA: a novel approach for accurate taxonomic classification of microbiome sequences. *Microbiome* 6: 140.
- Oksanen, J., Blanchet, F.G., Kindt, R., Legendre, P., Minchin, P.R., O’Hara, R.B., et al. (2015) OK-Package ‘vegan.’ Community Ecol Packag version 285 pp.
- Orata, F.D., Rosana, A.R.R., Xu, Y., Simkus, D.N., Bramucci, A.R., Boucher, Y., and Case, R.J. (2016) Polymicrobial Culture of Naked ( N-Type ) *Emiliana huxleyi*. *Genome Announc* 4: 9–10.
- Paasche, E. (2001) A review of the coccolithophorid *Emiliana huxleyi* (Prymnesiophyceae), with particular reference to growth, coccolith formation, and calcification-photosynthesis interactions. *Phycologia* 40: 503–529.
- Parada, A.E., Needham, D.M., and Fuhrman, J.A. (2016) Every base matters: Assessing small subunit rRNA primers for marine microbiomes with mock communities, time series and global field samples. *Environ Microbiol* 18: 1403–1414.
- Passow, U. (2002) Transparent exopolymer particles (TEP) in aquatic environments. *Prog Oceanogr* 55: 287–333.
- Patil, S.M., Mohan, R., Shetye, S.S., Gazi, S., Baumann, K.H., and Jafar, S. (2017) Biogeographic distribution of extant Coccolithophores in the Indian sector of the Southern Ocean. *Mar Micropaleontol* 137: 16–30.
- Pomeroy, L., leB. Williams, P., Azam, F., and Hobbie, J. (2007) The Microbial Loop. *Oceanography* 20: 28–33.
- Probert, I. (2019) K/2 Ian / K-ET. protocols.io.

- Probert, I. and Houdan, A. (2004) The Laboratory Culture of Coccolithophores BT - Coccolithophores: From Molecular Processes to Global Impact. In Thierstein, H.R. and Young, J.R. (eds). *Berlin, Heidelberg: Springer Berlin Heidelberg*, pp. 217–249.
- Quast, C., Pruesse, E., Yilmaz, P., Gerken, J., Schweer, T., Yarza, P., et al. (2013) The SILVA ribosomal RNA gene database project: improved data processing and web-based tools. *Nucleic Acids Res* 41: D590–D596.
- R Core Team (2017) R: A language and environment for statistical computing. R Foundation for Statistical Computing, Vienna, Austria. URL <https://www.R-project.org/>.
- Rhodes, L.L., Peake, B.M., MacKenzie, A.L., and Marwick, S. (1995) Coccolithophores *Gephyrocapsa oceanica* and *Emiliana huxleyi* (Prymnesiophyceae= Haptophyceae) in New Zealand's coastal waters: Characteristics of blooms and growth in laboratory culture. *New Zeal J Mar Freshw Res* 29: 345–357.
- Rognes, T., Flouri, T., Nichols, B., Quince, C., and Mahé, F. (2016) VSEARCH: a versatile open source tool for metagenomics. *PeerJ* 4: e2584–e2584.
- Romera-Castillo, C., Sarmiento, H., Alvarez-Salgado, X.A.Á., Gasol, J.M., and Marrasé, C. (2011) Net production and consumption of fluorescent colored dissolved organic matter by natural bacterial assemblages growing on marine phytoplankton exudates. *Appl Environ Microbiol* 77: 7490–7498.
- Rosana, A.R.R., Orata, F.D., Xu, Y., Simkus, D.N., Bramucci, A.R., Boucher, Y., and Case, R.J. (2016) Draft genome sequences of seven bacterial strains isolated from a polymicrobial culture of coccolith-bearing (C-type) *Emiliana huxleyi* M217. *Genome Announc* 4:.
- RStudio Team (2016) RStudio: Integrated Development for R. RStudio, Inc, Boston, MA.
- Ruiz-González, C., Mestre, M., Estrada, M., Sebastián, M., Salazar, G., Agustí, S., et al. (2020) Major imprint of surface plankton on deep ocean prokaryotic structure and activity. *Mol Ecol* 29: 1820–1838.
- Sanz-Sáez, I., Salazar, G., Sánchez, P., Lara, E., Royo-Llonch, M., Sà, E.L., et al. (2020) Diversity and distribution of marine heterotrophic bacteria from a large culture collection. *BMC Microbiol* 20: 1–16.
- Sebastián, M., Estrany, M., Ruiz-González, C., Forn, I., Montserrat Sala, M., Gasol, J.M., and Marrasé, C. (2019) High growth potential of long-term starved deep ocean opportunistic heterotrophic bacteria. *Front Microbiol* 10: 1–12.
- Segev, E., Wyche, T.P., Kim, K.H., Petersen, J., Ellebrandt, C., Vlamakis, H., et al. (2016) Dynamic metabolic exchange governs a marine algal-bacterial interaction. *Elife* 5:.

- Seyedsayamdost, M.R., Case, R.J., Kolter, R., and Clardy, J. (2011) The Jekyll-and-Hyde chemistry of *Phaeobacter gallaeciensis*. *Nat Chem* 3: 331–335.
- Seymour, J.R., Amin, S.A., Raina, J.B., and Stocker, R. (2017) Zooming in on the phycosphere: The ecological interface for phytoplankton-bacteria relationships. *Nat Microbiol* 2:.
- Seymour, J.R., Simó, R., Ahmed, T., and Stocker, R. (2010) Chemoattraction to dimethylsulfoniopropionate throughout the marine microbial food web. *Science* (80- ) 329: 342–345.
- Sher, D., Thompson, J.W., Kashtan, N., Croal, L., and Chisholm, S.W. (2011) Response of *Prochlorococcus* ecotypes to co-culture with diverse marine bacteria. *ISME J* 5: 1125–1132.
- Shi, Y., McCarren, J., and Delong, E.F. (2012) Transcriptional responses of surface water marine microbial assemblages to deep-sea water amendment. *Environ Microbiol* 14: 191–206.
- Shin, H., Lee, E., Shin, J., Ko, S.-R., Oh, H.-S., Ahn, C.-Y., et al. (2018) Elucidation of the bacterial communities associated with the harmful microalgae *Alexandrium tamarense* and *Cochlodinium polykrikoides* using nanopore sequencing. *Sci Rep* 8: 5323.
- Simon, M., Grossart, H.P., Schweitzer, B., and Ploug, H. (2002) Microbial ecology of organic aggregates in aquatic ecosystems. *Aquat Microb Ecol* 28: 175–211.
- Sison-Mangus, M.P., Jiang, S., Tran, K.N., and Kudela, R.M. (2014) Host-specific adaptation governs the interaction of the marine diatom, *Pseudo-nitzschia* and their microbiota. *ISME J* 8: 63–76.
- Sörenson, E., Bertos-Fortis, M., Farnelid, H., Kremp, A., Krüger, K., Lindehoff, E., and Legrand, C. (2019) Consistency in microbiomes in cultures of *Alexandrium* species isolated from brackish and marine waters. *Environ Microbiol Rep* 11: 425–433.
- Spring, S. and Riedel, T. (2013) Mixotrophic growth of bacteriochlorophyll a-containing members of the OM60/NOR5 clade of marine gammaproteobacteria is carbon-starvation independent and correlates with the type of carbon source and oxygen availability. *BMC Microbiol* 13: 1.
- Stamatakis, A. (2014) RAxML version 8: a tool for phylogenetic analysis and post-analysis of large phylogenies. *Bioinformatics* 30: 1312–1313.
- Stock, W., Blommaert, L., De Troch, M., Mangelinckx, S., Willems, A., Vyverman, W., and Sabbe, K. (2019) Host specificity in diatom-bacteria interactions alleviates antagonistic effects. *FEMS Microbiol Ecol* 95: 1–11.
- Stocker, R. (2012) Marine microbes see a sea of gradients. *Science* (80- ) 338: 628–633.

- Tada, Y., Taniguchi, A., Nagao, I., Miki, T., Uematsu, M., Tsuda, A., and Hamasaki, K. (2011) Differing growth responses of major phylogenetic groups of marine bacteria to natural phytoplankton blooms in the Western North Pacific Ocean. *Appl Environ Microbiol* 77: 4055–4065.
- Taylor, A.R., Brownlee, C., and Wheeler, G. (2017) Coccolithophore cell biology: chalking up progress. *Ann Rev Mar Sci* 9: 283–310.
- Taylor, J.D. and Cunliffe, M. (2017) Coastal bacterioplankton community response to diatom-derived polysaccharide microgels. *Environ Microbiol Rep* 9: 151–157.
- Teeling, H., Fuchs, B.M., Becher, D., Klockow, C., Gardebrecht, A., Bennke, C.M., et al. (2012) Substrate-controlled succession of marine bacterioplankton populations induced by a phytoplankton bloom. *Science* (80- ) 336: 608–611.
- Teeling, H., Fuchs, B.M., Bennke, C.M., Krüger, K., Chafee, M., Kappelmann, L., et al. (2016) Recurring patterns in bacterioplankton dynamics during coastal spring algae blooms. *Elife* 5: 1–31.
- Tyrrell, T. and Merico, A. (2004) *Emiliana huxleyi*: bloom observations and the conditions that induce them. In *Coccolithophores*. pp. 75–97.
- Vardi, A., Haramaty, L., Van Mooy, B.A.S., Fredricks, H.F., Kimmance, S.A., Larsen, A., and Bidle, K.D. (2012) Host-virus dynamics and subcellular controls of cell fate in a natural coccolithophore population. *Proc Natl Acad Sci U S A* 109: 19327–19332.
- Wang, H.B., Zheng, Y.L., Zhang, Y.Q., Li, X.S., Li, S.H., and Yan, B.L. (2014) Allelopathic effects of a novel *Marinobacter* strain (HY-3) on diatom. *Allelopath J* 33.
- Warnes, M.G.R., Bolker, B., Bonebakker, L., Gentleman, R., and Huber, W. (2016) Package ‘gplots.’ Var R Program tools plotting data.
- Wickham, H. (2016) *ggplot2: Elegant Graphics for Data Analysis*. Springer-Verlag New York ISBN 978-3:
- van den Wollenberg, A.D. (1977) Redundancy Analysis an alternative for Canonical Correlation Analysis. *Psychometrika* 42: 207–219.
- Young, J.R., Geisen, M., Cros, L., Kleijne, a, Sprengel, C., Probert, I., and Østergaard, J. (2003) A guide to extant coccolithophore taxonomy. *J Nannoplankt Res* 125.
- Young, J.R. and Westbroek, P. (1991) Genotypic variation in the coccolithophorid species *Emiliana huxleyi*. *Mar Micropaleontol* 18: 5–23.
- Zäncker, B., Engel, A., and Cunliffe, M. (2019) Bacterial communities associated with individual transparent exopolymer particles (TEP). *J Plankton Res* 41: 561–565.
- Zheng, Q., Wang, Y., Xie, R., Lang, A.S., Liu, Y., Lu, J., et al. (2018) Dynamics of

heterotrophic bacterial assemblages within *Synechococcus* cultures. *Appl Environ Microbiol* 84: e01517-17.

Zubkov, M. V., Fuchs, B.M., Archer, S.D., Kiene, R.P., Amann, R., and Burkill, P.H. (2001) Linking the composition of bacterioplankton to rapid turnover of dissolved dimethylsulphoniopropionate in an algal bloom in the North Sea. *Environ Microbiol* 3: 304–311.

## SUPPLEMENTARY MATERIAL

### The microbiome of the cosmopolitan coccolithophore *Emiliana huxleyi*

#### Supplementary Material and Methods

##### *Sequencing*

At the Genotoul platform, single multiplexing was performed using homemade 6 bp index, which were added to reverse primer during a second PCR with 12 cycles using forward primer (AATGATACGGCGACCACCGAGATCTACACTCTTTCCCTACACGAC) and reverse primer (CAAGCAGAAGACGGCATACGAGAT-index-GTGACTGGAGTTCAGACGTGT). The resulting PCR products were purified and loaded onto the Illumina MiSeq V3 cartridge according to the manufacturer instructions. The quality of the run was checked internally using PhiX, and then each pair-end sequence was assigned to its sample with the help of the previously integrated index.

##### *Global ocean sequence datasets*

###### *Datasets*

ASVs identified in coccolithophore cultures were compared to two datasets of Illumina 16S rRNA gene sequences retrieved across the world's oceans. The first dataset comprised a total of 723 samples collected during the *Tara Oceans 2009* and *Tara Oceans Polar Circle 2013* expeditions which covered the major oceanic provinces and latitudes (65° S - 80° N). Sampling strategy and methodology are described in (Pesant *et al.*, 2015). In this dataset, six size fractions were collected in the surface, DCM and mesopelagic layers [0.2-3 µm (50 samples), 0.8-5 µm (163 samples), 3-20 µm (36 samples), 5-20 µm (94 samples), 20-180 µm (188 samples), and 180-2,000 µm (192 samples)]. The second dataset comprised a total of 124 surface samples and 41 bathypelagic samples collected during the *Malaspina 2010* expedition across the world's oceans. Surface seawater (3m) samples were collected and filtered as described previously in (Ruiz-González *et al.*, 2019). For these surface samples we focused on the 0.2–3 µm fraction, which represents mostly free-living bacteria. On the other hand, bathypelagic samples (from 2150 to 4018 m depth) were collected and filtered as described in (Salazar *et al.*, 2016). In these cases, two different size fractions were analyzed representing the free-living (0.2-0.8 µm)

and the particle-attached (0.8-20  $\mu\text{m}$ ) bacterial communities. In both datasets, once seawater was processed, filters were flash-frozen in liquid nitrogen and stored at  $-80\text{ }^{\circ}\text{C}$  until DNA extraction.

### *DNA extraction, amplification and sequencing*

The DNA from the samples of the different datasets described was extracted with a phenol-chloroform protocol, as described elsewhere (Massana *et al.*, 1997; Salazar *et al.*, 2016; Alberti, 2017). Prokaryotic barcodes for each of the datasets was generated by amplifying the V4 and V5 hypervariable regions of the 16S rRNA gene using primers 515F-Y (5'-GTG YCA GCM GCC GCG GTA A-3') and 926R (5'-CCG YCA ATT YMT TTR AGT TT-3') described in (Parada *et al.*, 2016). Sequencing was performed in an Illumina MiSeq platform (iTAGs) using 2x250 bp paired-end approach at the Research and Testing Laboratory facility (Lubbock, TX, USA) for the *Malaspina* datasets and at Genoscope (Evry Cedex, France) for the *Tara* Oceans and *Tara* Polar Oceans dataset.

### *16S rRNA Illumina sequences processing*

The ASV table from the *Tara* Oceans dataset was obtained following the methods as described for the *E. huxleyi* microbiome dataset with few exceptions. First, since raw reads were in mixed orientation and R1 and R2 files contained reads with forward and reverse primers, the primer removal was run twice generating forward and reverse reads for each file. These two runs were performed in a non-anchored mode with the addition of the flag `--pair-adapters` and a length threshold of 75 (Martin, 2011). Additional steps of primer removal were added in order to remove remaining primers using the flag `--times 5`. Since R1 and R2 cycles can have different error rates, the forward and reverse reads obtained from each cycle were analyzed independently during all the DADA2 processing (Callahan *et al.*, 2016). Another difference was that default parameters were used at the `learnerrors` step. Then, after the ASV inference in pooled mode, the forward and reverse reads from the R1 file were merged using the function `mergePairs`. The reads coming from the R2 file were also merged but in an inverse position (reverse + forward). The sequences tables were built using the function `makeSequenceTable` and the sequence table obtained for R2 file was reverse complemented. Sequence tables from R1 and R2 files were merged and the chimera removal was done using method consensus. Finally, the taxonomic assignation was performed using IDtaxa (confidence

threshold of 40) (Murali *et al.*, 2018) and vsearch (using usearch\_global and 90% similarity) (Rognes *et al.*, 2016).

Computing analyses of the *Malaspina* dataset were run at the MARBITS bioinformatics platform at the Institut de Ciències del Mar and at the Euler scientific compute cluster of the ETH Zürich University. The obtained amplicons were processed through the bioinformatic pipeline described in the github repository [https://github.com/SushiLab/Amplicon\\_Recipes](https://github.com/SushiLab/Amplicon_Recipes). Briefly, pair-end reads were merged at a minimum 90% of identity alignment, and those with  $\leq 1$  expected error were selected (quality filtering). Primer matching was performed with CUTADAPT v.1.9.1 (Martin, 2011). Dereplication and zOTU (zero-radius OTUs) denoising at 100% similarity (UNOISE algorithm) were performed with USEARCH v.10.0.240 (Edgar, 2010). zOTUs were taxonomically annotated against the SILVA database v132 (2017) with the LCA (lowest common ancestor) approach. Finally, zOTUs were quantified to obtain zOTU-abundance tables. Non-prokaryotic ASVs and zOTUs (eukaryotes, chloroplast and mitochondria) were removed from the datasets.

## References

- Alberti, A. (2017) Data Descriptor : Viral to metazoan marine plankton nucleotide sequences from the Tara Oceans expedition. *Sci data* 1–20.
- Callahan, B.J., McMurdie, P.J., Rosen, M.J., Han, A.W., Johnson, A.J.A., and Holmes, S.P. (2016) DADA2: High-resolution sample inference from Illumina amplicon data. *Nat Methods* **13**: 581.
- Edgar, R.C. (2010) Search and clustering orders of magnitude faster than BLAST. *Bioinformatics* **26**: 2460–2461.
- Martin, M. (2011) Cutadapt removes adapter sequences from high-throughput sequencing reads. *EMBnet.journal*; Vol 17, No 1 Next Gener Seq Data Anal - 1014806/ej171200.
- Massana, R., Murray, A.E., Preston, C.M., and DeLong, E.F. (1997) Vertical distribution and phylogenetic characterization of marine planktonic Archaea in the Santa Barbara Channel. *Appl Environ Microbiol* **63**: 50–56.
- Murali, A., Bhargava, A., and Wright, E.S. (2018) IDTAXA: a novel approach for accurate taxonomic classification of microbiome sequences. *Microbiome* **6**: 140.
- Parada, A.E., Needham, D.M., and Fuhrman, J.A. (2016) Every base matters: Assessing small subunit rRNA primers for marine microbiomes with mock communities, time series and global field samples. *Environ Microbiol* **18**: 1403–1414.

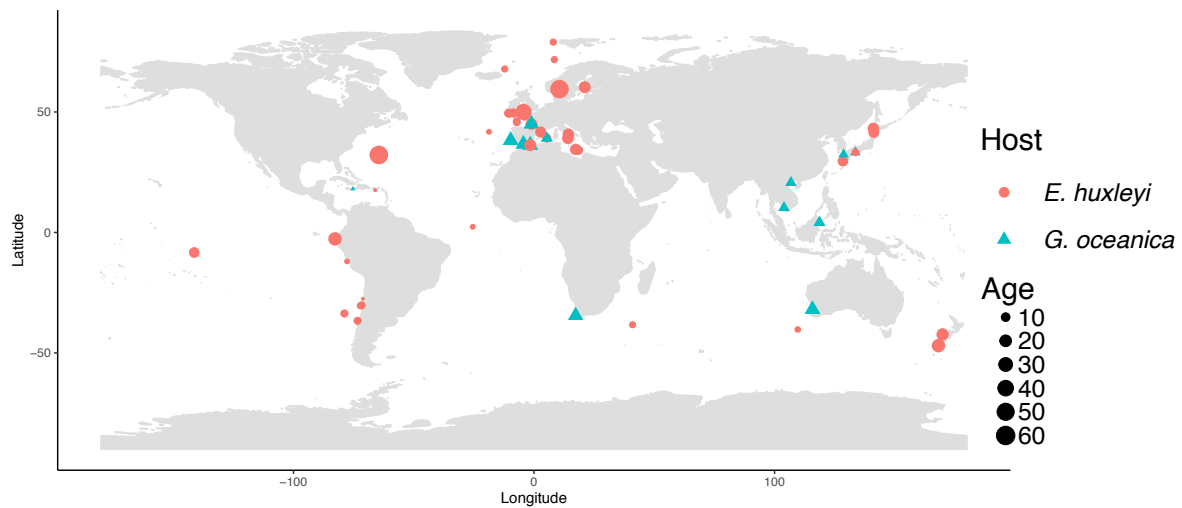
- Pesant, S., Not, F., Picheral, M., Kandels-Lewis, S., Le Bescot, N., Gorsky, G., et al. (2015) Open science resources for the discovery and analysis of Tara Oceans data. *Sci Data* **2**: 150023.
- Rognes, T., Flouri, T., Nichols, B., Quince, C., and Mahé, F. (2016) VSEARCH: a versatile open source tool for metagenomics. *PeerJ* **4**: e2584–e2584.
- Ruiz-González, C., Logares, R., Sebastián, M., Mestre, M., Rodríguez-Martínez, R., Galí, M., et al. (2019) Higher contribution of globally rare bacterial taxa reflects environmental transitions across the surface ocean. *Mol Ecol* **28**: 1930–1945.
- Salazar, G., Cornejo-Castillo, F.M., Benítez-Barrios, V., Fraile-Nuez, E., Álvarez-Salgado, X.A., Duarte, C.M., et al. (2016) Global diversity and biogeography of deep-sea pelagic prokaryotes. *ISME J* **10**: 596–608.

**Supplementary table 1.** Characteristics of strains sequenced at the study. Coccolithophore taxa, *E. huxleyi* cellular morphotype and morphogroups, place and date of isolation and temperature of maintenance. *E. huxleyi* cellular morphotypes and morphogroups were determined based on scanning electron microscopy.

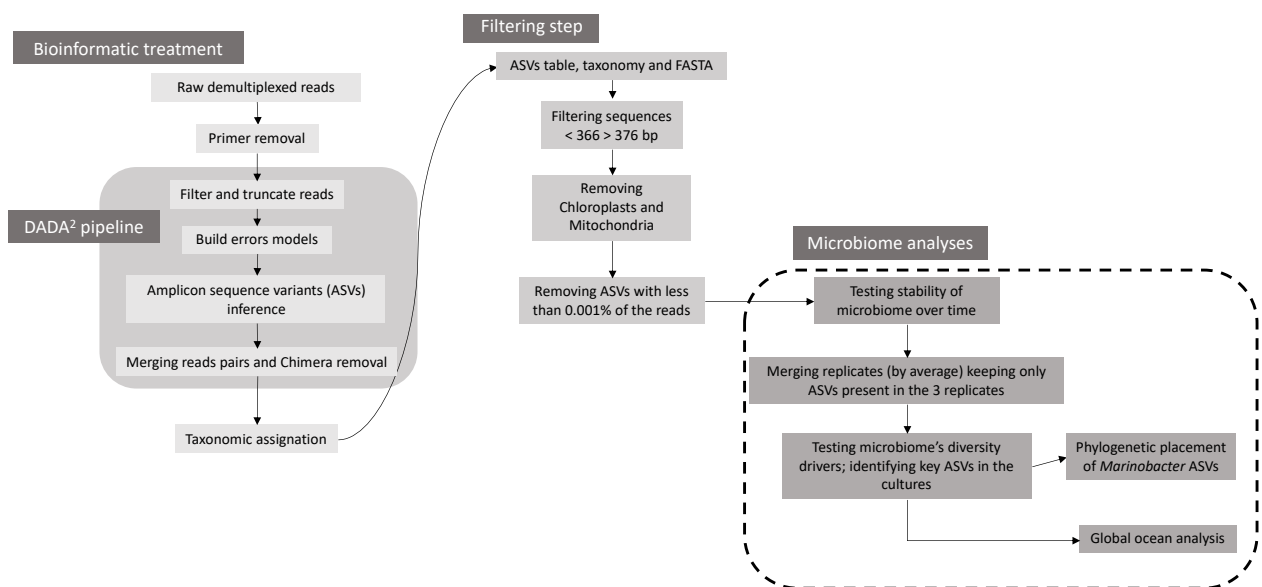
Culture code	Coccolithophore	Cellular morphotype	Cellular morphogroup	Place of isolation				Date of Isolation (DD/MM/YY)	Temperature of maintenance (°C)
				Lat	Long	Oceanic Region	Ocean/Sea of Origin		
ARC30-1	<i>E. huxleyi</i>	A	A	79.00	8.00	Western Coast of Svalbard	Arctic Ocean	01/07/12	15
ARC63-5	<i>E. huxleyi</i>	O	B	71.75	8.44	Norwegian Sea	Arctic Ocean	01/07/12	15
ARC68-3	<i>E. huxleyi</i>	O	B	67.83	-12.20	Northern Icelandic Sea	Arctic Ocean	01/07/12	15
CHC347	<i>E. huxleyi</i>	A	A	-30.25	-71.70	South Pacific	Pacific Ocean	01/11/12	18
NIES1311	<i>E. huxleyi</i>	O	B			Bering sea	Pacific Ocean	01/10/02	15
NIES1313	<i>E. huxleyi</i>	Non-calcifying	Non-calcifying	29.59	128.41	East China Sea	Pacific Ocean	09/09/03	20
NIES837	<i>E. huxleyi</i>	A	A			Great barrier reef australia	Pacific Ocean	01/11/90	20
PLY848	<i>E. huxleyi</i>	A	A	46.20	-7.21	Bay of Biscay	Atlantic Ocean	25/06/11	18
PLY850	<i>E. huxleyi</i>	A	A	45.70	-7.16	Bay of Biscay	Atlantic Ocean	20/06/11	18
RCC1210	<i>E. huxleyi</i>	A	A	59.77	20.64	Baltic Sea	Atlantic Ocean	03/07/98	18
RCC1212	<i>E. huxleyi</i>	B	B	-34.47	17.30	South Atlantic	Atlantic Ocean	01/09/00	18
RCC1213	<i>E. huxleyi</i>	A overcalcified	A	40.80	14.25	Tyrrhenian Sea	Mediterranean Sea	01/12/00	18
RCC1216	<i>E. huxleyi</i>	R	A	-42.30	169.83	Tasman Sea	Pacific Ocean	01/09/98	18
RCC1217	<i>E. huxleyi</i>	Haploid	Haploid	-42.30	169.83	Tasman Sea	Pacific Ocean	01/09/98	18
RCC1239	<i>E. huxleyi</i>	O	B	43.22	141.02		Pacific Ocean	22/04/02	18
RCC1240	<i>E. huxleyi</i>	A	A	41.50	141.25		Pacific Ocean	26/10/02	18
RCC1242	<i>E. huxleyi</i>	Non-calcifying	Non-calcifying	-2.67	-82.72	South Pacific	Pacific Ocean	07/05/91	18
RCC1245	<i>E. huxleyi</i>	A	A	45.00	-1.08	French coast	Atlantic Ocean	01/02/99	18
RCC1253	<i>E. huxleyi</i>	Non-calcifying	Non-calcifying	43.22	141.02		Pacific Ocean	22/04/02	18
RCC1255	<i>E. huxleyi</i>	Non-calcifying	Non-calcifying	59.50	10.60		Atlantic Ocean	12/05/59	18

RCC1260	<i>E. huxleyi</i>	Non-calcifying	Non-calcifying	32.17	-64.50	Sargasso Sea	Atlantic Ocean	20/04/60	18
RCC1265	<i>E. huxleyi</i>	Non-calcifying	Non-calcifying	49.58	-8.20		Atlantic Ocean	01/08/07	18
RCC1272	<i>E. huxleyi</i>	A	A	49.50	-10.50		Atlantic Ocean	01/08/07	18
RCC1322	<i>E. huxleyi</i>	A	A	36.25	-1.58	Alboran Sea	Mediterranean Sea	01/05/98	18
RCC173	<i>E. huxleyi</i>	Non-calcifying	Non-calcifying	32.17	-64.50	Sargasso Sea	Atlantic Ocean	20/04/60	18
RCC174	<i>E. huxleyi</i>	Non-calcifying	Non-calcifying	50.03	-4.37	English Channel	Atlantic Ocean	01/07/75	18
RCC1830	<i>E. huxleyi</i>	A overcalcified	A	39.10	5.35		Mediterranean Sea	01/09/08	18
RCC1844	<i>E. huxleyi</i>	A	A	34.13	18.45		Mediterranean Sea	01/09/08	18
RCC1844	<i>E. huxleyi</i>	A	A	34.13	18.45		Mediterranean Sea	01/09/08	18
RCC192	<i>E. huxleyi</i>	A	A				Atlantic Ocean		18
RCC3545	<i>E. huxleyi</i>	Non-calcifying	Non-calcifying						18
RCC3549	<i>E. huxleyi</i>	A overcalcified	A	-46.98	168.10	South Pacific	Pacific Ocean	01/01/92	18
RCC3716	<i>E. huxleyi</i>	A	A	33.25	133.63		Pacific Ocean	20/12/11	18
RCC3811	<i>E. huxleyi</i>	R	A	-30.25	-71.70	South East Pacific	Pacific Ocean	01/10/11	18
RCC3835	<i>E. huxleyi</i>	R	A	-30.25	-71.70	South East Pacific	Pacific Ocean	01/10/11	18
RCC3909	<i>E. huxleyi</i>	R	A	-36.65	-73.33	South East Pacific	Pacific Ocean	01/10/11	18
RCC3917	<i>E. huxleyi</i>	R	A	-36.65	-73.33	South East Pacific	Pacific Ocean	01/10/11	18
RCC3962	<i>E. huxleyi</i>	R	A	-33.63	-78.82	South East Pacific	Pacific Ocean	01/10/11	18
RCC3985	<i>E. huxleyi</i>	R	A	-33.63	-78.82	South East Pacific	Pacific Ocean	01/10/11	18
RCC4549	<i>E. huxleyi</i>	Non-calcifying	Non-calcifying	41.77	-18.75		Atlantic Ocean	30/09/14	18
RCC4560	<i>E. huxleyi</i>	Non-calcifying	Non-calcifying	2.35	-25.48		Atlantic Ocean	12/10/14	18
RCC458	<i>E. huxleyi</i>	Non-calcifying	Non-calcifying	48.75	-3.95	English Channel	Atlantic Ocean	16/05/01	18
RCC502	<i>E. huxleyi</i>	Non-calcifying	Non-calcifying	41.67	2.80	Balearic Sea	Mediterranean Sea	25/06/01	18
RCC5115	<i>E. huxleyi</i>	A overcalcified	A	-27.51	-71.13	South East Pacific	Pacific Ocean	07/12/15	18
RCC5134	<i>E. huxleyi</i>	O	B	-30.15	-71.97	South East Pacific	Pacific Ocean	23/11/15	18
RCC6302	<i>E. huxleyi</i>	A	A	17.51	-66.03	Caribbean Sea	Atlantic Ocean	20/12/15	18
RCC6354	<i>E. huxleyi</i>	A	A			South East Pacific	Pacific Ocean		18

RCC6536	<i>E. huxleyi</i>	B	B						20
RCC6617	<i>E. huxleyi</i>	A	A				Pacific Ocean	15/05/15	18
RCC6648	<i>E. huxleyi</i>	A overcalcified	A	-12.00	-77.42	South East Pacific	Pacific Ocean	15/05/14	18
RCC6676	<i>E. huxleyi</i>	Non-calcifying	Non-calcifying						18
RCC904	<i>E. huxleyi</i>	Non-calcifying	Non-calcifying	39.12	14.08		Mediterranean Sea	27/09/99	18
RCC955	<i>E. huxleyi</i>	Non-calcifying	Non-calcifying	-8.33	-	Marquesas islands	Pacific Ocean	29/10/04	18
RCC963	<i>E. huxleyi</i>	A	A	-8.33	-	Marquesas islands	Pacific Ocean	29/10/04	18
SOI-3	<i>E. huxleyi</i>	A	A	-38.32	40.96	Agulhas Front	Indian Ocean	01/04/13	15
SOI4-3	<i>E. huxleyi</i>	A	A	-40.26	109.63	Subtropical Front	Indian Ocean	01/04/13	15
SO63-03	<i>E. huxleyi</i>	A	A	-38.32	40.96	Agulhas Front	Indian Ocean	01/04/13	15
SO68-01	<i>E. huxleyi</i>	O	B	-38.32	40.96	Agulhas Front	Indian Ocean	01/04/13	15
RCC1281	<i>G. oceanica</i>			-31.93	115.73	Tasman Sea	Pacific Ocean	01/09/00	18
RCC1293	<i>G. oceanica</i>			-34.47	17.30	South Atlantic	Atlantic Ocean	01/09/00	18
RCC1296	<i>G. oceanica</i>			36.68	-4.42	Balearic Sea	Mediterranean Sea	01/04/98	18
RCC1300	<i>G. oceanica</i>					Gulf of California	Pacific Ocean		18
RCC1303	<i>G. oceanica</i>			45.00	-1.08		Atlantic Ocean	01/02/99	18
RCC1306	<i>G. oceanica</i>			38.23	-9.72		Atlantic Ocean	01/07/98	18
RCC1313	<i>G. oceanica</i>			36.25	-1.58	Alboran Sea	Mediterranean Sea	01/05/98	18
RCC1318	<i>G. oceanica</i>			-31.93	115.73	Tasman Sea	Pacific Ocean	01/09/00	18
RCC1792	<i>G. oceanica</i>			20.68	106.80	South China Sea	Pacific Ocean	13/03/09	22
RCC1804	<i>G. oceanica</i>			4.12	118.65	Celebes Sea	Pacific Ocean	09/12/08	22
RCC1836	<i>G. oceanica</i>			39.10	5.35		Mediterranean Sea	01/09/08	18
RCC3481	<i>G. oceanica</i>			10.27	103.92	South China Sea	Pacific Ocean	18/02/09	22
RCC3711	<i>G. oceanica</i>			33.25	133.63		Pacific Ocean	08/11/11	18
RCC3724	<i>G. oceanica</i>			32.42	128.67		Pacific Ocean	25/10/11	18
RCC6253	<i>G. oceanica</i>			18.11	-75.26	Caribbean Sea	Atlantic Ocean	18/12/15	18

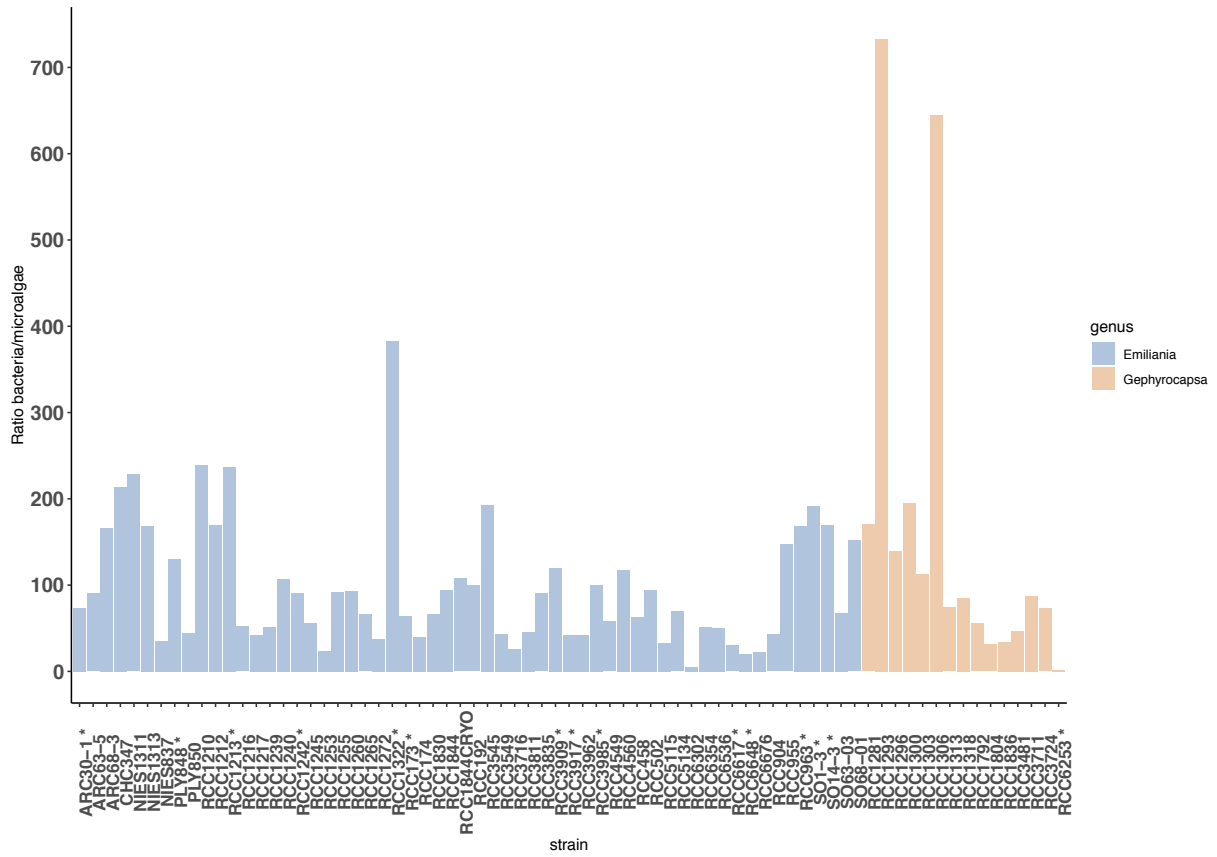


**Supplementary figure 1.** Map of *E. huxleyi* and *G. oceanica* cultures origin (color coded). The size of the shape corresponds to the age of the culture.

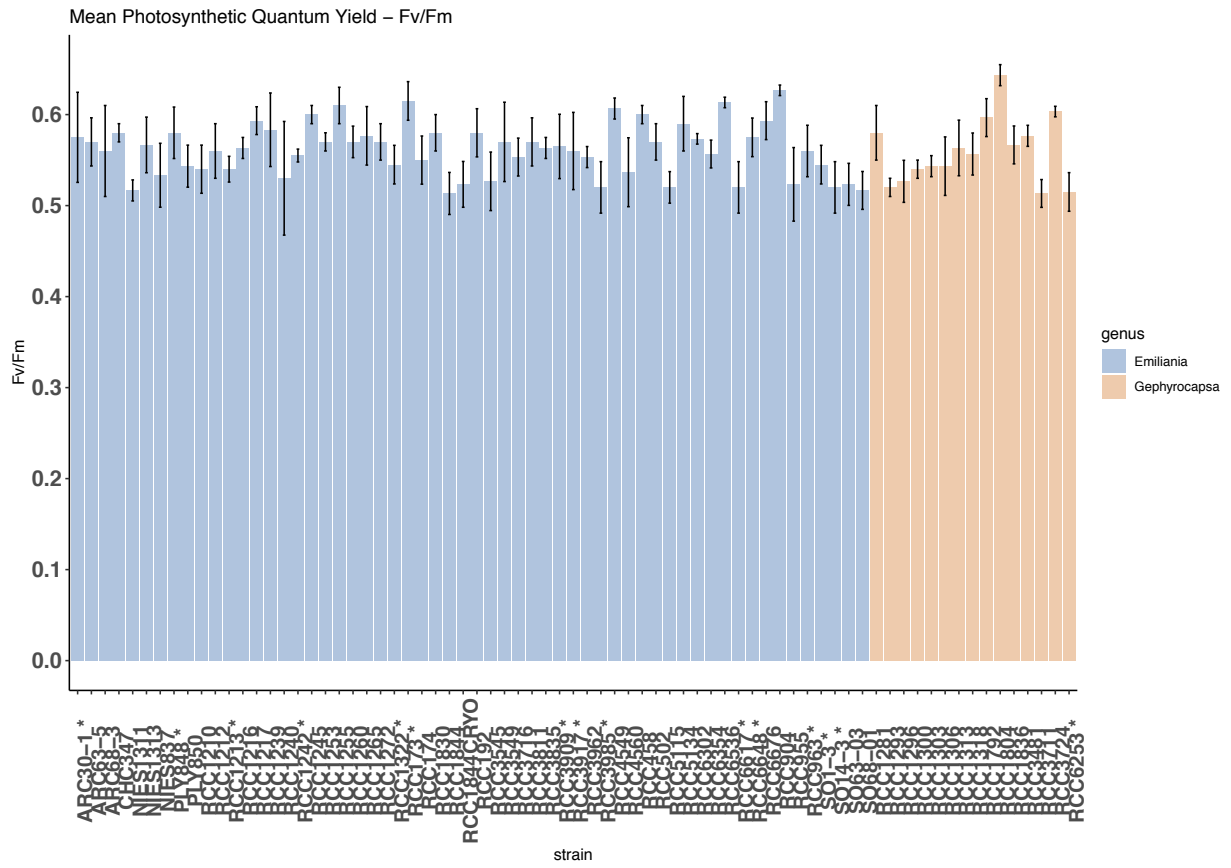


**Supplementary figure 2.** Workflow of analysis from raw demultiplexed reads. Details of the scripts used can be found at [https://github.com/mcamarareis/Coccolithophores\\_microbiomes](https://github.com/mcamarareis/Coccolithophores_microbiomes).

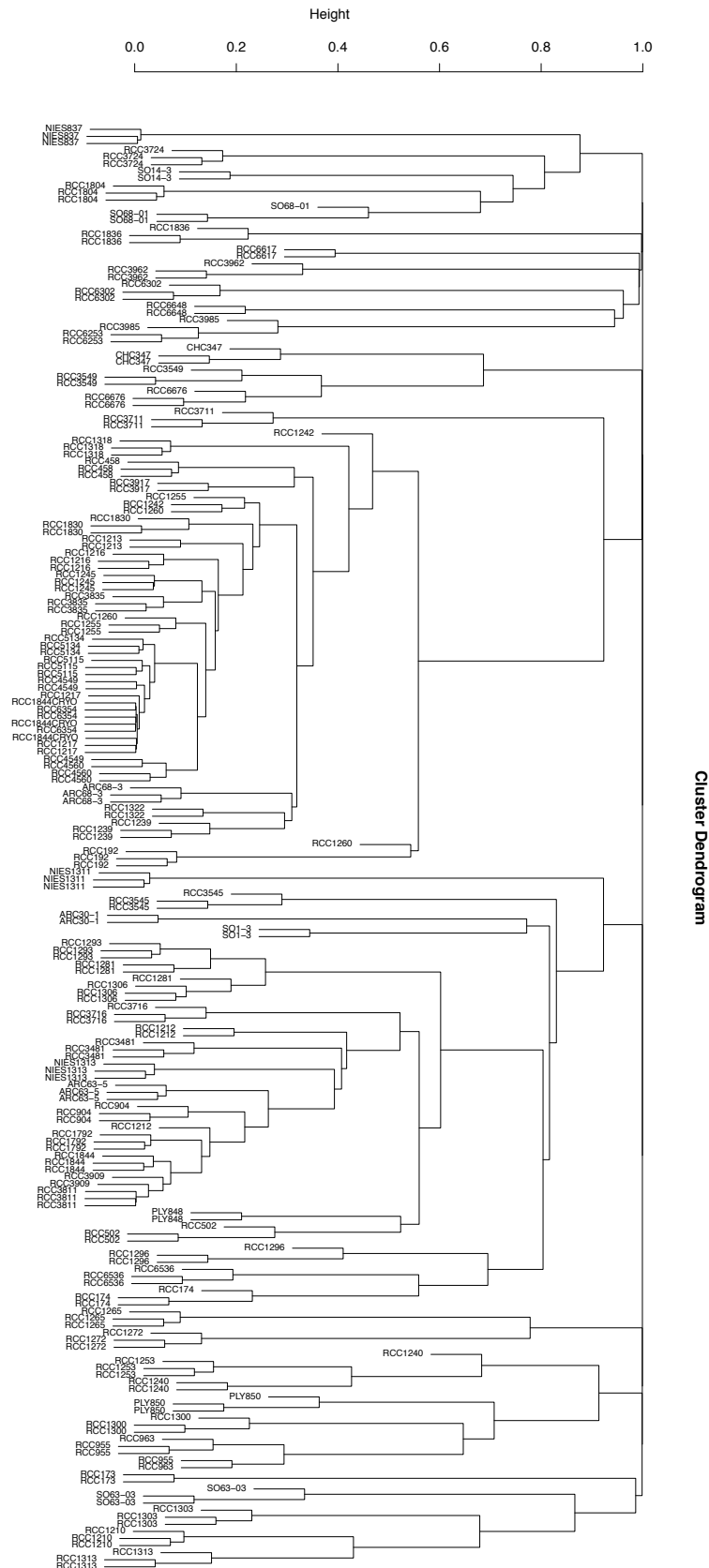




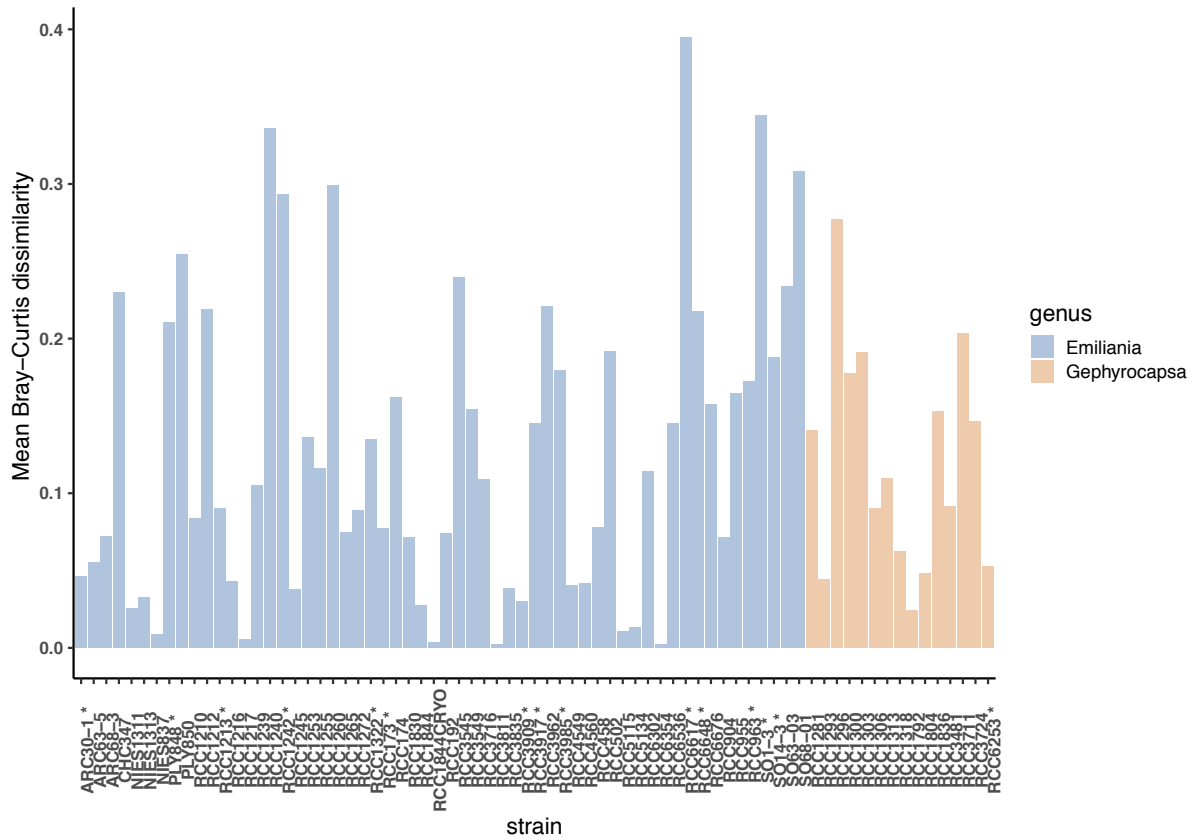
**Supplementary figure 4.** Mean Bacteria/coccolithophores ratio for each culture. Cultures with asterisk (\*) were sampled two times.



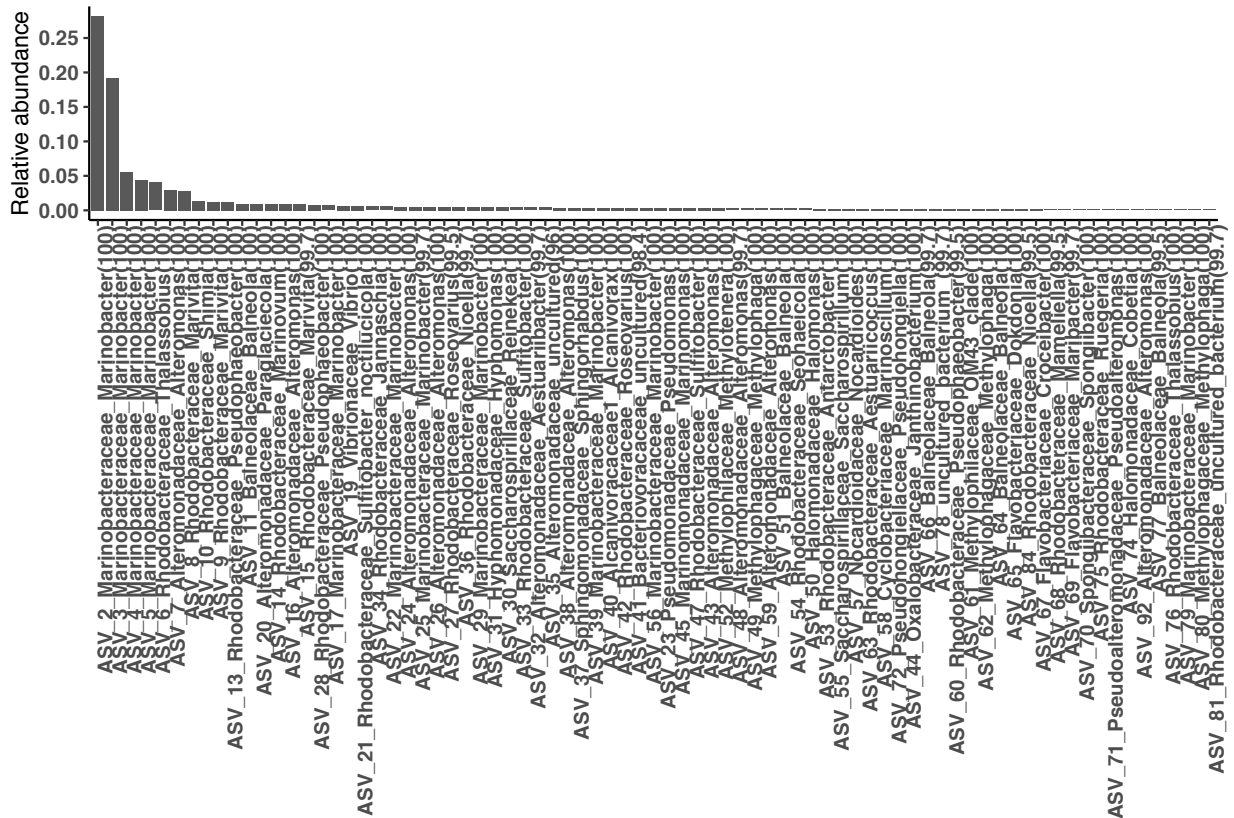
**Supplementary figure 5.** Mean and standard deviation of photosynthetic quantum yield over. Consecutive culture transfers for each culture. Cultures with asterisk (\*) were sampled two times.



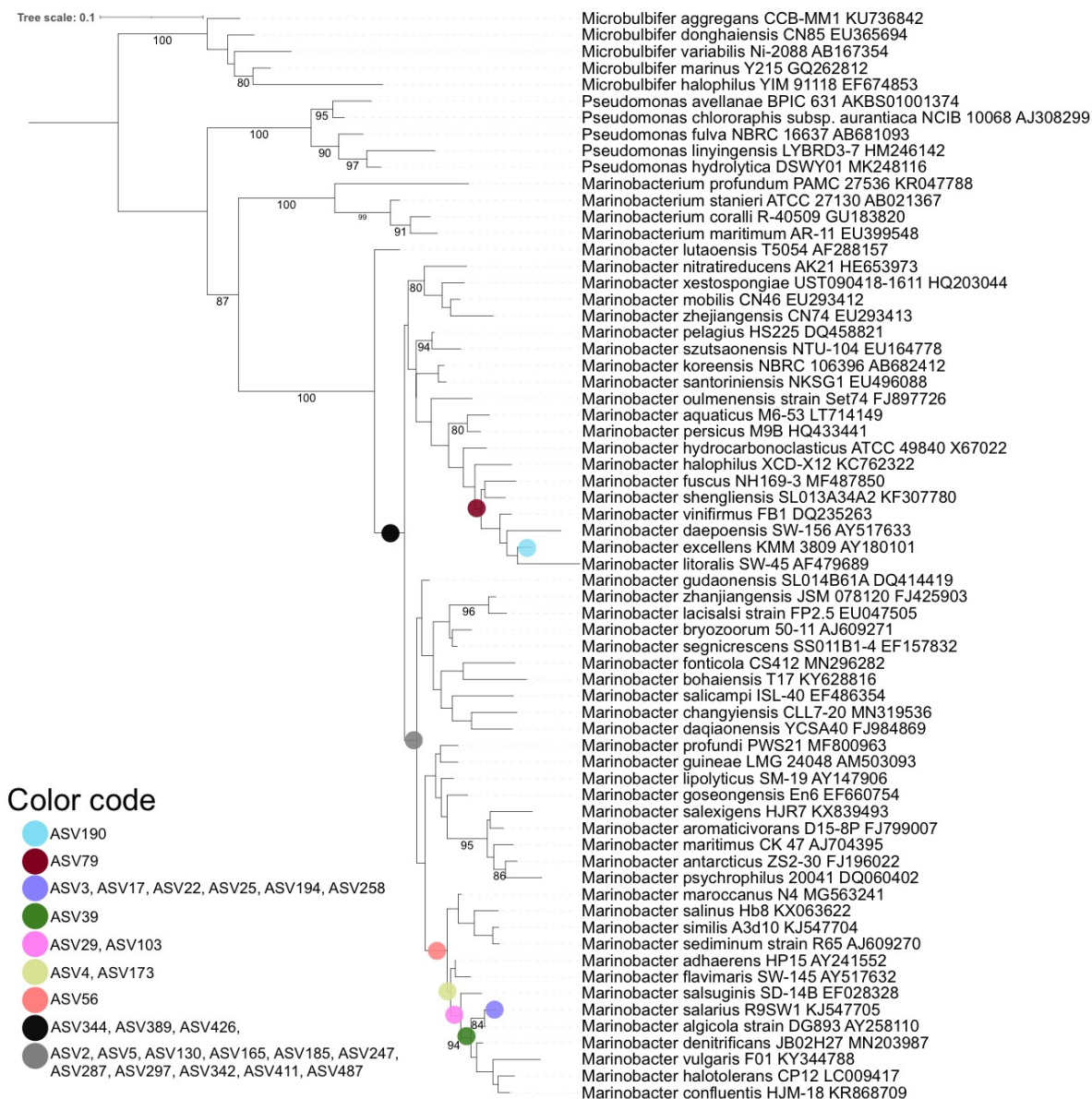
**Supplementary figure 6.** Hierarchical cluster analysis using complete linkage method of Bray-Curtis dissimilarity of the microbiomes sampled at two/three consecutive culture transfers for maintenance.



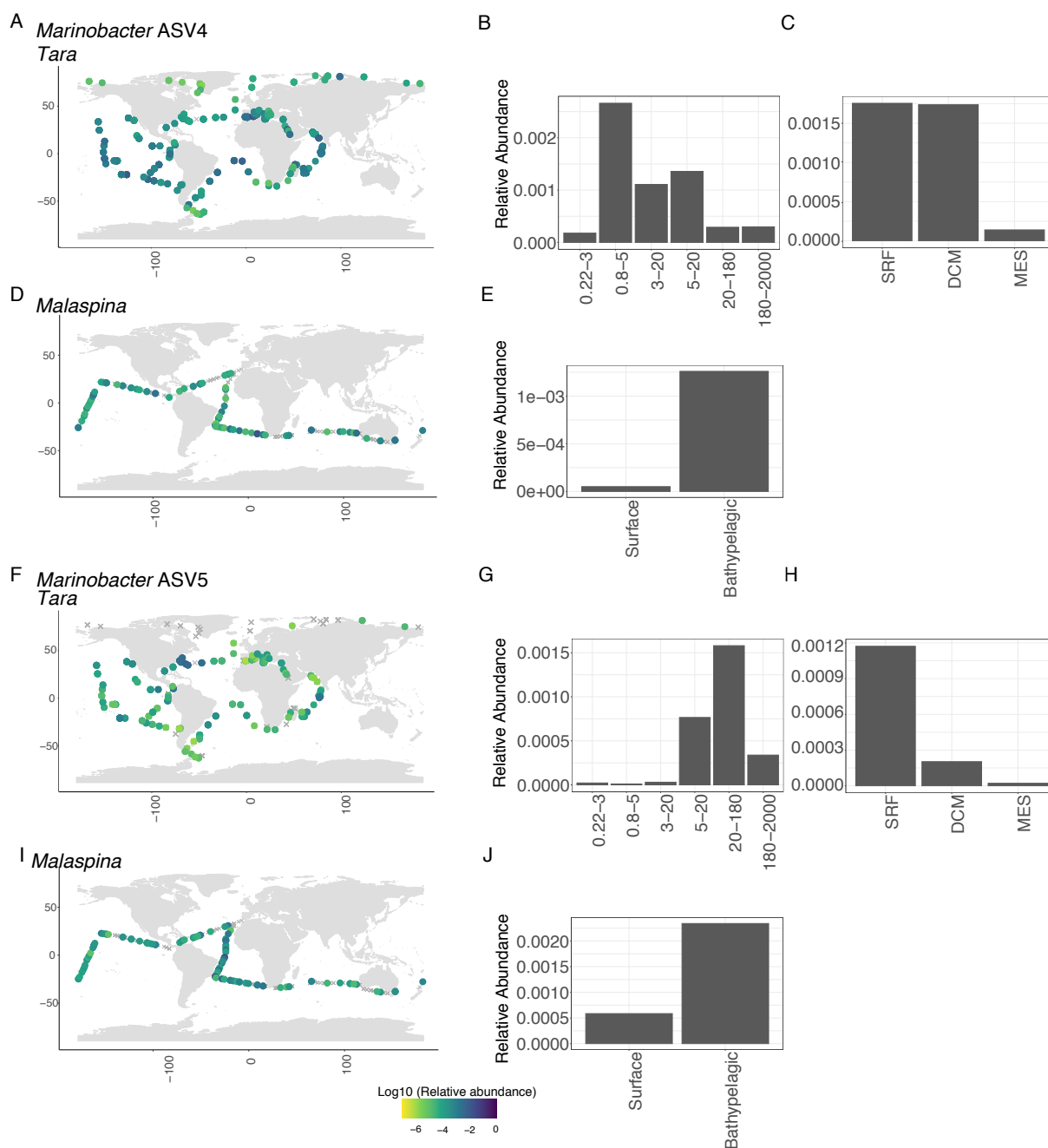
**Supplementary figure 7.** Mean Bray-Curtis dissimilarity between replicate cultures of coccolithophore strains. The asterisks indicate strains for which only 2 replicate cultures were obtained.



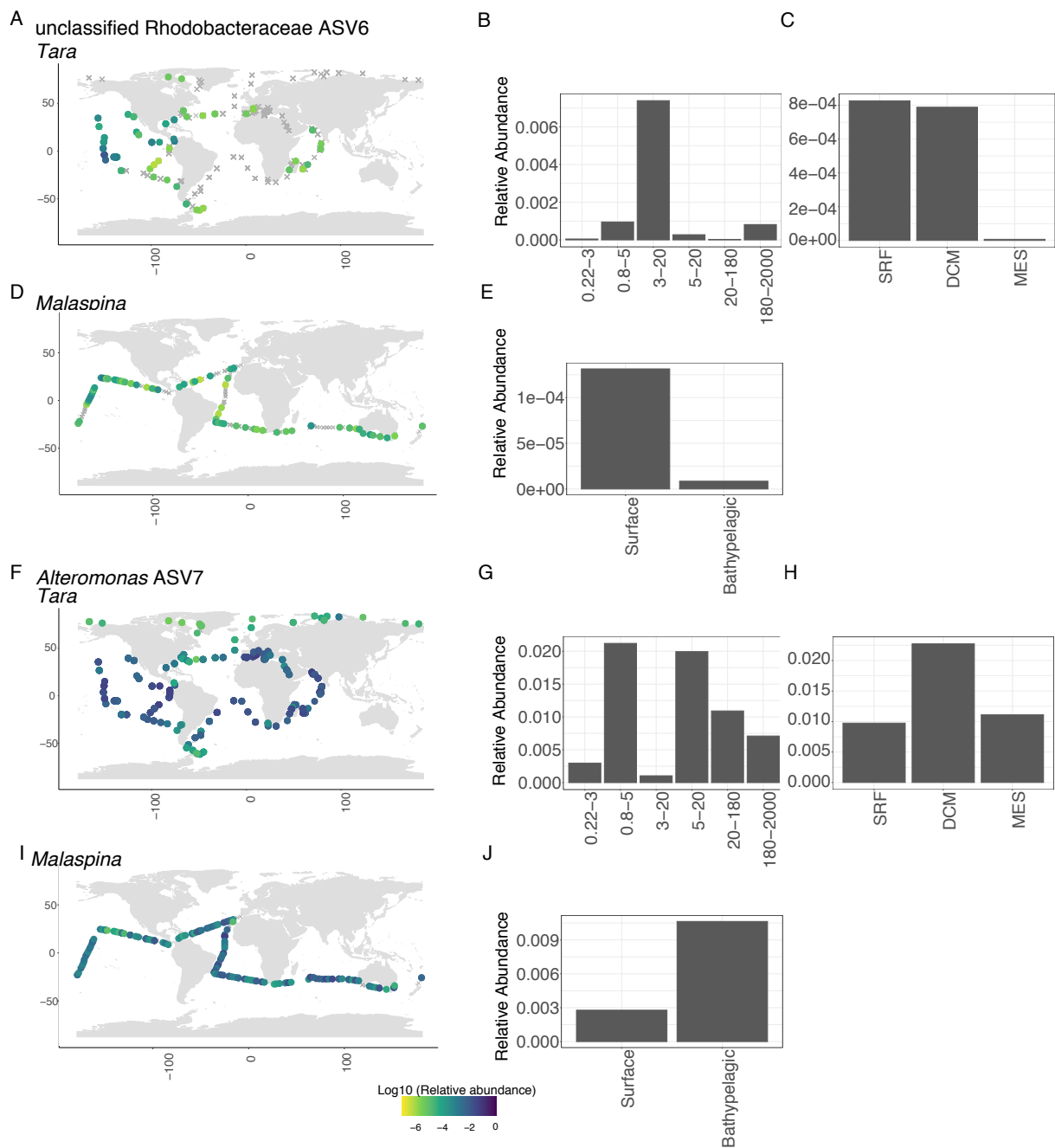
**Supplementary figure 8.** Relative abundance (proportion) and taxonomic classification (family\_genus\_(identity)) of ASVs accounting to more than 0.1% of the total of reads. Taxonomic assignment from vsearch.



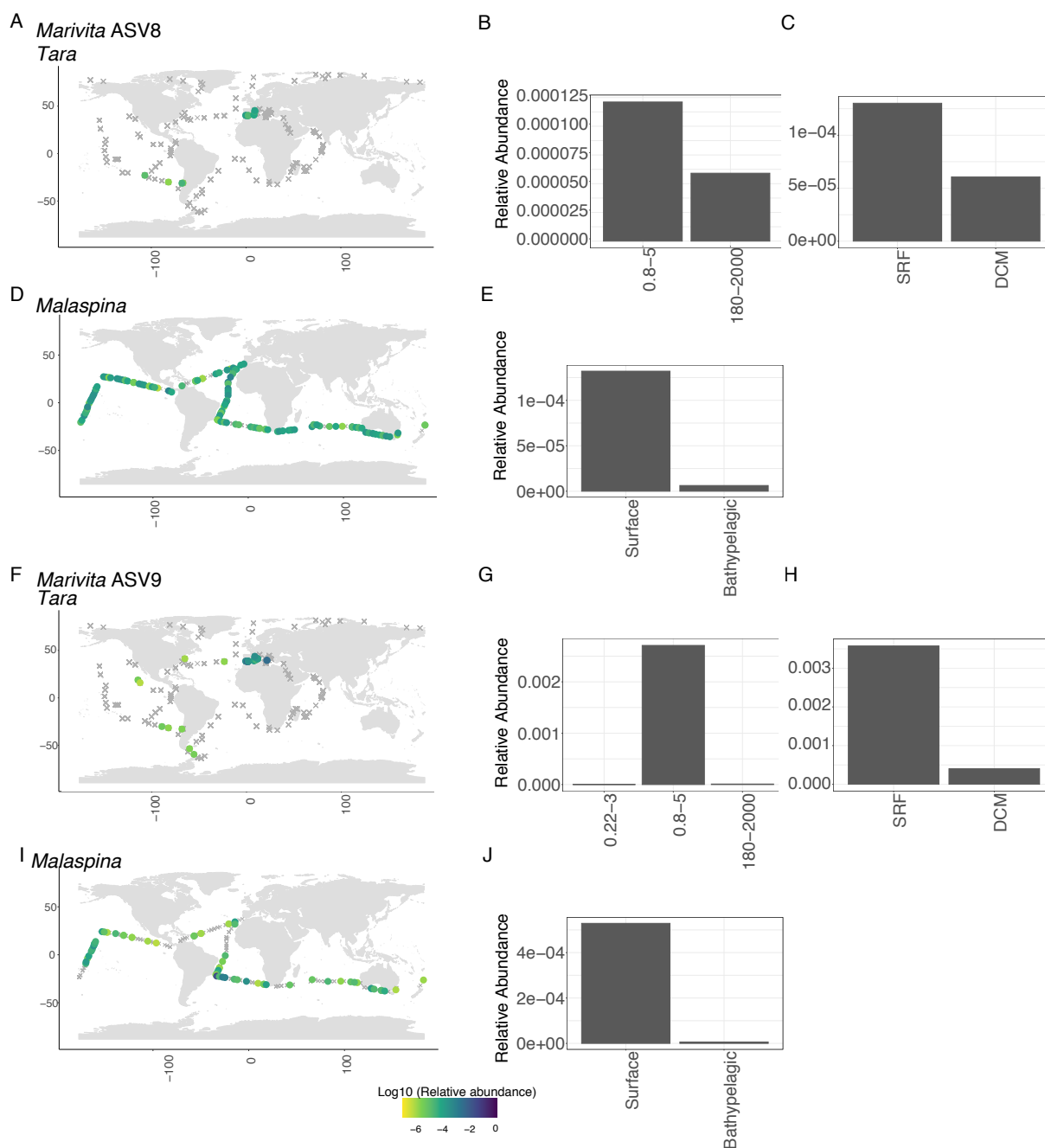
**Supplementary figure 9.** Phylogenetic placement of *Marinobacter* ASVs in the *Marinobacter* reference tree (sequences 1382 bp).



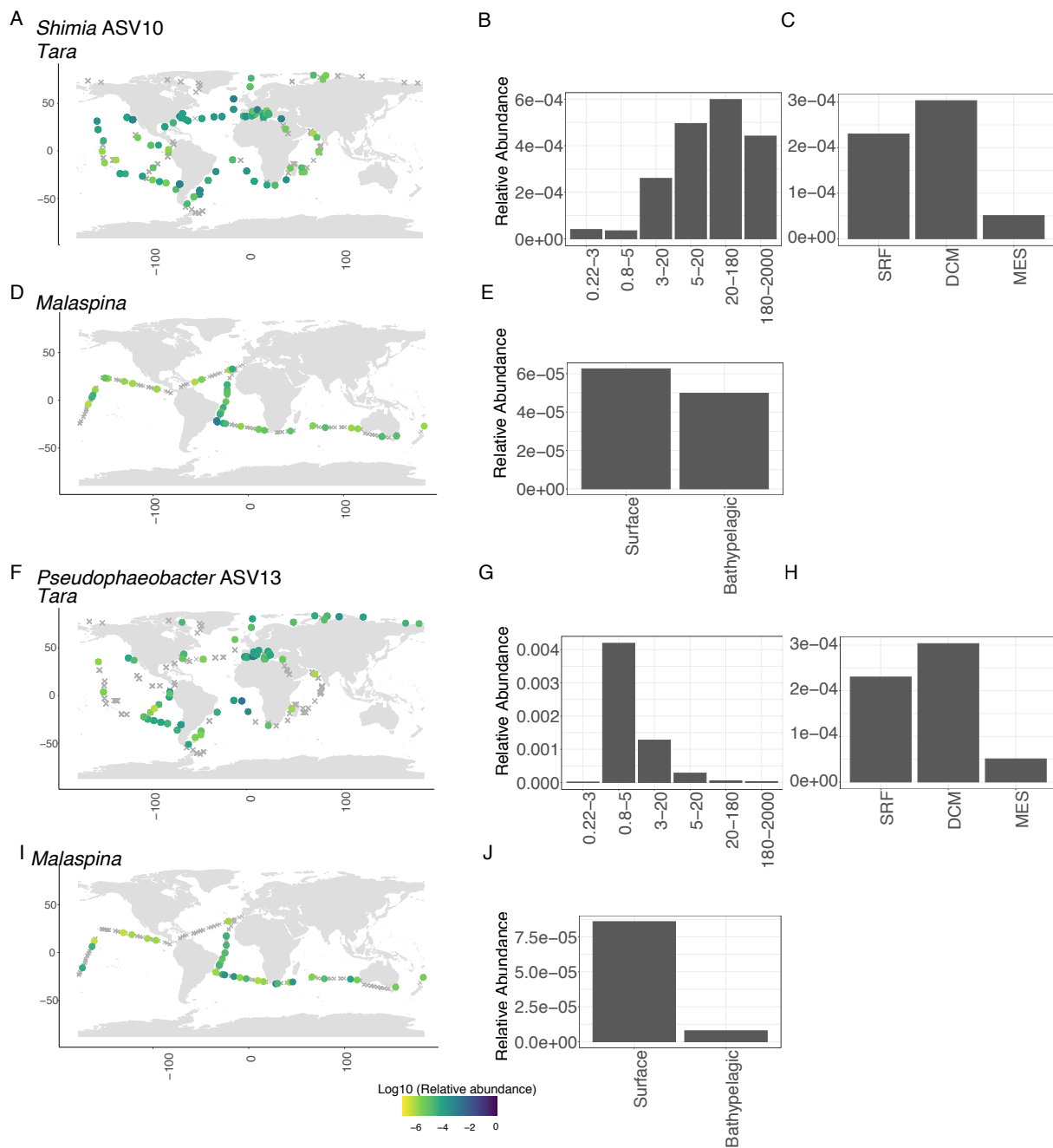
**Supplementary figure 10.** Relative abundance (proportion) and distribution of dominant coccolithophores-associated *Marinobacter* ASVs in the *Tara* Oceans and *Malaspina* expeditions. (A) Log<sub>10</sub>-transformed relative abundance of ASV4 in *Tara* Oceans dataset. (B) Relative abundance of ASV4 in *Tara* Oceans dataset by plankton size fraction. (C) by depth. (D) Log<sub>10</sub>-transformed relative abundance of ASV4 in the *Malaspina* dataset. (E) Relative abundance of ASV4 in *Malaspina* dataset by depth. (F) Log<sub>10</sub>-transformed relative abundance of ASV5 in *Tara* Oceans dataset. (G) Relative abundance of ASV5 in *Tara* Oceans dataset by size fraction. (H) by depth. (I) Log<sub>10</sub>-transformed relative abundance of ASV5 in the *Malaspina* dataset. (J) Relative abundance of ASV5 in *Malaspina* dataset by depth. Relative abundance was calculated as the number of reads of the ASV/zOTU by station/size fraction/depth divided by the total number of reads at the corresponding station/size fraction/depth.



**Supplementary figure 11.** Relative abundance (proportion) and distribution of dominant coccolithophores-associated ASVs in the *Tara* Oceans and *Malaspina* expeditions. (A) Log<sub>10</sub>-transformed relative abundance of ASV6 in *Tara* Oceans dataset. (B) Relative abundance of ASV6 in *Tara* Oceans dataset by plankton size fraction. (C) by depth. (D) Log<sub>10</sub>-transformed relative abundance of ASV6 in the *Malaspina* dataset. (E) Relative abundance of ASV6 in *Malaspina* dataset by depth. (F) Log<sub>10</sub>-transformed relative abundance of ASV7 in *Tara* Oceans dataset. (G) Relative abundance of ASV7 in *Tara* Oceans dataset by size fraction. (H) by depth. (I) Log<sub>10</sub>-transformed relative abundance of ASV7 in the *Malaspina* dataset. (J) Relative abundance of ASV7 in *Malaspina* dataset by depth. Relative abundance was calculated as the number of reads of the ASV/zOTU by station/size fraction/depth divided by the total number of reads at the corresponding size station/fraction/depth.



**Supplementary figure 12.** Relative abundance (proportion) and distribution of dominant coccolithophores-associated ASVs in the *Tara* Oceans and *Malaspina* expeditions. (A) Log<sub>10</sub>-transformed relative abundance of ASV8 in *Tara* Oceans dataset. (B) Relative abundance of ASV8 in *Tara* Oceans dataset by plankton size fraction. (C) by depth. (D) Log<sub>10</sub>-transformed relative abundance of ASV8 in the *Malaspina* dataset. (E) Relative abundance of ASV8 in *Malaspina* dataset by depth. (F) Log<sub>10</sub>-transformed relative abundance of ASV9 in *Tara* Oceans dataset. (G) Relative abundance of ASV9 in *Tara* Oceans dataset by size fraction. (H) by depth. (I) Log<sub>10</sub>-transformed relative abundance of ASV9 in the *Malaspina* dataset. (J) Relative abundance of ASV9 in *Malaspina* dataset by depth. Relative abundance was calculated as the number of reads of the ASV/zOTU by station/size fraction/depth divided by the total number of reads at the corresponding station/size fraction/depth.



**Supplementary figure 13.** Relative abundance (proportion) and distribution of dominant coccolithophores-associated ASVs in the *Tara* Oceans and *Malaspina* expeditions. (A) Log<sub>10</sub>-transformed relative abundance of ASV10 in *Tara* Oceans dataset. (B) Relative abundance of ASV10 in *Tara* Oceans dataset by plankton size fraction. (C) by depth. (D) Log<sub>10</sub>-transformed relative abundance of ASV10 in the *Malaspina* dataset. (E) Relative abundance of ASV10 in *Malaspina* dataset by depth. (F) Log<sub>10</sub>-transformed relative abundance of ASV13 in *Tara* Oceans dataset. (G) Relative abundance of ASV13 in *Tara* Oceans dataset by size fraction. (H) by depth. (I) Log<sub>10</sub>-transformed relative abundance of ASV13 in the *Malaspina* dataset. (J) Relative abundance of ASV13 in *Malaspina* dataset by depth. Relative abundance was calculated as the number of reads of the ASV/zOTU by station/size fraction/depth divided by the total number of reads at the corresponding station/size fraction/depth.





---

# CHAPTER 2

---



## Chapter 2

This second chapter is dedicated to the investigation of the processes of microbiome assembly in phytoplankton cultures. The study was guided by the results obtained in **Chapter 1**, where I did not find a significant influence of the parameters tested (host species, *E. huxleyi* morphogroups, age of the cultures and place of isolation) on the diversity of coccolithophores-associated bacteria. These results raised the question about the selection of microbiomes in cultures. Do they result from deterministic processes or are they randomly selected? To answer this question, I screened the Roscoff Culture Collection to extract phytoplankton species, including *E. huxleyi*, that were isolated from the same seawater samples and for which environmental parameters were available. Then, I compared their associated microbiomes with the objective of identifying and quantifying the influence of environmental filters, host specificity, culture media and random selection on their diversity.

We hypothesized that if the environmental filters drive the microbiome selection this would be identified by correlating community composition and environmental parameters. Conversely, if the host drives the assembly, we would find consistency in the microbiomes of each microalgal group whatever their sample of origin. Similar conclusions were expected if the medium contributed to the selection of phytoplankton microbiomes. Consequently, microalgae isolated using the same medium, independent of host or sample of origin would have the most similar microbiomes. Finally, if the assembly process was guided by random selection, we expected to find no consistency in the microbiomes at any level tested.

This chapter expanded the knowledge regarding the factors involved in microbiome selection by showing that environmental parameters at the time of isolation were significantly responsible for the microbiome composition in cultures while the influence of the hosts was low. In addition, we also identified the influence of the culture medium and a shared effect of medium and environment that could not be disentangled. To our knowledge, this is the first study investigating the influence of environmental parameters on the diversity of microbiomes maintained for many years (up to 22 years) in laboratory conditions. This work will be submitted to *Environmental Microbiology Reports*.



## **Microbiome assembly in phytoplankton cultures is partially driven by deterministic processes**

Mariana Câmara dos Reis<sup>1</sup>, Sarah Romac<sup>1</sup>, Florence Le Gall<sup>1</sup>, Nicolas Henry<sup>1,2</sup>,  
Colomban de Vargas<sup>1,2</sup>, Christian Jeanthon<sup>1</sup>

<sup>1</sup> Sorbonne Université/Centre National de la Recherche Scientifique, UMR7144, Adaptation et Diversité en Milieu Marin, ECOMAP, Station Biologique de Roscoff, Place Georges Teissier, Roscoff, France.

<sup>2</sup>Research Federation for the study of Global Ocean Systems Ecology and Evolution, FR2022/*Tara* GOSEE, Paris, France

**Running title:** Microbiome assembly in marine phytoplankton cultures

### **Abstract**

Phytoplankton and bacteria display tightly coupled interactions that have large scale impacts on aquatic ecosystem functioning. Although relationships between phytoplankton hosts and their associated microbiomes have been thoroughly studied over the last years, the understanding of community organization in phycosphere microbiomes is still limited. Here we investigated the influence of environmental filters, host types, and medium selection in the processes of bacterial community assembly in marine phytoplankton cultures. For this, we examined the microbiome composition of phytoplankton cultures from different taxonomic groups that were isolated from the same seawater samples collected from diverse marine regions. Variation partitioning analysis performed using five beta-diversity metrics revealed that environmental parameters (mainly temperature) from the original seawater samples consistently drove microbiome composition patterns, with additional effect of the culture medium used for isolation and maintenance. The influence of environmental parameters on cultured phytoplankton microbiomes was also supported by indicator bacterial species. On the other hand, host specificity had low influence on the process of microbiome assembly. Overall, our results suggest the influence of environmental filtering on phytoplankton-associated communities kept in culture for many years, highlighting the robustness of these communities.

## Introduction

Marine phytoplankton and bacteria display tightly connected interactions that can strongly influence global biogeochemical processes, such as the carbon and nutrient cycles in the oceans (Amin *et al.*, 2015; Seymour *et al.*, 2017). The surrounding region of the phytoplankton cell, the phycosphere, is characterized by a gradient of oxygen and organic compounds which connects phytoplankton to the surrounding bacterial communities through the exchanges of molecules (Seymour *et al.*, 2017; Kimbrel *et al.*, 2019). In the past decades, numerous studies documented the diversity of phycosphere-associated bacteria in marine natural phytoplankton populations (Buchan *et al.*, 2014; Zhou *et al.*, 2018, 2019) and in cultures (Grossart, 1999; Green *et al.*, 2015; Krohn-Molt *et al.*, 2017; Ajani *et al.*, 2018; Behringer *et al.*, 2018; Lawson *et al.*, 2018; Sörenson *et al.*, 2019; Mönnich *et al.*, 2020). Roseobacters, Flavobacteriia and members of the Gammaproteobacteria are typically the most dominant phytoplankton-associated bacteria (Buchan *et al.*, 2014; Amin *et al.*, 2015). However, little is known about the drivers determining the composition and structure of these complex assemblages.

Assembly process in the phycosphere is often discussed in the framework of the traditional niche-based theory, which postulates that specific variables (biotic and abiotic interactions, life history traits) determine how communities are organized (Hutchinson, 1957). Deterministic processes, such as the host genotypes (Eigemann *et al.*, 2013; Behringer *et al.*, 2018; Lawson *et al.*, 2018; Sörenson *et al.*, 2019) and the place of origin (Ajani *et al.*, 2018), were shown to have an important role on selecting the microbiome diversity of marine phytoplankton cultures. Phytoplankton species can release specific organic compounds which select for their phycosphere-associated bacteria (Smriga *et al.*, 2016; Fu *et al.*, 2020). Phytoplankton cultures can be affected by culture conditions (light intensity and medium composition), which are suspected to have also a critical role in the establishment and diversity of associated bacterial communities (Behringer *et al.*, 2018; Jackrel *et al.*, 2020). In the ocean, local physico-chemical conditions are key drivers of the abundance and distribution of phytoplankton and bacterial populations, which in turn, can impact their community composition (De Vargas *et al.*, 2015; Sunagawa *et al.*, 2015; Zhou *et al.*, 2018; Logares *et al.*, 2020). Finally, biological interactions are also forces that shape phytoplankton-associated bacterial communities in culture (Eigemann *et al.*, 2013; Majzoub *et al.*, 2019) and in the field (Zhou *et al.*, 2018).

Recently, assembly models such as the ‘competitive lottery’, that take into account the influence of stochasticity in determining the community structure, have been used in phycosphere studies (Kimbrel *et al.*, 2019; Zhou *et al.*, 2019; Mönnich *et al.*, 2020). The competitive lottery model proposes that a pool of species sharing the same niche are equally able to colonize it and the one arriving first wins the lottery (Sale, 1979). The model considers the redundancy of species that are equally able to colonize a niche and the influence of stochastic and priority effects determining which species will succeed. Increasing attention is currently brought to this model in microalgal microbiome studies because it can explain why bacterial groups present in low abundance in the natural environment (as free living) are typically enriched in phytoplankton blooms and cultures, suggesting that they represent a functional guild able to colonize the phycosphere (Buchan *et al.*, 2014). Meanwhile, this model can also explain how stochasticity is involved in the recruitment of different microbiomes within strains of the same phytoplankton species (Ajani *et al.*, 2018).

In this study, our objective was to disentangle deterministic and stochastic factors driving the diversity of phytoplankton-associated bacteria. We used cultures of different phytoplankton groups isolated from the same seawater samples in various oceanic regions. We identified their associated bacterial taxa and examined the effect of oceanic environmental parameters, hosts type, and culture media composition on the microbiome assembly. Our results demonstrate the detectable influence of environmental filtering on the bacterial communities associated with phytoplankton cultures even after years of laboratory maintenance and question the role of the host in the microbiome assembly.

## **Material and Methods**

### **Origin and growth conditions of phytoplankton cultures**

The 43 strains used in this study were isolated from six oceanographic cruises and were obtained from the Roscoff Culture Collection (RCC, <http://roscoff-culture-collection.org/>) (Supplementary table 1). These sampling cruises covered a wide variety of oceanic regions that displayed different trophic regimes in the Mediterranean Sea, the North to South Atlantic, and the South-East and South-West Pacific oceans (reference information on these cruises is detailed in the Supplementary Methods). Monoclonal phytoplankton batch cultures were established by isolating single cells either by micropipetting, filtration, serial dilution or flow cytometry cell sorting, transferred into culture medium and maintained under specific

conditions by the RCC (Supplementary Table 1). Upon receipt, cultures were grown using their routine maintenance conditions (Supplementary Table 1) in different culture media prepared using natural aged seawater collected at the SOMLIT-ASTAN monitoring site (48°46'18''N-3°58' 6''W) (Brittany, France). All the media recipes are available at: <http://roscoff-culture-collection.org/culture-media>. Cultures (20 mL) were grown in 50 mL vented tissue culture flasks on a 12h light and 12h dark cycle under a white light irradiance (Philips Master TL\_D 18W/865). Prior to experiments, cryopreserved cultures were acclimated to the growth conditions for at least two growth cycles. Cultures were established by transferring aliquots (200 µL) into 20 mL of medium.

### **DNA sampling, extraction, and 16S rRNA sequencing**

Once the cultures reached mid-late log phase (about 7 days after transfer), 2 mL was transferred to a sterile Eppendorf tube and centrifuged at 2,000 g for 30 sec to reduce the microalgal load. The supernatants were transferred into new tubes containing 2 µL of Poloxamer 188 solution 10% (Sigma-Aldrich) and centrifuged at 5,600 g for 5 min. Pelleted strains were extracted using a modified protocol from NucleoSpin PlantII® DNA Mini kit (Macherey-Nagel). First, cells were incubated 1 hour at 55°C with 400 µL of lysis buffer PL1, 25µL proteinase K (20mg/mL) and 100 µL lysozyme (20mg/mL). Nucleic acids were then extracted following the recommendations of the manufacturer and eluted in 100 µL of the buffer provided by the kit. Polymerase Chain Reaction (PCR) was conducted to amplify 16S ribosomal prokaryotic gene with the universal prokaryote primers 515F-Y 5'-GTGYCAGCMGCCGCGGTAA-3' and 926R 5'-CCGYCAATTYMTTTRAGTTT-3'(Parada *et al.*, 2016). The forward primer was 5'-labeled with an eight-nucleotide tag unique to each sample. Triplicate PCR reactions (30 µL) contained 10 ng of DNA, 0.625 units of GoTaq G2 Flexi polymerase (Promega), 1X of enzyme buffer, 1.5 mM of MgCl<sub>2</sub>, 0.4 mM of dNTPs, and 0.32 µM of each primer. The PCR program consisted in an initial denaturation step at 95°C during 10 min, 32 cycles of denaturation at 95°C for 30 sec, annealing at 50°C for 1 min and elongation at 72°C for 1 min, and a final step at 72°C for 10 min. PCR reactions were purified using the NucleoSpin Gel and PCR Clean-Up kit (Macherey-Nagel), and quantified with the Quant-It PicoGreen double stranded DNA Assay kit (ThermoFisher). The purified PCR products were pooled in equal concentrations. Library preparation and high-throughput sequencing using Illumina technology were performed at Fasteris SA (Plan-les-Ouates,

Switzerland). The DNA pool was sequenced using two independent Illumina runs (technical replicates).

### Sequencing data processing and bacterial community analysis

The first steps of the bioinformatic treatment and quality control were performed by FASTER SA. First, in order to separate the libraries, the base calling was done based on a 6 nt unique index, using the softwares MiSeq Control Software 2.6.2.1, RTA 1.18.54 and bcl2fastq2.17 v2.17.1.14 and allowing 1 mismatch. Then, Illumina standard adapters removal and quality trimming were done using the Trimmomatic package (version 0.32) (Bolger *et al.*, 2014). Briefly paired-end reads were globally aligned to ensure an end-to-end match. The adapters sequences were identified allowing a maximum of 2 mismatches and removed if the quality score was higher than 30. Then, bases were filtered by quality using a 4-base sliding window scan and trimming was done when the average quality per base dropped below 5. Reads without insert and with ambiguities were removed.

All the scripts used for the further bioinformatic analyses can be downloaded from: <https://github.com/mcamarareis/>. Briefly, raw reads from each sequencing run were demultiplexed based on the 8 nucleotide tag sequences with cutadapt (version 2.8.1) using anchored mode and allowing no mismatches, insertions or deletions (Martin, 2011). Since R1 and R2 files (corresponding to each cycle of paired-end sequencing) contained reads with forward and reverse primers (further called forward and reverse reads), the demultiplexing was run two times. The first and second demultiplexing searched for adapters in the R1 file and in the R2 file, respectively, which separated forward and reverse reads for each sample corresponding to each cycle. The primer sequences were removed using the same software allowing mismatches at a rate of 0.1 (insertions and deletions were not allowed) (Martin, 2011).

Since R1 and R2 cycles can have different error rates, they were analyzed independently. We used the DADA2 processing to obtain a table of amplicon sequence variants (ASVs) (Callahan *et al.*, 2016). First, the sequences were filtered using the function *filterAndTrim* with default values and trimmed according to the sequence quality. Then, a random subset of the reads ( $n_{bases} = 2e+08$ ) was used to learn the error models from forward and reverse reads using the function *learnerrors*. The ASVs were inferred in pooled mode. Following ASV inference, the forward and reverse reads of R1 were merged. The reads coming from the R2 file were also merged but in an inverse position (reverse + forward). The sequences

tables were built using the function *makeSequenceTable* and the sequence table obtained for R2 file was reverse complemented. Before chimera removal, the sequence tables obtained independently for R1 and R2 were merged. Six samples (3 biological replicates of 2 cultures) that were sequenced in a previous run (see **Chapter 1**) and processed independently were included in the sequence table for chimera removal, also performed in pooled mode. The sequences were filtered according to the range of length of the primers (from 366 to 376 bp) and the resulting fasta file was used to assign taxonomy using Silva database v138 by IDtaxa (using a confidence threshold of 50) (Quast *et al.*, 2013; Murali *et al.*, 2018). Chloroplasts and mitochondrial sequences were removed. Sequences not classified at the domain level by IDtaxa were classified using vsearch global alignment (90% identity) using Silva v138 (Rognes *et al.*, 2016) (Rognes *et al.*, 2016). These sequences were removed if they could not be classified and/or classified as chloroplasts or mitochondrial sequences by vsearch (Rognes *et al.*, 2016). In addition, since we noticed that IDtaxa failed to assign taxonomy to many Rhodobacteraceae sequences at the genus level, we used vsearch taxonomy (at 94.5% threshold (Yarza *et al.*, 2014)) for the taxonomic diversity plots. The resultant ASV table was filtered to remove ASVs accounting for less than 0.001% (24 reads) of the total number of reads. Consistency of technical replicates was evaluated by hierarchical cluster analysis (HCA) using Bray-Curtis dissimilarity of relative abundance data. After consistency was confirmed, independent replicates (technical and biological) of each culture were merged. Abundance and prevalence filters removed 58% of the total number of ASVs while keeping 99% of the reads.

### **Statistical analyses**

Statistical analyses were performed in R (v 4.0.2) using Rstudio (1.1.442) (RStudio Team, 2016; R Core Team, 2017) and graphs were produced using ggplot2 (v3.3.3) (Wickham, 2016), unless otherwise stated. Analyses of presence-absence data (alpha-diversity indexes, Jaccard dissimilarity and *IndVal* analysis) were performed using the rarefied ASV table. Analyses of relative abundance (diversity plots, relative abundance of groups and calculation of the other metrics) were performed using the non-rarefied ASV table to keep as much information as possible. The ASV table was rarefied 100 times at the minimum number of reads (8,522) using the function *rtk* (seed=1,000) from rtk package (v0.2.6.1) (Saary *et al.*, 2017). The mean alpha diversity indexes were obtained using the function *get.mean.diversity*. The diversity plot was produced using relative abundance of ASVs at the family level.

To investigate beta diversity patterns and their consistency we compared 5 beta-diversity metrics: Jaccard dissimilarity (using presence-absence) (Jaccard, 1901), Bray-Curtis dissimilarity calculated using the relative abundance data (Bray and Curtis, 1957), Euclidean distance of Hellinger-transformed data (Hellinger distance) (Legendre and Gallagher, 2001), Aitchison distance, *i.e.* Euclidean distance Centered-Log Ratio (CLR)-transformed data (Gloor *et al.*, 2017) and Euclidean distance of Phylogenetic Isometric-Log Ratio (PhILR)-transformed data (Silverman *et al.*, 2017). To account for the compositional nature of microbiome data from high-throughput sequencing we tested two compositional transformation methods (Gloor *et al.*, 2017). CLR and PhILR transformations take into account the compositional nature of microbiomes data by applying log-transformation (Gloor *et al.*, 2017; Silverman *et al.*, 2017). While CLR considers only the abundance of ASVs, PhILR additionally incorporates phylogenetic models to log-transform the abundance data (Silverman *et al.*, 2017). Prior to CLR transformation, we replaced zero abundance values using the simple multiplicative model of `zCompositions` package v1.3.4 (function `cmultRepl`) (Palarea-Albaladejo and Martín-Fernández, 2015). CLR transformation was performed by using the function `clr` from `easyCoda` package (v0.34.3) (Greenacre, 2018). For PhILR transformation, a constant of 1 was added to each abundance value on the community data to avoid zeros (Silverman *et al.*, 2017). This transformation uses phylogenetic information of the ASVs. For this, sequences were aligned using `mafft` 7.110 (Katoh and Standley, 2013) and the phylogenetic tree was built using GTRCAT model from `FastTree` Version 2.1.11 (Price *et al.*, 2010). In the absence of archaeal ASVs, the phylogenetic tree was rooted at 2 Planctomycetota ASVs using the function `root` of the `seqinr` package (v.2.5) (Charif and Lobry, 2007; Silverman *et al.*, 2017). Finally, PhILR transformation was carried using the phylogenetic tree by applying the function `philr` (package `philr` v1.14.0) (Silverman *et al.*, 2017).

To explore beta diversity patterns, we performed HCA for the different distance metrics using method Ward (`ward.D`, function `hclust`) (Borcard *et al.*, 2011). The influence of environmental parameters (temperature, salinity, phosphate and chlorophyll *a* (Chl *a*) concentrations transformed into z-scores) on the microbiome's diversity was tested by constrained distance-based redundancy analysis (db-RDA) for Jaccard and Bray-Curtis dissimilarities (Legendre and Andersson, 1999) and by RDA for CLR, Hellinger and PhILR transformed data (van den Wollenberg, 1977). The significance of the model was tested by *anova*-like permutation test (1,000 permutations) and plots of the influence of the environmental data on the community were produced using the function `plot`.

To quantify and disentangle the influence of the environment and microalgal hosts on the microbiome assembly, we performed variation partitioning (function *varpart*) including hosts [grouped as *Emiliana huxleyi* (14 strains), Pelagophyceae (10 strains) and other (19 strains)] and transformed environmental parameters (Borcard *et al.*, 1992). Before running the variation partitioning, homogeneity of multivariate beta-dispersion in the microalgal groups was checked using the function *betadisper* (using *bias.adjust* to account for different sample size among groups) and significance of the model and variables was tested using *anova*-like permutation test (Anderson and Walsh, 2013). The categorical variable corresponding to hosts was converted in numerical data by using the function *model.matrix*. Significance of the partitions was tested by partial db-RDA and RDA and *anova*-like permutation test (1,000 permutations). Variation partitioning was also used to quantify the influence of culture media and environmental parameters driving the microbiome composition. For this, we selected groups of culture media that displayed homogeneous multivariate beta-dispersion (tested as before). Microbiomes from phytoplankton strains grown in K+Si (4 strains), L1 (11 strains), F/2 (4 strains) and K/2 (6 strains) media were included in the analysis (Supplementary Table 2). F/2 and L1 media have a similar nutrient composition but different trace metal solutions (Guillard and Ryther, 1962; Guillard and Hargraves, 1993). K+Si and K/2 media are two variations of the medium designed by Keller *et al.*, (1987), with addition of silica to allow diatom growth and diluted two times, respectively. Then, variation partitioning was performed as before. Significance of individual variables in both models was tested by Type III *anova*-like permutation test, which is more robust to unbalanced sampling design (Legendre and Andersson, 1999).

In order to identify the ASVs responsible for the differences in Jaccard db-RDA, we plotted the 20 ASVs that accounted for most of the variance (presence-absence) among the samples. Then, indicative species were identified by Indicator Value tests (*IndVal*) (Dufrene and Legendre, 1997; De Cáceres and Legendre, 2009). The *IndVal* was based on the comparison of occurrences of taxa across predefined groups of microbiomes. The analysis provides an index ranging between 0 and 1, the maximum value indicating an ASV exclusively present in all samples of one group. *IndVal* is calculated as the product of *A* (specificity, *i.e.*, the probability that a site belongs to the group given the fact that a given species is found in that site) and *B* (fidelity, *i.e.*, the probability of finding a given taxon at a site when the site belongs to that group) (Dufrière & Legendre, 1997). To test for the presence of indicative ASVs in the Jaccard HCA groups, hosts and medium, *Indval* analysis using the rarefied table was run using the

function *multipatt* (package *indicspecies* v1.7.9) with 10,000 permutations (De Cáceres and Legendre 2009). P-values were adjusted for multiple comparison using false discovery rate correction (*p.adjust* function).

## Results and Discussion

The phytoplankton cultures used in this study were isolated from 13 different seawater samples collected during 6 oceanographic cruises. The sampling stations covered different oceanic regions (South West and East Pacific, North to South Atlantic, and Mediterranean Sea) (Supplementary Figure 1A) and encompassed large ranges of salinities, temperatures, distinct nutrient status, depths, and oceanic regimes (Supplementary Figure 1B, Supplementary Table 1). The 43 diverse phytoplankton cultures originating from these samples spanned 7 phyla (Hapophyta, Ochrophyta, Chlorophyta, Bacillariophyta, Myzozoa, Cercozoa and Chytridophyta) and more than 15 genera (Supplementary Figure 1A and Supplementary Table 2).

### Bacterial diversity associated to phytoplankton cultures

Comparative sequence analysis of the 16S rRNA amplicons revealed a total of 275 ASVs and 2,346,348 reads remaining after abundance and prevalence filters. Alpha diversity indexes of bacterial communities associated with phytoplankton cultures from the same water samples were variable and rather low (Figure 1A). Overall, richness values ranged from 9 to 48 ASVs with a mean and standard deviation of  $24 \pm 10$  (n=43) and Shannon index ranged from 0.22 to 2.85 (mean of  $1.42 \pm 0.76$ ). The highest richness values were observed in microbiomes of phytoplankton cultures from the BIOSOPE cruise (average of  $30 \pm 9$  ASVs; n=15), while TAN1810 displayed the lowest ones ( $13 \pm 4$  ASVs; n=6).

The taxonomic diversity was dominated by the phylum Proteobacteria (91.0% of the total of reads), followed by Bacteroidota (8.6% of the reads). Other phyla (Planctomycetota, Desulfobacterota, Firmicutes, Actinobacteriota, Myxococcota) accounted for 0.4% of the reads. Gammaproteobacteria (62%) and Alphaproteobacteria (29%) were the most abundant classes followed by Bacteroidia (6.2%). These bacterial classes are typically the most abundant in natural blooms (Buchan *et al.*, 2014; Teeling *et al.*, 2016; Zhou *et al.*, 2018, 2019) and in phytoplankton cultures (Krohn-Molt *et al.*, 2017; Ajani *et al.*, 2018; Behringer *et al.*, 2018; Lawson *et al.*, 2018; Kimbrel *et al.*, 2019; Sörenson *et al.*, 2019; Mönnich *et al.*, 2020; Kearney *et al.*, 2021).

Differences in the taxonomic composition at the family level could be observed between the microbiomes of phytoplankton cultures isolated from the same seawater sample (Figure 1B). The most abundant family Marinobacteraceae (56% of the total number of reads) dominated most TAN1702 and TAN1810 phytoplankton-associated communities, as well as some microbiomes from all other cruises. Rhodobacteraceae (17% of the total reads) were also found to dominate in cultures from diverse geographical origins. Although they were absent or low in most cultures, Thalassospiraceae (4%) and Alteromonadaceae (3%) were relatively abundant in one PROSOPE culture, and in two cultures from TAN1810 and AMT 24, respectively. Flavobacteriaceae (4%) were commonly found but never dominated (Figure 1B).

At the genus level, *Marinobacter* dominated (56.2% of the total of reads) and was present in all our phytoplankton cultures (non rarefied ASV table). *Marinobacter* spp. are well-known to be associated with cultures of cyanobacteria, coccolithophores, dinoflagellates, and a chlorophyte (*Ostreococcus*) as the dominant genus (Green *et al.*, 2015; Lupette *et al.*, 2016; Kearney *et al.*, 2021) or a core member (Lawson *et al.*, 2018; Sörenson *et al.*, 2019). A comparison of bacterial communities associated to diverse phytoplankton cultures (Sörenson *et al.*, 2019; Kearney *et al.*, 2021) revealed that *Marinobacter* was the most prevalent operational taxonomic unit (OTU) shared between coccolithophores, cyanobacteria, and *Alexandrium* sp. (**Chapter 1**). Among the other most abundant genera, *Marinovum* (4%), *Marivita* (3%), *Roseovarius* (3%), *Alteromonas* (2%), and *Balneola* (2%) are frequently associated with phytoplankton (Pradella *et al.*, 2010; Taniguchi *et al.*, 2011; Zhang *et al.*, 2015; Rosana *et al.*, 2016; Ajani *et al.*, 2018; Hou *et al.*, 2018; Zheng *et al.*, 2020). On the other hand, potential relationships with hydrocarbon-degraders of the genus *Thalassospira* (4%), commonly found on plastic debris, are yet not established for phytoplankton (Kodama *et al.*, 2008; Wright *et al.*, 2021). Cultivated representatives of the Roseobacter clade, *Marinobacter*, *Pseudoalteromonas* and *Alteromonas* are frequently isolated from blooms and phytoplankton cultures (Schäfer *et al.*, 2002; Berg *et al.*, 2009; Green *et al.*, 2015; Hahnke *et al.*, 2015; Crenn *et al.*, 2018). The presence in our cultures of these genera and other less abundant but prevalent ones (*Hyphomonas*, *Muricauda*, and *Alcanivorax*) may be due to their capacity to degrade hydrocarbon molecules and complex organic compounds produced by phytoplankton (Chernikova *et al.*, 2020). Co-culture experiments have shown intimate interactions between these copiotrophic bacteria and their phytoplankton hosts that range from mutualistic to parasitic (Amin *et al.*, 2012; Seymour *et al.*, 2017), suggesting that strong chemotaxis towards

phytoplankton organic matter has an important role in shaping phycosphere-associated communities (Slightom and Buchan, 2009; Sonnenschein *et al.*, 2012; Smriga *et al.*, 2016).

Importantly, the constant association of different phytoplankton groups that diversified hundreds of millions of years ago (Karlusich *et al.*, 2020) with the same bacterial taxa raises important questions into the functional aspects of microbiomes. Copiotrophic bacteria are involved in broad functions such as the degradation of organic compounds (Cottrell and Kirchman, 2016; Smriga *et al.*, 2016). This can assure the release of inorganic nutrients to the microalga (Amin *et al.*, 2012) in addition of the degradation of toxic compounds, such as hydrocarbons (Mishamandani *et al.*, 2016) and reactive oxygen species (Bolch *et al.*, 2011). Copiotrophic bacteria can also display specific functions such as the production of vitamins (Cruz-López and Maske, 2016) and of specific siderophores which increase microalgal uptake of iron (Amin *et al.*, 2009). However, the extent to which the specific functions are spread among interactions with different phytoplankton taxa is still poorly understood. Experimental approaches involving a bacterium isolate and multiple phytoplankton species will provide further insights into the mechanism of interaction of copiotrophs and phytoplankton and their impact on ecosystem function in the oceans.

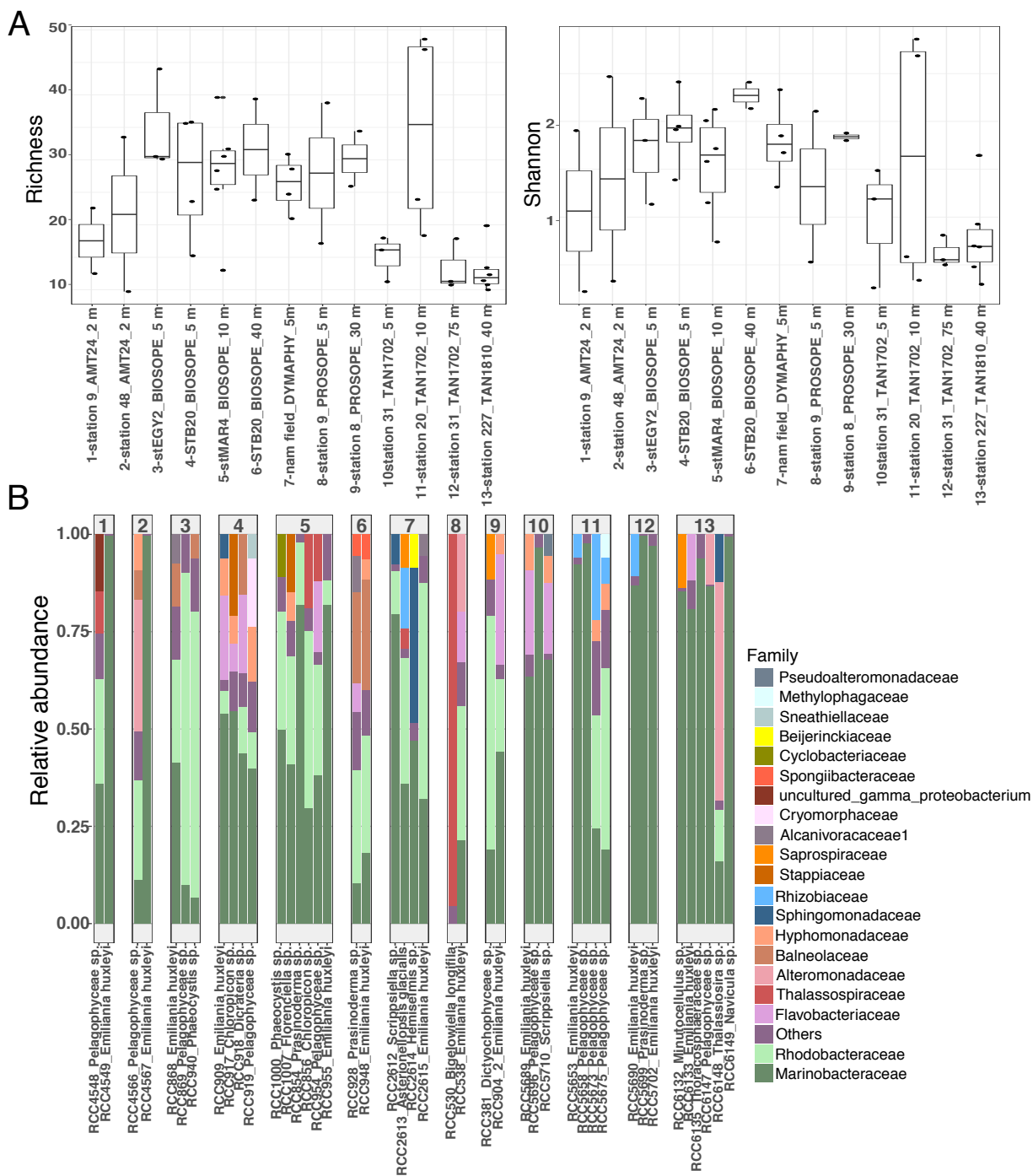


**Figure 1.** **A**) Box plots of alpha diversity indexes (richness and Shannon) of the microbiomes for each sample. The boxes mark the interquartile range. The thin horizontal lines represent the 25th and 75th percentiles while the thick horizontal line represents the median. The vertical lines indicate the minimum and maximum values (using 1.5 coefficients above and below the percentiles). The dots represent the values obtained for each culture. Dots further than the vertical lines represent potential outliers. Indexes were calculated from 100 rarefactions of the ASV table at the minimum of reads (8,522). **B**) Taxonomic diversity of the phytoplankton-associated microbiomes at the family level. Microbiomes are sorted according to the water samples from where the phytoplankton species were isolated. The relative abundance at family level was calculated on the raw ASV table. Families accounting to less than 5% of the total of reads at each microbiome were merged as “others” to ease visualization.

## Disentangling the influence of environment, hosts, and culture medium

Exploratory HCA using Jaccard dissimilarity separated the microbiomes associated with the 43 phytoplankton cultures into two main clusters, group A containing mainly strains isolated from warm waters ( $>15^{\circ}\text{C}$ ) and group B that consisted in most of strains isolated from cold waters (Supplementary Figure 2). Constrained analyses (db-RDA and RDA) that included physicochemical parameters as explanatory variables revealed the significant effect of environmental parameters on the beta diversity patterns of phytoplankton-associated bacterial assemblages ( $p = 0.01$ ) (Figure 2 and Supplementary Figure 3). The axis 1 of the constrained analysis plot, negatively correlated with temperature and salinity, discriminated microbiomes from cold and warm samples (Figure 2), confirming the clustering results (Supplementary Figure 2). Two TAN1702 microbiomes (RCC5673 and RCC5675), that both clustered into group A (warm samples) in the hierarchical clustering (Supplementary Figure 2), were closer to cold samples in the constrained analysis (Figure 2). This trend was also observed with three BIOSOPE samples that clustered in the cold group B in the hierarchical clustering (Figure 2 and Supplementary Figure 2). Similar conclusions regarding cold and warm waters groups could be drawn from the other distance metrics tested, although the importance of environmental parameters varied (Supplementary Figure 3). Axis 2 discriminated microbiomes associated with phytoplankton cultures from TAN1810 which are linked to relatively high Chl *a* concentrations (Figure 2).

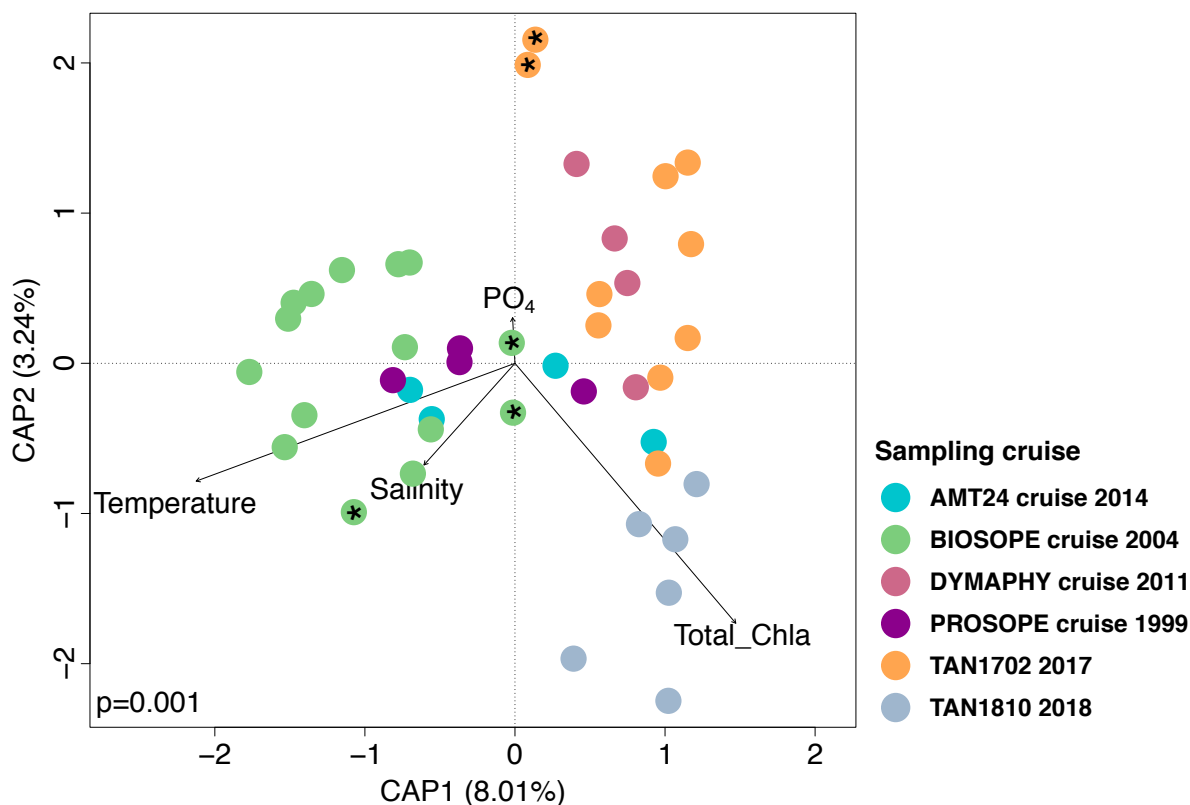


**Figure 2.** Distance-based redundancy analysis bi-plot using Jaccard dissimilarity matrix and environmental parameters (temperature, salinity, phosphate (PO<sub>4</sub>) and total Chl *a* concentration). The two main axes explain the highest proportion of the variation of the data. Vectors represent the environmental variables; their direction represents the correlation with each axis and the length of the vector is proportional to its importance in the ordination. Asterisks indicate outliers identified in the HCA (Supplementary Figure 2).

To disentangle the influence of environmental parameters and phytoplankton hosts on the observed beta diversity patterns, we performed variation partitioning using several beta-diversity metrics that consider different features of the data (presence-absence, relative abundance, phylogenetic-weighted abundance, compositional transformation). Multivariate beta dispersion of the phytoplankton groups was only significant for PhILR matrix ( $p=0.03$ ) (data not shown). Using the full dataset, environmental parameters alone explained consistently and significantly most of the variance whatever the metric used, whereas microalgal hosts, categorized as *E. huxleyi*, Pelagophyceae and other microalgae, were low contributors (Table 1). Temperature (F-value ranging from 2.6 to 10.6) was consistently identified as the main factor responsible for the differences observed between the microbiomes (Supplementary Table 3), the significance of other parameters (salinity, phosphate and Chl *a* concentrations) being metric-dependent.

**Table 1.** Disentangling the influence of microalgal host and environmental parameters on the beta diversity patterns of microbiomes. Adjusted R<sup>2</sup> of variation partitioning analysis using different beta diversity metrics. Aitchison distance was produced as the Euclidean distance of the centered log-ratio transformed data. Bray-Curtis dissimilarity was calculated on the relative abundance data. Hellinger was calculated as the Euclidean distance of the Hellinger transformed data. Jaccard dissimilarity was calculated with presence/absence of ASVs of the rarefied table. PhILR was produced as the Euclidean distance of the phylogenetic isometric log-ratio transformed data. For the all the metrics (except Jaccard) the raw table was used. Significance of the partitions was tested by partial db-RDA (Jaccard and Bray-Curtis) and partial RDA (PhILR, Aitchison and Hellinger). Significance code: \*\*\* p < 0.001; \*\* p < 0.01; \* p < 0.05. - indicates adjusted R<sup>2</sup> close to 0.

Metric tested	Microalgae	Intersection	Environmental parameters	Microalgae + Environmental parameters
Aitchison	0.01	-	0.08**	0.09***
Bray-Curtis	0.03*	-	0.18***	0.19***
Hellinger	0.03**	-	0.15***	0.18***
Jaccard	0.02**	-	0.08***	0.09***
PhILR	0.03	-	0.28**	0.30**

A variation partitioning analysis carried out on a subset of the data was performed to evaluate the influence of culture media in the selection of the phytoplankton-associated microbiomes. To identify medium effect on the significance (and not dispersion effect), we selected a subset of the data which contained homogeneous multivariate beta dispersion among the groups of culture media (Anderson and Walsh 2013). Similar explained variations were generally obtained for media and environmental parameters among the different beta diversity metrics (Table 2). However, the significance of the partial tests varied. Pure contribution of medium was found significant with Jaccard, Hellinger and Bray-Curtis metrics, while pure environmental parameters were only significant with Jaccard and Hellinger metrics (Table 2). Importantly, both variables shared an important proportion (from 6 to 17%) of the explained variation. Significance of individual parameters of the model are detailed in Supplementary Table 4.

**Table 2.** Disentangling the influence of cultivation media and environmental parameters on the beta diversity patterns of microbiomes. Adjusted R<sup>2</sup> of variation partitioning analysis using different beta diversity metrics. Aitchison distance was produced as the Euclidean distance of the centered log-ratio transformed data. Bray-Curtis dissimilarity was calculated on the relative abundance data. Hellinger was calculated as the Euclidean distance of the Hellinger transformed data. Jaccard dissimilarity was calculated with presence/absence of ASVs of the rarefied table. PhilR was produced as the Euclidean distance of the phylogenetic isometric log-ratio transformed data. For the all the metrics (except Jaccard) the raw table was used. Significance of the partitions was tested by partial db-RDA (Jaccard and Bray-Curtis) and partial RDA (PhilR, Aitchison and Hellinger). Significance code: \*\*\* p < 0.001; \*\* p < 0.01; \* p < 0.05. - indicates adjusted R<sup>2</sup> close to 0.

Metric tested	Medium	Intersection	Environmental parameters	Medium + Environmental parameters
Aitchison	0.05	0.07	0.07	0.20**
Bray-Curtis	0.13**	0.07	0.09	0.29***
Hellinger	0.11**	0.06	0.09*	0.26***
Jaccard	0.05*	0.07	0.05*	0.17***
PhilR	0.05	0.17	-	0.20*

Marine phytoplankton and bacteria are submitted to variable physicochemical and biological conditions which are known to influence their abundance and distribution (De Vargas *et al.*, 2015; Sunagawa *et al.*, 2015; Logares *et al.*, 2020). Among these parameters, temperature is considered as the main driver of prokaryotic communities in the global ocean (Sunagawa *et al.*, 2015; Logares *et al.*, 2020). Phytoplankton composition, abundance, as well as the quantity and quality of organic matter they excrete, also affect the prokaryotic community (Landa *et al.*, 2016, 2018; Sarmiento *et al.*, 2016). Temperature and other environmental parameters (salinity and nutrients) were found to account for a substantial part of the variation in the bacterioplankton community structure associated with a bloom of the dinoflagellate *Scyrsiella trochoidea* (Zhou *et al.*, 2018). To our knowledge, no studies have evaluated the influence of environmental parameters from the isolation place on the diversity of cultivated microbiomes. Ajani *et al.*, (2018) showed that the place/time of isolation had also a stronger influence on the microbiome diversity in cultures than host genotypes on diatom-associated bacteria in culture. Other cultivation experiments demonstrated the significant influence of the host selection on the microbiome assembly (Jackrel *et al.*, 2020; Mönnich *et al.*, 2020). Here, we showed that the environmental conditions at the time of sampling, and mainly temperature, had detectable effects on heterotrophic bacterial communities associated with phytoplankton cultures that have been maintained in the laboratory for years, while the host influence, although

it was detectable, was low. A possible explanation for the weak influence of hosts in our study could be the limited number of strains of each phytoplankton species in our dataset and the grouping of different species together (*i.e.* Pelagophyceae group assembled different species). However, since *E. huxleyi*-associated microbiomes did not cluster together (Supplementary Figure 2), it indicates that other variables, *e.g.*, temperature, had stronger influence than host specificity.

A concern regarding the use of phytoplankton cultures to study the microbiome composition is the possible effect of the culture medium on the bacterial community (Kearney *et al.*, 2021). Up to now, most studies that characterized phytoplankton-associated microbiomes did not investigate the influence of the culture medium on the microbiome composition (Ajani *et al.*, 2018; Behringer *et al.*, 2018; Lawson *et al.*, 2018; Kimbrel *et al.*, 2019; Sörenson *et al.*, 2019; Mönnich *et al.*, 2020). Lupette *et al.*, (2016) showed however that different culture media and photoperiods affected the growth of a strain of *Ostreococcus tauri* but they had no effects on the associated microbiomes diversity, dominated by *Marinobacter* in all culture conditions and phases of growth. Here, using a subset of the data, we showed that the culture medium had an influence similar to that of the environmental parameters on the microbiome composition. Since it has been shown that different media and culture conditions can affect growth and cellular metabolism of microalgae (Wang *et al.*, 2014; Sánchez-Bayo *et al.*, 2020), a possibility was that the medium composition (*e.g.* inorganic nutrient and vitamins concentrations) may have selected for particular phytoplankton species during the initial isolation/enrichment phase of our phytoplankton cultures and that the dissolved organic matter they excreted may have favored specific bacterial communities (Sarmiento and Gasol, 2012). However, our variation partitioning results consistently demonstrated that phytoplankton hosts had a weak influence on the variation of the microbiome structure. We cannot also fully exclude that the media formulation had a direct effect on the bacterial composition. However, since environmental parameters and medium have a shared effect (adjusted  $R^2 = 0.07-0.17$ ) on the microbiome composition that we could not disentangle, we rather hypothesize that the initial composition of heterotrophic bacteria in the seawater collected during the cruises and initial culture conditions were probably decisive. A balanced design of experiments comparing different media would help to tackle this question.

## Identification of indicator species

To identify species that could be indicative of the two main clusters defined by the hierarchical clustering and constrained analyses using Jaccard index (Supplementary Figure 2 and Figure 2), we performed *IndVal* analysis (De Cáceres and Legendre, 2009). Among the 20 ASVs that accounted for most of the variance among the microbiomes, *IndVal* analysis identified 8 bacterial species indicative of group A (Figure 3), mostly associated with phytoplankton from the BIOSOPE and PROSOPE cruises, (Supplementary Figure 2). These indicator species, that displayed high specificity (0.7-1), were mostly present in the microbiomes of group A but not in all cultures (Figure 3 and Supplementary Table 5).

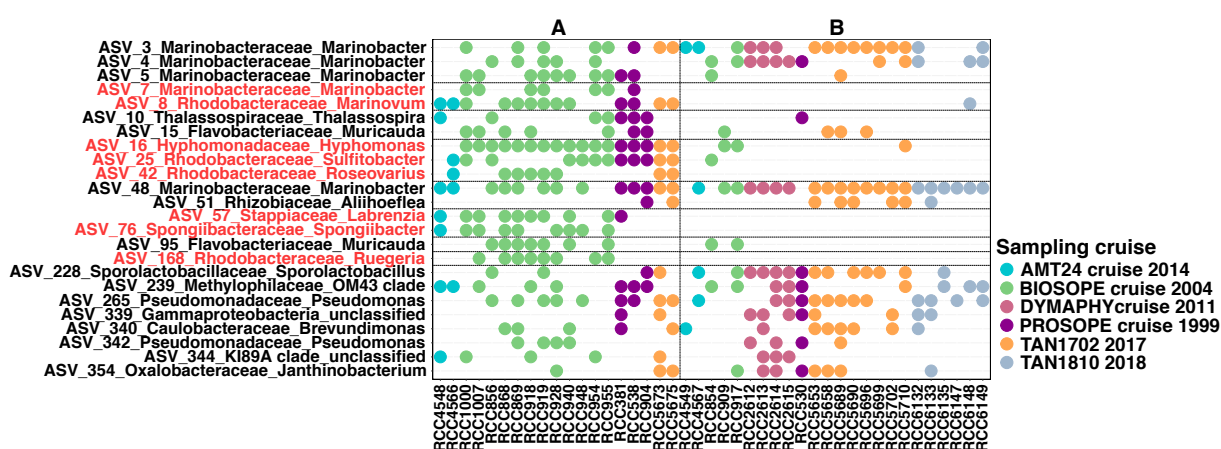


**Figure 3.** Presence-absence of the 20 ASVs that accounted for most of the variance (presence-absence) among the microbiomes. The ASVs in red represent significant indicator ASVs of group A. The groups were extracted from hierarchical cluster analysis and were consistent with the groups obtained at the db-RDA using Jaccard dissimilarity (Supplementary Figure 2).

High specificity and fidelity values (Supplementary Table 5) of ASV8 (*Marinovum*), ASV16 (*Hyphomonas*), ASV25 (*Sulfitobacter*) and ASV57 (*Labrenzia*), identified them as the best indicators for group A. These taxa, commonly associated with phytoplankton blooms (Buchan *et al.*, 2014; Landa *et al.*, 2018; Li *et al.*, 2018) and cultures (Amin *et al.*, 2015; Lupette *et al.*, 2016; Ajani *et al.*, 2018; Kimbrel *et al.*, 2019; Mönnich *et al.*, 2020; Kearney *et al.*, 2021), are known to produce and exchange infochemicals within the phycosphere. *Sulfitobacter* provides indole-3-acetic acid, one of the most important plant auxins, and ammonium to diatoms in exchange of tryptophan (Amin *et al.*, 2015). Other Rhodobacteraceae, such as *Roseobacter* symbionts display sophisticated quorum-sensing guided behavior to colonize the diatom phycosphere (Fei *et al.*, 2020). *Labrenzia*, the most abundant core member of *Symbiodinium*-associated communities is notable for its ability to

produce dimethylsulfoniopropionate (Curson *et al.*, 2017) which has central role in mutualistic interactions (Miller and Belas, 2004; Pohnert *et al.*, 2007; Seymour *et al.*, 2010). Phytoplankton-*Hyphomonas* interactions are not well documented but several *Hyphomonas* strains significantly influenced the development of normal morphology in axenic protoplasts of the red alga *Pyropia yezoensis* (Fukui *et al.*, 2014), whose normal development is entirely dependent on the incubation with certain bacteria.

The presence of indicator ASVs in the group formed mainly by bacterial communities associated with phytoplankton isolated from relatively warm (>15°C) samples can have ecological implications regarding the influence of temperature on phytoplankton-bacteria interactions. Temperature can influence bacterial community composition directly as well as through bacterial interactions with phytoplankton. The concentration and composition of DOC excreted by phytoplankton depend on temperature conditions (Zlotnik and Dubinsky, 1989; Parker and Armbrust, 2005). Experimental manipulation of natural communities showed that an increase of temperature induces a mutualistic relationship between microalgae and heterotrophic bacteria through exchange of metabolites (C transfer to bacteria) or nutrients (N uptake by microalgae) mediated by attachment (Arandia-Gorostidi *et al.*, 2017). The effect of temperature was also shown to significantly increase the carbon assimilation of copiotrophic Rhodobacteraceae and Flavobacteria commonly associated with phytoplankton (Arandia-Gorostidi *et al.*, 2020). It is worth mentioning that we tested also for indicator species related to the microalgal hosts and culture media but did not find any.

## Conclusions

We found that deterministic processes (environmental filtering and medium) significantly contribute to shape the microbiome composition in phytoplankton cultures while hosts had a low influence. In light of these results, we propose that the initial environmental conditions act as a primary filter selecting the bacterial community in the inoculum (Ajani *et al.*, 2018). Once the microalgae are isolated, the culture medium will represent another force (possibly stronger than the environment) determining the diversity of the microbiomes. However, we observed that most of the variation was unexplained (ranging from 0.71 to 0.84) in addition to high differences among the phytoplankton-associated microbiomes originating from the same samples. This high unexplained variation could be related to the decrease of the predictive power of environmental factors over the cultivation time as recently

shown by Jackrel *et al.*, (2020). Indeed, these authors demonstrated that the magnitude of the host and environmental signatures decreased over the 30-day duration of their experiment (Jackrel *et al.*, 2020). The microbiomes analyzed in our study were kept in cultivation from 3 to 22 years. During this time, many biotic and abiotic processes could have influenced their composition. For example, bacterial communities may have experienced ecological drift and bottlenecks imposed through weekly culture transfers and changing conditions (light, natural seawater used in the medium formulation) leading to possible selection by their algal hosts (Jackrel *et al.*, 2020). A recent study showed that the enrichment of phytoplankton-attached bacterial community induced stochasticity in the composition of selected microbiomes (Kimbrel *et al.*, 2019), and favored the competitive lottery hypothesis (Sale, 1979). The principle behind, is that the bacterial community present in the cultures represent a guild with similar capacity of colonizing a niche (Sale, 1979; Kimbrel *et al.*, 2019). Priority effects and stochasticity could therefore induce changes in the bacterial community composition that may explain the high dissimilarity among microbiomes originating from the same samples. Our results bring light to the complex process of microbiome assembly in phytoplankton cultures. Future experimental studies incorporating phytoplankton and heterotrophic model organisms could clarify the role of environment, host, and stochastic processes in shaping host microbiome composition.

### **Acknowledgements**

This work was supported by the Sorbonne University, the Région Bretagne, the Centre National de la Recherche Scientifique (CNRS, France), and the French Government “Investissements d’Avenir” programmes OCEANOMICS (ANR-11-BTBR-0008). The DYMAPHY cruise was financed by INTERREG IVA “2 Mers Seas Zeeën” European cross-border project DYMAPHY (Development of a DYnamic observation system for the assessment of MARine water quality, based on PHYtoplankton analysis), and the EU FP7 PROTOOL (PROductivity TOOLS: Automated Tools to Measure Primary Productivity in European Seas). We are also thankful to Veronique Creach, Andres Gutierrez-Rodriguez, and Monica Hanley for providing the ancillary data from DYPMAPHY, TAN1702/1810, and AMT24 cruises, respectively. Finally, we would like to thank the ABiMS bioinformatic platform (<http://abims.sb-roscoff.fr>) for the computational resources, the RCC team for the phytoplankton resources, and Miguel Méndez-Sandín for his contribution in improving the manuscript.

## References

- Ajani, P.A., Kahlke, T., Siboni, N., Carney, R., Murray, S.A., and Seymour, J.R. (2018) The microbiome of the cosmopolitan diatom *Leptocylindrus* reveals significant spatial and temporal variability. *Front Microbiol* **9**: 2758.
- Amin, S.A., Green, D.H., Hart, M.C., Kupper, F.C., Sunda, W.G., and Carrano, C.J. (2009) Photolysis of iron-siderophore chelates promotes bacterial-algal mutualism. *Proc Natl Acad Sci* **106**: 17071–17076.
- Amin, S.A., Hmelo, L.R., Van Tol, H.M., Durham, B.P., Carlson, L.T., Heal, K.R., *et al.* (2015) Interaction and signalling between a cosmopolitan phytoplankton and associated bacteria. *Nature* **522**: 98–101.
- Amin, S.A., Parker, M.S., and Armbrust, E. V. (2012) Interactions between Diatoms and Bacteria. *Microbiol Mol Biol Rev* **76**: 667–684.
- Anderson, M.J. and Walsh, D.C.I. (2013) PERMANOVA, ANOSIM, and the Mantel test in the face of heterogeneous dispersions: What null hypothesis are you testing? *Ecol Monogr* **83**: 557–574.
- Arandia-Gorostidi, N., Alonso-Sáez, L., Stryhanyuk, H., Richnow, H.H., Morán, X.A.G., and Musat, N. (2020) Warming the phycosphere: Differential effect of temperature on the use of diatom-derived carbon by two copiotrophic bacterial taxa. *Environ Microbiol* **22**: 1381–1396.
- Arandia-Gorostidi, N., Weber, P.K., Alonso-Sáez, L., Morán, X.A.G., and Mayali, X. (2017) Elevated temperature increases carbon and nitrogen fluxes between phytoplankton and heterotrophic bacteria through physical attachment. *ISME J* **11**: 641–650.
- Behringer, G., Ochsenkühn, M.A., Fei, C., Fanning, J., Koester, J.A., and Amin, S.A. (2018) Bacterial communities of diatoms display strong conservation across strains and time. *Front Microbiol* **9**:
- Berg, K.A., Lyra, C., Sivonen, K., Paulin, L., Suomalainen, S., Tuomi, P., and Rapala, J. (2009) High diversity of cultivable heterotrophic bacteria in association with cyanobacterial water blooms. *ISME J* **3**: 314–325.
- Bolch, C.J.S., Subramanian, T.A., and Green, D.H. (2011) The toxic dinoflagellate *Gymnodinium catenatum* (Dinophyceae) requires marine bacteria for growth. *J Phycol* **47**: 1009–1022.
- Bolger, A.M., Lohse, M., and Usadel, B. (2014) Trimmomatic: a flexible trimmer for Illumina sequence data. *Bioinformatics* **30**: 2114–2120.
- Borcard, D., Gillet, F., and Legendre, P. (2011) Numerical Ecology with R, Springer.
- Borcard, D., Legendre, P., and Drapeau, P. (1992) Partialling out the spatial component of ecological variation. *Ecology* **73**: 1045–1055.
- Bray, J.R. and Curtis, J.T. (1957) An ordination of the upland forest communities of southern Wisconsin. *Ecol Monogr* **27**: 325–349.
- Buchan, A., LeCleir, G.R., Gulvik, C.A., and González, J.M. (2014) Master recyclers: features and functions of bacteria associated with phytoplankton blooms. *Nat Rev Microbiol* **12**: 686–698.
- De Cáceres, M. and Legendre, P. (2009) Associations between species and groups of sites: Indices and statistical inference. *Ecology* **90**: 3566–3574.
- Callahan, B.J., McMurdie, P.J., Rosen, M.J., Han, A.W., Johnson, A.J.A., and Holmes, S.P. (2016) DADA2: High-resolution sample inference from Illumina amplicon data. *Nat Methods* **13**: 581.
- Charif, D. and Lobry, J. (2007) Seqin{R} 1.0-2: a contributed package to the {R} project for statistical computing devoted to biological sequences retrieval and analysis. In *Biomedical*

- Engineering*. Bastolla U, Porto M, Roman H, V.M. (ed). Springer Verlag, pp. 207–232.
- Chernikova, T.N., Bargiela, R., Toshchakov, S. V., Shivaraman, V., Lunev, E.A., Yakimov, M.M., *et al.* (2020) Hydrocarbon-degrading bacteria *Alcanivorax* and *Marinobacter* associated with microalgae *Pavlova lutheri* and *Nannochloropsis oculata*. *Front Microbiol* **11**.
- Cottrell, M.T. and Kirchman, D.L. (2016) Transcriptional control in marine copiotrophic and oligotrophic bacteria with streamlined genomes. *Appl Environ Microbiol* **82**: 6010–6018.
- Crenn, K., Duffieux, D., and Jeanthon, C. (2018) Bacterial epibiotic communities of ubiquitous and abundant marine diatoms are distinct in short- and long-term associations. *Front Microbiol* **9**: 1–12.
- Cruz-López, R. and Maske, H. (2016) The vitamin B1 and B12 required by the marine dinoflagellate *Lingulodinium polyedrum* can be provided by its associated bacterial community in culture. *Front Microbiol* **7**: 1–13.
- Curson, A.R.J., Liu, J., Bermejo Martínez, A., Green, R.T., Chan, Y., Carrión, O., *et al.* (2017) Dimethylsulfoniopropionate biosynthesis in marine bacteria and identification of the key gene in this process. *Nat Microbiol* **2**: 17009.
- Dufrene, M. and Legendre, P. (1997) Species assemblages and indicator species: the need for a flexible asymmetrical approach. *Ecol Monogr* **67**: 345–366.
- Eigemann, F., Hilt, S., Salka, I., and Grossart, H.P. (2013) Bacterial community composition associated with freshwater algae: Species specificity vs. dependency on environmental conditions and source community. *FEMS Microbiol Ecol* **83**: 650–663.
- Fei, C., Ochsenkühn, M.A., Shibl, A.A., Isaac, A., Wang, C., and Amin, S.A. (2020) Quorum sensing regulates ‘swim-or-stick’ lifestyle in the phycosphere. *Environ Microbiol* **22**: 4761–4778.
- Fu, H., Uchimiya, M., Gore, J., and Moran, M.A. (2020) Ecological drivers of bacterial community assembly in synthetic phycospheres. *Proc Natl Acad Sci U S A* **117**: 3656–3662.
- Fukui, Y., Abe, M., Kobayashi, M., Yano, Y., and Satomi, M. (2014) Isolation of *Hyphomonas* strains that induce normal morphogenesis in protoplasts of the marine red alga *Pyropia yezoensis*. *Microb Ecol* **68**: 556–566.
- Gloor, G.B., Macklaim, J.M., Pawlowsky-Glahn, V., and Egozcue, J.J. (2017) Microbiome datasets are compositional: And this is not optional. *Front Microbiol* **8**: 1–6.
- Green, D.H., Echavarrri-Bravo, V., Brennan, D., and Hart, M.C. (2015) Bacterial diversity associated with the coccolithophorid algae *Emiliania huxleyi* and *Coccolithus pelagicus* f. *braarudii*. *Biomed Res Int* **2015**.
- Greenacre, M. (2018) Compositional Data Analysis in Practice. *Chapman Hall / CRC Press*.
- Grossart, H.P. (1999) Interactions between marine bacteria and axenic diatoms (*Cylindrotheca fusiformis*, *Nitzschia laevis*, and *Thalassiosira weissflogii*) incubated under various conditions in the lab. *Aquat Microb Ecol* **19**: 1–11.
- Guillard, R.R.L. and Hargraves, P.E. (1993) *Stichochrysis immobilis* is a diatom, not a chrysophyte. *Phycologia* **32**: 234–236.
- Guillard, R.R.L. and Ryther, J.H. (1962) Studies of marine planktonic diatoms: I. *Cyclotella nana* Hustedt, and *Detonula confervacea* (Cleve) Gran. *Can J Microbiol* **8**: 229–239.
- Hahnke, R.L., Bennke, C.M., Fuchs, B.M., Mann, A.J., Rhiel, E., Teeling, H., *et al.* (2015) Dilution cultivation of marine heterotrophic bacteria abundant after a spring phytoplankton bloom in the North Sea. *Environ Microbiol* **17**: 3515–3526.
- Hou, S., López-Pérez, M., Pfreundt, U., Belkin, N., Stüber, K., Huettel, B., *et al.* (2018) Benefit from decline: the primary transcriptome of *Alteromonas macleodii* str. Te101 during *Trichodesmium* demise. *ISME J* **12**: 981–996.
- Hutchinson, G.E. (1957) Concluding remarks. *Cold Spring Harb Symp Quant Biol* **224**: 415–

427.

- Jaccard, P. (1901) Étude comparative de la distribution florale dans une portion des Alpes et des Jura. *Bull Soc Vaudoise Sci Nat* **37**: 547–579.
- Jackrel, S.L., Yang, J.W., Schmidt, K.C., and Deneff, V.J. (2020) Host specificity of microbiome assembly and its fitness effects in phytoplankton. *ISME J*.
- Karlusich, J.J.P., Ibarbalz, F.M., and Bowler, C. (2020) Exploration of marine phytoplankton: from their historical appreciation to the omics era. *J Plankton Res* 1–18.
- Katoh, K. and Standley, D.M. (2013) MAFFT Multiple Sequence Alignment Software Version 7: Improvements in Performance and Usability. *Mol Biol Evol* **30**: 772–780.
- Kearney, S.M., Thomas, E., Coe, A., and Chisholm, S.W. (2021) Microbial diversity of co-occurring heterotrophs in cultures of marine picocyanobacteria. *Environ Microbiomes* **16**: 1–15.
- Keller, M.D., Selvin, R.C., Claus, W., and Guillard, R.R.L. (1987) Media for the culture of oceanic ultraphytoplankton. *J Phycol* **23**: 633–638.
- Kimbrel, J.A., Samo, T.J., Ward, C., Nilson, D., Thelen, M.P., Siccardi, A., *et al.* (2019) Host selection and stochastic effects influence bacterial community assembly on the microalgal phycosphere. *Algal Res* **40**: 101489.
- Kodama, Y., Stiknowati, L.I., Ueki, A., Ueki, K., and Watanabe, K. (2008) *Thalassospira tepidiphila* sp. nov., a polycyclic aromatic hydrocarbon-degrading bacterium isolated from seawater. *Int J Syst Evol Microbiol* **58**: 711–715.
- Krohn-Molt, I., Alawi, M., Förstner, K.U., Wiegandt, A., Burkhardt, L., Indenbirken, D., *et al.* (2017) Insights into Microalga and bacteria interactions of selected phycosphere biofilms using metagenomic, transcriptomic, and proteomic approaches. *Front Microbiol* **8**: 1–14.
- Landa, M., Blain, S., Christaki, U., Monchy, S., and Obernosterer, I. (2016) Shifts in bacterial community composition associated with increased carbon cycling in a mosaic of phytoplankton blooms. *ISME J* **10**: 39–50.
- Landa, M., Blain, S., Harmand, J., Monchy, S., Rapaport, A., and Obernosterer, I. (2018) Major changes in the composition of a Southern Ocean bacterial community in response to diatom-derived dissolved organic matter. *FEMS Microbiol Ecol* **94**: 1–16.
- Lawson, C.A., Raina, J.B., Kahlke, T., Seymour, J.R., and Suggett, D.J. (2018) Defining the core microbiome of the symbiotic dinoflagellate, *Symbiodinium*. *Environ Microbiol Rep* **10**: 7–11.
- Legendre, P. and Andersson, M. (1999) Distance-based redundancy analysis: Testing multispecies responses in multifactorial ecological experiments. *Ecol Monogr* **69**: 1–24.
- Legendre, P. and Gallagher, E.D. (2001) Ecologically meaningful transformations for ordination of species data. *Oecologia* **129**: 271–280.
- Li, D.X., Zhang, H., Chen, X.H., Xie, Z.X., Zhang, Y., Zhang, S.F., *et al.* (2018) Metaproteomics reveals major microbial players and their metabolic activities during the blooming period of a marine dinoflagellate *Prorocentrum donghaiense*. *Environ Microbiol* **20**: 632–644.
- Logares, R., Deutschmann, I.M., Junger, P.C., Giner, C.R., Krabberød, A.K., Schmidt, T.S.B., *et al.* (2020) Disentangling the mechanisms shaping the surface ocean microbiota. *Microbiome* **8**: 55.
- Lupette, J., Lami, R., Krasovec, M., Grimsley, N., Moreau, H., Piganeau, G., and Sanchez-Ferandin, S. (2016) *Marinobacter* dominates the bacterial community of the *Ostreococcus tauri* phycosphere in culture. *Front Microbiol* **7**:.
- Majzoub, M.E., Beyersmann, P.G., Simon, M., Thomas, T., Brinkhoff, T., and Egan, S. (2019) *Phaeobacter inhibens* controls bacterial community assembly on a marine diatom. *FEMS Microbiol Ecol* **95**:.
- Martin, M. (2011) Cutadapt removes adapter sequences from high-throughput sequencing

- reads. *EMBNET Journal*; Vol 17, No 1 Next Gener Seq Data Anal - 1014806/ej171200.
- Miller, T.R. and Belas, R. (2004) Dimethylsulfoniopropionate metabolism by *Pfiesteria* - associated *Roseobacter* spp. †. **70**: 3383–3391.
- Mishamandani, S., Gutierrez, T., Berry, D., and Aitken, M.D. (2016) Response of the bacterial community associated with a cosmopolitan marine diatom to crude oil shows a preference for the biodegradation of aromatic hydrocarbons. *Environ Microbiol* **18**: 1817–1833.
- Mönnich, J., Tebben, J., Bergemann, C., Case, R.J., Sylke Wohlrab, and Harder, T. (2020) Niche-based assembly of bacterial consortia on the diatom *Thalassiosira rotula* is stable and reproducible. *ISME J* **14**: 1614–1625.
- Murali, A., Bhargava, A., and Wright, E.S. (2018) IDTAXA: a novel approach for accurate taxonomic classification of microbiome sequences. *Microbiome* **6**: 140.
- Palarea-Albaladejo, J. and Martín-Fernández, J.A. (2015) ZCompositions - R package for multivariate imputation of left-censored data under a compositional approach. *Chemom Intell Lab Syst* **143**: 85–96.
- Parker, M.S. and Armbrust, E.V. (2005) Synergistic effects of light, temperature, and nitrogen source on transcription of genes for carbon and nitrogen metabolism in the centric diatom *Thalassiosira pseudonana* (Bacillariophyceae) 1. *J Phycol* **41**: 1142–1153.
- Pohnert, G., Steinke, M., and Tollrian, R. (2007) Chemical cues, defence metabolites and the shaping of pelagic interspecific interactions. **22**.
- Pradella, S., Päuker, O., and Petersen, J. (2010) Genome organisation of the marine *Roseobacter* clade member *Marinovum algicola*. *Arch Microbiol* **192**: 115–126.
- Price, M.N., Dehal, P.S., and Arkin, A.P. (2010) FastTree 2 - Approximately maximum-likelihood trees for large alignments. *PLoS One* **5**.
- Quast, C., Pruesse, E., Yilmaz, P., Gerken, J., Schweer, T., Yarza, P., *et al.* (2013) The SILVA ribosomal RNA gene database project: improved data processing and web-based tools. *Nucleic Acids Res* **41**: D590–D596.
- R Core Team (2017) R: A language and environment for statistical computing. R Foundation for Statistical Computing, Vienna, Austria. URL <https://www.R-project.org/>.
- Rognes, T., Flouri, T., Nichols, B., Quince, C., and Mahé, F. (2016) VSEARCH: a versatile open source tool for metagenomics. *PeerJ* **4**: e2584–e2584.
- Rosana, A.R.R., Orata, F.D., Xu, Y., Simkus, D.N., Bramucci, A.R., Boucher, Y., and Case, R.J. (2016) Draft genome sequences of seven bacterial strains isolated from a polymicrobial culture of coccolith-bearing (C-type) *Emiliana huxleyi* M217. *Genome Announc* **4**.
- RStudio Team (2016) RStudio: Integrated Development for R. *RStudio, Inc, Boston, MA*.
- Saary, P., Forslund, K., Bork, P., and Hildebrand, F. (2017) RTK: efficient rarefaction analysis of large datasets.
- Sale, P.F. (1979) Recruitment, loss and coexistence in a guild of territorial coral reef fishes. *Oecologia* **42**: 159–177.
- Sánchez-Bayo, A., Morales, V., Rodríguez, R., Vicente, G., and Bautista, L.F. (2020) Cultivation of microalgae and cyanobacteria: effect of operating conditions on growth and biomass composition. *Molecules* **25**: 2834.
- Sarmiento, H. and Gasol, J.M. (2012) Use of phytoplankton-derived dissolved organic carbon by different types of bacterioplankton. *Environ Microbiol* **14**: 2348–2360.
- Sarmiento, H., Morana, C., and Gasol, J.M. (2016) Bacterioplankton niche partitioning in the use of phytoplankton-derived dissolved organic carbon: Quantity is more important than quality. *ISME J* **10**: 2582–2592.
- Schäfer, H., Abbas, B., Witte, H., and Muyzer, G. (2002) Genetic diversity of ‘satellite’ bacteria present in cultures of marine diatoms. *FEMS Microbiol Ecol* **42**: 25–35.
- Seymour, J.R., Amin, S.A., Raina, J.B., and Stocker, R. (2017) Zooming in on the phycosphere:

- The ecological interface for phytoplankton-bacteria relationships. *Nat Microbiol* **2**:
- Seymour, J.R., Simó, R., Ahmed, T., and Stocker, R. (2010) Chemoattraction to dimethylsulfoniopropionate throughout the marine microbial food web. *Science (80- )* **329**: 342–345.
- Silverman, J.D., Washburne, A.D., Mukherjee, S., and David, L.A. (2017) A phylogenetic transform enhances analysis of compositional microbiota data. *Elife* **6**: 1–20.
- Slightom, R.N. and Buchan, A. (2009) Surface colonization by marine *Roseobacters*: Integrating genotype and phenotype. *Appl Environ Microbiol* **75**: 6027–6037.
- Smriga, S., Fernandez, V.I., Mitchell, J.G., and Stocker, R. (2016) Chemotaxis toward phytoplankton drives organic matter partitioning among marine bacteria. *Proc Natl Acad Sci U S A* **113**: 1576–1581.
- Sonnenschein, E.C., Syit, D.A., Grossart, H.P., and Ullrich, M.S. (2012) Chemotaxis of *Marinobacter adhaerens* and its impact on attachment to the diatom *Thalassiosira weissflogii*. *Appl Environ Microbiol* **78**: 6900–6907.
- Sörenson, E., Bertos-Fortis, M., Farnelid, H., Kremp, A., Krüger, K., Lindehoff, E., and Legrand, C. (2019) Consistency in microbiomes in cultures of *Alexandrium* species isolated from brackish and marine waters. *Environ Microbiol Rep* **11**: 425–433.
- Sunagawa, S., Coelho, L.P., Chaffron, S., Kultima, J.R., Labadie, K., Salazar, G., *et al.* (2015) Structure and function of the global ocean microbiome. *Science (80- )* **348**: 1261359–1261359.
- Taniguchi, A., Tada, Y., and Hamasaki, K. (2011) Seasonal variations in the community structure of actively growing bacteria in neritic waters of Hiroshima bay, western Japan. *Microbes Environ* **26**: 339–46.
- Teeling, H., Fuchs, B.M., Bennke, C.M., Krüger, K., Chafee, M., Kappelmann, L., *et al.* (2016) Recurring patterns in bacterioplankton dynamics during coastal spring algae blooms. *Elife* **5**: 1–31.
- De Vargas, C., Audic, S., Henry, N., Decelle, J., Mahé, F., Logares, R., *et al.* (2015) Eukaryotic plankton diversity in the sunlit ocean. *Science (80- )* **348**:
- Wang, W., Han, F., Li, Y., Wu, Y., Wang, J., Pan, R., and Shen, G. (2014) Medium screening and optimization for photoautotrophic culture of *Chlorella pyrenoidosa* with high lipid productivity indoors and outdoors. *Bioresour Technol* **170**: 395–403.
- Wickham, H. (2016) ggplot2: Elegant Graphics for Data Analysis. *Springer-Verlag New York ISBN 978-3*:
- van den Wollenberg, A.D. (1977) Redundancy Analysis an alternative for Canonical Correlation Analysis. *Psychometrika* **42**: 207–219.
- Wright, R.J., Langille, M.G.I., and Walker, T.R. (2021) Food or just a free ride? A meta-analysis reveals the global diversity of the Plastisphere. *ISME J* **15**: 789–806.
- Yarza, P., Yilmaz, P., Pruesse, E., Glöckner, F.O., Ludwig, W., Schleifer, K.H., *et al.* (2014) Uniting the classification of cultured and uncultured bacteria and archaea using 16S rRNA gene sequences. *Nat Rev Microbiol* **12**: 635–645.
- Zhang, Z., Chen, Y., Wang, R., Cai, R., Fu, Y., and Jiao, N. (2015) The fate of marine bacterial exopolysaccharide in natural marine microbial communities. *PLoS One* **10**: e0142690.
- Zheng, Q., Wang, Y., Lu, J., Lin, W., Chen, F., and Jiao, N. (2020) Metagenomic and metaproteomic insights into photoautotrophic and heterotrophic interactions in a *Synechococcus* culture. *MBio* **11**: 1–18.
- Zhou, J., Chen, G.F., Ying, K.Z., Jin, H., Song, J.T., and Cai, Z.H. (2019) Phycosphere microbial succession patterns and assembly mechanisms in a marine dinoflagellate bloom. *Appl Environ Microbiol* **85**: 1–17.
- Zhou, J., Richlen, M.L., Sehein, T.R., Kulis, D.M., Anderson, D.M., and Cai, Z. (2018) Microbial Community Structure and Associations During a Marine Dinoflagellate Bloom.

Zlotnik, I. and Dubinsky, Z. (1989) The effect of light and temperature on DOC excretion by phytoplankton. *Limnol Oceanogr* **34**: 831–839.

## SUPPLEMENTARY MATERIAL

### Microbiome assembly in phytoplankton cultures is partially driven by deterministic processes

#### Supplementary Methods

#### Origin of phytoplankton cultures

The 43 strains used in this study were isolated from 6 oceanographic cruises that covered a variety of oceanic regions. The PROSOPE (PROductivity of Oceanic PELagic Systems) cruise onboard the RV *Thalassa* (9 September - 3 October 1999) explored the biogeochemical processes in waters of different trophic status in the Mediterranean Sea (Claustre *et al.*, 2020). The BIOSOPE (BIogeochemistry and Optics SOUTh Pacific Experiment) cruise that took place between Tahiti and Chile during the Austral Summer (26 October - 11 December 2004) onboard the RV *Atalante* explored the biological, biogeochemical and bio-optical properties of different trophic regimes in the South East Pacific (Claustre *et al.*, 2008). Samples from the North Sea were collected during the PROTOOL/DYMAPHY project cruise (8 - 12 May 2011) onboard the RV *Cefas Endeavour* (Thyssen *et al.*, 2015). The Atlantic Meridional Transect 24 (AMT24) cruise took place between the United Kingdom and Falkland Islands during boreal autumn (30 September - 1 November 2014). It covered most biogeochemical provinces of the Atlantic Ocean (Lange *et al.*, 2020). TAN1702 and TAN1810 cruises onboard RV *Tangaroa* were part of the Ross Sea Environment and Ecosystem voyages. The TAN1702 voyage was mainly a physical oceanographic study with focus on the Campbell Plateau (16 March - 1 April 2017) (<https://niwa.co.nz/static/web/Vessels/TRG-July-2016-to-June-2017-Voyage-Summaries-NIWA.pdf>). TAN1810 (21 October - 21 November 2018) explored the carbon flows in the Chatham Rise, east of New Zealand (<https://niwa.co.nz/static/web/Vessels/TRG-July-2018-to-June-2019-Voyage-Summaries-NIWA.pdf>)

#### References

- Claustre, H., Antoine, D., Babin, M., Belviso, S., Begovic, M., Bianchi, M., *et al.* (2020) BIOGEOCHEMICAL dataset collected during the PROSOPE cruise. *SEANOE*.
- Claustre, H., Sciandra, A., and Vaultot, D. (2008) Introduction to the special section bio-optical and biogeochemical conditions in the South East Pacific in late 2004: the BIOSOPE program. *Biogeosciences* 5: 679–691.
- Lange, P.K., Jeremy Werdell, P., Erickson, Z.K., Dall’Olmo, G., Brewin, R.J.W., Zubkov, M.

V., *et al.* (2020) Radiometric approach for the detection of picophytoplankton assemblages across oceanic fronts. *Opt Express* 28: 25682.

Thyssen, M., Alvain, S., Lefèbvre, A., Dessailly, D., Rijkeboer, M., Guiselin, N., *et al.* (2015) High-resolution analysis of a North Sea phytoplankton community structure based on in situ flow cytometry observations and potential implication for remote sensing. *Biogeosciences* 12: 4051–4066.

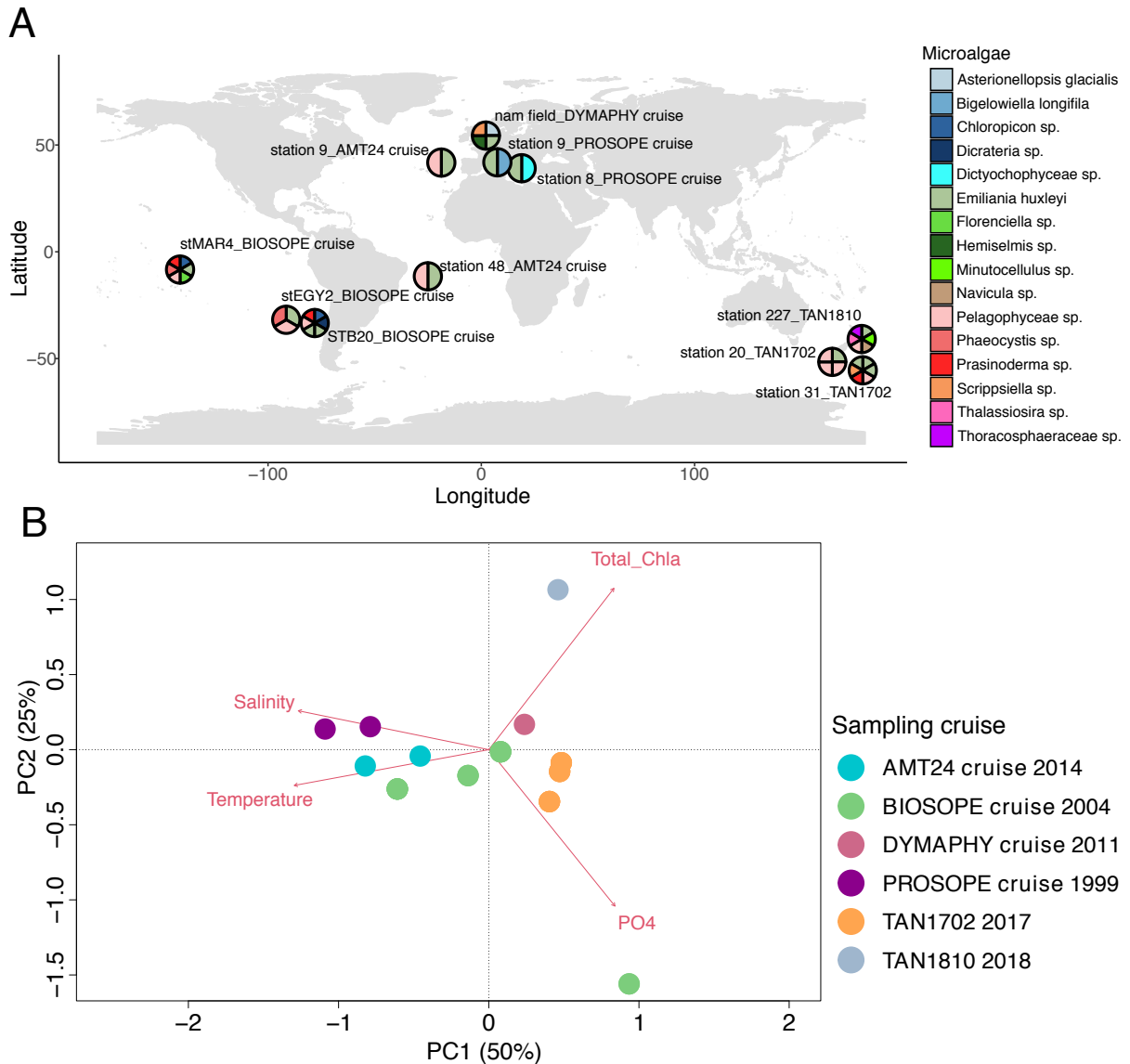
**Supplementary Table 1.** Depth, temperature, salinity, phosphate (PO<sub>4</sub>) and chlorophyll *a* concentration, Latitude and Longitude (decimal degrees) of each sample from where the microalgae used in this study were isolated.

<i>Sampling cruise/Year</i>	<i>Sampling station</i>	<i>Sampling depth (m)</i>	<i>Temperature (°C)</i>	<i>Salinity (PSU)</i>	<i>PO<sub>4</sub> (μM)</i>	<i>Chlorophyll a (mg/m<sup>3</sup>)</i>	<i>Latitude</i>	<i>Longitude</i>
<i>AMT24</i>	9	2	19.900	35.770	0.030	0.047	41.770	-18.750
<i>AMT24</i>	48	2	25.354	36.648	0.120	0.026	-11.480	-25.050
<i>BIOSOPE</i>	stMAR4	10	27.788	35.563	0.351	0.163	-8.330	-141.250
<i>BIOSOPE</i>	stEGY2	5	18.083	34.699	0.177	0.064	-31.820	-91.470
<i>BIOSOPE</i>	STB20	5	17.565	33.947	0.095	0.311	-33.350	-78.100
<i>BIOSOPE</i>	STB20	40	14.801	33.993	3.302	0.524	-33.350	-78.100
<i>DYMAPHY</i>	namfield	5	11.997	34.385	0.120	0.436	53.820	3.420
<i>PROSOPE</i>	9	5	23.931	38.195	0.003	0.082	41.900	10.430
<i>PROSOPE</i>	8	30	18.113	37.743	0.007	0.046	39.120	14.080
<i>TANI702</i>	20	10	9.853	34.435	0.835	0.199	-51.537	167.482
<i>TANI702</i>	31	75	9.877	34.346	0.770	0.453	-51.643	171.119
<i>TANI702</i>	31	5	9.892	34.345	0.740	0.515	-51.643	171.119
<i>TANI810</i>	227	40	13.276	34.987	0.242	1.811	-42.771	178.346

**Supplementary Table 2.** Detailed taxonomic information, source of isolation and culturing conditions of the phytoplankton strains. \* indicate strains recovered from cryopreservation. NA indicates that no sequences are available in GenBank and that corresponding cultures were identified by microscopy visualization.

<i>Strain</i>	<i>Taxonomic information</i>				<i>Source of isolation</i>		<i>Culture conditions</i>		
	<b>Phylum</b>	<b>Taxonomy</b>	<b>GenBank accession</b>	<b>Gene</b>	<b>Cruise (Year)</b>	<b>Station of isolation</b>	<b>Growth temperature (°C)</b>	<b>Growth medium</b>	<b>Light intensity (<math>\mu\text{mol s}^{-1}\text{m}^{-2}</math>)</b>
<i>RCC4548</i>	Ochrophyta	<i>Pelagomonas calceolata</i>	KX014627	18S rRNA	AMT24 (2014)	station 9	22	K	100
<i>RCC4549</i>	Haptophyta	<i>Emiliana huxleyi</i>	KX014628	18S rRNA	AMT24 (2014)	station 9	18	K/2	60
<i>RCC4566</i>	Ochrophyta	<i>Pelagomonas calceolata</i>	KX014639	18S rRNA	AMT24 (2014)	station 48	22	K	100
<i>RCC4567</i>	Haptophyta	<i>Emiliana huxleyi</i>	KX014640	18S rRNA	AMT24 (2014)	station 48	20	K	100
<i>RCC909</i>	Haptophyta	<i>Emiliana huxleyi</i>	KT861255	18S rRNA	BIOSOPE (2004)	STB20_5m	20	K	100
<i>RCC917</i>	Chlorophyta	<i>Chloropicon roscoffensis</i>	EU106769	18S rRNA	BIOSOPE (2004)	STB20_5m	20	K	100
<i>RCC918</i>	Haptophyta	<i>Dicrateria sp.</i>	KF899845	18S rRNA	BIOSOPE (2004)	STB20_5m	20	K	100
<i>RCC919</i>	Ochrophyta	<i>Pelagomonas calceolata</i>	KT861049	18S rRNA	BIOSOPE (2004)	STB20_5m	20	K	100
<i>RCC928</i>	Chlorophyta	<i>Prasinoderma singularis</i>	KT860930	18S rRNA	BIOSOPE (2004)	STB20_40m	20	K	100
<i>RCC948</i>	Haptophyta	<i>Emiliana huxleyi</i>	JN098172	cox3	BIOSOPE (2004)	STB20_40m	17	K/2	25
<i>RCC868*</i>	Haptophyta	<i>Emiliana huxleyi</i>	EU106749	18S rRNA	BIOSOPE (2004)	EGY2	19	K/2	100
<i>RCC869</i>	Ochrophyta	<i>Pelagomonas calceolata</i>	LN735476	16S rRNA	BIOSOPE (2004)	EGY2	20	K	100
<i>RCC940</i>	Haptophyta	<i>Phaeocystis globosa</i>	EU106787	18S rRNA	BIOSOPE (2004)	EGY2	15	K/2ET	100
<i>RCC1000</i>	Haptophyta	<i>Phaeocystis sp.</i>	JX660991	18S rRNA	BIOSOPE (2004)	stMAR4	15	K/2ET	100
<i>RCC1007</i>	Ochrophyta	<i>Florenciella sp.</i>	KT861110	18S rRNA	BIOSOPE (2004)	stMAR4	20	K	100
<i>RCC854*</i>	Chlorophyta	<i>Prasinoderma coloniale</i>	KT860905	18S rRNA	BIOSOPE (2004)	stMAR4	20	K	100
<i>RCC856</i>	Chlorophyta	<i>Chloropicon laureae</i>	MK086001	genome	BIOSOPE (2004)	stMAR4	20	K	100
<i>RCC954</i>	Ochrophyta	<i>Pelagomonas calceolata</i>	KT861051	18S rRNA	BIOSOPE (2004)	stMAR4	20	K	100
<i>RCC955</i>	Haptophyta	<i>Emiliana huxleyi</i>	KT861256	18S rRNA	BIOSOPE (2004)	stMAR4	18	K/2	60
<i>RCC2612</i>	Myzozoa	<i>Scrippsiella sp.</i>	KT860944	18S rRNA	DYMAPHY (2011)	nam field	15	F/2	100

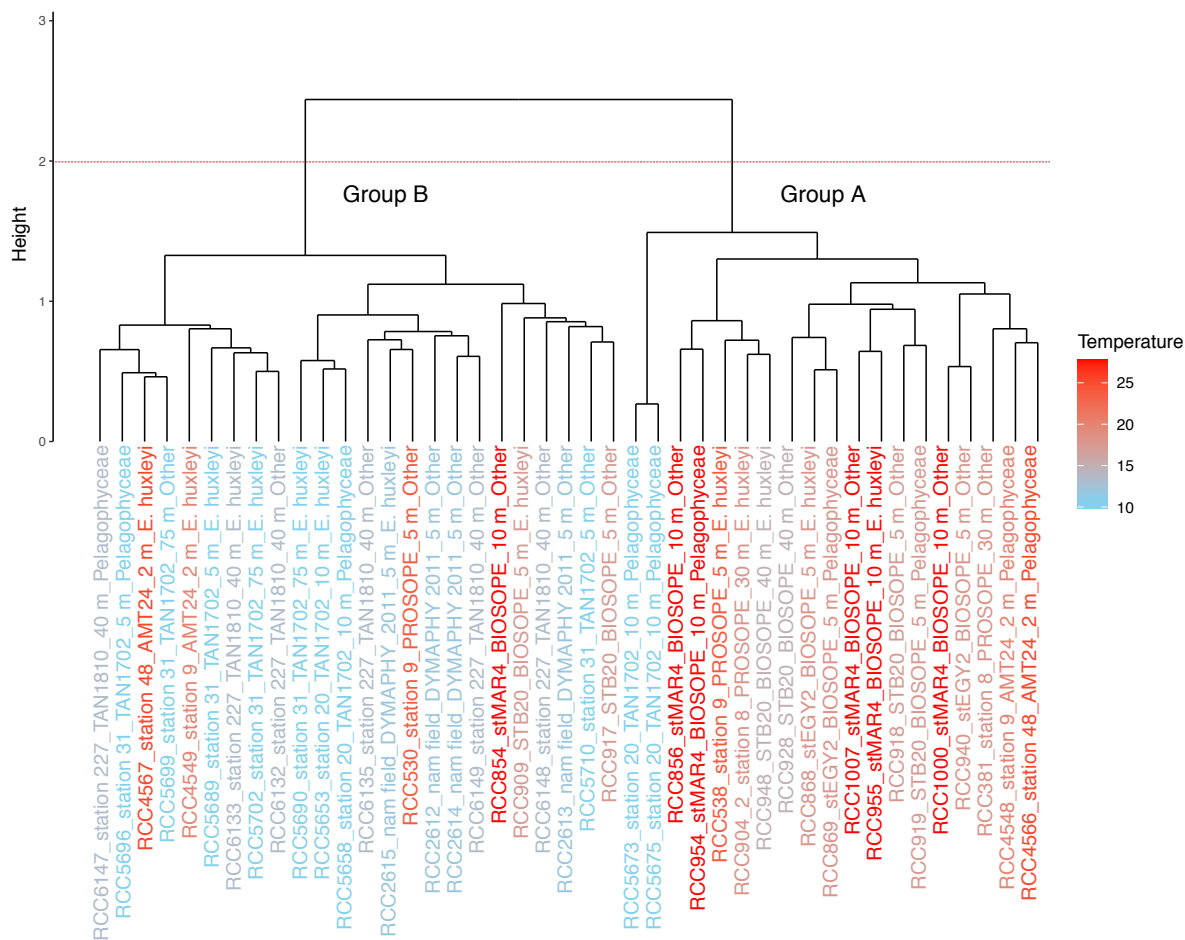
RCC2613	Bacillariophyta	<i>Asterionellopsis glacialis</i>	KT861146	18S rRNA	DYMAPHY (2011)	nam field	15	F/2	100
RCC2614	Cryptophyta	<i>Hemiselmis sp.</i>	KT861344	18S rRNA	DYMAPHY (2011)	nam field	15	F/2	100
RCC2615	Haptophyta	<i>Emiliana huxleyi</i>	KT861276	18S rRNA	DYMAPHY (2011)	nam field	15	F/2	100
RCC381	Ochrophyta	<i>Dictyochophyceae sp</i>	NA	NA	PROSOPE (1999)	station 8	20	K	100
RCC904	Haptophyta	<i>Emiliana huxleyi</i>	NA	NA	PROSOPE (1999)	station 8	17	K/2	25
RCC538	Haptophyta	<i>Emiliana huxleyi</i>	KT861253	18S rRNA	PROSOPE (1999)	station 9	17	K/2	25
RCC530	Cercozoa	<i>Bigelowiella longifila</i>	KT861355	18S rRNA	PROSOPE (1999)	station 9	20	K	100
RCC5689	Haptophyta	<i>Emiliana huxleyi</i>	MH764617	18S rRNA	TAN1702 (2017)	station 31_5m	12	L1	80
RCC5696	Ochrophyta	<i>Pelagococcus sp.</i>	MH764647	18S rRNA	TAN1702 (2017)	station 31_5m	12	L1	80
RCC5710	Myzozoa	<i>Scrippsiella sp.</i>	MH764679	18S rRNA	TAN1702 2017	station 31_5m	12	L1	80
RCC5653	Haptophyta	<i>Emiliana huxleyi</i>	MH764614	18S rRNA	TAN1702 2017	station 20_10m	12	L1	80
RCC5658	Ochrophyta	<i>Pelagococcus sp.</i>	MH764634	18S rRNA	TAN1702 2017	station 20_10m	12	L1	80
RCC5673	Ochrophyta	<i>Pelagophyceae sp.</i>	MH764655	18S rRNA	TAN1702 2017	station 20_10m	12	L1	80
RCC5675	Ochrophyta	<i>Pelagophyceae sp.</i>	NA	NA	TAN1702 2017	station 20_10m	12	L1	80
RCC5690	Haptophyta	<i>Emiliana huxleyi</i>	NA	NA	TAN1702 2017	station 31_75m	12	L1	80
RCC5699	Chlorophyta	<i>Prasinoderma singularis</i>	MH764667	18S rRNA	TAN1702 2017	station 31_75m	12	L1	80
RCC5702	Haptophyta	<i>Emiliana huxleyi</i>	NA	NA	TAN1702 2017	station 31_75m	12	L1	80
RCC6132	Bacillariophyta	<i>Minutocellulus sp.</i>	MN121039	18S rRNA	TAN1810 2018	station 227	13	K+Si	80
RCC6133	Haptophyta	<i>Emiliana huxleyi</i>	MN121040	18S rRNA	TAN1810 2018	station 227	13	L1	100
RCC6135	Myzozoa	<i>Thoracosphaeraceae sp.</i>	MN121042	18S rRNA	TAN1810 2018	station 227	13	K	100
RCC6147	Ochrophyta	<i>Pelagococcus sp.</i>	MN121048	18S rRNA	TAN1810 2018	station 227	13	K+Si	100
RCC6148	Bacillariophyta	<i>Thalassiosira sp.</i>	MN121049	18S rRNA	TAN1810 2018	station 227	13	K+Si	100
RCC6149	Bacillariophyta	<i>Navicula sp.</i>	MN121050	18S rRNA	TAN1810 2018	station 227	13	K+Si	100



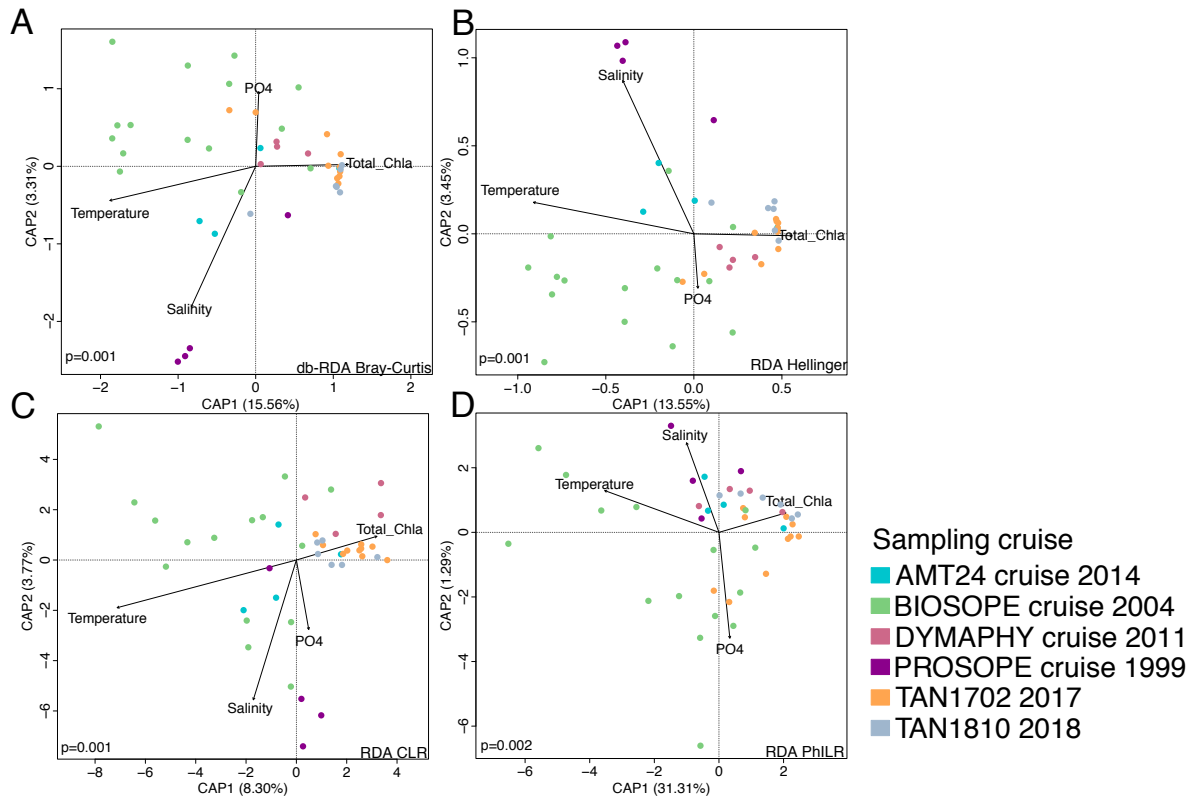
**Supplementary Figure 1. (A)** Map showing the sampling locations where phytoplankton cultures used at this study were retrieved. The pie charts indicate the taxonomy of microalgae isolated at each sampling site. Note that depth profiles from TAN1702 and BIOSOPE STB20 are merged for improving visualization. **(B)** Principal component analysis (PCA) showing ordination of samples according to temperature, salinity, phosphate ( $\text{PO}_4$ ) and total chlorophyll *a* concentration (z-score normalization).







**Supplementary Figure 2.** Dendrogram showing clustering of phytoplankton-associated bacteria composition using Jaccard dissimilarity matrix and method “ward.D”. The dashed line represents the threshold that separates the two groups of samples used in the indicator species analysis (*IndVal*). The two groups are consistent with the ordination produced by the db-RDA using Jaccard dissimilarity.



**Supplementary Figure 3. Constrained analysis including community and environmental data. (A)** Distance-based redundancy analysis (db-RDA) using Bray-Curtis dissimilarity. **(B)** Redundancy analysis (RDA) using Hellinger-transformed data, **(C)** CLR-transformed data (Aitchinson distance), and **(D)** PhILR-transformed data.

**Supplementary Table 3.** Individual statistics of parameters that drive significantly the microbiome diversity in the models including hosts and environmental parameters. *Anova*-like permutation test Type III (margin) was used. - Not significant. Total chl a: Total chlorophyll *a*

<i>Metric</i>	<i>Host</i>	<i>Temperature</i>	<i>Salinity</i>	<i>PO<sub>4</sub></i>	<i>Total chl a</i>
Aitchison	-	F= 3.12 p=0.001	F= 1.84 p=0.033	-	-
Bray-Curtis	F= 1.62 p=0.045	F= 4.31 p=0.002	-	F=1.90 p=0.045	-
Hellinger	F= 1.79 p=0.009	F= 3.89 p=0.002	F= 1.70 p=0.046	-	-
Jaccard	F= 1.39 p=0.026	F= 2.62 p=0.001	F= 1.47 p=0.035	-	F= 1.67 p=0.023
PhILR	-	F=10.56 p=0.001	-	-	-

**Supplementary Table 4.** Individual statistics of parameters that drive significantly microbiome diversity in the models including media and environmental parameters. *Anova*-like permutation test Type III (margin) was used. - Not significant. Total chl a: Total chlorophyll *a*

<i>Metric</i>	<i>Medium</i>	<i>Temperature</i>	<i>Salinity</i>	<i>PO<sub>4</sub></i>	<i>Total chl a</i>
Aitchison	-	-	F= 2.27 p=0.021	-	-
Bray-Curtis	F= 2.19 p=0.005	F= 2.71 p=0.005	-	F=2.07 p=0.036	-
Hellinger	F= 1.97 p=0.001	F= 2.30 p=0.002	-	F= 1.85 p=0.022	-
Jaccard	F= 1.39 p=0.017	-	F= 1.74 p=0.011	F= 1.50 p=0.031	-
PhILR	-	-	-	-	-

**Supplementary Table 5.** Significant indicator ASVs and their indicator values. The p-values were adjusted to multiple comparison using false discovery rate (FRD) correction.

<i>ASV Id</i>	<i>Component A Specificity</i>	<i>Component B Fidelity</i>	<i>Indicator value (IndVal)</i>	<i>p.value</i>	<i>Corrected p.value</i>
ASV_8	0.9999	0.6842	0.8271	0.0001	0.0116
ASV_16	0.732	0.8947	0.8093	0.0003	0.0140
ASV_25	0.8527	0.6316	0.7338	0.0002	0.0140
ASV_57	1	0.5263	0.7255	0.0001	0.0116
ASV_76	1	0.4737	0.6882	0.0003	0.0140
ASV_42	1	0.4211	0.6489	0.0012	0.0349
ASV_168	1	0.4211	0.6489	0.0007	0.0272
ASV_7	1	0.3684	0.6070	0.0012	0.0349



---

# CHAPTER 3

---



## Chapter 3

This chapter brings answers to questions opened in previous parts of this work. In **Chapter 1**, we could not associate beta diversity patterns of the microbiomes with any of the variables tested (place of isolation, host genotype, etc). This questions whether the microbiomes in cultures result from environmental selection at the place of isolation and/or through host specificities. In **Chapter 2**, we partially answered this question by showing that environmental filters and culture media were the main drivers of the microbiome composition of different phytoplankton cultures that were isolated from the same seawater samples. However, we were not able to identify the influence of host selection. Importantly, in previous chapters we used cultures isolated many years ago and for which the initial microbiome composition was unknown. Although we showed in **Chapter 1** that the cultures are stable over culture transfers for maintenance across a short period of time (three consecutive culture transfers), we did not test for putative microbiome changes over longer periods of time. To answer these questions, this chapter brings results of an experiment of microbiome selection by an axenic *E. huxleyi* strain.

We took the opportunity of the *Tara Breizh* Bloom cruise organized by the Ecology of Marine Plankton team (ECOMAP, Roscoff) and the *Tara Ocean* Foundation in Spring 2019 to tackle these questions. This cruise was set up to follow an *E. huxleyi* bloom in the Celtic Sea for five days using a Lagrangian strategy. This was achieved by the deployment of an Argo float at the bloom patch. Every day, the positions of the sampling sites were determined next to the position of the drifting float. Besides analyzing the prokaryotic and eukaryotic microbial community dynamics during this natural bloom, we used environmental samples collected inside and outside the bloom to inoculate an axenic *E. huxleyi* culture and followed the microbiome changes over one year. The main objectives of this study were (i) to investigate how the microbiome composition of different sources influence the microbiomes grown from axenic *E. huxleyi* cultures; (ii) to identify the short-to-long term changes in the microbiome composition; and (iii) to identify whether the exposition of the natural bacterial community to high *E. huxleyi* cell concentrations in the bloom would result in different microbiomes in cultures.



---

**Microbiome assembly in axenic *Emiliana huxleyi* cultures is influenced by the source community composition and is resilient to disturbance**

Mariana Câmara dos Reis<sup>1,5</sup>, Sarah Romac<sup>1</sup>, Florence Le Gall<sup>1</sup>, Dominique Marie<sup>1</sup>, Miguel Frada<sup>2,3</sup>, Thierry Cariou<sup>4,\*</sup>, Colomban de Vargas<sup>1,5</sup>, Christian Jeanthon<sup>1,5</sup>

<sup>1</sup>Sorbonne Université/Centre National de la Recherche Scientifique, UMR7144, Adaptation et Diversité en Milieu Marin, Station Biologique de Roscoff, Roscoff, France

<sup>2</sup>The Interuniversity Institute for Marine Sciences in Eilat, 88103 Eilat, Israel

<sup>3</sup>Department of Ecology, Evolution and Behavior, Alexander Silberman Institute of Life Sciences, Hebrew University of Jerusalem, Israel

<sup>4</sup>Sorbonne Université/Centre National de la Recherche Scientifique, FR2424, Station Biologique de Roscoff, Roscoff, France

<sup>5</sup>Research Federation for the study of Global Ocean Systems Ecology and Evolution, FR2022/*Tara* GOSEE, Paris, France

\*New address: IRD, US191, Instrumentation, Moyens Analytiques, Observatoires en Géophysique et Océanographie (IMAGO), Technopôle de Brest-Iroise, Plouzané, France

## Abstract

Phytoplankton and heterotrophic bacteria are the major primary producers and decomposers in the oceans. Understanding their interactions is critical to assess the individual contribution of the associated bacterial community and phytoplankton to their success in ocean ecosystems. Questions remain regarding how the phytoplankton microbiomes are selected, and the role of the host in the process of selection. Here, we used the globally spread coccolithophore *Emiliana huxleyi* to investigate these questions. During a 5 days cruise following an *E. huxleyi* bloom patch in the Celtic Sea in Spring 2019, we collected bacterial communities from surface and deep chlorophyll maximum depth samples within and outside the bloom and inoculated them in axenic *E. huxleyi* cultures. The cultures were then followed over one year in order to evaluate the short-to-long term changes in microbiomes composition. Although the culture conditions led to the severe reduction of the initial bacterioplankton diversity, the resulting microbiomes were dependent on the composition of the initial bacterioplankton community. The inoculum involving bacterial populations collected at the *E. huxleyi* bloom depth resulted in a more diverse microbiome that maintained over time several specific Flavobacteriaceae members typically associated with the degradation of polysaccharides produced during bloom demises. The microbiomes selected were stable over time and resilient to disturbance. Overall, this work sheds new light on the importance of the initial inoculum composition in microbiome recruitment and elucidates the temporal dynamics of its composition and resilience.

## Introduction

The oceans cover more than 70% of the world's surface harboring key processes, such as photosynthesis and organic matter degradation, that sustain and control the nutrient and carbon cycles and global productivity (Falkowski, 1997; Behrenfeld *et al.*, 2006). Phytoplankton and heterotrophic bacteria, as major primary producers and decomposers, respectively, are two fundamental actors in these processes (Falkowski, 1994; Field *et al.*, 1998; Pomeroy *et al.*, 2007; Falkowski, Fenchel and Delong, 2008; Jiao *et al.*, 2010). To investigate interactions between these major contributors is of central relevance to better understand microbial processes in the oceans.

The surrounding region of a microalgal cell is enriched in organic molecules which attract chemotactic bacteria (Smriga *et al.*, 2016; Seymour *et al.*, 2017). This area, known as the phycosphere, is an analogous of the rhizosphere in plants (Seymour *et al.*, 2017). It is at the phycosphere level that the interactions, including exchanges of molecules and metabolites (Cirri and Pohnert, 2019) between both partners, take place. Heterotrophic bacteria take advantage of the complex organic matter released by microalgae to sustain their growth while in exchange they can stimulate microalgal growth by releasing promoters (Amin *et al.*, 2015), by providing vitamins (such as vitamin B12) (Cruz-López and Maske, 2016), by facilitating iron uptake (Amin *et al.*, 2009), or by protecting them against pathogenic bacteria (Seyedsayamdost *et al.*, 2014). Microalgae can release specific metabolites which will select the bacteria growing in the phycosphere (Buchan *et al.*, 2014; Shibl *et al.*, 2020). On the other hand, the bacterial composition of the phycosphere will determine how the organic matter will be degraded and which molecules will be made available to the microalga (Fu *et al.*, 2020). However, to study the bacterial composition and selection in the phycosphere still represents a challenge considering the microscale where this process takes place. As a consequence, the selection processes of many phytoplankton groups remain poorly explored (however see **Chapter 2**; Kimbrel *et al.*, 2019; Mönnich *et al.*, 2020).

To overcome this challenge, one strategy is to study the processes of selection in natural algal blooms (Zhou *et al.*, 2019) or by experimental manipulation (*e.g.* meso/microcosms and cultures) (Ajani *et al.*, 2018; Kimbrel *et al.*, 2019; Sörenson *et al.*, 2019; Fu *et al.*, 2020; Mönnich *et al.*, 2020), when phytoplankton cells are at high concentrations. Natural blooms are short-lived phenomena that happen when specific physical, chemical and biological

conditions allow microalgae to reach enormous cell concentrations and spread over kilometers in the sunlit layer of the aquatic systems (Assmy and Smetacek, 2009). Although phytoplankton blooms are common, less than 5% of the described phytoplankton species have been reported so far as to contribute to these phenomena in lakes and oceans (Assmy and Smetacek, 2009). *Emiliania huxleyi* is the most abundant and cosmopolitan coccolithophore species and is able to form massive annual blooms in temperate and subpolar oceans mostly in Spring (Tyrrell and Merico, 2004). *E. huxleyi* blooms are characterized by blue turquoise waters that can be observed from satellite images (Tyrrell and Merico, 2004). These blooms have a critical relevance for carbon and sulfur cycles due to the ecological and biogeochemical roles of coccolithophores as primary producers, calcifiers, and main contributors to the emission of dimethylsulfoniopropionate (DMSP) to the atmosphere (Malin and Steinke, 2004; Rost *et al.*, 2004). Although the role of viruses in bloom termination has been thoroughly investigated (*e.g.* Bratbak, Egge and Heldal, 1993; Vardi *et al.*, 2012; Lehahn *et al.*, 2014), only few studies have targeted the microbiome diversity associated with *E. huxleyi* in natural environments (Gonzalez *et al.*, 2000; Zubkov *et al.*, 2001) and cultures (Green *et al.*, 2015; Orata *et al.*, 2016; Rosana *et al.*, 2016; **Chapter 1**). Roseobacters and SAR86 have been pointed out as the main bacterial groups in natural *E. huxleyi* blooms (Gonzalez *et al.*, 2000; Zubkov *et al.*, 2001). Meanwhile, the microbiome of *E. huxleyi* in cultures is highly dominated by *Marinobacter* members (**Chapter 1**) and by Rhodobacteraceae members (including Roseobacter clade members) (Green *et al.*, 2015).

In this study, we allied investigation in a natural *E. huxleyi* bloom and selection experiment in a manipulated phycosphere to explore the microbiome selection by an axenic *E. huxleyi* culture. By following the prokaryotic community composition in the natural bloom patch over five days, we were able to detect changes in alpha and beta diversity patterns and the taxonomic diversity of the dominant groups. In parallel, to identify the influence of the initial inoculum on the microbiome selected by an axenic *E. huxleyi* culture, we collected prokaryotic communities from two sites (located 34 km apart, inside and outside the bloom event), and from two depths (surface and deep chlorophyll maximum – DCM) to inoculate in 12 independent cultures. The composition and dynamics of the established prokaryotic communities were followed for more than a year. More specifically, we aimed to identify if the exposition of the bacterial community to high concentrations of *E. huxleyi* in the bloom would be reflected in the final microbiomes. Finally, by following the microbiome cell concentrations and diversity from the establishment of the cultures (9 days after inoculation)

until day 392, we also aimed at identifying short-to-long term microbiome diversity changes that are poorly documented (Behringer *et al.*, 2018). We hypothesized that established microbiomes would be enriched in *Marinobacter* and Rhodobacteraceae members often found in *E. huxleyi* cultures and that selected microbiomes would differ according to the initial inoculum. All our cultures experienced a severe stress during the first weeks of cultivation. Our results showed that compositional changes were induced by this event and that microbiomes tend to partially recover their initial composition once normal growth of the algal host was restored.

## **Material and Methods**

### **Study site and sample collection**

Samples used in this study were collected aboard the schooner *Tara* (Sunagawa *et al.*, 2020) in the Celtic Sea (from 48°19-48°24 N/6°28-7°02 W; Figure 1A), during the ‘*Tara BreizhBloom*’ cruise from May 27 to June 2, 2019. To follow an *E. huxleyi* bloom event that was occurring in this area (Figure 1B), an Argo float was deployed in the center of the bloom patch and its position was used twice a day (early morning and end of afternoon) to determine the geographical locations of the sampling stations.

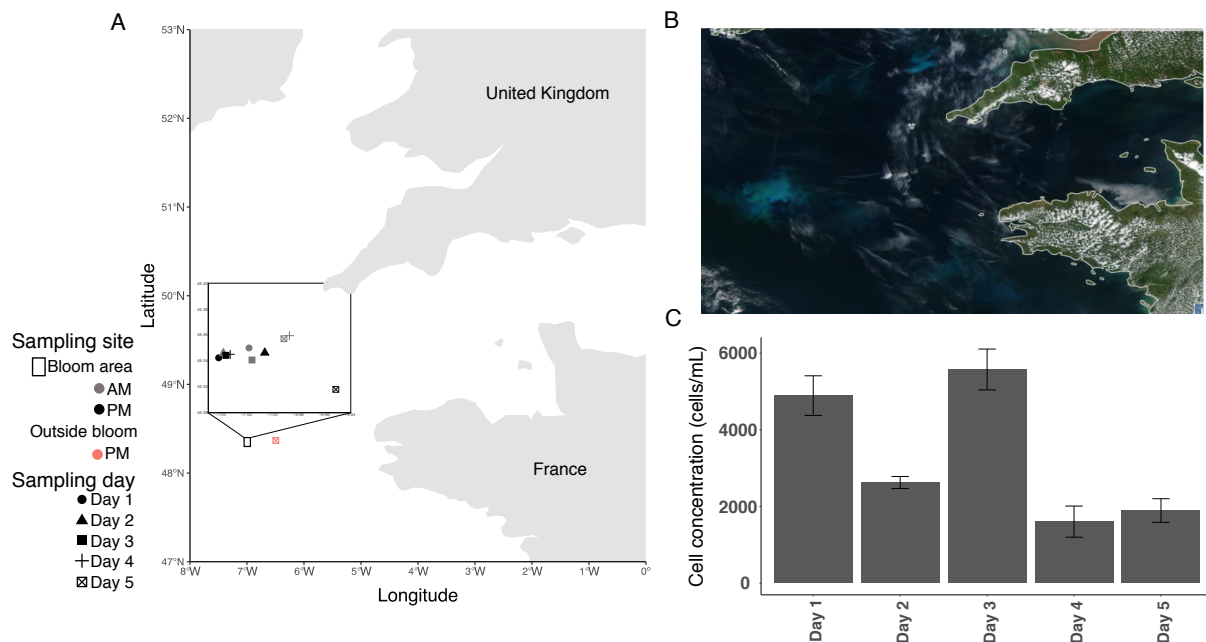


**Figure 1:** Sampling area and characteristics of the *E. huxleyi* bloom in the Celtic sea. **A)** Map showing the bloom area (black rectangle). The sampling strategy covered daily sampling for five days (shape coded) in the morning (AM, grey symbol) and the afternoon (PM, black symbol). The red square indicates the location of the sampling performed outside the bloom, 34 km apart from the last bloom station sampled. **B)** Satellite image showing the bloom area. Source: <https://www.star.nesdis.noaa.gov/sod/mecb/color/ocview/ocview.html>; May 21, 2019. **C)** *E. huxleyi* cell concentrations at AM bloom sites during the survey. Cell concentrations were calculated from duplicate filters using scanning electron microscopy (20 images per filter were analyzed).

On the last sampling day, a site about 34 km apart from the bloom area was sampled to serve as a reference (Figure 1A). For each sampling event, surface to 50 m depth profiles of temperature, salinity, turbidity, pressure, photosynthetic active radiation (PAR), chlorophyll *a* (chl<sub>a</sub>) fluorescence, oxygen concentrations and pH were conducted by deploying the SBE19+ profiler. Water samples from surface and bloom depth were collected twice a day using an 8L Niskin bottle for nutrient analyses. After collection, nutrient samples (125 mL) were stored at -20°C for further analysis. Concentrations of nitrate, nitrite, phosphate and silicate were measured using a AA3 auto-analyzer (Seal Analytical) following the methods described by Tréguer and Le Corre, (1975). Samples for flow cytometry (FCM), scanning electron microscopy (SEM), and metabarcoding analysis, were collected at the bloom depth and

prefiltered through a 20 µm mesh to eliminate large microzooplankton. For FCM analysis of photosynthetic eukaryotes and prokaryotic communities, two replicates (1.5 mL) were fixed twice a day using glutaraldehyde (0.25% final concentration) and Poloxamer 10% (0.1% final concentration) and incubated for 15 min at 4°C before flash freezing in liquid nitrogen. At the last bloom site (Day 5) and at the reference site, samples for nutrients and FCM were collected from surface and bloom depth (DCM for reference site). For SEM analysis, samples of morning sites (two replicates of 250 mL) were gently filtered onto PC membranes (47 mm in diameter; 1.2 µm pore-size) (Millipore). Filters were placed onto Petri slides, dried at least 2h at 50°C, and finally stored at room temperature. For metagenomic analysis, cell biomass was collected from ~ 14 L of seawater by successive filtration onto large (142 mm in diameter) 3 µm pore-size and then 0.2 µm pore-size polycarbonate membranes (Millipore). Filters were flash-frozen and stored in liquid nitrogen. Back in the lab, filters were transferred to -80°C until DNA extraction and purification steps.

### Scanning electron microscopy analysis

Representative filter portions were fixed in aluminum stubs and sputter coated with gold–palladium (20 nm) (Keuter *et al.*, 2019). Quantitative assessment of *E. huxleyi* cells was performed using a Phenom Pro scanning electron microscope. Cells were counted in twenty random screens (area analyzed = 0.16 mm) and cell concentrations were calculated based on the filtered sample volume corresponding to the area analyzed (0.042 mL).

### Community assembly experiments

**(i) Axenization.** *E. huxleyi* strain RCC1212, isolated from the Atlantic Ocean near to South Africa on September 1st, 2000, was obtained from the Roscoff Culture Collection. This strain was axenized following a sequence of washing and centrifugation steps, and variable incubation periods with increasing concentrations of an antibiotic solution mixture (ASM). The original detailed protocol developed at the Scottish Association for Marine Science (SAMS, Oban, UK) is available at: [assemblemarine.org/assets/Uploads/Documents/toolbox/Antibiotic-treatmentSAMS.pdf](https://assemblemarine.org/assets/Uploads/Documents/toolbox/Antibiotic-treatmentSAMS.pdf).

Briefly, 15 mL of an exponential phase culture (~ 10<sup>6</sup> cells/mL) were centrifuged at 1600 g for 4 min. The pellet was resuspended in sterile K/2 medium (Keller *et al.*, 1987; Probert, 2019) prepared with reconstituted red sea water (<https://www.redseafish.com/red-sea->

salts/red-sea-salt/; 37.7 grams of salts in 1L of ultrapure water, boiled 100°C for 20 min) and sterilized using 0.1 µm filtration unit. After centrifugation at 1600 g for 2 min, the supernatant was discarded, and the same process was repeated for 6 times. The final pellet resuspended in sterile K/2 medium was further used as inoculum. The axenization medium (final volume per tube, 2 mL) contained variable volumes of K/2 medium (according to the ASM concentration used), increasing concentrations (from 0 to 35%) of the ASM, and 25 µL of Marine Broth (1/10 strength) added to promote bacterial growth. The 10X ASM contained the following antibiotics: cefotaxime (5 g/L), carbenicillin (5 g/L), kanamycin (2 g/L) and augmentin (2 g/L). The ASM was filtered sterilized (0.1 µm) and kept at -20°C for long-term storage. Culture tubes (one tube per ASM condition) inoculated with 100 µL of prewashed RCC1212 culture were incubated at 17°C with an irradiance of  $70 \pm 20 \mu\text{mol photons s}^{-1}\text{m}^{-2}$ . Culture aliquots (50 µL) of each ASM condition were sampled daily for 5 days and transferred into new culture tubes containing sterile K/2 medium that were incubated as before.

Once these new cultures were dense (about 15 days later), the presence of bacteria was checked by FCM. For FCM, 196 µL of each positive culture was fixed with glutaraldehyde 25% (0.25% final concentration) for 15 min in the dark. Then fixed cultures were stained with SYBR green (1/10,000 final concentration). Samples were analyzed in an FACSCanto flow cytometer (Becton Dickinson, San Jose, CA, USA) equipped with 488 and 633 nm lasers and standard filter setup. Bacterial data acquisition was triggered on the green fluorescence signal and non-diluted samples were run for 1 min at medium rate (~50 µL/min). Bacteria-free cultures were transferred into fresh K/2 medium and reinspected by FCM after the next culture cycle. For maintenance, axenic cultures were grown in K/2 medium prepared as previously mentioned. They were routinely checked for bacterial contamination by FCM as mentioned above. When used for specific experiments, culture aliquots (3-5 mL) stained with SYBR green (1/10,000 final concentration) and filtered onto 0.2 µm polycarbonate black membrane (Millipore Isopore) were examined by fluorescence microscopy to ensure cultures remained axenic.

**(ii) Sample preparation and inoculation.** Four seawater samples were used in the bacterial community assembly experiment. They consisted of a surface and a DCM sample collected in the bloom area on day 5 (station D5\_IN\_PM) and a surface and a DCM sample collected the same day apart the bloom area (station D5\_OUT\_PM). Seawater was collected using the Niskin and immediately processed. In order to remove the autotrophic picoeukaryotes and

cyanobacteria from the inoculum, samples were gently filtered through a 0.45  $\mu\text{m}$  pore size membrane (Millipore). To estimate the number of prokaryotic cells lost during the filtration step, aliquots of total and filtered seawater samples were fixed for FCM analysis using the methods previously mentioned. After filtration, 150  $\mu\text{L}$  of each prokaryotic community were transferred in triplicates into 50 mL culture flasks filled with 15 mL of K/2 medium prepared as described before. Finally, 150  $\mu\text{L}$  of stationary phase (17 days old) RCC1212 axenic culture was added to each flask. Six axenic RCC1212 cultures were used as controls. Overall, the 18 cultures (12 treatments and 6 controls) were incubated at 15°C and a 12:12 photoperiod regime. For the first 27 days the light intensity was set up to 20  $\mu\text{mol photons s}^{-1}\text{m}^{-2}$  and a blue filter was used to mimic in situ conditions of the natural bloom. After 27 days, in order to recover the *E. huxleyi* cultures that were crashing (see results section), the light was increased to  $70 \pm 20$   $\mu\text{mol photons s}^{-1}\text{m}^{-2}$  intensity and the blue filter was removed.

**(iii) Molecular survey of the microbiomes in culture.** Once the inoculated *E. huxleyi* cultures reached the exponential growth phase (9 days after inoculation), the axenic controls were checked by FCM to confirm that no contamination happened during the experiment's preparation. Once the axeny was confirmed, 13 flasks (12 treatments + one axenic control) were transferred by inoculating 100  $\mu\text{L}$  of the culture in 10 mL of fresh K/2 medium. Then each treatment was sampled for prokaryotic community composition and FCM analyses. For community composition analysis, 2 mL of culture was centrifuged at 2,000 g for 30 sec to reduce the microalgal load. The supernatants were transferred into new tubes containing 2  $\mu\text{L}$  of Poloxamer 188 solution 10% (Sigma-Aldrich) and centrifuged at 5,600 g for 5 min. The supernatants were discarded, and the pellets were stored at -80°C until DNA extraction. For FCM analysis, duplicate samples were fixed as previously described for environmental samples and stored at -80°C. Cultures were transferred and sampled using the same procedures every 11-14 days for the first 70 days of maintenance. Two additional samplings were performed at days 175 and 392, while still ensuring culture transfers every 3 weeks. The axenic control was regularly checked to ensure the clean handling of the cultures. In addition, culture flasks were daily randomized in the incubator in order to achieve homogeneous light conditions.

### FCM analysis

**(i) Environmental samples.** Back to the laboratory, samples were thawed at room temperature. Fluorescent microspheres (0.95  $\mu\text{m}$  PolySciences) were added to each sample as internal reference at a final concentration between 6000 to 8000 per mL. Phytoplanktonic cells were first analyzed based on their autofluorescence using a FaCSARIA flow cytometer (Becton Dickinson, CA, USA) equipped with 488 and 633 nm lasers and the standard filter setup at a flow rate of 64  $\mu\text{L}/\text{min}$ . A second analysis was run after staining samples with SYBR Green-I (1/10,000, final concentration) to enumerate heterotrophic microorganisms.

**(ii) Laboratory experimental samples.** A FACSCanto flow cytometer (Becton Dickinson, San Jose, CA, USA) equipped with 488 and 633 nm lasers and standard filter setup was used to enumerate *E. huxleyi* and bacterial cells (Marie *et al.*, 1999). For *E. huxleyi*, data acquisition was triggered on the red fluorescence signal and samples were run for 1 min for cultures at medium rate ( $\sim 50 \mu\text{L}/\text{min}$ ). To quantify prokaryotes, samples were diluted 1:10 to 1:100 in TE (10 mM Tris, 1 mM EDTA [pH 7.5]), stained with SYBR Green (1/10,000 final concentration) and incubated for 15 min in the dark. The discriminator was set on green fluorescence, and the samples were analyzed as before.

### DNA extraction and sequencing

DNA from environmental samples was extracted using the method described by (Alberti, 2017). Prokaryotic DNA extraction from cultures and PCR amplification were performed as previously described (**Chapter 2**). Pooled amplicons were sent to Fasteris SA (Plan-les-Ouates, Switzerland) for Illumina high throughput sequencing. The first 84 DNA samples (first 7 time points) were sequenced together using two independent Illumina runs (technical replicates). The last 12 DNA samples (day 392) were sequenced in another Illumina run without sequencing replicates.

## Bioinformatics

The first steps of the bioinformatic treatment and quality control were performed by FASTER SA. First, in order to separate the libraries, the base calling was done based on a 6 nt unique index, using the softwares MiSeq Control Software 2.6.2.1, RTA 1.18.54 and bcl2fastq2.17 v2.17.1.14 and allowing 1 mismatch. Then, Illumina standard adapters removal and quality trimming were done using the Trimmomatic package (version 0.32) (Bolger *et al.*, 2014). Briefly paired-end reads were globally aligned to ensure an end-to-end match. The adapters sequences were identified allowing a maximum of 2 mismatches and removed if the quality score was higher than 30. Then, bases were filtered by quality using a 4-base sliding window scan and trimming was done when the average quality per base dropped below 5. Reads without insert and with ambiguities were removed. All the scripts used for the further bioinformatic analyses can be downloaded from: <https://github.com/mcamarareis/>. Briefly, raw reads from each sequencing run were demultiplexed based on the 8 nucleotide tag sequences with cutadapt (version 2.8.1) using anchored mode and allowing no mismatches, insertions or deletions (Martin, 2011). Since R1 and R2 files (corresponding to each cycle of paired-end sequencing) contained reads with forward and reverse primers (further called forward and reverse reads), the demultiplexing was run two times. The first and second demultiplexing searched for adapters in the R1 file and in the R2 file, respectively, which separated forward and reverse reads for each sample corresponding to each cycle. The primer sequences were removed using the same software allowing mismatches at a rate of 0.1 (insertions and deletions were not allowed) (Martin, 2011). The demultiplexed primer-free sequences were processed to obtain an amplicon sequence variant (ASV) table using the DADA2 pipeline (version 1.14.0 in R 3.6.1) (Callahan *et al.*, 2016; R Core Team, 2017). Since R1 and R2 cycles can have different error rates, they were analyzed independently during all the DADA2 processing. The same was done for the different sequencing runs. First, the sequences were filtered using the function *filterAndTrim* with default values and trimmed according to the sequence quality (see scripts for details). Then, a random subset of the reads was used to learn the error models from forward and reverse reads using the function *learnErrors*. The ASVs were inferred in pooled mode. Following ASV inference, the forward and reverse reads of R1 were merged. The reads coming from the R2 file were also merged but in an inverse position (reverse + forward). The sequences tables were built using the function *makeSequenceTable* and the sequence table obtained for R2 file was reverse complemented. To correct the mixed orientation, the reverse

reads of the R2 were reverse complemented before merging with the forward reads. Before chimera removal, the sequence tables obtained independently for R1 and R2 were merged.

Sequences from the last time point were processed independently using the same methods. Then, all the independent processed data were included in the sequence table for chimera removal, also performed in pooled mode. The sequences were filtered according to the range of length of the primers (from 366 to 376 bp) and the resulting fasta file was used to assign taxonomy using the Silva database v138 by IDtaxa (using a confidence threshold of 50) (Quast *et al.*, 2013; Murali *et al.*, 2018). Chloroplasts and mitochondrial sequences were removed. Sequences not classified at the domain level by IDtaxa were classified using vsearch global alignment using Silva v138 (Rognes *et al.*, 2016). These sequences were removed if they could not be classified and/or were classified as chloroplasts or mitochondrial sequences by vsearch. In addition, because IDtaxa failed in assigning taxonomy to many Rhodobacteraceae sequences at the genus level we used vsearch taxonomy (at 94.5% threshold (Yarza *et al.*, 2014)) for the taxonomic diversity plots. The resultant ASV table was filtered to remove ASVs accounting for less than 0.001% (61 reads) of the total number of reads. Consistency of technical replicates was evaluated by hierarchical cluster analysis (HCA) using Bray-Curtis distance of relative abundance data. After consistency was confirmed, independent technical replicates of each culture were merged by the sum of the number of reads of the ASVs present in the two replicates of the same culture. The abundance and prevalence filters applied removed about 68% of the total number of ASVs while keeping 99% of the number of reads.

### **Community composition and statistical analyzes**

*(i) Environmental samples.* All the analyses were conducted in R version 4.0.2 in Rstudio (1.1.442) and the plots were produced with ggplot2 (RStudio Team, 2016; Wickham, 2016; R Core Team, 2017). Taxonomy pie charts of environmental samples were produced at the genus level. To facilitate visualization, low abundant genus (accounting to less than 3% of relative abundance at each sample) present at the raw community table were grouped and named as “others”. In order to compare the alpha diversity indexes in environmental samples and cultures, the ASV table was rarefied 100 times at the minimum number of reads (3,465) using the function *rtk* (seed=1,000) (Saary *et al.*, 2017). Richness and Shannon indexes were obtained using the function *get.mean.diversity*. HCA was used to identify differences among sampling sites using the Euclidean distance of the Hellinger-transformed data using method “ward.D2”

(function *hclust*) (Legendre and Gallagher, 2001; Oksanen *et al.*, 2015). Heatmap was produced using the function *pheatmap* (Kolde and Kolde, 2015).

**(ii) Experiment.** To analyze alpha diversity dynamics of the cultures, rarefaction was performed at a reads depth of 5,957 reads as previously mentioned. The rarefied matrix was transformed in presence-absence (*decostand* function) and the Jaccard dissimilarity was calculated (*vegdist* function) for beta-diversity analysis (Oksanen *et al.*, 2015). Hellinger distance (Euclidean distance of Hellinger-transformed matrix) was calculated from the non rarefied table (Legendre and Gallagher, 2001; Oksanen *et al.*, 2015). To test the influence of the treatments, replicates and time on the microbiome beta diversity, we performed permutational analysis of variance (PERMANOVA) (Anderson, 2005). Before running the analysis, the functions *betadisper* and *anova*-like permutation test were used to identify significant deviations on the multivariate beta dispersion of the data for treatments, replicates, and time (Oksanen *et al.*, 2015). The effect of treatments and replicates (nested within treatments) was tested using the function *nested.npmanova* (Kindt and Coe, 2005), which calculates the correct statistics for two factors in a nested design. To test the effect of time and the interaction between treatments and time, we used the function *adonis* (Oksanen *et al.*, 2015) including treatments, replicates, and time (number of days) as fixed variables in the model. The permutations of *adonis* were restricted to the replicates level using *strata*. To identify pairwise differences among treatments (including replicates), *nested.npmanova* function was used to test combinations of each pair (total of six combinations). In this case, the number of permutations for treatments was not enough to estimate the p-value, so we focused the interpretation on the R<sup>2</sup> values. HCA was done using the Hellinger distance (Euclidean distance of Hellinger-transformed data) and “ward.D2” method using the function *hclust* (Oksanen *et al.*, 2015). Taxonomy barplots were produced by showing the three most abundant genera, while the less abundant were merged as “others”. In order to identify the shared and specific ASVs in each treatment, we used the rarefied community table and considered all ASVs. *IndVal* analyses were run to identify indicative species of each treatment using the function *multipatt* (package *indicspecies* v1.7.9) with 10,000 permutations (De Cáceres and Legendre, 2009). P-values were adjusted for multiple comparisons using false discovery rate method (function *p.adjust*) (Oksanen *et al.*, 2015).

## Results

The samples used in the community assembly experiment were collected during the *Tara Breizh* Bloom oceanographic cruise that sampled an *E. huxleyi* bloom during 5 days in the Celtic Sea (Figure 1A and 1B). Although these samples were obtained only at the end of the cruise, we present here the ancillary and prokaryotic diversity data to contextualize the results gathered from the laboratory experiment.

### Abiotic and biotic parameters characterizing the *E. huxleyi* bloom in the Celtic sea

Coccolithophore blooms occur seasonally from April to June in the Bay of Biscay along the continental shelf to the Celtic Sea in June and the North-Sea in July and August (Holligan *et al.*, 1983; Van Oostende *et al.*, 2012; Poulton *et al.*, 2014; Perrot *et al.*, 2018). We followed the bloom patch in end May-June 2019 in the Celtic Sea using near-real time interpolated images of non-algal suspended particulate matter (SPM) derived from satellite reflectance data (Perrot *et al.*, 2018) as provided by Ifremer at <http://marc.ifremer.fr/en/results/turbidite>.

Over the duration of the sampling period, temperature and salinity ranged from 12.4°C to 15.4°C and from 35.4 to 35.5 PSU, respectively (Supplementary Table 1). Nutrient concentrations were low with NO<sub>2</sub> + NO<sub>3</sub> and PO<sub>4</sub> ranging from the detection threshold to 1.25 µmol and 0.05 to 0.2 µmol/L, respectively. These low values were typical of a bloom event where cells consume most of the nutrients. *E. huxleyi* cell densities ranged from 1.6 x 10<sup>3</sup> to 5.6 x 10<sup>3</sup> cells/mL over the sampling period (Figure 1C). Total prokaryotic abundance ranged from 8.1 × 10<sup>5</sup> to 2.0 × 10<sup>6</sup> cells/mL.

FCM data evidenced an average of total photosynthetic eukaryotic cell concentration of 2.47 x 10<sup>4</sup> cells/mL (min: 9.57 x 10<sup>3</sup> cells/mL and max: 3.68 x 10<sup>4</sup> cells/mL). The most abundant photosynthetic organisms identified by FCM were *Synechococcus* with cell concentrations ranging from 2.1 x 10<sup>4</sup> to 1.1 x 10<sup>5</sup> cells/mL. On the other hand, cell concentrations of heterotrophic bacteria ranged from 8.1 x 10<sup>5</sup> to 2.0 x 10<sup>6</sup> cells/mL. The lowest cell concentration was observed in the outside bloom samples (Supplementary Table 1).

Overall, the environmental samples displayed a prokaryotic richness of 146 ± 26 ASVs (mean ± SD, n=19) (Supplementary Figure 1A). Richness increased over the course of the bloom and reached a maximum at day 4 (174 ± 11 ASVs, n=4) and decreased the fifth day.

The samples collected for the community assembly experiments (0.2-3  $\mu\text{m}$  fractions of day 5 PM inside bloom and day 5 PM outside bloom) contained 158 and 139 ASVs, respectively. Note that the Shannon index, which is less affected by sampling effort, displayed homogeneous values (mean  $3.9 \pm 0.4$  SD,  $n=19$ ) across the samples (Supplementary Figure 1B). Hierarchical clustering revealed three groups of samples that clearly delineated the evolution of the prokaryotic communities across the bloom in a time-dependent manner (Supplementary Figure 2). Prokaryotic community collected from days 2 to 4 where the richness increased clustered together and were distinct from that sampled on the fifth day. Surprisingly, prokaryotic communities outside the bloom grouped with those collected a few hours before in the bloom area.

We found a diverse prokaryotic community at the genus level over the course of the bloom at AM and PM sites (Supplementary Figure 3). SAR11 clade (11% of the total reads,  $n=11$ ) and *Synechococcus* sp. (7%) were present in all samples. Members of the genus *Pseudoalteromonas* emerged at day 2 and became the most abundant (12%), dominating over SAR11 on the fifth day in and outside the *E. huxleyi* bloom. Both members of the Roseobacter clade, assigned to *Ascidiaehabitans* and *Sulfitobacter*, prevailed in the periods where richness increased. While *Sulfitobacter* was not observed after richness peaked, proportions of *Ascidiaehabitans* remained stable. The Flavobacteriaceae were moderately abundant (11% of the total reads), the NS4 group being the most prevalent while NS5 group and *Polaribacter* were occasionally found. Thermoplasmata (4%) emerged at day 3 and were present until the end of the sampling. Some genera were detected in only one sample in which they predominated like *Vibrio* (12% in day 2 PM sample) and *Nitrosopumilus* (18% in day 3 AM sample) or were substantial such as the members of OCS116 clade (4% in day 2 PM sample).

Regarding the samples that served as inocula for the community assembly experiment, the main observed differences were the presence of *Lentimonas* (5.5%) in the bloom site sample and the presence of the OM60 (NOR5) clade (3.6%) and Thermoplasmata (4%) in the outside bloom sample.

## Community assembly experiment

### *(i) Dynamics of cell concentrations and alpha-diversity patterns in the cultures*

Seawater samples used to inoculate axenic *E. huxleyi* cultures were filtered through 0.45  $\mu\text{m}$  membranes to remove the abundant autotrophic eukaryotes and *Synechococcus* populations they contained. A loss of about 40% of the initial bacterial cell concentration was observed after this filtration step (data not shown). A clear decrease of *E. huxleyi* cell concentrations ( $80\% \pm 0.04$  SD,  $n=12$ ) was noticed in all the treatments between the inoculation and the 3 first culture transfers (from day 9 to day 32) (Figure 2A). To prevent culture death, light intensity was increased at day 32 to  $70 \pm 20 \mu\text{mol photons s}^{-1}\text{m}^{-2}$  and a larger microalgal inoculum (10% of the final culture volume instead of 1%) was transferred. Cultures recovered growth. Their cell densities gradually increased at each next transfer until day 70 where they reached highest cell concentration ( $9.9 \times 10^5 \pm 1.2 \times 10^5$  cells/mL) and remained stable up to the end of the experiment (Figure 2A).

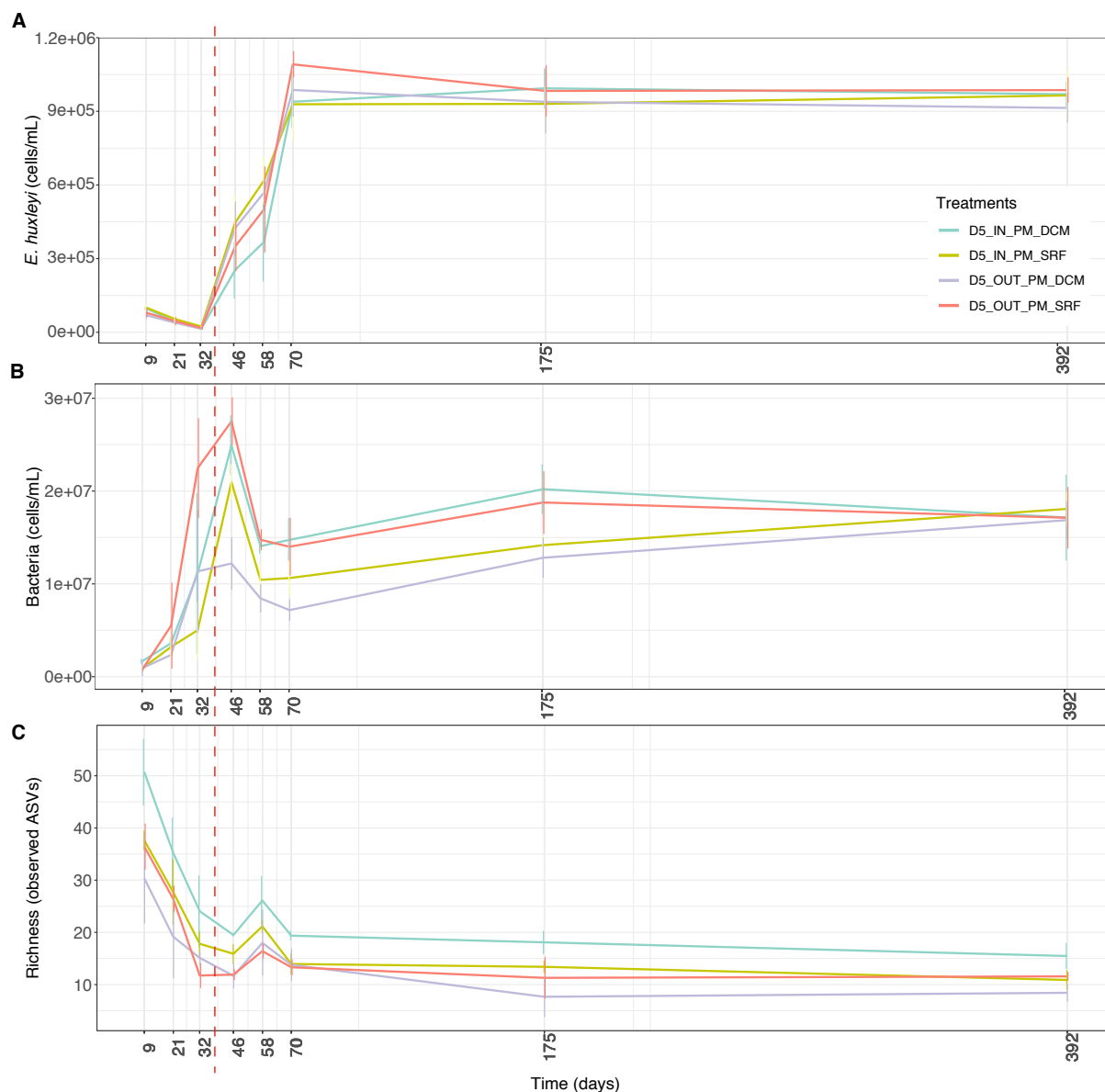


**Figure 2.** Dynamics of (A) *E. huxleyi* and (B) bacterial cell concentration (cell/mL) over time (mean  $\pm$  SD,  $n=3$  for the four first time points and  $n=6$  for the last four). (C) Richness, expressed as number of prokaryotic ASVs over time for each treatment (mean  $\pm$  SD,  $n=3$ ). Colors of the curves indicated the different water samples used as inoculum: D5\_IN\_PM\_DCM (DCM sample inside the bloom); D5\_IN\_PM\_SRF (surface sample inside the bloom); D5\_OUT\_PM\_DCM (DCM sample outside the bloom); D5\_OTU\_PM\_SRF (surface sample outside the bloom). The red dotted line represents the moment following the increase of the inoculum at the culture transfer to recover *E. huxleyi* cell concentration.

Bacterial cell concentrations increased during the crash period and decreased once algal cultures recovered (Figure 2B). Regarding the structure of the bacterial community, a severe loss of richness between the natural and culture samples was observed (Supplementary Figure 1A). At day 9, the bacterial richness in the cultures was about one fourth of the richness in the environmental samples ( $33 \pm 8$  SD,  $n=12$ ) (Supplementary figure 1A). This reflected also a parallel decrease in the Shannon index, which at day 9, was about one third the values recorded in environmental samples ( $1.4 \pm 0.6$  SD,  $n=12$ , Supplementary figure 1B). Over the course experiment, we could observe a decrease in richness along the first five weeks (mean decrease  $24 \pm 7$  SD,  $n=12$ , until day 46) (Figure 2C). After an increase at day 58 that corresponded to the period of culture recovery, the richness values decreased again and remained stable until day 392 ( $11$  ASVs  $\pm 3$ ). The decrease of richness was mainly associated with the loss of low abundance ASVs, while the dominant ones remained over the course of the experiment (Supplementary Figure 4). In general, the Shannon index also decreased over the first three time points (mean decrease  $0.55 \pm 0.63$  SD,  $n=12$ ) and then gradually increased to values similar to that from day 21 (day 392:  $1.21 \pm 0.4$ ,  $n=12$ ) (data not shown). The highest richness and Shannon indexes were obtained in the treatments amended with the bloom DCM sample (richness:  $26 \pm 11$ ; Shannon  $1.6 \pm 0.4$ ,  $n=24$ ).

### **Beta diversity patterns among treatments and over time**

In order to identify the influence of the different initial prokaryotic communities and to follow the changes in the microbiome beta diversity with time, we used two metrics, Hellinger distance (Euclidean distance of Hellinger-transformed data) and Jaccard dissimilarity. Principal component analysis using Jaccard dissimilarity demonstrated that *E. huxleyi* cultures inoculated with surface samples grouped together (Figure 3A), while those inoculated with inside and outside bloom DCM samples formed two other independent clusters.

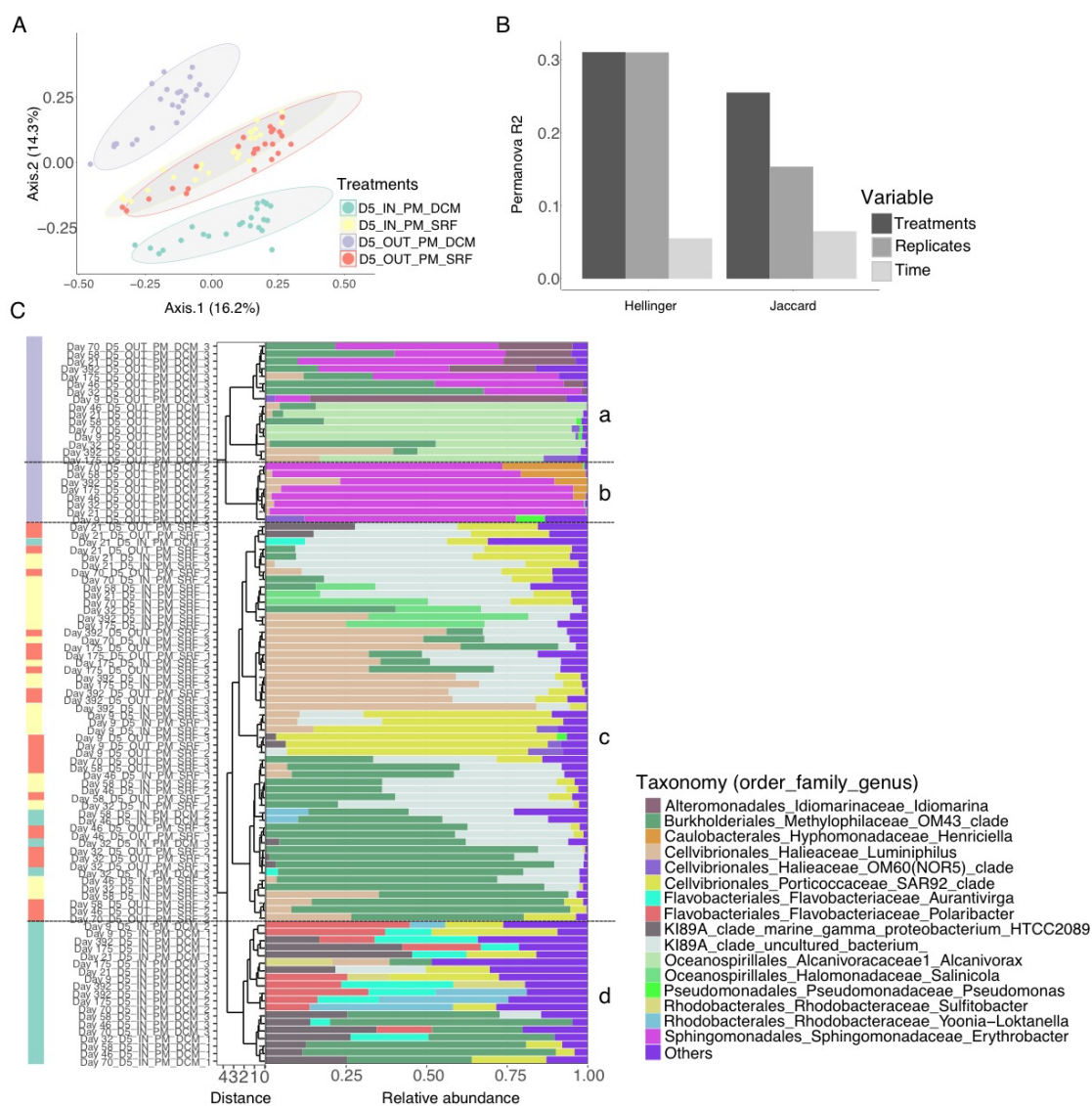


**Figure 3.** Beta-diversity patterns of *E. huxleyi* microbiomes across treatments and time. **(A)** Principal coordinates analysis (PCoA) using Jaccard dissimilarity matrix of the presence-absence transformed rarefied table. Colors correspond to each treatment that received prokaryotic communities from different water samples: D5\_IN\_PM\_DCM (DCM sample inside the bloom); D5\_IN\_PM\_SRF (surface sample inside the bloom); D5\_OUT\_PM\_DCM (DCM sample outside the bloom); D5\_OTU\_PM\_SRF (surface sample outside the bloom). Ellipses represent 95% confidence. **(B)** R2 of permutational multivariate analysis of variance (PERMANOVA) and nested PERMANOVA using two metrics (see material and methods for details). **(C)** Hierarchical clustering produced with the Hellinger distance matrix using “ward.D2” method. Codes of each microbiome are experiment sampling day\_treatment\_replicate. Bar plots indicate the taxonomy of the 3 most abundant genera. The other genera were merged as “others”.

Statistical significance of the effect of treatments, replicates and time on the diversity of the microbiomes was assessed by PERMANOVA and nested PERMANOVA. Before performing PERMANOVA analysis we tested the beta-dispersion of the microbiomes grouped by treatments, time and replicates. We observed significant beta-dispersion across treatments for both metrics tested ( $p = 0.001$ ) while beta-dispersion of replicates was only significant using Hellinger metric ( $p = 0.007$ ). Beta-dispersion was not significant over time for both metrics. Still PERMANOVA results are robust to dispersion for balanced designs like ours (Anderson and Walsh, 2013). PERMANOVA results of Hellinger and Jaccard dissimilarity showed that treatments, replicates and time had a significant influence on the microbiomes beta diversity (Supplementary Tables 2 and 3). Treatments explained from 26% ( $F_{\text{Jaccard}} = 4.43$ ;  $p_{\text{Jaccard}} = 0.001$ ) to 31% ( $F_{\text{Hellinger}} = 2.67$ ;  $p_{\text{Hellinger}} = 0.002$ ) of the patterns observed, while replicates were responsible for 15% ( $F_{\text{Jaccard}} = 2.72$ ;  $p_{\text{Jaccard}} = 0.001$ ) to 31% ( $F_{\text{Hellinger}} = 8.56$ ;  $p_{\text{Hellinger}} = 0.001$ ) (Figure 3B and Supplementary Tables 2 and 3). Time was responsible for explaining only a small proportion of the variance, ranging from 6% ( $F_{\text{Hellinger}} = 14.76$ ;  $p_{\text{Hellinger}} = 0.001$ ) to 7% ( $F_{\text{Jaccard}} = 10.31$ ;  $p_{\text{Jaccard}} = 0.001$ ) (Figure 3B and Tables 2 and 3). The interaction between treatments and time was significant using Hellinger distance ( $F = 2.23$ ;  $p = 0.019$ ) however it explained a small proportion of the variance ( $R^2 = 0.025$ ). In addition, pairwise comparisons of treatments (including replicates) using nested PERMANOVA (Supplementary Table 4) indicated that treatments explained a higher proportion of the variance between bloom DCM and bloom surface and/outside bloom treatments ( $R^2$  from 0.19 to 0.25) (Supplementary Table 4). In comparisons between surfaces (bloom and outside bloom) treatments, a larger proportion of the variance was explained by replicates (0.14) rather than treatments (0.07) (Supplementary Table 4).

Clustering using Hellinger distance revealed that the prokaryotic community composition of all the cultures clustered into three main groups according to the inoculum origin (Figure 3C). The outside bloom DCM treatments formed the two clusters (a and b) (Figure 3C), highlighting the compositional differences between the 3 replicates, which were dominated by different bacterial genera. Replicate 1 (cluster a) was dominated by *Alcanivorax* (77%,  $n=8$ ), while replicates 2 (cluster a) and 3 (cluster a) were dominated by two different *Erythrobacter* (83% and 41%, respectively). The second main cluster (c) mainly consisted in treatments inoculated by both surface water samples (Figure 3C). Surface treatments were dominated by OM43 clade (20% and 35 % in the inside and outside bloom sample, respectively), KI89A clade (35% and 24% in the inside and outside bloom sample,

respectively). The composition of both surface treatments was differentiated by the presence of SAR92 clade members in the outside bloom (17%) and *Luminiphilus* in the inside bloom (18%). Finally, the third cluster (d) formed by microbiomes from the inside bloom DCM treatment was dominated by members of the OM43 clade (25%), the KI89A clade (23%), and *Polaribacter* (10.5%) (Figure 3C). ASVs that dominate in cultures amended with bloom DCM and outside bloom DCM samples were in low abundance or were not detected in the original water mass (Figure 3C and Supplementary Figure 3).

Besides the differences among treatments, we observed a somehow cyclic pattern of the beta-diversity over time using Hellinger distance (Figure 4). Bacterial communities from days 9, 21 and 32 clearly differed from each other. However, from days 49 to 392 their composition gradually tended to become similar to their initial status. This trend was consistently observed in all treatments, except in the outside bloom DCM cultures where it happened at the replicate level (replicates 1 and 3). This dynamic was mainly driven by the transient dominance OM43 clade during the alga crash (Supplementary Figure 5) and the increased abundance of *Luminiphilus* after the algal recovery.

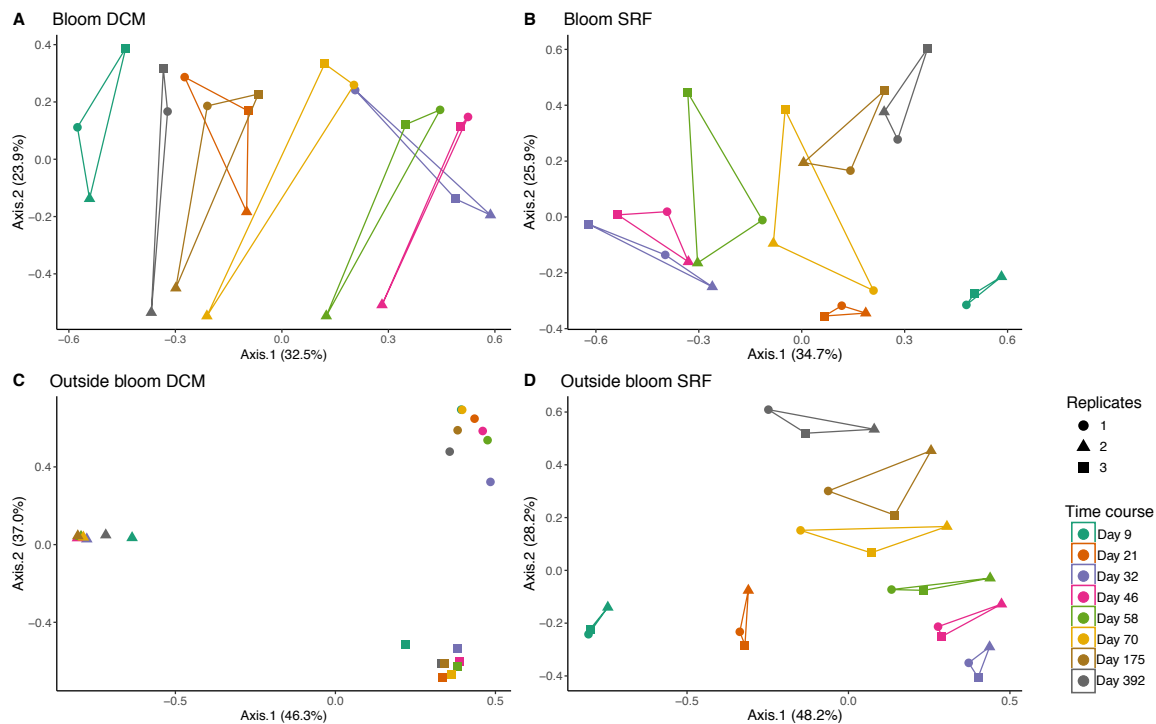


**Figure 4.** Principal components analysis (PCA) showing the cyclic patterns of the microbiome beta diversity. Community distances (Euclidian distances of Hellinger-transformed data) are shown for microbiomes from bloom DCM (D5\_IN\_PM\_DCM) (A), bloom surface (D5\_IN\_PM\_SRF) (B), outside bloom DCM (D5\_OUT\_PM\_DCM) (C), and outside bloom surface (D5\_OUT\_PM\_SRF) (D). In C., the cyclic pattern is observed at the replicate level for replicates 1 and 3. The polygons link replicates (shape coded) at each time point (color coded).

### Shared, specific ASVs and indicative ASVs among treatments

In total, 46 ASVs were shared between the microbiomes of the four treatments. Among the most prevalent (> 70%), *Luminiphilus*, OM43 and KI89A clades were the most abundant while, an Oxalobacteraceae assigned to *Janthinobacterium* by vsearch and *Pseudomonas* were lower (Supplementary Table 5). Among the shared ASVs, one (ASV2, KI89A clade) was identified as indicative (*i.e.*, indicator value – *IndVal* – which measures specificity and fidelity of an ASV) of both surface treatments (Supplementary Table 6) (De Cáceres and Legendre, 2009). ASVs assigned to SAR92 and OM43 clades, were indicative of inside bloom treatments and outside bloom surface (*IndVal* from 0.7 to 1).

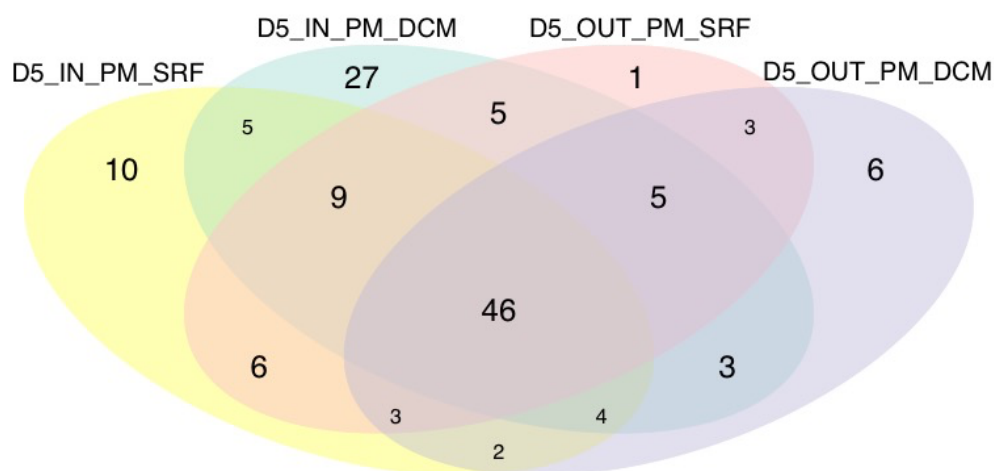


**Figure 5.** Venn diagram showing the number of ASVs shared by the different treatments. Acronym of different treatments: D5\_IN\_PM\_DCM, bloom DCM sample; D5\_IN\_PM\_SRF, bloom surface sample; D5\_OTU\_PM\_DCM, outside bloom DCM sample; D5\_OTU\_PM\_SRF, outside bloom site SRF.

The microbiomes grown from the inside bloom DCM sample displayed the highest number of specific ASVs (27 ASVs) and indicative ASVs (13 ASVs) (Figure 5 and Supplementary Table 6). Nine of the specific ASVs belonged to the family Flavobacteriaceae, four being assigned to the genus *Polaribacter* (Supplementary Table 5). The most prevalent among the indicative flavobacterial ASVs, assigned to *Aurantivirga* and *Polaribacter*, were present in all and in 18 out of 24 ‘bloom-DCM’ microbiomes, respectively, and displayed (*Indval* 1 and 0.87 respectively) (Supplementary Table 6). Other specific bloom DCM indicative ASVs belonged to Rhodobacteraceae (*Sulfitobacter* as classified by vsearch and *Yoonia-Loktanella*) and Tenderiaceae (Supplementary Table 6). In addition, some indicative ASVs with *Indval* higher than 0.86 (*Polaribacter*, KI89 clade and *Aurantivirga*) were shared with other treatments (Supplementary Table 6).

Outside bloom surface and DCM treatments displayed the lower number of specific ASVs. *Alcanivorax*, *Herinciella* and *Joostela* were significantly indicative of outside bloom DCM treatment (Supplementary Table 6) and the most prevalent. Outside bloom surface treatments harbored only a single specific ASV (*Porticoccus*) in a unique sample (1 out of 24 microbiomes).

## Discussion

In this study, we explored the 2019 *E. huxleyi* bloom in the Celtic Sea and collected bacterioplankton samples for conducting a microbiome selection experiment in *E. huxleyi* axenic cultures. Satellite images and biological data we obtained indicate that the bloom was already in its decaying phase when we started the sampling.

First, the high reflectance patch visible on the satellite images (Figure 1B) and the daily vanishing of the coccolith-derived turbidity signal observed from the interpolated images of non-algal suspended particulate matter as provided by Ifremer (see Results section) were both indicative of detached coccoliths from dead *E. huxleyi* cells (Neukermans and Fournier, 2018; Perrot *et al.*, 2018). This assumption was confirmed by the complete disappearance of the coccolith-derived turbidity signal a couple of days after we left the sampling area. Second, a suite of ongoing experiments on the bloom samples using diagnostic lipid- and gene-based molecular biomarkers (Vardi *et al.*, 2009; Hunter *et al.*, 2015; Ziv *et al.*, 2016; Vincent *et al.*, 2021) revealed the detection of specific viral polar lipids and visualized *E. huxleyi* infected cells during bloom succession, suggesting that the demise of the *E. huxleyi* bloom was mediated by Coccothovirus infections (Vardi *et al.*, pers. comm.) as often proposed (Bratbak *et al.*, 1993; Vardi *et al.*, 2012; Laber *et al.*, 2018). Third, the composition of the bacterial community, *e.g.* the presence of Flavobacteriaceae and Pseudoalteromonadaceae, is another indicator of the bloom demise (Lovejoy *et al.*, 1998; Buchan *et al.*, 2014). Flavobacteria, are reported amongst the main bacteria present in the declining phase of phytoplankton blooms (Teeling *et al.*, 2012, 2016; Landa *et al.*, 2016), which seems linked to their capacity to degrade high molecular weight substrates such as proteins and polysaccharides (Cottrell and Kirchman, 2000; Kirchman, 2002; Fernández-Gomez *et al.*, 2013; Kappelmann *et al.*, 2019). TonB-dependent transporters, often specific for polysaccharide uptake, were recently identified as the most highly expressed protein class, split approximately evenly between the Gammaproteobacteria and Bacteroidetes, during a spring phytoplankton bloom in the southern North Sea (Francis *et al.*, 2021). Finally, the algicidal effects of *Pseudoalteromonas* strains and species have been documented in many microalgae (Holmström and Kjelleberg, 1999; Mayali and Azam, 2004; Li *et al.*, 2018), which calls attention to their potential role in the *E. huxleyi* bloom termination (Lovejoy *et al.*, 1998).

Besides the presence of Flavobacteriaceae and Pseudomonadaceae, our results are in agreement with the only two past studies on the diversity of the bacterioplankton associated

with *E. huxleyi* blooms (Gonzalez *et al.*, 2000; Zubkov *et al.*, 2001). These molecular surveys also reported the dominance of SAR11, roseobacters, and SAR86 as main contributors among active prokaryotes (Gonzalez *et al.*, 2000; Zubkov *et al.*, 2001). Concomitantly to the predominance of SAR11, the most abundant organism in the oceans (Morris *et al.*, 2002; Giovannoni, 2017) and common inhabitant of blooms (Gonzalez *et al.*, 2000; Teeling *et al.*, 2012, 2016; Landa *et al.*, 2016), we found abundant members of the Roseobacter clade, most notably assigned to the genera *Sulfitobacter* and *Ascidiaceihabitans* (formerly Roseobacter OCT lineage), whose relative abundances typically fluctuate during phytoplankton blooms (Hahnke *et al.*, 2015; Lucas *et al.*, 2016; Chafee *et al.*, 2018; Choi *et al.*, 2018; Kappelmann *et al.*, 2019). Interestingly, a *Sulfitobacter* ASV was present at all sites. This is in agreement with the cooccurrence of a *Sulfitobacter* strain and *E. huxleyi* in the water column during the demise phase of an *E. huxleyi* bloom in the North Atlantic (Barak-Gavish *et al.*, 2018). Since this *Sulfitobacter* strain was found to display a strong DMSP-mediated virulence when co-cultured with *E. huxleyi*, its possible contribution to the bloom termination as a complementary mortality agent to viral infection was suggested by these authors.

The experimental selection of *E. huxleyi*-associated microbiomes allowed us to capture the temporal dynamics of simultaneous crashes of all cultures followed by their growth recovery. During the first month of culture, the opposite dynamics of *E. huxleyi* and bacteria coupled to the sharp decrease of the bacterial alpha diversity indicated that a few bacterial taxa were outcompeting the others. A first possibility could be that inoculation with natural bacterioplankton communities propagated a virus infection in the cultures since diagnostic signatures of the presence of coccolithoviruses were found in the samples of the bloom site. However, cultures inoculated with samples from the outside bloom showed the same pattern, although no *E. huxleyi* bloom was detected in this area during the entire sampling period. A second possibility could be the overgrowth of algicidal bacteria because (i) several bacteria of the Roseobacter clade and the genus *Pseudomonas* are known to kill phytoplankton, including *E. huxleyi* (Mayali and Azam, 2004; Seyedsayamdost *et al.*, 2011; Segev *et al.*, 2016; Barak-Gavish *et al.*, 2018) and (ii) Roseobacter-like members and *Pseudoalteromonas* sp. were abundant during the bloom. This possibility is however unlikely because we did not find any Rhodobacteraceae and Pseudoalteromonaceae sequences in most of the cultures collected at the lowest algal cell abundance (day 32). All cultures were systematically dominated by members of clades OM43 (38-81% of the reads) and KI89A (15-45%), and both clades were associated with *Erythrobacter* (44%) in cultures inoculated with the outside bloom DCM

sample. Almost systematically dominant, members of the OM43 clade are methylotrophic bacteria which can utilize methanol and methylated compounds as sole growth substrates (Anthony, 1983). This clade is commonly found at low levels in coastal ecosystems (Rappé *et al.*, 2000; Sekar *et al.*, 2004; Song *et al.*, 2009) and has been observed to increase in abundance to ~2% of bacterial cells during phytoplankton blooms (Morris *et al.*, 2006). In the field, its abundance was found to increase during phytoplankton blooms (Rich *et al.*, 2011; Yang *et al.*, 2015) and to correlate with diatom abundance (Morris *et al.*, 2006). To explain the simultaneous crashes of all the cultures, we favor a severe abiotic stress experienced by *E. huxleyi* in the first weeks of culture that could be due to growth-limiting light conditions since growth recovery was immediately observed after increasing light intensity. However, we cannot exclude that the inoculated diversified bacterial communities may have also contributed to a stress for the axenic alga. While this remains speculative, a likely hypothesis is however that algal stress/death induced the release of methylated compounds by the alga providing a selective advantage to members of the OM43 clade over bacteria in the phycosphere. We suspect that the unfavorable light conditions might have induced algal cell death and lysis promoting the release of methylated compounds further used as a carbon source by the specialist OM43 clade methylotrophs, similarly as other marine methylotrophs (Vila-Costa *et al.*, 2006; Schäfer, 2007; Neufeld *et al.*, 2008). Among the possible produced substrates, methylated sugars and uronic acid methyl esters prevalent in polysaccharides were suggested as candidates (Sosa *et al.*, 2015). In addition, dimethyl sulfide (Wolfe and Steinke, 1996) and methylated volatile organic compounds (Reese *et al.*, 2019; Fisher *et al.*, 2020) have been identified as indicators of algal stress/death.

Upon culture recovery, we observed that the bacterial community composition followed a cyclic pattern suggesting that it reverted back to a composition similar to its initial community at day 9 of culture. Such cyclic pattern has been shown in the mucus microbiome of the coral *Porites astreoides* (Glasl *et al.*, 2016) and the surface microbiome of the seaweed *Delisea pulchra* (Longford *et al.*, 2019) after experimental disturbances. This cyclic pattern of recovery was consistently observed in the four separate treatments, with some variability (*e.g.* in the outside bloom DCM treatment, cyclic pattern was observed at the replicate level). With the exception of the outside bloom DCM treatment, in general we observed low levels of between-replicate variability at all time points, indicating a high degree of uniformity among cultures at corresponding times in the survey. The microbiomes resulting from both surface treatments were remarkable in this respect. It is surprising that community composition remained so

uniform across replicates at corresponding times, and that succession patterns were indeed reproducible. Although these samples were collected 34 km apart, they were both composed of *Luminiphilus*, SAR92 and KI89A clades as main components, suggesting the similarity of the initial bacterioplankton composition of both epipelagic surface waters and the functional complementarity between microbiome species.

Our results also illustrate the importance of niche differentiation in natural communities. In particular, we showed that bacterial species or phylogenetic groups from surface and bloom depth did not respond equally to the organic or inorganic nutrients provided in *E. huxleyi* cultures. Although no major differences were observed in the bacterioplankton samples from inside and outside bloom DCM communities, the resulting *E. huxleyi* microbiomes differed. Other microbiome studies of phytoplankton cultures have highlighted the impact of the initial community composition on microbiomes after short (Ajani *et al.*, 2018; Sörenson *et al.*, 2019; Jackrel *et al.*, 2020), and long-term selection (**Chapter 2**). We cannot explain the variability of outside DCM treatment, although patchiness of bacterioplankton communities can be argued. However, remarkable features were found in the microbiomes resulting from inside bloom DCM waters where several specific flavobacterial ASVs, mainly assigned to *Polaribacter* and *Aurantivirga*, were initially selected and were amongst the most prevalent and abundant ASVs after the host crash. Both genera were identified as the main degraders of diatom polysaccharides during spring blooms in the Southern North Sea (Krüger *et al.*, 2019). *Aurantivirga* was found more abundant in early stages of diatom blooms (Krüger *et al.*, 2019; Liu *et al.*, 2020) while *Polaribacter* abundance was higher in late bloom stages (Teeling *et al.*, 2012; Landa *et al.*, 2016). This may be related to the differential capacity of these bacteria to degrade phytoplankton-derived polysaccharides during blooms (Teeling *et al.*, 2012; Krüger *et al.*, 2019). Indeed, expression profiles of TonB-dependent transporters have recently predicted that *Aurantivirga* produced the most abundant putative alpha-glucan transporter during the early phase of a bloom (Francis *et al.*, 2021). Interestingly, in the same bloom, SAR92 and *Luminiphilus*, which are often viewed as oligotrophic bacteria (Spring and Riedel, 2013; Cottrell and Kirchman, 2016), were important degraders of algal polysaccharides (Francis *et al.*, 2021), suggesting their potential role in our cultures. Another important trait of the inside bloom DCM treatment was the presence of many indicative ASVs, including several flavobacterial ASVs and members of the Roseobacter clade (*Sulfitobacter* and *Yoonia-Loktanella*). These last genera are known to be part of the bacterial community associated with phytoplankton blooms (Zubkov *et al.*, 2001; Barak-Gavish *et al.*, 2018).

Based on previous reports of the *E. huxleyi* microbiomes diversity, we expected to find a dominance of *Marinobacter* in the cultured microbiomes (**Chapter 1**; Green *et al.*, 2015). Since *Marinobacter* species display relatively large cell sizes (Bowman and McMeekin, 2005), a plausible explanation for their very low representation might be due to the 0.45  $\mu\text{m}$  filtration step in our experimental design. However, we detected a few *Marinobacter* sequences in the cultures, suggesting that the filtration step does not fully explain their abundance. We acknowledge that the filtration step might have induced other modifications in the initial composition of the inocula. Many studies have indeed demonstrated that communities of free-living and particle-associated bacteria (including those associated with algae) are different (*e.g.* DeLong, Franks and Alldredge, 1993; Simon *et al.*, 2002; Grossart *et al.*, 2005; Bachmann *et al.*, 2018). This situation was probably the case in our samples because *E. huxleyi* bloom demises are coupled with particle aggregation of organic molecules from dying phytoplankton. However, as our primary objective was to study the role of the host in bacterial community selection and assembly, we opted to remove other autotrophic phytoplankton cells, mainly *Synechococcus* and picoeukaryotes found in high abundance at both the sampling sites (see Supplementary Table 1). Despite these limitations, we can draw several conclusions from this work.

We assume that exopolysaccharides/exudates of axenic *E. huxleyi* cultures have strongly influenced which bacteria emerged first (day 9), which has crucial effects on the resulting community and its long-term stability. Our results suggest that the decrease of OM43 clade abundance after day 32 provided an open niche, which was recolonized by opportunistic bacteria that remained stable (*SAR92*, *Alcanivorax*, *Erythrobacter*, *Yoonia*, and *Idiomarina*) or increased with time (*Luminiphilus*) (data not shown). Since this situation was however limited to few ASVs, we hypothesize that the complete re-establishment of the initially grown prokaryotic community after disturbance depends on the degree of disruption of the microbiome and the initial microbiome diversity. The later factor, which may facilitate stability, was exemplified by the contrasting results obtained with the inside and outside bloom DCM samples. The bacterioplankton communities of the inside bloom DCM sample were the more diverse from the two samples and they resulted in more diverse microbiomes after 9 days of culture. The microbiomes grown from the inside bloom DCM sample displayed also the highest number of specific ASVs and indicative species. More importantly, they were composed of 13 ASVs with relative abundance higher than 2% whereas microbiomes from other treatments contained 3 to 5 ASVs displaying abundance higher than this threshold (data

not shown). This is also the likely explanation of the almost complete cyclic pattern followed by the microbiomes resulting from inside bloom DCM samples (Figure 4A). Contrary to the other treatments, this bacterial community was collected in the *E. huxleyi* bloom and we hypothesize that pre-adaptation of the community to the different substrates produced by the future host promoted microbiomes of larger diversity.

Some of the bacterial groups that we found in the treatments were not reported previously in phytoplankton cultures or in low abundance, notably *Luminiphilus*, SAR92, KI89A and OM43 clades (**Chapter 1**, Green *et al.*, 2015). This is easily understandable because *Luminiphilus*, SAR92 and KI89A clades belong to an important group of oligotrophic marine Gammaproteobacteria that do not grow in the high nutrient concentrations provided by phytoplankton cultures (Cho and Giovannoni, 2004; Spring and Riedel, 2013). Although they are widely distributed in the oceans, only a few OMG and clade OM43 isolates exist (Cho and Giovannoni, 2004; Yang *et al.*, 2016). Our experimental approach combining prefiltration of natural samples and co-culture with *E. huxleyi* demonstrates that these bacteria are free-living in a bloom context and are stimulated by *E. huxleyi*-derived organic substrates. We believe that this experimental approach could give valuable conditions to isolate them and expand the collection of marine bacterial isolates resistant to traditional cultivation techniques. This approach could also be used to isolate *Janthinobacterium* whose low abundance but prevalence and specific presence in *E. huxleyi* cultures when compared with other studies (**Chapter 1**) was questionable. Sequences assigned to *Janthinobacterium* also prevailed in the new cultures and they emerged in the first microbiomes of the survey at day 9. Since we carefully checked the axenic status of the *E. huxleyi* culture before the experiment, we hypothesize that *Janthinobacterium* is a member of the rare biosphere particularly adapted to coccolithophore-derived organic matter. Of note, an isolate of this genus has been shown to produce siderophores and auxins triggering an increase in *Chlorella vulgaris* growth by 163% (Krug *et al.*, 2020).

## Conclusions

In this work, we showed that the source of the initial bacterioplankton communities influences the resulting composition of *E. huxleyi* microbiomes. Our experimental approach demonstrated the stability of microalgal microbiomes to stressful conditions as it has also been reported for other phytoplankton microbiomes (Geng *et al.*, 2016; Camp *et al.*, 2020). Although species losses still occurred in the last sampled microbiomes of the survey, they were associated with low abundance taxa and did not induce major restructuring of the community, as previously shown in long-term experiments by Behringer *et al.*, (2018). Overall, we bring evidence that microbiomes associated with phytoplankton collection cultures represent a valuable resource to explore phytoplankton-bacteria interactions. Isolation of several bacteria that correspond to specific and shared ASV will be necessary to investigate the role and functions of stable core bacterial members interacting with *E. huxleyi*. Future co-culture experiments coupled with transcriptomic and metabolomic analyses will provide valuable information about the genes and molecules involved in these ecologically key interactions.

## Acknowledgments

This work was supported by Sorbonne University, the Région Bretagne, the Centre National de la Recherche Scientifique (CNRS, France), and the French Government ‘‘Investissements d’Avenir’’ programmes OCEANOMICS (ANR-11-BTBR-0008). We are grateful to the *Tara* Ocean Foundation, led by Romain Trouble and Etienne Bourgois, for the sampling opportunity and facilities onboard *Tara*, and to all the scientific and logistic team involved in the *Tara* Breizh Bloom cruise, notably captain Martin Herteau and his crew. We are thankful to the ABiMS bioinformatic platform (<http://abims.sb-roscoff.fr>) for the computational resources, and to Nicolas Henry and Lydia White for their help in statistical analysis. This article is contribution number XX of *Tara* Oceans.

## References

- Ajani, P.A., Kahlke, T., Siboni, N., Carney, R., Murray, S.A., and Seymour, J.R. (2018) The microbiome of the cosmopolitan diatom *Leptocylindrus* reveals significant spatial and temporal variability. *Front Microbiol* 9: 2758.
- Alberti, A. (2017) Data Descriptor : Viral to metazoan marine plankton nucleotide sequences from the *Tara* Oceans expedition. *Sci data* 1–20.
- Amin, S.A., Green, D.H., Hart, M.C., Kupper, F.C., Sunda, W.G., and Carrano, C.J. (2009) Photolysis of iron-siderophore chelates promotes bacterial-algal mutualism. *Proc Natl Acad Sci* 106: 17071–17076.
- Amin, S.A., Hmelo, L.R., Van Tol, H.M., Durham, B.P., Carlson, L.T., Heal, K.R., *et al.* (2015) Interaction and signalling between a cosmopolitan phytoplankton and associated bacteria. *Nature* 522: 98–101.
- Anderson, M.J. (2005) PERMANOVA. Permutational multivariate analysis of variance. Department of Statistics, University of Auckland, Auckland.
- Anderson, M.J. and Walsh, D.C.I. (2013) PERMANOVA, ANOSIM, and the Mantel test in the face of heterogeneous dispersions: What null hypothesis are you testing? *Ecol Monogr* 83: 557–574.
- Anthony, C. (1983) Methanol oxidation and growth yields in methylotrophic bacteria: a review. *Acta Biotechnol* 3: 261–268.
- Assmy, P. and Smetacek, V. (2009) Algal Blooms. *Encycl Microbiol* 3: 27–41.
- Bachmann, J., Heimbach, T., Hassenrück, C., Kopprio, G.A., Iversen, M.H., Grossart, H.P., and Gärdes, A. (2018) Environmental drivers of free-living vs. particle-attached bacterial community composition in the Mauritania upwelling system. *Front Microbiol* 9: 2836.
- Barak-Gavish, N., Frada, M.J., Ku, C., Lee, P.A., DiTullio, G.R., Malitsky, S., *et al.* (2018) Bacterial virulence against an oceanic bloom-forming phytoplankton is mediated by algal DMSP. *Sci Adv* 4: eaau5716.
- Behrenfeld, M.J., O'Malley, R.T., Siegel, D.A., McClain, C.R., Sarmiento, J.L., Feldman, G.C., *et al.* (2006) Climate-driven trends in contemporary ocean productivity. *Nature* 444: 752–755.
- Behringer, G., Ochsenkühn, M.A., Fei, C., Fanning, J., Koester, J.A., and Amin, S.A. (2018) Bacterial communities of diatoms display strong conservation across strains and time. *Front Microbiol* 9:.
- Bolger, A.M., Lohse, M., and Usadel, B. (2014) Trimmomatic: a flexible trimmer for Illumina sequence data. *Bioinformatics* 30: 2114–2120.
- Bowman, J.P. and McMeekin, T.A. (2005) Order X. Alteromonadales ord. nov. *Bergey's Man Syst Bacteriol* 2: 443.
- Bratbak, G., Egge, J.K., and Heldal, M. (1993) Viral mortality of the marine alga *Emiliania huxleyi* (Haptophyceae) and termination of algal blooms. *Mar Ecol Prog Ser* 93: 39–48.
- Buchan, A., LeClerc, G.R., Gulvik, C.A., and González, J.M. (2014) Master recyclers: features and functions of bacteria associated with phytoplankton blooms. *Nat Rev Microbiol* 12: 686–698.
- De Cáceres, M. and Legendre, P. (2009) Associations between species and groups of sites: Indices and statistical inference. *Ecology* 90: 3566–3574.
- Callahan, B.J., McMurdie, P.J., Rosen, M.J., Han, A.W., Johnson, A.J.A., and Holmes, S.P. (2016) DADA2: High-resolution sample inference from Illumina amplicon data. *Nat Methods* 13: 581.
- Camp, E.F., Kahlke, T., Nitschke, M.R., Varkey, D., Fisher, N.L., Fujise, L., *et al.* (2020) Revealing changes in the microbiome of Symbiodiniaceae under thermal stress. *Environ Microbiol* 22: 1294–1309.

- Chafee, M., Fernández-Guerra, A., Buttigieg, P.L., Gerds, G., Eren, A.M., Teeling, H., and Amann, R.I. (2018) Recurrent patterns of microdiversity in a temperate coastal marine environment. *ISME J* 12: 237–252.
- Cho, J.-C. and Giovannoni, S.J. (2004) Cultivation and growth characteristics of a diverse group of oligotrophic marine Gammaproteobacteria. *Appl Environ Microbiol* 70: 432–440.
- Choi, D.H., An, S.M., Yang, E.C., Lee, H., Shim, J., Jeong, J., and Noh, J.H. (2018) Daily variation in the prokaryotic community during a spring bloom in shelf waters of the East China Sea. *FEMS Microbiol Ecol* 94: fiy134.
- Cirri, E. and Pohnert, G. (2019) Algae–bacteria interactions that balance the planktonic microbiome. *New Phytol* 223: 100–106.
- Cottrell, M.T. and Kirchman, D.L. (2000) Natural assemblages of marine proteobacteria and members of the Cytophaga-Flavobacter cluster consuming low- and high-molecular-weight dissolved organic matter. *Appl Environ Microbiol* 66: 1692–1697.
- Cottrell, M.T. and Kirchman, D.L. (2016) Transcriptional control in marine copiotrophic and oligotrophic bacteria with streamlined genomes. *Appl Environ Microbiol* 82: 6010–6018.
- Cruz-López, R. and Maske, H. (2016) The vitamin B1 and B12 required by the marine dinoflagellate *Lingulodinium polyedrum* can be provided by its associated bacterial community in culture. *Front Microbiol* 7: 1–13.
- DeLong, E.F., Franks, D.G., and Alldredge, A.L. (1993) Phylogenetic diversity of aggregate-attached vs. free-living marine bacterial assemblages. *Limnol Oceanogr* 38: 924–934.
- Falkowski, P.G. (1997) Evolution of the nitrogen cycle and its influence on the biological sequestration of CO<sub>2</sub> in the ocean. *Nature* 387: 272–275.
- Falkowski, P.G. (1994) The role of phytoplankton photosynthesis in global biogeochemical cycles. 235–258.
- Falkowski, P.G., Fenchel, T., and DeLong, E.F. (2008) The microbial engines that drive earth's biogeochemical cycles. *Science* (80-) 320: 1034–1039.
- Fernández-Gómez, B., Richter, M., Schüller, M., Pinhassi, J., Acinas, S.G., González, J.M., and Pedros-Alio, C. (2013) Ecology of marine Bacteroidetes: a comparative genomics approach. *ISME J* 7: 1026–1037.
- Field, C.B., Behrenfeld, M.J., Randerson, J.T., and Falkowski, P. (1998) Primary Production of the Biosphere: Integrating Terrestrial and Oceanic Components. *Science* (80-) 281: 237 LP – 240.
- Fisher, C.L., Lane, P.D., Russell, M., Maddalena, R., and Lane, T.W. (2020) Low Molecular Weight Volatile Organic Compounds Indicate Grazing by the Marine Rotifer *Brachionus plicatilis* on the Microalgae *Microchloropsis salina*. *Metabolites* 10: 361.
- Francis, T. Ben, Bartosik, D., Sura, T., Sichert, A., Hehemann, J.-H., Markert, S., et al. (2021) Changing expression patterns of TonB-dependent transporters suggest shifts in polysaccharide consumption over the course of a spring phytoplankton bloom. *ISME J* 1–15.
- Fu, H., Uchimiya, M., Gore, J., and Moran, M.A. (2020) Ecological drivers of bacterial community assembly in synthetic phycospheres. *Proc Natl Acad Sci U S A* 117: 3656–3662.
- Geng, H., Sale, K.L., Tran-Gyamfi, M.B., Lane, T.W., and Yu, E.T. (2016) Longitudinal Analysis of Microbiota in Microalga *Nannochloropsis salina* Cultures. *Microb Ecol* 72: 14–24.
- Giovannoni, S.J. (2017) SAR11 bacteria: the most abundant plankton in the oceans. *Ann Rev Mar Sci* 9: 231–255.
- Glasl, B., Herndl, G.J., and Frade, P.R. (2016) The microbiome of coral surface mucus has a key role in mediating holobiont health and survival upon disturbance. *ISME J* 10: 2280–

2292.

- Gonzalez, J.M., Simó, R., Massana, R., Covert, J.S., Casamayor, E.O., Pedrós-Alió, C., and Moran, M.A. (2000) Bacterial community structure associated with a dimethylsulfoniopropionate-producing North Atlantic algal bloom. *Appl Environ Microbiol* 66: 4237–4246.
- Green, D.H., Echavarrri-Bravo, V., Brennan, D., and Hart, M.C. (2015) Bacterial diversity associated with the coccolithophorid algae *Emiliania huxleyi* and *Coccolithus pelagicus* f. *braarudii*. *Biomed Res Int* 2015:.
- Grossart, H.P., Levold, F., Allgaier, M., Simon, M., and Brinkhoff, T. (2005) Marine diatom species harbour distinct bacterial communities. *Environ Microbiol* 7: 860–873.
- Hahnke, R.L., Bennke, C.M., Fuchs, B.M., Mann, A.J., Rhiel, E., Teeling, H., et al. (2015) Dilution cultivation of marine heterotrophic bacteria abundant after a spring phytoplankton bloom in the North Sea. *Environ Microbiol* 17: 3515–3526.
- Holligan, P.M., Viollier, M., Harbour, D.S., Camus, P., and Champagne-Philippe, M. (1983) Satellite and ship studies of coccolithophore production along a continental shelf edge. *Nature* 304: 339–342.
- Holmström, C. and Kjelleberg, S. (1999) Marine *Pseudoalteromonas* species are associated with higher organisms and produce biologically active extracellular agents. *FEMS Microbiol Ecol* 30: 285–293.
- Hunter, J.E., Frada, M.J., Fredricks, H.F., Vardi, A., and Van Mooy, B.A.S. (2015) Targeted and untargeted lipidomics of *Emiliania huxleyi* viral infection and life cycle phases highlights molecular biomarkers of infection, susceptibility, and ploidy. *Front Mar Sci* 2: 81.
- Jackrel, S.L., Yang, J.W., Schmidt, K.C., and Deneff, V.J. (2020) Host specificity of microbiome assembly and its fitness effects in phytoplankton. *ISME J*.
- Jiao, N., Herndl, G.J., Hansell, D.A., Benner, R., Kattner, G., Wilhelm, S.W., et al. (2010) Microbial production of recalcitrant dissolved organic matter: Long-term carbon storage in the global ocean. *Nat Rev Microbiol* 8: 593–599.
- Kappelmann, L., Krüger, K., Hehemann, J.H., Harder, J., Markert, S., Unfried, F., et al. (2019) Polysaccharide utilization loci of North Sea Flavobacteriia as basis for using SusC/D-protein expression for predicting major phytoplankton glycans. *ISME J* 13: 76–91.
- Keller, M.D., Selvin, R.C., Claus, W., and Guillard, R.R.L. (1987) Media for the culture of oceanic ultraphytoplankton. *J Phycol* 23: 633–638.
- Keuter, S., Young, J.R., and Frada, M.J. (2019) Life cycle association of the coccolithophore *Syracosphaera gaarderae* comb. nov. (ex *Alveosphaera bimurata*): Taxonomy, ecology and evolutionary implications. *Mar Micropaleontol* 148: 58–64.
- Kimbrel, J.A., Samo, T.J., Ward, C., Nilson, D., Thelen, M.P., Siccardi, A., et al. (2019) Host selection and stochastic effects influence bacterial community assembly on the microalgal phycosphere. *Algal Res* 40: 101489.
- Kindt, R. and Coe, R. (2005) Tree diversity analysis. A manual and software for common statistical methods for ecological and biodiversity studies. World Agrofor Cent.
- Kirchman, D.L. (2002) The ecology of Cytophaga–Flavobacteria in aquatic environments. *FEMS Microbiol Ecol* 39: 91–100.
- Krug, L., Erlacher, A., Markut, K., Berg, G., and Cernava, T. (2020) The microbiome of alpine snow algae shows a specific inter-kingdom connectivity and algae-bacteria interactions with supportive capacities. *ISME J* 14: 2197–2210.
- Krüger, K., Chafee, M., Ben Francis, T., Glavina del Rio, T., Becher, D., Schweder, T., et al. (2019) In marine Bacteroidetes the bulk of glycan degradation during algae blooms is mediated by few clades using a restricted set of genes. *ISME J* 13: 2800–2816.
- Laber, C.P., Hunter, J.E., Carvalho, F., Collins, J.R., Hunter, E.J., Schieler, B.M., et al. (2018)

- Coccolithovirus facilitation of carbon export in the North Atlantic. *Nat Microbiol* 1–11.
- Landa, M., Blain, S., Christaki, U., Monchy, S., and Obernosterer, I. (2016) Shifts in bacterial community composition associated with increased carbon cycling in a mosaic of phytoplankton blooms. *ISME J* 10: 39–50.
- Legendre, P. and Gallagher, E.D. (2001) Ecologically meaningful transformations for ordination of species data. *Oecologia* 129: 271–280.
- Lehahn, Y., Koren, I., Schatz, D., Frada, M., Sheyn, U., Boss, E., *et al.* (2014) Decoupling physical from biological processes to assess the impact of viruses on a mesoscale algal bloom. *Curr Biol* 24: 2041–2046.
- Li, D.X., Zhang, H., Chen, X.H., Xie, Z.X., Zhang, Y., Zhang, S.F., *et al.* (2018) Metaproteomics reveals major microbial players and their metabolic activities during the blooming period of a marine dinoflagellate *Prorocentrum donghaiense*. *Environ Microbiol* 20: 632–644.
- Liu, Y., Blain, S., Crispi, O., Rembauville, M., and Obernosterer, I. (2020) Seasonal dynamics of prokaryotes and their associations with diatoms in the Southern Ocean as revealed by an autonomous sampler. *Environ Microbiol* 22: 3968–3984.
- Longford, S.R., Campbell, A.H., Nielsen, S., Case, R.J., Kjelleberg, S., and Steinberg, P.D. (2019) Interactions within the microbiome alter microbial interactions with host chemical defences and affect disease in a marine holobiont. *Sci Rep* 9: 1–13.
- Lovejoy, C., Bowman, J.P., and Hallegraeff, G.M. (1998) Algicidal effects of a novel marine *Pseudoalteromonas* isolate (class Proteobacteria, gamma subdivision) on harmful algal bloom species of the genera *Chattonella*, *Gymnodinium*, and *Heterosigma*. *Appl Environ Microbiol* 64: 2806–2813.
- Lucas, J., Koester, I., Wichels, A., Niggemann, J., Dittmar, T., Callies, U., *et al.* (2016) Short-term dynamics of North Sea bacterioplankton-dissolved organic matter coherence on molecular level. *Front Microbiol* 7: 321.
- Malin, G. and Steinke, M. (2004) Dimethyl sulfide production: what is the contribution of the coccolithophores? *Coccolithophores* 127–164.
- Marie, D., Brussaard, C.P.D., Partensky, F., and Vaultot, D. (1999) Flow cytometric analysis of phytoplankton, bacteria and viruses. *Curr Protoc Cytom* 11.11: 1–15.
- Martin, M. (2011) Cutadapt removes adapter sequences from high-throughput sequencing reads. *EMBnet.journal*; Vol 17, No 1 Next Gener Seq Data Anal - 1014806/ej171200.
- Mayali, X. and Azam, F. (2004) Algicidal bacteria in the sea and their impact on algal blooms. *J Eukaryot Microbiol* 51: 139–144.
- Mönnich, J., Tebben, J., Bergemann, Case, R.J., Sylke Wohlrab, and Harder, T. (2020) Niche-based assembly of bacterial consortia on the diatom *Thalassiosira rotula* is stable and reproducible. *ISME J* 14: 1614–1625.
- Morris, R.M., Longnecker, K., and Giovannoni, S.J. (2006) *Pirellula* and OM43 are among the dominant lineages identified in an Oregon coast diatom bloom. *Environ Microbiol* 8: 1361–1370.
- Morris, R.M., Rappé, M.S., Connon, S.A., Vergin, K.L., Siebold, W.A., Carlson, C.A., and Giovannoni, S.J. (2002) SAR11 clade dominates ocean surface bacterioplankton communities. *Nature* 420: 806–810.
- Murali, A., Bhargava, A., and Wright, E.S. (2018) IDTAXA: a novel approach for accurate taxonomic classification of microbiome sequences. *Microbiome* 6: 140.
- Neufeld, J.D., Boden, R., Moussard, H., Schäfer, H., and Murrell, J.C. (2008) Substrate-specific clades of active marine methylotrophs associated with a phytoplankton bloom in a temperate coastal environment. *Appl Environ Microbiol* 74: 7321–7328.
- Neukermans, G. and Fournier, G. (2018) Optical modeling of spectral backscattering and remote sensing reflectance from *Emiliania huxleyi* Blooms. *Front Mar Sci* 5: 1–20.

- Oksanen, J., Blanchet, F.G., Kindt, R., Legendre, P., Minchin, P.R., O'Hara, R.B., *et al.* (2015) OK-Package 'vegan.' Community Ecol Packag version 285 pp.
- Van Oostende, N., Harlay, J., Vanellander, B., Chou, L., Vyverman, W., and Sabbe, K. (2012) Phytoplankton community dynamics during late spring coccolithophore blooms at the continental margin of the Celtic Sea (North East Atlantic, 2006–2008). *Prog Oceanogr* 104: 1–16.
- Orata, F.D., Rosana, A.R.R., Xu, Y., Simkus, D.N., Bramucci, A.R., Boucher, Y., and Case, R.J. (2016) Polymicrobial Culture of Naked ( N-Type ) *Emiliana huxleyi*. *Genome Announc* 4: 9–10.
- Perrot, L., Gohin, F., Ruiz-Pino, D., Lampert, L., Huret, M., Dessier, A., *et al.* (2018) Coccolith-derived turbidity and hydrological conditions in May in the Bay of Biscay. *Prog Oceanogr* 166: 41–53.
- Pomeroy, L., leB. Williams, P., Azam, F., and Hobbie, J. (2007) The Microbial Loop. *Oceanography* 20: 28–33.
- Poulton, A.J., Stinchcombe, M.C., Achterberg, E.P., Bakker, D.C.E., Dumousseaud, C., Lawson, H.E., *et al.* (2014) Coccolithophores on the north-west European shelf: calcification rates and environmental controls. *Biogeosciences* 11: 3919–3940.
- Probert, I. (2019) K/2 Ian / K-ET. protocols.io.
- Quast, C., Pruesse, E., Yilmaz, P., Gerken, J., Schweer, T., Yarza, P., *et al.* (2013) The SILVA ribosomal RNA gene database project: improved data processing and web-based tools. *Nucleic Acids Res* 41: D590–D596.
- R Core Team (2017) R: A language and environment for statistical computing. R Foundation for Statistical Computing, Vienna, Austria. URL <https://www.R-project.org/>.
- Rappé, M.S., Vergin, K., and Giovannoni, S.J. (2000) Phylogenetic comparisons of a coastal bacterioplankton community with its counterparts in open ocean and freshwater systems. *FEMS Microbiol Ecol* 33: 219–232.
- Reese, K.L., Fisher, C.L., Lane, P.D., Jaryenneh, J.D., Moorman, M.W., Jones, A.D., *et al.* (2019) Chemical profiling of volatile organic compounds in the headspace of algal cultures as early biomarkers of algal pond crashes. *Sci Rep* 9: 1–10.
- Rich, V.I., Pham, V.D., Eppley, J., Shi, Y., and DeLong, E.F. (2011) Time-series analyses of Monterey Bay coastal microbial picoplankton using a 'genome proxy' microarray. *Environ Microbiol* 13: 116–134.
- Rognes, T., Flouri, T., Nichols, B., Quince, C., and Mahé, F. (2016) VSEARCH: a versatile open source tool for metagenomics. *PeerJ* 4: e2584–e2584.
- Rosana, A.R.R., Orata, F.D., Xu, Y., Simkus, D.N., Bramucci, A.R., Boucher, Y., and Case, R.J. (2016) Draft genome sequences of seven bacterial strains isolated from a polymicrobial culture of coccolith-bearing (C-type) *Emiliana huxleyi* M217. *Genome Announc* 4:.
- Rost, B., Riebesell, U., Röst, B., and Riebesell, U. (2004) Coccolithophores and the biological pump: Responses to environmental changes. Coccolithophores From Mol Process to Glob Impact 99–125.
- RStudio Team (2016) RStudio: Integrated Development for R. RStudio, Inc, Boston, MA.
- Saary, P., Forslund, K., Bork, P., and Hildebrand, F. (2017) RTK: efficient rarefaction analysis of large datasets.
- Schäfer, H. (2007) Isolation of *Methylophaga* spp. from marine dimethylsulfide-degrading enrichment cultures and identification of polypeptides induced during growth on dimethylsulfide. *Appl Environ Microbiol* 73: 2580–2591.
- Segev, E., Wyche, T.P., Kim, K.H., Petersen, J., Ellebrandt, C., Vlamakis, H., *et al.* (2016) Dynamic metabolic exchange governs a marine algal-bacterial interaction. *Elife* 5:.
- Sekar, R., Fuchs, B.M., Amann, R., and Pernthaler, J. (2004) Flow sorting of marine

- bacterioplankton after fluorescence in situ hybridization. *Appl Environ Microbiol* 70: 6210–6219.
- Seyedsayamdost, M.R., Case, R.J., Kolter, R., and Clardy, J. (2011) The Jekyll-and-Hyde chemistry of *Phaeobacter gallaeciensis*. *Nat Chem* 3: 331–335.
- Seyedsayamdost, M.R., Wang, R., Kolter, R., and Clardy, J. (2014) Hybrid biosynthesis of roseobactin from algal and bacterial precursor molecules. *J Am Chem Soc* 136: 15150–15153.
- Seymour, J.R., Amin, S.A., Raina, J.B., and Stocker, R. (2017) Zooming in on the phycosphere: The ecological interface for phytoplankton-bacteria relationships. *Nat Microbiol* 2:.
- Shibl, A.A., Isaac, A., Ochsenkühn, M.A., Cárdenas, A., Fei, C., Behringer, G., *et al.* (2020) Diatom modulation of select bacteria through use of two unique secondary metabolites. *Proc Natl Acad Sci U S A* 117: 27445–27455.
- Simon, M., Grossart, H.-P., Schweitzer, B., and Ploug, H. (2002) Microbial ecology of organic aggregates in aquatic ecosystems. *Aquat Microb Ecol* 28: 175–211.
- Smriga, S., Fernandez, V.I., Mitchell, J.G., and Stocker, R. (2016) Chemotaxis toward phytoplankton drives organic matter partitioning among marine bacteria. *Proc Natl Acad Sci U S A* 113: 1576–1581.
- Song, J., Oh, H.-M., and Cho, J.-C. (2009) Improved culturability of SAR11 strains in dilution-to-extinction culturing from the East Sea, West Pacific Ocean. *FEMS Microbiol Lett* 295: 141–147.
- Sörenson, E., Bertos-Fortis, M., Farnelid, H., Kremp, A., Krüger, K., Lindehoff, E., and Legrand, C. (2019) Consistency in microbiomes in cultures of *Alexandrium* species isolated from brackish and marine waters. *Environ Microbiol Rep* 11: 425–433.
- Sosa, O.A., Gifford, S.M., Repeta, D.J., and DeLong, E.F. (2015) High molecular weight dissolved organic matter enrichment selects for methylotrophs in dilution to extinction cultures. *ISME J* 9: 2725–2739.
- Spring, S. and Riedel, T. (2013) Mixotrophic growth of bacteriochlorophyll a-containing members of the OM60/NOR5 clade of marine gammaproteobacteria is carbon-starvation independent and correlates with the type of carbon source and oxygen availability. *BMC Microbiol* 13: 1.
- Sunagawa, S., Acinas, S.G., Bork, P., Bowler, C., Acinas, S.G., Babin, M., *et al.* (2020) Tara Oceans: towards global ocean ecosystems biology. *Nat Rev Microbiol* 18: 428–445.
- Teeling, H., Fuchs, B.M., Becher, D., Klockow, C., Gardebrecht, A., Bennke, C.M., *et al.* (2012) Substrate-controlled succession of marine bacterioplankton populations induced by a phytoplankton bloom. *Science* (80- ) 336: 608–611.
- Teeling, H., Fuchs, B.M., Bennke, C.M., Krüger, K., Chafee, M., Kappelmann, L., *et al.* (2016) Recurring patterns in bacterioplankton dynamics during coastal spring algae blooms. *Elife* 5: 1–31.
- Tréguer, P. and Le Corre, P. (1975) Manuel d'analyse des sels nutritifs dans l'eau de mer (utilisation de l'autoanalyseur Technicon R). Rapp l'Université Bretagne Occident.
- Tyrrell, T. and Merico, A. (2004) *Emiliania huxleyi*: bloom observations and the conditions that induce them. In *Coccolithophores*. pp. 75–97.
- Vardi, A., Haramaty, L., Van Mooy, B.A.S., Fredricks, H.F., Kimmance, S.A., Larsen, A., and Bidle, K.D. (2012) Host-virus dynamics and subcellular controls of cell fate in a natural coccolithophore population. *Proc Natl Acad Sci U S A* 109: 19327–19332.
- Vardi, A., Van Mooy, B.A.S., Fredricks, H.F., Popendorff, K.J., Ossolinski, J.E., Haramaty, L., and Bidle, K.D. (2009) Viral glycosphingolipids induce lytic infection and cell death in marine phytoplankton. *Science* (80- ) 326: 861–865.
- Vila-Costa, M., Del Valle, D.A., González, J.M., Slezak, D., Kiene, R.P., Sánchez, O., and Simó, R. (2006) Phylogenetic identification and metabolism of marine dimethylsulfide-

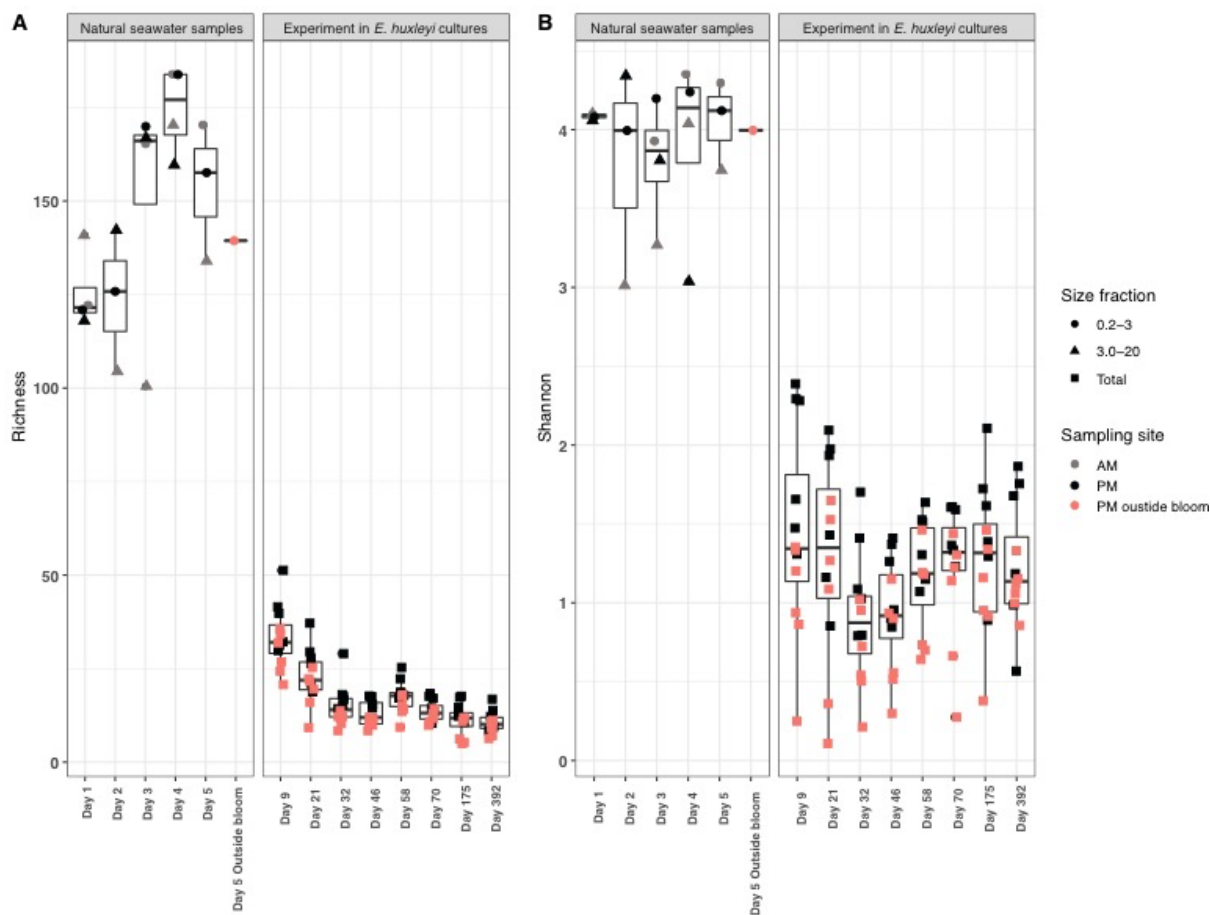
- consuming bacteria. *Environ Microbiol* 8: 2189–2200.
- Vincent, F., Sheyn, U., Porat, Z., Schatz, D., and Vardi, A. (2021) Visualizing active viral infection reveals diverse cell fates in synchronized algal bloom demise. *Proc Natl Acad Sci* 118: e2021586118.
- Wickham, H. (2016) *ggplot2: Elegant Graphics for Data Analysis*. Springer-Verlag New York ISBN 978-3:
- Wolfe, G. V and Steinke, M. (1996) Grazing-activated production of dimethyl sulfide (DMS) by two clones of *Emiliana huxleyi*. *Limnol Oceanogr* 41: 1151–1160.
- Yang, C., Li, Y., Zhou, B., Zhou, Y., Zheng, W., Tian, Y., *et al.* (2015) Illumina sequencing-based analysis of free-living bacterial community dynamics during an Akashiwo sanguine bloom in Xiamen sea, China. *Sci Rep* 5: 1–11.
- Yang, S.-J., Kang, I., and Cho, J.-C. (2016) Expansion of cultured bacterial diversity by large-scale dilution-to-extinction culturing from a single seawater sample. *Microb Ecol* 71: 29–43.
- Yarza, P., Yilmaz, P., Pruesse, E., Glöckner, F.O., Ludwig, W., Schleifer, K.H., *et al.* (2014) Uniting the classification of cultured and uncultured bacteria and archaea using 16S rRNA gene sequences. *Nat Rev Microbiol* 12: 635–645.
- Zhou, J., Chen, G.F., Ying, K.Z., Jin, H., Song, J.T., and Cai, Z.H. (2019) Phycosphere microbial succession patterns and assembly mechanisms in a marine dinoflagellate bloom. *Appl Environ Microbiol* 85: 1–17.
- Ziv, C., Malitsky, S., Othman, A., Ben-Dor, S., Wei, Y., Zheng, S., *et al.* (2016) Viral serine palmitoyltransferase induces metabolic switch in sphingolipid biosynthesis and is required for infection of a marine alga. *Proc Natl Acad Sci* 113: E1907–E1916.
- Zubkov, M. V., Fuchs, B.M., Archer, S.D., Kiene, R.P., Amann, R., and Burkill, P.H. (2001) Linking the composition of bacterioplankton to rapid turnover of dissolved dimethylsulphoniopropionate in an algal bloom in the North Sea. *Environ Microbiol* 3: 304–311.

## Supplementary Material

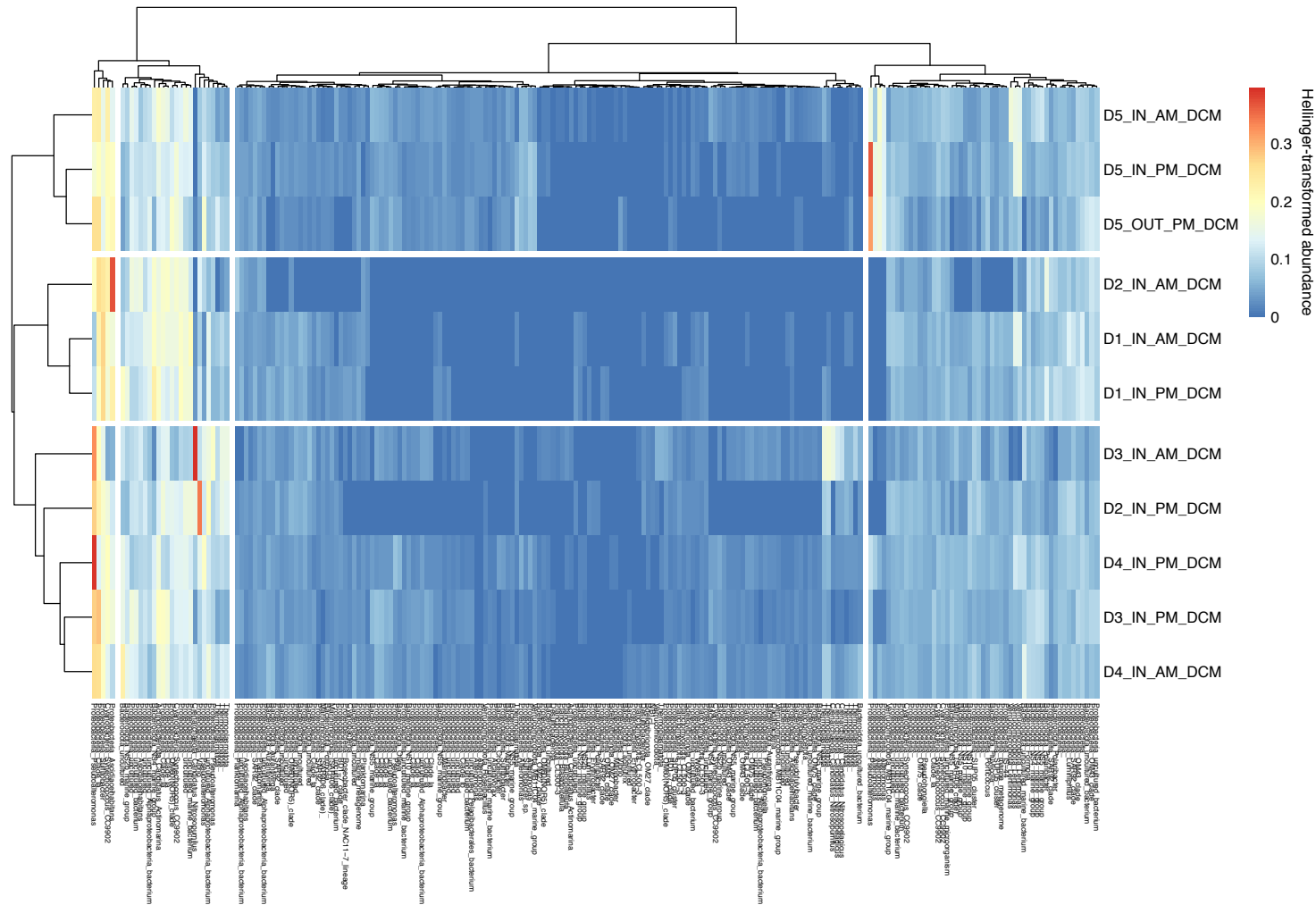
**Microbiome assembly in axenic *Emiliana huxleyi* cultures is influenced by the source community composition and is resilient to disturbance**

**Supplementary Table 1.** Environmental parameters sampled over the course of the bloom. The codes correspond to the day of sampling, the place where it was collected (inside or outside the bloom), the time of the day (morning - AM or afternoon - PM) and the depth (surface – SRF and deep chlorophyll maximum – DCM).

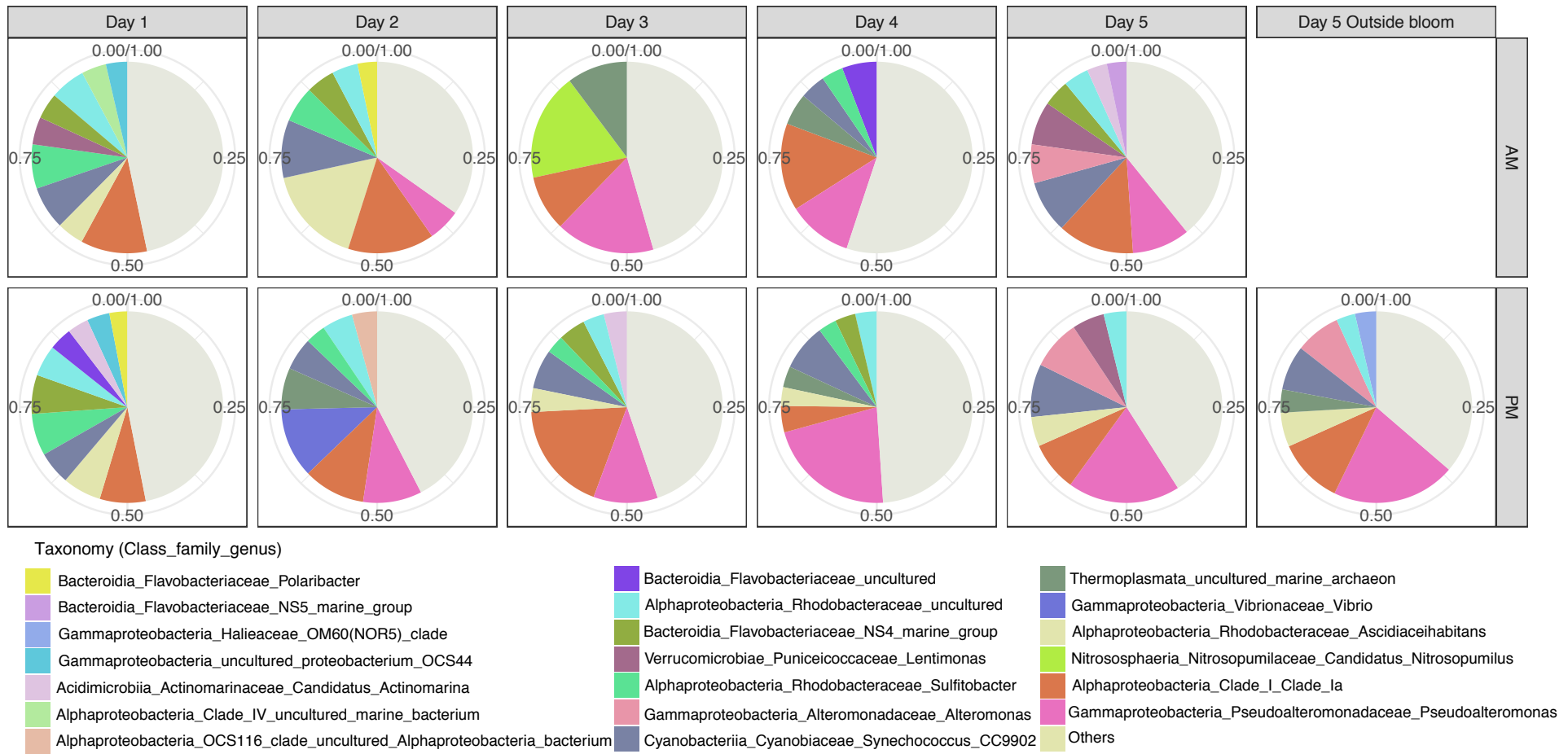
Site code	Date	Lat N	Long W	Time UTC	Sampling depth m	Nitrite $\mu\text{mol/L}$	Nitrate + nitrite $\mu\text{mol/L}$	Phosphate $\mu\text{mol/L}$	Silicate $\mu\text{mol/L}$	Temperature $^{\circ}\text{C}$	Salinity PSU	Par	Fluorescence	Turbidity WETntu0	Oxygen Volts	Oxygen mL/L	Total Eukaryotes cells/mL	Synechococcus cells/mL	Bacteria cells/mL
D1_IN_AM_DCM	20190529	48°21.000	7°01.114	09:21	20	0.159	0.989	0.162	1.245	13.308	35.5042	6.55E+00	2.0457	1.8356	2.1988	5.3034	2.43E+04	4.20E+04	1.01E+06
D1_IN_PM_DCM	20190529	48°20.543	7°02.520	16:10	20	0.017	DL	0.078	0.986	14.2163	35.4004	2.01E+01	0.9833	2.0452	2.3406	5.56827	2.95E+04	6.40E+04	1.62E+06
D2_IN_AM_DCM	20190530	48°20.794	7°02.301	06:50	15	0.0119	1.246	0.197	1.515	14.1133	35.3901	1.27E+01	0.7179	2.1609	2.1143	4.89932	2.46E+04	6.30E+04	1.39E+06
D2_IN_PM_DCM	20190530	48°20.817	7°00.384	16:31	20	0.021	DL	0.076	1.138	14.264	35.3993	3.42E+01	1.0677	2.0305	2.3299	5.52171	2.71E+04	6.25E+04	1.35E+06
D3_IN_AM_DCM	20190531	48°20.441	7°00.976	10:18	20	0.028	0.103	0.084	1.202	13.4539	35.376	5.85E+01	2.4072	1.9514	2.3633	5.73291	9.57E+03	2.08E+04	1.11E+06
D3_IN_PM_DCM	20190531	48°20.658	7°02.183	18:32	25	0.026	DL	0.068	1.117	13.2655	35.3729	1.44E+01	3.1488	2.048	2.335	5.6121	3.05E+04	7.48E+04	1.54E+06
D4_IN_AM_DCM	20190601	48°21.568	6°59.241	09:41	20	0.02	DL	0.083	1.067	12.4174	35.4077	1.51E+01	2.6518	1.8822	2.2428	5.39943	3.68E+04	1.10E+05	2.03E+06
D4_IN_PM_DCM	20190601	48°20.705	7°01.985	17:07	20	0.027	0.053	0.102	1.111	ND	ND	ND	ND	ND	ND	ND	3.21E+04	7.16E+04	1.45E+06
D5_IN_AM_DCM	20190602	48°21.427	6°59.496	09:40	15	0.035	0.04	0.061	0.922	13.2725	35.3667	8.69E+00	2.0143	1.9281	2.3174	5.58092	2.19E+04	1.01E+05	1.33E+06
D5_IN_PM_SRF	20190602	48°19.160	6°58.717	14:16	3	0.028	0.033	0.048	1.13	ND	ND	ND	ND	ND	ND	ND	ND	ND	ND
D5_IN_PM_DCM	20190602	48°19.081	6°57.090	13:45	25	0.03	0.035	0.094	0.276	ND	ND	ND	ND	ND	ND	ND	2.51E+04	9.15E+04	1.16E+06
D5_OUT_PM_SRF	20190602	48°21.961	6°28.519	18:00	3	0.034	0.039	0.073	0.197	15.3573	35.375	2.59E+02	0.4863	1.6543	2.3532	5.46434	ND	ND	ND
D5_OUT_PM_DCM	20190602	48°22.026	6°29.658	17:12	15	0.031	0.037	0.086	0.158	14.3971	35.3501	4.21E+01	1.3364	1.5285	2.3578	5.62631	1.05E+04	3.40E+04	8.06E+05



**Supplementary Figure 1.** Composite representation of the dynamics of the prokaryotic richness (A) and Shannon (B) indexes in natural samples (bloom and DCM depths only) and cultures experiments. The community tables were rarefied at the minimum number of reads of the environmental samples (3,465). The boxes represent the interquartile range. The thin horizontal lines represent the 25th and 75th percentiles and while the thick horizontal line represents the median. The vertical lines indicate the minimum and maximum values (using 1.5 coefficients above and below the percentiles). The dots represent the values measured for each culture. Dots further than the vertical lines represent potential outliers.

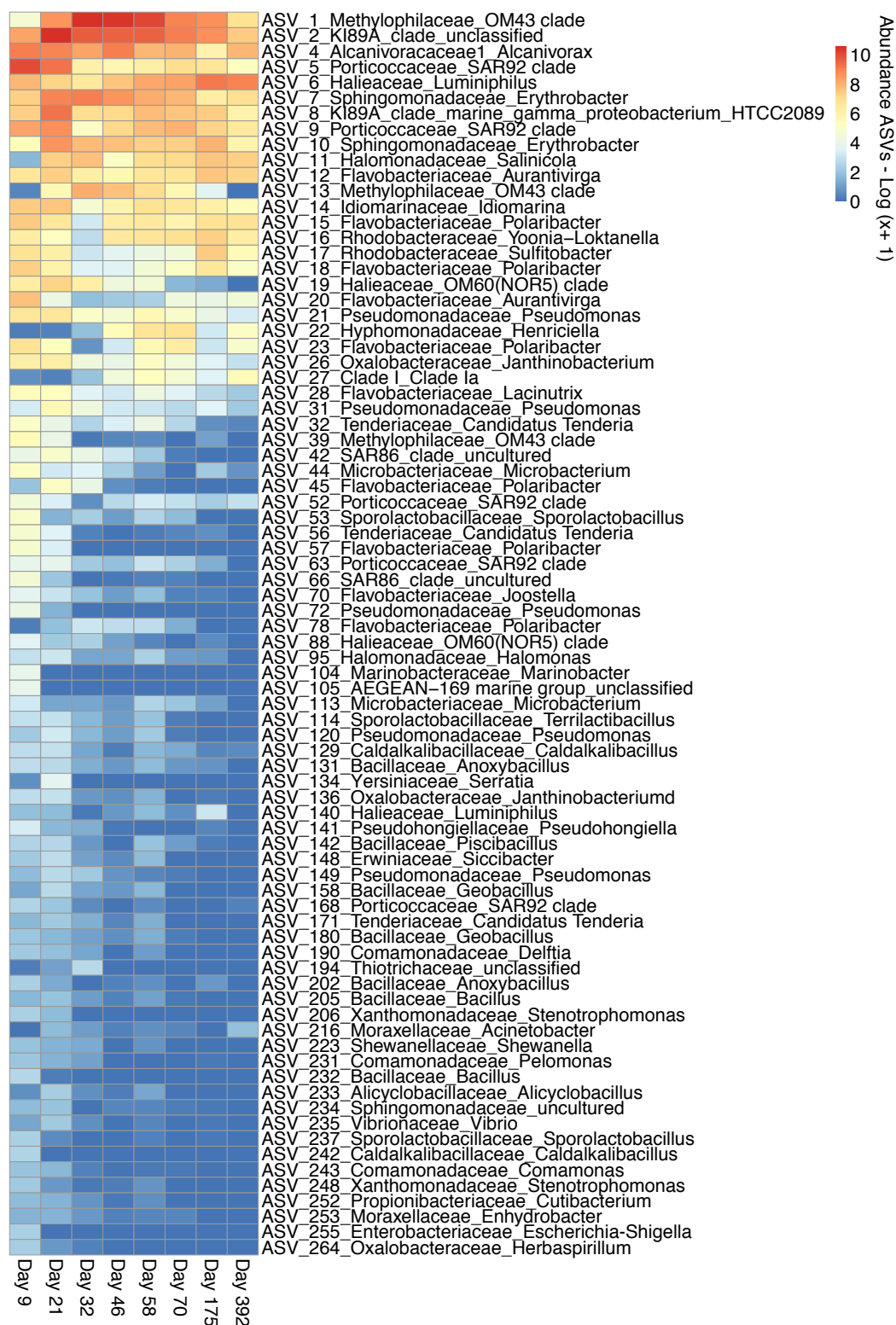


**Supplementary Figure 2.** Heatmap representing the hierarchical clustering of free-living (0.2-3  $\mu\text{m}$ ) prokaryotic communities at the sampling sites. The hierarchical clustering was built using the method “ward.D2” and Euclidean distances of the Hellinger-transformed community data. Taxomy is represented by phylum and genus level.



**Supplementary Figure 3.** Taxonomic composition (class\_family\_genus) of the free-living (0.2-3  $\mu\text{m}$ ) prokaryotic community at the bloom depths along the cruise. Genera accounting for less than 3% of the sample relative abundance were merged as “others”.





**Supplementary Figure 4.** Heatmap showing the ASVs dynamics over time. ASVs abundances over time were obtained by the mean number of reads of all the samples at each time point. Abundances were log transformed - Log (x+1) - to facilitate visualization. Only ASVs with a mean number of reads higher than 10 are represented in the plot.

**Supplementary Table 2.** Permutational multivariate analysis of variance (PERMANOVA) and nested PERMANOVA results (*nested.npmanova*) using Euclidean distance of Hellinger-transformed data. ‘Treatments’ is a fixed factor with four levels (D5\_IN\_PM\_SRF, D5\_IN\_PM\_DCM, D5\_OUT\_PM\_SRF and D5\_OUT\_PM\_DCM). ‘Replicates’ is a fixed factor with 12 levels (3 replicates x 4 treatments) nested within treatments. ‘Time’ is a fixed continuous factor (days after the starting of the experiment). Permutations were restricted to the replicates in traditional *adonis* (strata). •F.model and P-value correctly calculated using *nested.npmanova*. \* Significant results.

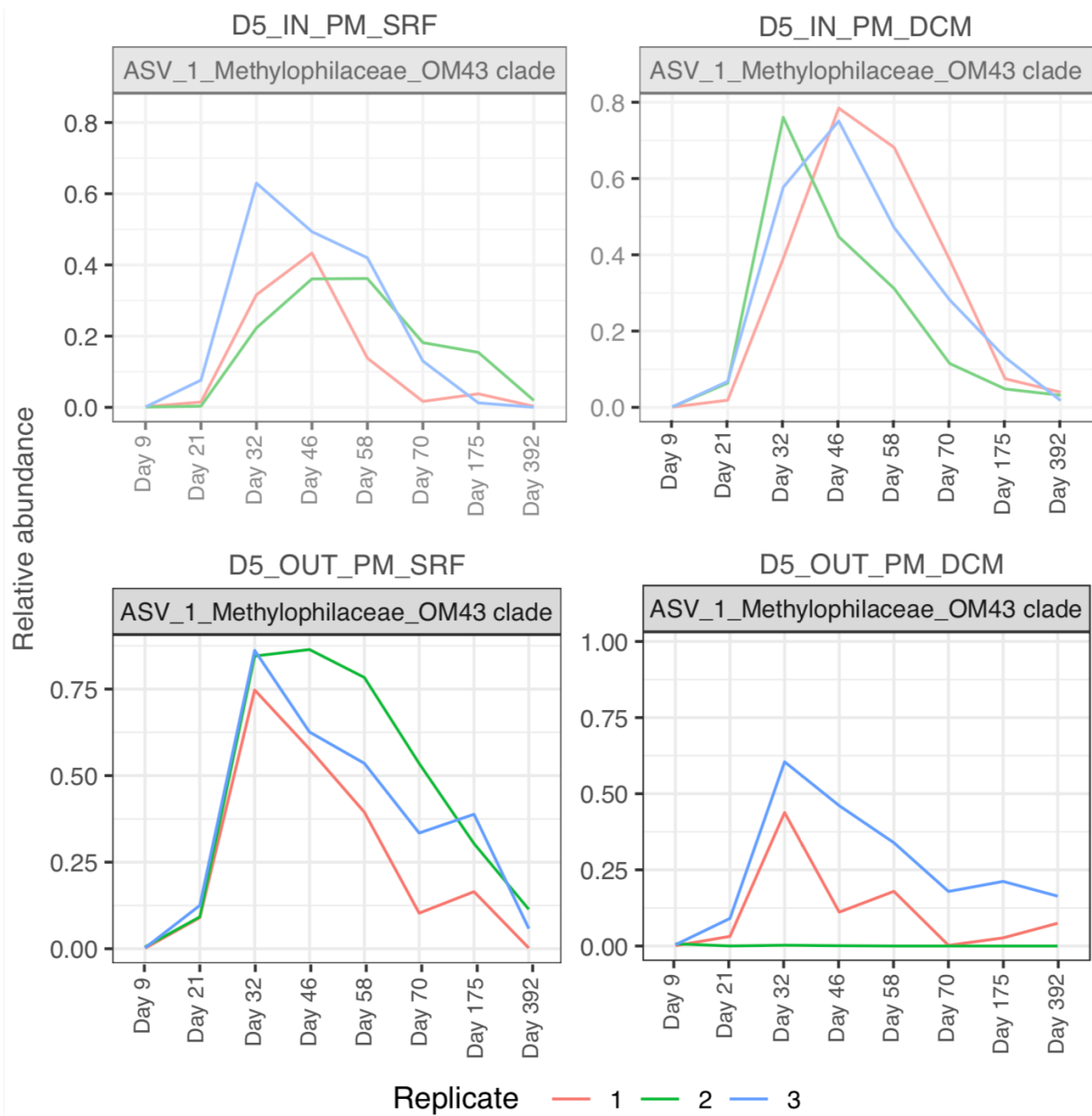
<i>Hellinger</i>	<i>Df</i>	<i>Sum of Squares</i>	<i>Mean sum of squares</i>	<i>F.Model</i>	<i>R2</i>	<i>P-value</i>
<i>Treatments</i> •	3	17.944	5.981	2.670	0.310	0.002*
<i>Replicates</i> •	8	17.923	2.240	8.561	0.310	0.001*
<i>Time</i>	1	3.199	3.199	14.762	0.055	0.001*
<i>Treatments x Time</i>	3	1.447	0.482	2.226	0.025	0.019*
<i>Residuals</i>	80	17.337	0.217	NA	0.300	NA
<i>Total</i>	95	57.850	NA	NA	1	NA

**Supplementary Table 3.** Permutational multivariate analysis of variance (PERMANOVA) and nested PERMANOVA results (*nested.npmanova*) using Jaccard dissimilarity. ‘Treatments’ is a fixed factor with four levels (D5\_IN\_PM\_SRF, D5\_IN\_PM\_DCM, D5\_OUT\_PM\_SRF and D5\_OUT\_PM\_DCM). ‘Replicates’ is a fixed factor with 12 levels (3 replicates x 4 treatments) nested within treatments. ‘Time’ is a fixed continuous factor (days after the starting of the experiment). Permutations were restricted to the replicates in traditional *adonis*. •F.model and P-value correctly calculated using *nested.npmanova*. \* Significant results.

<i>Jaccard</i>	<i>Df</i>	<i>Sum of Squares</i>	<i>Mean sum of squares</i>	<i>F.Model</i>	<i>R2</i>	<i>P-value</i>
<i>Treatments</i> •	3	5.917	1.972	4.430	0.255	0.001*
<i>Replicates</i> •	8	3.562	0.445	2.722	0.153	0.001*
<i>Time</i>	1	1.508	1.508	10.316	0.065	0.001*
<i>Treatments x Time</i>	3	0.536	0.179	1.222	0.023	0.180
<i>Residuals</i>	80	11.693	0.146	NA	0.504	NA
<i>Total</i>	95	23.215	NA	NA	1	NA

**Supplementary Table 4.** Pairwise nested PERMANOVA results using Jaccard dissimilarity of community composition data. ‘Treatments’ is a fixed factor with four levels (D5\_IN\_PM\_SRF, D5\_IN\_PM\_DCM, D5\_OUT\_PM\_SRF and D5\_OUT\_PM\_DCM). ‘Replicates’ is a fixed factor with 12 levels (3 replicates x 4 treatments) nested within treatments. Numbers of samples were not enough to achieve the number of permutations necessary to calculate the p-value.

<i>Pairwise comparison</i>	<i>R2</i>	<i>R2_replicates</i>
<i>D5_IN_PM_DCM - D5_IN_PM_SRF</i>	0.21964543	0.1348233
<i>D5_IN_PM_DCM - D5_OUT_PM_DCM</i>	0.25431716	0.1898008
<i>D5_IN_PM_DCM - D5_OUT_PM_SRF</i>	0.18826695	0.1231075
<i>D5_IN_PM_SRF - D5_OUT_PM_DCM</i>	0.17439807	0.2024069
<i>D5_IN_PM_SRF - D5_OUT_PM_SRF</i>	0.06653704	0.1370241
<i>D5_OUT_PM_DCM - D5_OUT_PM_SRF</i>	0.17692212	0.1918391



**Supplementary Figure 5.** ASV1 relative abundance dynamics in replicates of different treatments. Relative abundance was calculated from the non-rarefied ASV table.

**Supplementary Table 5.** Shared and specific ASVs among the treatments. Prevalence corresponds to the number of samples where the ASV was found. The percentage of prevalence is equal to the prevalence divided by the total of samples. The percentage of reads corresponds to the number of reads of the ASV divided by the total number of reads of the rarefied table. N corresponds to the number of samples used to calculate the prevalence. Prevalence of ASVs that were shared among all treatments was calculated based on the total number of samples (96). For specific ASVs, the number of samples considered was the total of each treatment (24). The taxonomy was assigned by vsearch using 94.5% identity to identify genus level. Status indicates if the ASV is specific to the treatment or shared among all treatments.

<i>ASVId</i>	<i>Prevalence</i>	<i>Prevalence in N samples</i>	<i>N</i>	<i>% of total of reads</i>	<i>Taxonomy</i>	<i>Status</i>
<i>ASV_21</i>	95	0.990	96	0.004	Proteobacteria;Gammaproteobacteria;Pseudomonadales;Pseudomonadaceae;Pseudomonas	shared
<i>ASV_6</i>	94	0.979	96	0.109	Proteobacteria;Gammaproteobacteria;Cellvibrionales;Haliaceae; <i>Luminiphilus</i>	shared
<i>ASV_1</i>	91	0.948	96	0.230	Proteobacteria;Gammaproteobacteria;Burkholderiales;Methylophilaceae;OM43_clade	shared
<i>ASV_26</i>	91	0.948	96	0.003	Proteobacteria;Gammaproteobacteria;Burkholderiales;Oxalobacteraceae;Janthinobacterium	shared
<i>ASV_31</i>	81	0.844	96	0.001	Proteobacteria;Gammaproteobacteria;Pseudomonadales;Pseudomonadaceae;Pseudomonas	shared
<i>ASV_2</i>	70	0.729	96	0.173	Proteobacteria;Gammaproteobacteria;KI89A_clade;uncultured_bacterium;	shared
<i>ASV_13</i>	57	0.594	96	0.013	Proteobacteria;Gammaproteobacteria;Burkholderiales;Methylophilaceae;OM43_clade	shared
<i>ASV_72</i>	52	0.542	96	0.000	Proteobacteria;Gammaproteobacteria;Pseudomonadales;Pseudomonadaceae;Pseudomonas	shared
<i>ASV_19</i>	30	0.313	96	0.007	Proteobacteria;Gammaproteobacteria;Cellvibrionales;Haliaceae;OM60(NOR5)_clade	shared
<i>ASV_53</i>	30	0.313	96	0.001	Firmicutes;Bacilli;Bacillales;Sporolactobacillaceae;Sporolactobacillus	shared
<i>ASV_120</i>	30	0.313	96	0.000	Proteobacteria;Gammaproteobacteria;Pseudomonadales;Pseudomonadaceae;Pseudomonas	shared
<i>ASV_104</i>	27	0.281	96	0.000	Proteobacteria;Gammaproteobacteria;Alteromonadales; <i>Marinobacteraceae;Marinobacter</i>	shared
<i>ASV_129</i>	26	0.271	96	0.000	Firmicutes;Bacilli;Caldalkalibacillales;Caldalkalibacillaceae;Caldalkalibacillus	shared
<i>ASV_136</i>	25	0.260	96	0.000	Proteobacteria;Gammaproteobacteria;Burkholderiales;Oxalobacteraceae;Janthinobacterium	shared
<i>ASV_149</i>	23	0.240	96	0.000	Proteobacteria;Gammaproteobacteria;Pseudomonadales;Pseudomonadaceae;Pseudomonas	shared
<i>ASV_95</i>	21	0.219	96	0.000	Proteobacteria;Gammaproteobacteria;Oceanospirillales;Halomonadaceae;Halomonas	shared
<i>ASV_134</i>	21	0.219	96	0.000	Proteobacteria;Gammaproteobacteria;Enterobacteriales;Yersiniaceae;Serratia	shared
<i>ASV_131</i>	17	0.177	96	0.000	Firmicutes;Bacilli;Bacillales;Bacillaceae;Anoxybacillus	shared

ASV_142	17	0.177	96	0.000	Firmicutes;Bacilli;Bacillales;Bacillaceae;Piscibacillus	shared
ASV_158	17	0.177	96	0.000	Firmicutes;Bacilli;Bacillales;Bacillaceae;Geobacillus	shared
ASV_114	16	0.167	96	0.000	Firmicutes;Bacilli;Bacillales;Sporolactobacillaceae;Terrilactibacillus	shared
ASV_56	15	0.156	96	0.000	Proteobacteria;Gammaproteobacteria;Tenderiales;Tenderiaceae;Candidatus_Tenderia	shared
ASV_202	14	0.146	96	0.000	Firmicutes;Bacilli;Bacillales;Bacillaceae;Anoxybacillus	shared
ASV_223	14	0.146	96	0.000	Proteobacteria;Gammaproteobacteria;Alteromonadales;Shewanellaceae;Shewanella	shared
ASV_180	13	0.135	96	0.000	Firmicutes;Bacilli;Bacillales;Bacillaceae;Geobacillus	shared
ASV_206	12	0.125	96	0.000	Proteobacteria;Gammaproteobacteria;Xanthomonadales;Xanthomonadaceae;Stenotrophomonas	shared
ASV_216	12	0.125	96	0.000	Proteobacteria;Gammaproteobacteria;Pseudomonadales;Moraxellaceae;Acinetobacter	shared
ASV_190	11	0.115	96	0.000	Proteobacteria;Gammaproteobacteria;Burkholderiales;Comamonadaceae;Delftia	shared
ASV_232	11	0.115	96	0.000	Firmicutes;Bacilli;Bacillales;Bacillaceae;Bacillus	shared
ASV_66	10	0.104	96	0.000	Proteobacteria;Gammaproteobacteria;SAR86_clade;uncultured_bacterium;	shared
ASV_88	9	0.094	96	0.000	Proteobacteria;Gammaproteobacteria;Cellvibrionales;Halieaceae;OM60(NOR5)_clade	shared
ASV_148	9	0.094	96	0.000	Proteobacteria;Gammaproteobacteria;Enterobacteriales;Erwiniaceae;Siccibacter	shared
ASV_231	9	0.094	96	0.000	Proteobacteria;Gammaproteobacteria;Burkholderiales;Comamonadaceae;Pelomonas	shared
ASV_237	8	0.083	96	0.000	Firmicutes;Bacilli;Bacillales;Sporolactobacillaceae;Sporolactobacillus	shared
ASV_301	8	0.083	96	0.000	Proteobacteria;Gammaproteobacteria;Oceanospirillales;Halomonadaceae;Halomonas	shared
ASV_239	7	0.073	96	0.000	Proteobacteria;Gammaproteobacteria;Alteromonadales;Marinobacteraceae;Marinobacter	shared
ASV_242	7	0.073	96	0.000	Firmicutes;Bacilli;Caldalkalibacillales;Caldalkalibacillaceae;Caldalkalibacillus	shared
ASV_252	7	0.073	96	0.000	Actinobacteriota;Actinobacteria;Propionibacteriales;Propionibacteriaceae;Cutibacterium	shared
ASV_260	7	0.073	96	0.000	Actinobacteriota;Actinobacteria;Micrococcales;Micrococcaceae;Pseudarthrobacter	shared
ASV_264	7	0.073	96	0.000	Proteobacteria;Gammaproteobacteria;Burkholderiales;Oxalobacteraceae;Herbaspirillum	shared
ASV_256	6	0.063	96	0.000	Proteobacteria;Gammaproteobacteria;Xanthomonadales;Xanthomonadaceae;Stenotrophomonas	shared
ASV_259	6	0.063	96	0.000	Proteobacteria;Gammaproteobacteria;Pseudomonadales;Pseudomonadaceae;Pseudomonas	shared
ASV_295	6	0.063	96	0.000	Firmicutes;Bacilli;Bacillales;Sporolactobacillaceae;Terrilactibacillus	shared
ASV_302	6	0.063	96	0.000	Proteobacteria;Gammaproteobacteria;Pseudomonadales;Moraxellaceae;Acinetobacter	shared
ASV_248	5	0.052	96	0.000	Proteobacteria;Gammaproteobacteria;Xanthomonadales;Xanthomonadaceae;Stenotrophomonas	shared
ASV_324	5	0.052	96	0.000	Firmicutes;Negativicutes;Veillonellales-Selenomonadales;uncultured;uncultured_bacterium	shared

ASV_12	24	1.000	24	0.024	Bacteroidota;Bacteroidia;Flavobacteriales;Flavobacteriaceae;Aurantivirga	specific D5_IN_PM_DCM
ASV_23	18	0.750	24	0.006	Bacteroidota;Bacteroidia;Flavobacteriales;Flavobacteriaceae;Polaribacter	specific D5_IN_PM_DCM
ASV_17	11	0.458	24	0.007	Proteobacteria;Alphaproteobacteria;Rhodobacterales;Rhodobacteraceae;Sulfitobacter	specific D5_IN_PM_DCM
ASV_16	8	0.333	24	0.016	Proteobacteria;Alphaproteobacteria;Rhodobacterales;Rhodobacteraceae;Yoonia-Loktanella	specific D5_IN_PM_DCM
ASV_28	8	0.333	24	0.003	Bacteroidota;Bacteroidia;Flavobacteriales;Flavobacteriaceae;Lacinutrix	specific D5_IN_PM_DCM
ASV_57	7	0.292	24	0.000	Bacteroidota;Bacteroidia;Flavobacteriales;Flavobacteriaceae;Polaribacter	specific D5_IN_PM_DCM
ASV_171	7	0.292	24	0.000	Proteobacteria;Gammaproteobacteria;Tenderiales;Tenderiaceae;Candidatus_Tenderia	specific D5_IN_PM_DCM
ASV_45	6	0.250	24	0.001	Bacteroidota;Bacteroidia;Flavobacteriales;Flavobacteriaceae;Polaribacter	specific D5_IN_PM_DCM
ASV_78	6	0.250	24	0.000	Bacteroidota;Bacteroidia;Flavobacteriales;Flavobacteriaceae;Polaribacter	specific D5_IN_PM_DCM
ASV_34	3	0.125	24	0.000	Proteobacteria;Alphaproteobacteria;Rhodobacterales;Rhodobacteraceae;Asciidiaceihabitans	specific D5_IN_PM_DCM
ASV_36	2	0.083	24	0.000	Bacteroidota;Bacteroidia;Flavobacteriales;Flavobacteriaceae;uncultured	specific D5_IN_PM_DCM
ASV_108	2	0.083	24	0.000	Proteobacteria;Alphaproteobacteria;SAR11_clade;Clade_I;Clade_Ia	specific D5_IN_PM_DCM
ASV_141	2	0.083	24	0.000	Proteobacteria;Gammaproteobacteria;Oceanospirillales;Pseudohongiellaceae;Pseudohongiella	specific D5_IN_PM_DCM
ASV_169	2	0.083	24	0.000	Proteobacteria;Alphaproteobacteria;Rhodobacterales;Rhodobacteraceae;Planktomarina	specific D5_IN_PM_DCM
ASV_184	2	0.083	24	0.000	Proteobacteria;Alphaproteobacteria;Rhodospirillales;AEGEAN-169_marine_group;marine_metagenome	specific D5_IN_PM_DCM
ASV_263	2	0.083	24	0.000	Firmicutes;Thermoanaerobacteria;Caldicellulosiruptorales;Caldicellulosiruptoraceae;Caldicellulosiruptor	specific D5_IN_PM_DCM
ASV_54	1	0.042	24	0.000	Proteobacteria;Alphaproteobacteria;SAR11_clade;Clade_I;uncultured	specific D5_IN_PM_DCM
ASV_59	1	0.042	24	0.000	Verrucomicrobiota;Verrucomicrobiae;Opitutales;Puniceicoccaceae;Lentimonas	specific D5_IN_PM_DCM
ASV_76	1	0.042	24	0.000	Bacteroidota;Bacteroidia;Flavobacteriales;Flavobacteriaceae;NS4_marine_group	specific D5_IN_PM_DCM
ASV_94	1	0.042	24	0.000	Proteobacteria;Gammaproteobacteria;Cellvibrionales;Porticoccaceae;SAR92_clade	specific D5_IN_PM_DCM
ASV_107	1	0.042	24	0.000	Proteobacteria;Gammaproteobacteria;Thiomicrospirales;Thioglobaceae;SUP05_cluster	specific D5_IN_PM_DCM
ASV_128	1	0.042	24	0.000	Proteobacteria;Gammaproteobacteria;Thiomicrospirales;Thioglobaceae;SUP05_cluster	specific D5_IN_PM_DCM
ASV_221	1	0.042	24	0.000	Proteobacteria;Gammaproteobacteria;SAR86_clade;uncultured_gamma_proteobacterium;	specific D5_IN_PM_DCM
ASV_279	1	0.042	24	0.000	Proteobacteria;Gammaproteobacteria;Pseudomonadales;Pseudomonadaceae;Pseudomonas	specific D5_IN_PM_DCM
ASV_281	1	0.042	24	0.000	Bacteroidota;Bacteroidia;Flavobacteriales;Flavobacteriaceae;NS2b_marine_group	specific D5_IN_PM_DCM
ASV_352	1	0.042	24	0.000	Planctomycetota;Planctomycetes;Pirellulales;Pirellulaceae;Blastopirellula	specific D5_IN_PM_DCM
ASV_338	1	0.042	24	0.000	Proteobacteria;Gammaproteobacteria;Cellvibrionales;Haliaceae;Luminiphilus	specific D5_IN_PM_DCM
ASV_11	8	0.333	24	0.022	Proteobacteria;Gammaproteobacteria;Oceanospirillales;Halomonadaceae;Salinicola	specific D5_IN_PM_SRF

<i>ASV_44</i>	8	0.333	24	0.001	Actinobacteriota;Actinobacteria;Micrococcales;Microbacteriaceae;Microbacterium	specific D5_IN_PM_SRF
<i>ASV_38</i>	2	0.083	24	0.000	Proteobacteria;Alphaproteobacteria;Rhodobacterales;Rhodobacteraceae;uncultured	specific D5_IN_PM_SRF
<i>ASV_98</i>	2	0.083	24	0.000	Proteobacteria;Gammaproteobacteria;SAR86_clade;uncultured_bacterium;	specific D5_IN_PM_SRF
<i>ASV_116</i>	2	0.083	24	0.000	Proteobacteria;Gammaproteobacteria;OM182_clade;marine_gamma_proteobacterium_HTCC2151;	specific D5_IN_PM_SRF
<i>ASV_194</i>	2	0.083	24	0.000	Proteobacteria;Gammaproteobacteria;Thiotrichales;Thiotrichaceae;uncultured	specific D5_IN_PM_SRF
<i>ASV_350</i>	2	0.083	24	0.000	Firmicutes;Clostridia;Thermincolales;Thermincolaceae;Thermincola	specific D5_IN_PM_SRF
<i>ASV_99</i>	1	0.042	24	0.000	Proteobacteria;Alphaproteobacteria;Puniceispirillales;SAR116_clade;uncultured_marine_bacterium	specific D5_IN_PM_SRF
<i>ASV_137</i>	1	0.042	24	0.000	Proteobacteria;Gammaproteobacteria;SAR86_clade;uncultured_marine_bacterium;	specific D5_IN_PM_SRF
<i>ASV_356</i>	1	0.042	24	0.000	Proteobacteria;Gammaproteobacteria;Burkholderiales;Methylophilaceae;OM43_clade	specific D5_IN_PM_SRF
<i>ASV_4</i>	8	0.333	24	0.064	Proteobacteria;Gammaproteobacteria;Oceanospirillales;Alcanivoracaceae1; <i>Alcanivorax</i>	specific D5_OUT_PM_DCM
<i>ASV_22</i>	6	0.250	24	0.007	Proteobacteria;Alphaproteobacteria;Caulobacterales;Hyphomonadaceae;Henriciella	specific D5_OUT_PM_DCM
<i>ASV_70</i>	6	0.250	24	0.001	Bacteroidota;Bacteroidia;Flavobacteriales;Flavobacteriaceae;Joostella	specific D5_OUT_PM_DCM
<i>ASV_287</i>	2	0.083	24	0.000	Firmicutes;Bacilli;Caldalkalibacillales;Caldalkalibacillaceae;Caldalkalibacillus	specific D5_OUT_PM_DCM
<i>ASV_41</i>	1	0.042	24	0.000	Actinobacteriota;Acidimicrobiia;Actinomarinales;Actinomarinaceae;Candidatus_Actinomarina	specific D5_OUT_PM_DCM
<i>ASV_312</i>	1	0.042	24	0.000	Proteobacteria;Gammaproteobacteria;Xanthomonadales;Xanthomonadaceae;Stenotrophomonas	specific D5_OUT_PM_DCM
<i>ASV_130</i>	1	0.042	24	0.000	Proteobacteria;Gammaproteobacteria;Cellvibrionales;Porticoccaceae;Porticoccus	specific D5_OUT_PM_SRF

**Supplementary Table 6.** Detailed results of IndVal analysis. The grey-shaded polygons indicate the group to which the ASV is indicative. The components A and B are used to calculate the indicator value (IndVal). P-values were adjusted for multiple comparison using false discovery rate correction. Prevalence corresponds to the number of samples where the ASV was found. Status indicates if the ASV is specific of the treatment or shared with others.

ASVId	IN DCM	IN SRF	OUT DCM	OUT SRF	A (specificity)	B (fidelity)	IndVal	P-value	Taxonomy	Prevalence	status
ASV12					1	1	1.000	0.001	Bacteroidota;Bacteroidia;Flavobacteriales;Flavobacteriaceae; Aurantivirga	24	specific D5_IN_PM_DCM
ASV18					0.9997	0.9583	0.979	0.001	Bacteroidota;Bacteroidia;Flavobacteriales;Flavobacteriaceae; <i>Polaribacter</i>	24	shared D5_IN_PM_DCM:D5_OUT_PM_SRF
ASV8					0.8421	1	0.918	0.001	Proteobacteria;Gammaproteobacteria;KI89A clade; marine_gamma_proteobacterium_HTCC2089 ;unclassified	38	shared D5_IN_PM_DCM:D5_OUT_PM_SRF
ASV15					0.9998	0.8333	0.913	0.001	Bacteroidota;Bacteroidia;Flavobacteriales;Flavobacteriaceae; <i>Polaribacter</i>	21	shared D5_IN_PM_DCM:D5_OUT_PM_DC M
ASV20					0.9997	0.7917	0.890	0.001	Bacteroidota;Bacteroidia;Flavobacteriales;Flavobacteriaceae; Aurantivirga	20	shared D5_IN_PM_DCM:D5_OUT_PM_DC M
ASV23					1	0.75	0.866	0.001	Bacteroidota;Bacteroidia;Flavobacteriales;Flavobacteriaceae; <i>Polaribacter</i>	18	specific D5_IN_PM_DCM
ASV17					1	0.4583	0.677	0.001	Proteobacteria;Alphaproteobacteria;Rhodobacterales;Rhodobacteraceae;Sulfitobacter	11	specific D5_IN_PM_DCM
ASV16					1	0.3333	0.577	0.001	Proteobacteria;Alphaproteobacteria;Rhodobacterales;Rhodobacteraceae;Yoonia-Loktanella	8	specific D5_IN_PM_DCM
ASV28					1	0.3333	0.577	0.001	Bacteroidota;Bacteroidia;Flavobacteriales;Flavobacteriaceae;Lacinutrix	8	specific D5_IN_PM_DCM

ASV57		1	0.2917	0.540	0.001	Bacteroidota;Bacteroidia;Flavobacteriales;Flavobacteriaceae; <i>Polaribacter</i>	7	specific D5_IN_PM_DCM
ASV17		1	0.2917	0.540	0.001	Proteobacteria;Gammaproteobacteria;Tenderiales;Tenderiaceae;Candidatus Tenderia	7	specific D5_IN_PM_DCM
ASV78		1	0.25	0.500	0.003	Bacteroidota;Bacteroidia;Flavobacteriales;Flavobacteriaceae; <i>Polaribacter</i>	6	specific D5_IN_PM_DCM
ASV45		1	0.25	0.500	0.004	Bacteroidota;Bacteroidia;Flavobacteriales;Flavobacteriaceae; <i>Polaribacter</i>	6	specific D5_IN_PM_DCM
ASV7		0.9998	0.4583	0.677	0.001	Proteobacteria;Alphaproteobacteria;Sphingomonadales;Sphingomonadaceae; <i>Erythrobacter</i>	14	shared D5_IN_PM_SRF:D5_OUT_PM_SRF: D5_OUT_PM_DCM
ASV4		1	0.3333	0.577	0.001	Proteobacteria;Gammaproteobacteria;Oceanospirillales;Alcanivoracaceae1; <i>Alcanivorax</i>	8	specific D5_OUT_PM_DCM
ASV10		0.9999	0.3333	0.577	0.001	Proteobacteria;Alphaproteobacteria;Sphingomonadales;Sphingomonadaceae; <i>Erythrobacter</i>	9	shared D5_IN_PM_SRF:D5_OUT_PM_DCM
ASV14		0.9999	0.3333	0.577	0.001	Proteobacteria;Gammaproteobacteria;Alteromonadales;Idiomarinaceae;Idiomarina	9	shared D5_IN_PM_SRF:D5_OUT_PM_DCM
ASV22		1	0.25	0.500	0.004	Proteobacteria;Alphaproteobacteria;Caulobacteriales;Hyphomonadaceae;Henriciella	6	specific D5_OUT_PM_DCM
ASV70		1	0.25	0.500	0.003	Bacteroidota;Bacteroidia;Flavobacteriales;Flavobacteriaceae;Jostella	6	specific D5_OUT_PM_DCM
ASV11		1	0.3333	0.577	0.001	Proteobacteria;Gammaproteobacteria;Oceanospirillales;Halomonadaceae;Salinicola	8	specific D5_IN_PM_SRF
ASV44		1	0.3333	0.577	0.001	Actinobacteriota;Actinobacteria;Micrococcales;Microbacteriaceae;Microbacterium	8	specific D5_IN_PM_SRF
ASV11		3	0.9846	0.2083	0.010	Actinobacteriota;Actinobacteria;Micrococcales;Microbacteriaceae;Microbacterium	6	shared D5_IN_PM_SRF:D5_OUT_PM_SRF

ASV9				1	1	1.000	0.001	Proteobacteria;Gammaproteobacteria;Cellvibrionales;Porticocaceae;SAR92 clade	72	shared D5_IN_PM_SRF:D5_IN_PM_DCM:D5_OUT_PM_SRF
ASV2				1	0.9583	0.979	0.001	Proteobacteria;Gammaproteobacteria;KI89A clade;uncultured_bacterium;unclassified	70	shared all
ASV5				1	0.9444	0.972	0.001	Proteobacteria;Gammaproteobacteria;Cellvibrionales;Porticocaceae;SAR92 clade	68	shared D5_IN_PM_SRF:D5_IN_PM_DCM:D5_OUT_PM_SRF
ASV39				1	0.5	0.707	0.001	Proteobacteria;Gammaproteobacteria;Burkholderiales;Methylphilaceae;OM43 clade	36	shared D5_IN_PM_SRF:D5_IN_PM_DCM:D5_OUT_PM_SRF
ASV63				0.9576	0.6458	0.786	0.001	Proteobacteria;Gammaproteobacteria;Cellvibrionales;Porticocaceae;SAR92 clade	40	shared D5_IN_PM_SRF:D5_IN_PM_DCM:D5_OUT_PM_SRF
ASV32				1	0.6528	0.808	0.001	Proteobacteria;Gammaproteobacteria;Tenderiales;Tenderiaceae;Candidatus Tenderia	47	shared D5_IN_PM_DCM:D5_OUT_PM_SRF:D5_OUT_PM_DCM







---

# DISCUSSION AND PERSPECTIVES

---



## Discussion and Perspectives

The overall objective of this thesis was to characterize the bacterial diversity associated with coccolithophores in cultures and to investigate the patterns and processes of microbiome selection. In this last part, I will discuss the pitfalls of the approaches used here and the strategies applied to overcome the challenges. I also discuss the major contributions of this thesis to the current state of the art on phytoplankton microbiomes. Perspectives based on preliminary results obtained from co-culture experiments were proposed.

### **High-throughput sequencing technologies and the microbiomes studies: advances and challenges**

In the past decade, the advances in molecular tools such as Illumina Miseq sequencing allowed exploration of the microbiomes of several phytoplankton (Ajani *et al.*, 2018; Behringer *et al.*, 2018; Lawson *et al.*, 2018; Sörenson *et al.*, 2019). Still, one of the main challenges of microbiome studies using amplicon data is how to get biologically meaningful information and separate true diversity from errors (Prodan *et al.*, 2020). Although this thesis did not focus on the development of methods to assess microbiomes, I carefully tuned the protocols used, starting with the choice of primers. I used primers that show lower bias for important bacterial groups (Alpha and Gammaproteobacteria), giving results very close to the ones expected in mock communities and natural samples (Parada *et al.*, 2016). However, we could observe that the length of the amplicons and the region sequenced is not resolute enough to perform differentiation within some genera, such as *Marinobacter* (See **Chapter 1** - Supplementary Figure 8). New technologies involving long-reads sequencing (*e.g.*, Nanopore MinION) propose a solution for increasing taxonomic resolution. Association of both sequencing technologies have been applied to investigate microbiomes of dinoflagellates and showed promising results, with a better evaluation of the abundance at the species level (Shin *et al.*, 2018). However, the limitation of this technology (accuracy and low throughput) still favors the use of Illumina short reads in microbiome studies (Pollock *et al.*, 2018).

Furthermore, each step from the DNA collection until the DNA sequencing are subject to the introduction of contaminations and sequencing errors, which potentially introduce false-positive and inflate diversity indexes if not corrected (Bokulich *et al.*, 2013; Nearing *et al.*, 2018). There are different strategies developed for correction and minimization of errors on

microbiome data from amplicon sequencing. Different studies have shown that the use of mock communities and negative controls can be effective for controlling the various technical, biological and human errors that arise at the processing and sequencing, in addition to control contaminations (see Bokulich *et al.*, 2020 and references therein). However, their laborious preparation and cost, make that they are not routinely applied. In the absence of mock communities, I applied other practices in order to decrease biases associated with errors. First, I compared different commonly used workflows to obtain a diversity table (Mothur (Schloss *et al.*, 2009), QIIME2 using vsearch OTU clustering (Bolyen *et al.*, 2019), Amplitools workflow (Kahlke, 2018) and FROGS (Escudié *et al.*, 2018)) and the DADA2 denoising (Callahan *et al.*, 2016). In general, workflows disagreed in number OTUs/ASVs, however the beta-diversity patterns were highly correlated. Based on this preliminary work, I selected DADA2 because it performs a good control of errors while allowing the easy comparison between different studies (Callahan *et al.*, 2016).

Here, the sequencing of biological (**Chapter 1**) and technical replicates (**Chapters 2 and 3**) allowed to inspect variations in the diversity that could be associated with errors. By carefully inspecting the biological replicates, I could observe that they were consistent regarding the most abundant ASVs (in presence-absence and number of reads) although low abundance transient ASVs were also present. Considering a phytoplankton culture as a closed system, with no migration processes, these ASVs can be: (i) ASVs close to the detection limit of the methods and thus they are not consistently detected or (ii) errors and/or contaminations. Either situation is difficult to pinpoint and thus after comparing abundance filters, I removed ASVs representing less than 0.001% of the total of reads and considered only those that were found in all replicates for each strain. The same reasoning was used for the technical replicates of **chapters 2 and 3**. Although this choice might decrease the power to detect the natural variability in the communities, it increases the certainty of the sequences investigated (Alberdi *et al.*, 2018). I acknowledge that even though abundance filters can be effective at removing low abundance contamination and spurious diversity, they are also criticized by removing true diversity (Prodan *et al.*, 2020). Here, the choice was at most guided by limits on drawing conclusions about the rare biosphere based solely on sequencing methods. To put these in numbers, the filters used in the different chapters (prevalence in replicates and abundance) removed from 57% to 74% of the total number of ASVs, while keeping 99% of the reads. This demonstrates the very high number of singletons and low abundance ASVs which are very difficult to distinguish from errors and add rather low information for beta diversity analyses.

In addition to that, it has been shown that statistical methods and ordinations can perform better when low abundance features are removed because it decreases sparsity (zero inflated estimation due to rare species appearing only in one sample) (Alberdi and Gilbert, 2019). Although it might be argued that the application of abundance filters can influence the alpha-diversity measurements based on total number of observed and unobserved species (*e.g.* richness and Chao1 indexes), their use on molecular data is also controversial (Alberdi and Gilbert, 2019). Alpha diversity indexes in molecular data are highly affected by sequence depth, number of copies of the gene and other issues, which make it very difficult to get a real estimation of diversity. Moreover, not performing any filtering can be more damaging than filtering low abundance ASVs (*e.g.*, increasing dissimilarity among replicates, overestimation of diversity) (Alberdi *et al.*, 2018). Here, alpha diversity indexes were carefully used to compare samples from the same study which received the same bioinformatic treatment.

A last aspect that can be considered in microbiome studies is the association of strategies to validate the ecological relevance of the observations. Here I looked for the dominant ASVs from cultures in global oceans surveys and compared coccolithophore microbiomes with published datasets from other microalgae by applying the same methods (**Chapter 1**). Altogether, these approaches helped to draw a better connection between culture-based *in vitro* studies and surveys of natural *in situ* samples and to get a general view of phytoplankton-associated bacterial diversity. I still acknowledge that even the most careful treatment is not free of errors. For this reason, I believe that more than choosing the methods that better allow investigating the scientific question, sharing is a crucial step to guarantee fully reproducibility, comparison and improvement of the methods. For this reason, all the codes I have generated in this work are available online for further studies (<https://github.com/mcamarareis>).

### **Investigating microalgal microbiomes in culture: when simplified communities bring valuable insights into phytoplankton-bacteria interactions**

One of the greatest challenges on investigating phycosphere-associated communities is on how to precisely tackle the diversity at such a small scale (Fu *et al.*, 2020). In marine environmental surveys, biomass from a seawater sample is concentrated on a filter before being processed for metabarcoding analysis. This approach has allowed identification of co-occurring organisms and major driving forces at a global scale (Sunagawa *et al.*, 2015; Logares *et al.*, 2020). However, it is difficult to precisely resolve how the microbial diversity is shaped within the phycosphere. In this scenario, the association of different approaches is a promising

solution. Investigating simplified systems such as cultured microbiomes allows to draw hypotheses that can then be addressed in a large-scale perspective. However, studying the diversity of microbiomes that have been kept for years in laboratory conditions is still a matter of debate. In this thesis, I responded to fundamental questions regarding the study of microbiomes of clonal phytoplankton cultures that can be used as pavement for future studies on phytoplankton-bacteria interactions.

First, an important gap regarding the bacterial diversity associated with two coccolithophores (*E. huxleyi* and *G. oceanica*) in cultures was filled out by our results (**Chapter 1**). We found a striking dominance of Gammaproteobacteria in the coccolithophore microbiomes, which differs from other microalgae (*e.g.* diatoms) microbiomes (Ajani *et al.*, 2018; Behringer *et al.*, 2018). Surprisingly coccolithophore microbiomes have common points with that of cyanobacterial and *Alexandrium* sp. cultures with about 52% and 42% of the taxa shared respectively, including the most dominant one (Sörenson *et al.*, 2019; Kearney *et al.*, 2021). A considerable diversity of *Marinobacter* was found associated with coccolithophore cultures, most of which could not be assigned to known species by phylogenetic placement. This indicates a high diversity of yet unknown *Marinobacter* species associated with coccolithophores which deserves further attention. *Marinobacter* spp. are considered ‘opportunotrophs’ because they take advantage of nutrient pulses to grow (Handley and Lloyd, 2013). However, their high dominance in the microbiomes of different phytoplankton cannot be reduced only to an opportunistic presence. *Marinobacter* isolates are shown to increase the growth of different phytoplankton in co-cultures (Amin *et al.*, 2009; Bolch *et al.*, 2017). This enhancement has been attributed to their capacity to produce modified siderophores which increase iron uptake by phytoplankton (Amin *et al.*, 2009). Still, the metabolic exchanges among *Marinobacter* and phytoplankton other than diatoms are largely unexplored and might not be restricted to siderophores production.

I also showed that the dominant ASVs from the coccolithophore phycosphere are globally distributed in the world ocean, agreeing with their presence in cultures isolated from different oceanic regions, although they are found in low abundance in the surface ocean. Furthermore, our results indicate the possible association of these taxa to large sinking particles in the oceans. Importantly, their higher abundance in deep waters suggest that, through the sinking of particles, these taxa are inoculated the deep realm, where they thrive, and contribute to its function and structure (Mestre *et al.*, 2018). Altogether, our results point out to an

important role of the phycosphere as a ‘seed bank’ of bacterial taxa displaying variable functions depending on their habitat. These taxa can bloom when conditions are favorable, following a ‘bloom and burst’ dynamic (Alonso-Sáez *et al.*, 2014, 2015). Large blooms of phycosphere-associated taxa have been observed (Morris *et al.*, 2006; Alonso-Sáez *et al.*, 2014). Their transient behavior in the oceans seems mainly related to the seasonality of favorable conditions, however the precise conditions are still not known and may vary for each taxon (Alonso-Sáez *et al.*, 2015). In cultures, homogeneous conditions, concentrated organic matter, and reduced competition might be decisive for the dominance and long-term persistence of these taxa.

Short-to-long time scale persistency and robustness/resilience of microbiomes were other key findings from this thesis (Chapters 1 and 3). I confirmed the hypothesis that phytoplankton microbiomes in culture represent long-lasting and stable relationships (Krohn-Molt *et al.*, 2017). Importantly, these microbiomes are robust and coupled to changes in the health state of the host (**Chapter 3**). Among microalgae, robustness/resilience of microbiomes to environmental perturbations were shown for *N. salina* and *Symbiodinium* (Geng *et al.*, 2016; Camp *et al.*, 2020). This coupling can have important evolutionary implications in phytoplankton-bacteria interactions. While the host is in a healthy state, interactions are stable, however, stress can trigger changes in these interactions and modify the microbiome dominant taxa. The coupling between host and microbiome health state has been demonstrated in corals, which experienced parasitism by its *Symbiodinium* partners under thermal stress (Baker *et al.*, 2018). Concerning *E. huxleyi*, studies have shown that an associated bacterium can switch from mutualistic to parasitic according to senescence signals released by the host (Seyedsayamdost, Case, *et al.*, 2011; Segev, Wyche, *et al.*, 2016). We cannot characterize the patterns observed here as a switch in the interactions however they demonstrate that stable conditions are necessary for the maintenance of these associations. Further studies involving different levels of disturbance would help to better understand the relationships between the diversity and taxonomic structure of the microbiomes and their capacity to recover from disturbance, and ultimately the consequences of a failure to recover. These questions are of crucial importance to understand the impacts of environmental global changes on major processes driven by symbiotic interactions in the oceans.

Another key result from this work regards the processes of microbiome assembly. I showed that even if the most dominant taxa are shared among cultures, we can still identify

patterns related to the assembly of microbiomes (**Chapters 2 and 3**). The local conditions of the place of isolation were shown to display an important role in the microbiome assembly. Both abiotic parameters at the time of sampling and culture conditions (**Chapter 2**) and biotic factors (*e.g.* pre-exposition to *E. huxleyi* in the bloom) (**Chapter 3**) were detected as drivers of microbiome composition. These results reinforce the influence of deterministic processes on the assembly of phytoplankton microbiomes (Ajani *et al.*, 2018; Sörenson *et al.*, 2019). These forces might act at different scales. While the environmental factors select the bacterial community at a larger scale, the effect of the host is more pronounced at the phycosphere level where the organic matter released is more concentrated (Landa *et al.*, 2016; Fu *et al.*, 2020). This local effect of the phycosphere is clear from the results of the **Chapter 3**, showing that the bacterial community sampled at the *E. huxleyi* bloom depth favored the presence of groups not found in the other treatments (even from the same site at upper depth). Altogether these results point out to a high complexity of the processes involved in microbiome assembly at multiple scales.

To conclude with the contributions of this thesis to the knowledge on phytoplankton-bacteria interactions, an important catalogue of the bacterial diversity found in microalgal cultures that were isolated from different places in the world, with different metabolic requirements (specially *E. huxleyi*, but not only) was also provided (**Chapters 1 and 2**). This unique dataset is being included in a global analysis of the *Tara* Oceans 16S rRNA metabarcodes as a reference for phytoplankton-associated bacteria. This reinforces the already mentioned importance of using microbiomes in culture to obtain insights and draw hypotheses that can be tested in other contexts.

### **Towards a functional exploitation of microalgal microbiomes and beyond**

Many fundamental questions regarding phytoplankton microbiomes are yet to be answered. Especially for coccolithophores, the metabolic exchanges with mutualistic bacteria are still largely unexplored. Studying the interactions between bacterial isolates and *E. huxleyi* was one of the initial objectives of my thesis. During the last three years, in parallel to the experiments I detailed before, I also isolated many bacterial taxa associated with *E. huxleyi* and established axenic cultures that were both used in co-culture experiments. Together, the results presented here, and preliminary co-culture experiments opened new avenues in the study of phytoplankton-bacteria interactions at multiple scales.

One of the main paradigms of microbiomes is that they provide to the host conditions to grow better (Amin *et al.*, 2012), to fight pathogens (Seyedsayamdost *et al.*, 2014), to thrive in different environments (Amin *et al.*, 2009), and to co-exist with competitors (Jackrel *et al.*, 2020). Different studies propose that genes, or clusters of genes, might be more important than species for understanding the roles and assembly processes of microbiomes associated with various systems (Burke, Steinberg, *et al.*, 2011; Fan *et al.*, 2012; Louca *et al.*, 2016). Macroalgal investigations have shown that although disagreements can be found regarding the microbiome diversity of a host grown in different environments, much more agreement is found if we investigate the functional diversity (Burke *et al.*, 2011). Furthermore, a study on the global ocean microbiome evidenced a high functional redundancy across oceanic regions which harbored different taxonomic compositions (Sunagawa *et al.*, 2015). Thus, it is expected that functional redundancy is also present in phytoplankton microbiomes. Investigation of the phycosphere of *Microcystis aeruginosa* from different lakes agrees with this hypothesis by showing functional convergence and coupling between host and microbiome function (Jackrel *et al.*, 2019). Still, functional diversity in phytoplankton microbiomes remains largely unexplored.

Here, results of **chapters 1 and 3** raised the question about the functional diversity in *E. huxleyi* microbiomes. In both chapters the communities were dominated by gammaproteobacterial members, however the dominant taxa varied. In **Chapter 1** *Marinobacter* and *Alteromonas* were dominant while in **Chapter 3** dominance among the treatments and specific replicates was displayed by other taxa, such as OM43 clade, *Luminiphilus*, SAR92 clade, KI89 clade and *Alcanivorax*. The hypothesis for these differences is discussed in **Chapter 3**. The remaining question is, do these microbiomes present the same or complementary functional potential?

Functional assignment of the ASVs accounting for more than 1% of relative abundance per sample in each study revealed microbiomes highly similar regarding dominance and low abundance functions (see Annex 2 for the methods used). Although a considerable fraction of the ASVs (42% and 44% in **chapters 1 and 3**, respectively) of each study could not be assigned to a function, the remaining ones were assigned to 12 functions from which 10 were shared between both studies (Figure 1).

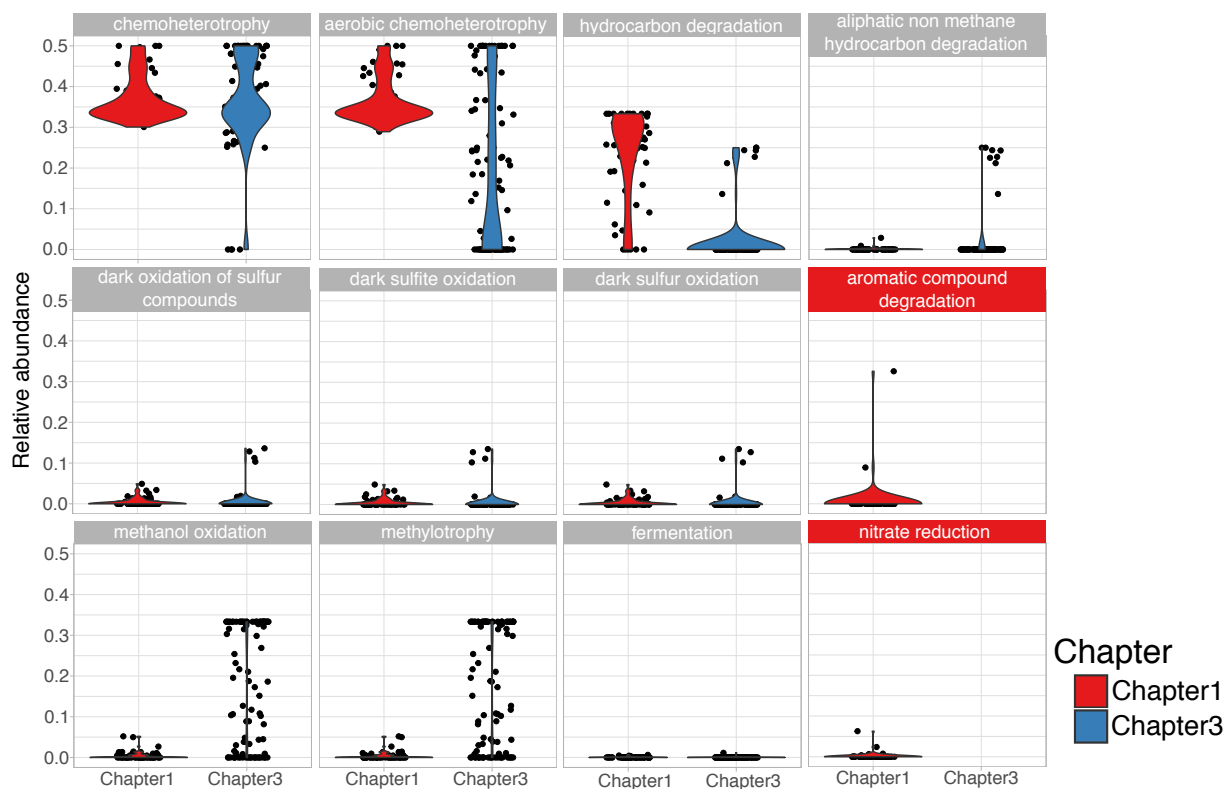


**Figure 1.** Functional classification of ASVs, found in **chapters 1** and **3**, having more than 1% of relative abundance. Classification was done based in FAPROTAX database v1.2.4 (Louca *et al.*, 2016). Grey boxes represent shared functions while red boxes are functions specific to ASVs from **Chapter 1**.

Among the identified functions, chemoheterotrophy and aerobic chemoheterotrophy displayed mainly by copiotrophic bacteria were the most dominant in both studies. These functions were assigned mainly to Rhodobacteraceae, Alteromonadaceae and Marinobacteraceae in **Chapter 1**, and to Flavobacteriaceae and Pseudomonadaceae in **Chapter 3**. Aerobic chemoheterotrophy is the function comprising the highest diversity of taxa in the oceans (Louca *et al.*, 2016). Both incorporate activities involved in the degradation of various organic compounds and for this reason they are spread in most of bacterial taxa (Louca *et al.*, 2016).

In addition, we identified interesting patterns regarding more specific functions. Regarding the bacterial diversity, our results evidenced a dominance of *Marinobacter* and *Alteromonas*, well known hydrocarbon degraders, in the **Chapter 1** one while in **Chapter 3** they were absent. Functional assignment demonstrated that in the absence of *Marinobacter* and *Halomonas*, another hydrocarbon degrader, *Alcanivorax* (100% similar to *Alcanivorax*

*venustensis*) succeeded in one of the replicates in **Chapter 3** (see **Chapter 3** - Figure 3C). This calls attention to the important role of hydrocarbon-degrading bacteria in *E. huxleyi* microbiomes and shows that the function can be filled by other taxa in the absence of *Marinobacter*. Recent studies pointed out the phycosphere as a niche for hydrocarbon-degrading bacteria (Chernikova *et al.*, 2020; Thompson *et al.*, 2020; Kearney *et al.*, 2021). The main compounds hypothesized to be degraded by these bacteria in phytoplankton cultures are polycyclic aromatic hydrocarbons (PAHs) and long-chain hydrocarbon-like compounds (Mishamandani *et al.*, 2016). Genomic evidence highlights the potential of *E. huxleyi* to produce lipidic compounds, however metabolic pathways involved in the production of PAHs are yet not established (Read *et al.*, 2013). Moreover, bacteria have been shown to modulate *E. huxleyi* production of lipidic compounds, which might be a mechanism involved in their interactions (Segev, Castañeda, *et al.*, 2016). *Alcanivorax* is considered as the most cosmopolite obligate hydrocarbon-degrading genus (Yakimov *et al.*, 2007). However, members of this genus are much less dominant in phytoplankton cultures than *Marinobacter* (Lupette *et al.*, 2016; Kearney *et al.*, 2021). For example, in the **Chapter 1** *Alcanivorax* accounted to 0.42% of the reads, while *Marinobacter* to 61%. This might be attributed to the versatility of *Marinobacter*, which can explore diverse types of substrates while most *Alcanivorax* members specifically degrade hydrocarbons (Yakimov *et al.*, 2007; Handley and Lloyd, 2013).

A similar pattern was observed for methylotrophs, such as OM43 clade and *Methylophaga*. In coccolithophore-associated microbiomes (**Chapter 1**), methylotrophs mainly represented by *Methylophaga* were present in low abundance. In **Chapter 3**, OM43 clade dominated the community composition of the four treatments at days 32 and 46 (**Chapter 3** - Figure 3C). Methylotrophic bacteria metabolize and assimilate one-carbon (C1) compounds and have been identified in *E. huxleyi* blooms (Neufeld *et al.*, 2008). *Methylophaga* is also considered as putative hydrocarbon-degrading bacteria although the database that we used did not classify them as such (Mishamandani *et al.*, 2016). In phytoplankton blooms, methylotrophic bacteria seem to rely on phytoplankton for carbon and energy sources in addition to compete for cobalamin (Bertrand *et al.*, 2015). However, their ecological role and interactions with phytoplankton are not well investigated. Genomic analysis of an OM43 isolate evidenced a narrow substrate range and a streamlined genome (Giovannoni *et al.*, 2008). Their presence and overdominance under certain conditions indicate that *E. huxleyi* can produce a specific suite of compounds which stimulate their growth.

Finally, metabolism of sulfur compounds was consistently represented by *Sulfitobacter* in both studies. *Sulfitobacter* members are important actors in the phycosphere, displaying interactions that range from mutualism to parasitism (Amin *et al.*, 2015; Barak-Gavish *et al.*, 2018). Draft genomes of *Sulfitobacter* isolates from naked and coccolith-bearing *E. huxleyi* cultures showed that they encode genes involved in symbiotic relationships (type IV secretion system) besides degradation of lignin and DMSP (Orata *et al.*, 2016; Rosana *et al.*, 2016). However, symbiotic interactions of *E. huxleyi* and *Sulfitobacter* have not been described up to now. On the other hand, parasitic interactions are known and hypothesized to contribute to *E. huxleyi* bloom demise (Barak-Gavish *et al.*, 2018).

Although preliminary, this functional screening allowed to identify interesting patterns in *E. huxleyi* microbiomes. Further investigations focusing on interactions between *E. huxleyi* and isolates of different bacterial groups supposedly displaying the same functions will help to understand how functional redundancy is important in phytoplankton microbiomes. Moreover, a functional approach will help to disentangle the influence of dominant taxa and of the rare biosphere on the host. Fundamental opened questions are: Do dominant taxa contribute more to the host because of their high abundance? Are interactions between host and dominant groups stronger because their metabolic exchanges are more pronounced? What is the role of the rare biosphere in phytoplankton microbiomes? How rare taxa display important roles for the host when they are constantly in low abundance? Which conditions can promote the increase of their relative abundance? Do they wait for the hosts' weakness for blooming and killing it?

### **Exploring *Emiliania huxleyi* aggregates**

From my experience with axenic *E. huxleyi* cultures I could observe that, contrary to other microalgae, *E. huxleyi* is able to grow steadily in axenic conditions (Bolch *et al.*, 2011) (see Annex 3 for the methods used). However, growth rates of the axenic cultures are significantly lower than when compared to the xenic ones (host with its associated microbiome) (Figure 2A).

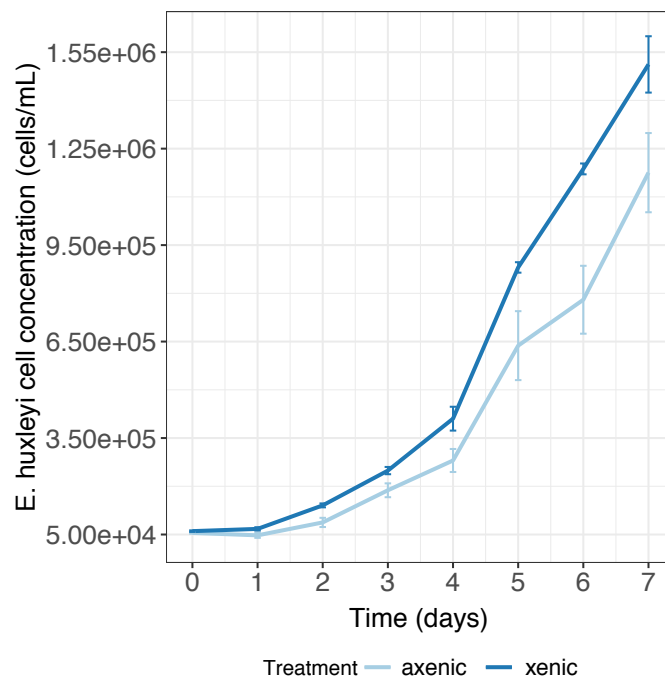


**Figure 2.** Growth curves comparing axenic (antibiotic-treated culture) and xenic (culture with its associated microbiome) *Emiliana huxleyi* cultures.

Furthermore, I observed the formation of cell clumps difficult to dissolve in the axenic cultures when they reached higher concentrations that were not visible in xenic cultures in the same phase of growth. These clumps are suggestive of a high production of polysaccharides which accumulate and catalyze the formation of transparent exopolymer particles (TEP) resulting in the formation of large aggregates (Passow, 2002). I hypothesize two reasons for this formation of aggregates. One could be a response of *E. huxleyi* to the stress in the absence of its microbiome. This phenomena has been observed when *E. huxleyi* is submitted to different stressors (Engel *et al.*, 2004; Vardi *et al.*, 2012). The TEP production dramatically increased during viral infection and it has been hypothesized as a defense strategy (Vardi *et al.*, 2012; Nissimov *et al.*, 2018). Moreover, higher CO<sub>2</sub> concentrations induce the TEP production by *E. huxleyi* as a response when nutrients are exhausted (Engel *et al.*, 2004). Considering that bacteria in cultures can provide better conditions to the microalgal growth, such as the release of vitamins and growth promoters, their absence can represent a stressor (Amin *et al.*, 2012). A second hypothesis is that bacteria consumes the TEP produced by *E. huxleyi*, which accumulates in their absence. Bacteria have been shown to affect the aggregation of different microalgae (Grossart, Czub, *et al.*, 2006; Gärdes *et al.*, 2011; Cruz and Neuer, 2019). For some (*e.g. Thalassiosira rotula* and *Synechococcus* sp.), bacteria stimulate the aggregation (Grossart, Czub, *et al.*, 2006; Gärdes *et al.*, 2011; Cruz and Neuer, 2019), but for others (*Skeletonema*

*costatum*), they prevent microalgal aggregation by consuming the TEP and protein-containing particles (Grossart *et al.*, 2006).

During my PhD, I co-cultured several bacterial isolates from *E. huxleyi* cultures with an axenic *E. huxleyi* culture (Figure 3). The bacterial candidates were shown to enhance *E. huxleyi* growth and decrease cell aggregation. These isolates belong to *Marinobacter*, *Nioella*, *Halomonas* and *Sulfitobacter* (Figure 3) (see Annex 3 for the methods used).

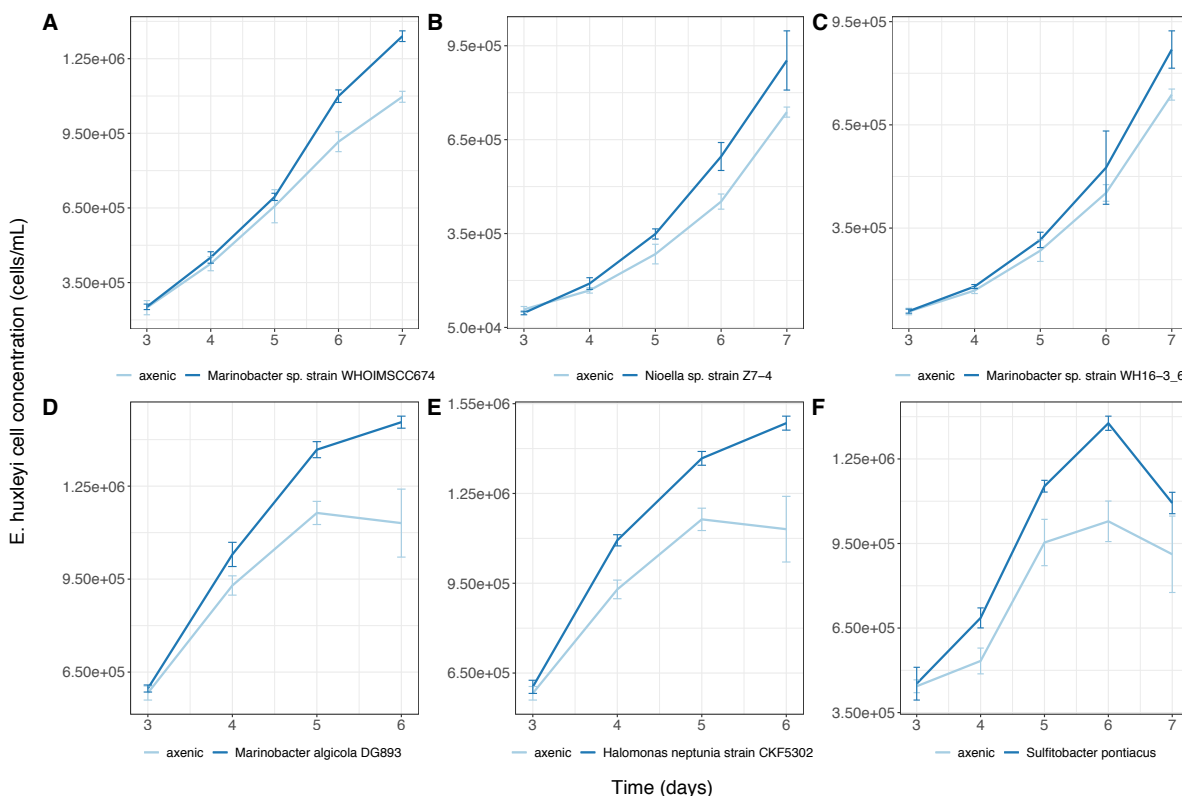


**Figure 3.** Growth curves of co-culture experiments comparing the axenic *E. huxleyi* culture alone (control) and with a bacterial isolate. The curves shown start at the beginning of exponential phase (day 3) and stop at the end of exponential growth (days 6/7).

Investigation using transcriptomics in co-cultures and individual partners associated with quantification of exopolysaccharides under manipulated conditions will help to understand the involvement of these bacteria in TEP degradation. Differentially expressed genes can be explored in data available from global surveys (such as the ‘Ocean gene atlas’) in order to understand the distribution of these genes in the global oceans and their potential large-scale impacts in global processes (Villar *et al.*, 2018). Furthermore, such hypotheses can be explored at larger scales, in *E. huxleyi* blooms surveys, by the quantification and characterization of the

bacterial community associated with sinking particles. Association of satellite images, lipidomic- and gene-based molecular approaches, in situ optical sensors and sediment traps has been used to investigate the influence of viral infection on carbon export during an *E. huxleyi* bloom (Laber *et al.*, 2018). Similar approach applied to the investigation of bacterial communities will bring valuable information on the role of phycosphere-associated bacteria on aggregate formation in a large-scale perspective.

## **Concluding remarks**

Using molecular approaches, this thesis shed light on fundamental questions regarding the diversity and assembly processes in the phycosphere. Still, 49 years after the publication of the pioneer work of Bell and Mitchell (1972) on the phycosphere, we are far from understanding all the processes underlying the complex interactions in this microscale environment. Multiscale studies involving multiple hosts, culture-based experiments, meta- and single cell ‘omics’ techniques, field observations and systems biology modelling, will provide the knowledge necessary to decipher the complexity and dynamics of these interactions and their impact on major ecological processes in the oceans.



## References

### A

- Abby, S., Touchon, M., de Jode, A., Grimsley, N., and Piganeau, G. (2014) Bacteria in *Ostreococcus tauri* cultures - friends, foes or hitchhikers? *Front Microbiol* 5:.
- Ajani, P.A., Kahlke, T., Siboni, N., Carney, R., Murray, S.A., and Seymour, J.R. (2018) The microbiome of the cosmopolitan diatom *Leptocylindrus* reveals significant spatial and temporal variability. *Front Microbiol* 9: 2758.
- Alberdi, A., Aizpurua, O., Gilbert, M.T.P., and Bohmann, K. (2018) Scrutinizing key steps for reliable metabarcoding of environmental samples. *Methods Ecol Evol* 9: 134–147.
- Alberdi, A. and Gilbert, M.T.P. (2019) A guide to the application of Hill numbers to DNA-based diversity analyses. *Mol Ecol Resour* 19: 804–817.
- Alcolombri, U., Ben-Dor, S., Feldmesser, E., Levin, Y., Tawfik, D.S., and Vardi, A. (2015) Identification of the algal dimethyl sulfide-releasing enzyme: A missing link in the marine sulfur cycle. *Science* (80-) 348: 1466–1469.
- Alonso-Sáez, L., Díaz-Pérez, L., and Morán, X.A.G. (2015) The hidden seasonality of the rare biosphere in coastal marine bacterioplankton. *Environ Microbiol* 17: 3766–3780.
- Alonso-Sáez, L., Zeder, M., Harding, T., Pernthaler, J., Lovejoy, C., Bertilsson, S., and Pedrós-Alió, C. (2014) Winter bloom of a rare betaproteobacterium in the Arctic Ocean. *Front Microbiol* 5: 1–9.
- Amin, S.A., Green, D.H., Hart, M.C., Kupper, F.C., Sunda, W.G., and Carrano, C.J. (2009) Photolysis of iron-siderophore chelates promotes bacterial-algal mutualism. *Proc Natl Acad Sci* 106: 17071–17076.
- Amin, S.A., Parker, M.S., and Armbrust, E. V. (2012) Interactions between Diatoms and Bacteria. *Microbiol Mol Biol Rev* 76: 667–684.
- Armbrust, E.V. (2009) The life of diatoms in the world's oceans. *Nature* 459: 185–192.
- Assmy, P. and Smetacek, V. (2009) Algal Blooms. *Encycl Microbiol* 3: 27–41.
- Azam, F., Fenchel, T., Field, J.G., Gray, J.S., Meyer-Reil, L.A., and Thingstad, F. (1983) The ecological role of water-column microbes in the sea. *Mar Ecol Prog Ser* 257–263.

**B**

- Baker, D.M., Freeman, C.J., Wong, J.C.Y., Fogel, M.L., and Knowlton, N. (2018) Climate change promotes parasitism in a coral symbiosis. *ISME J* 12: 921–930.
- Baquero, F. and Nombela, C. (2012) The microbiome as a human organ.
- Barak-Gavish, N., Frada, M.J., Ku, C., Lee, P.A., DiTullio, G.R., Malitsky, S., *et al.* (2018) Bacterial virulence against an oceanic bloom-forming phytoplankton is mediated by algal DMSP. *Sci Adv* 4: eaau5716.
- Bates, S.S., Douglas, D.J., Doucette, G.J., and Léger, C. (1995) Effects of reintroducing bacteria on domoic acid production by axenic cultures of the diatom *Pseudonitzschia pungens* f. *multiseries*. *Nat Toxins* 3: 428–435.
- Beaufort, L., Probert, I., De Garidel-Thoron, T., Bendif, E.M., Ruiz-Pino, D., Metzl, N., *et al.* (2011) Sensitivity of coccolithophores to carbonate chemistry and ocean acidification. *Nature* 476: 80–83.
- Behringer, G., Ochsenkühn, M.A., Fei, C., Fanning, J., Koester, J.A., and Amin, S.A. (2018) Bacterial communities of diatoms display strong conservation across strains and time. *Front Microbiol* 9:.
- Bekker, A., Holland, H.D., Wang, P.L., Rumble, D., Stein, H.J., Hannah, J.L., *et al.* (2004) Dating the rise of atmospheric oxygen. *Nature* 427: 117–120.
- Bell, W. and Mitchell, R. (1972) Chemotactic and growth responses of marine bacteria to algal extracellular products. *Biol Bull* 143: 265–277.
- Bendif, E.M., Nevado, B., Wong, E.L.Y., Hagino, K., Probert, I., Young, J.R., *et al.* (2019) Repeated species radiations in the recent evolution of the key marine phytoplankton lineage *Gephyrocapsa*. *Nat Commun* 10: 4234.
- Bendif, E.M., Probert, I., Carmichael, M., Romac, S., Hagino, K., and de Vargas, C. (2014) Genetic delineation between and within the widespread coccolithophore morpho-species *Emiliana huxleyi* and *Gephyrocapsa oceanica* (Haptophyta). *J Phycol* 50: 140–148.
- Bendif, E.M., Probert, I., Díaz-Rosas, F., Thomas, D., van den Engh, G., Young, J.R., and von Dassow, P. (2016) Recent reticulate evolution in the ecologically dominant lineage of coccolithophores. *Front Microbiol* 7:.
- Bendif, E.M., Probert, I., Young, J.R., and von Dassow, P. (2015) Morphological and Phylogenetic Characterization of New *Gephyrocapsa* Isolates Suggests Introgressive Hybridization in the *Emiliana/Gephyrocapsa* Complex

- (Haptophyta). *Protist* 166: 323–336.
- Berg, G., Rybakova, D., Fischer, D., Cernava, T., Vergès, M.C.C., Charles, T., *et al.* (2020) Microbiome definition re-visited: old concepts and new challenges. *Microbiome* 8: 1–22.
- Bertrand, E.M., McCrow, J.P., Moustafa, A., Zheng, H., McQuaid, J.B., Delmont, T.O., *et al.* (2015) Phytoplankton-bacterial interactions mediate micronutrient colimitation at the coastal Antarctic sea ice edge. *Proc Natl Acad Sci USA* 112: 9938–9943.
- Bigalke, A. and Pohnert, G. (2019) Algicidal bacteria trigger contrasting responses in model diatom communities of different composition. *Microbiologyopen* 8: 1–14.
- Billard, C. and Inouye, I. (2004) What is new in coccolithophore biology? In *Coccolithophores*. Springer, pp. 1–29.
- Bird, D.F. and Kalff, J. (1984) Empirical Relationships between Bacterial Abundance and Chlorophyll Concentration in Fresh and Marine Waters. *Can J Fish Aquat Sci* 41: 1015–1023.
- Blackburn, S.I. and Cresswell, G. (1993) A coccolithophorid bloom in Jervis Bay, Australia. *Mar Freshw Res* 44: 253–260.
- Bokulich, N.A., Subramanian, S., Faith, J.J., Gevers, D., Gordon, J.I., Knight, R., *et al.* (2013) Quality-filtering vastly improves diversity estimates from Illumina amplicon sequencing. *Nat Methods* 10: 57–59.
- Bokulich, N.A., Ziemski, M., Robeson, M.S., and Kaehler, B.D. (2020) Measuring the microbiome: Best practices for developing and benchmarking microbiomics methods. *Comput Struct Biotechnol J* 18: 4048–4062.
- Bolch, C.J.S., Bejoy, T.A., and Green, D.H. (2017) Bacterial associates modify growth dynamics of the dinoflagellate *Gymnodinium catenatum*. *Front Microbiol* 8:.
- Bolch, C.J.S., Subramanian, T.A., and Green, D.H. (2011) The toxic dinoflagellate *Gymnodinium catenatum* (Dinophyceae) requires marine bacteria for growth. *J Phycol* 47: 1009–1022.
- Bollmann, J. (1997) Morphology and biogeography of *Gephyrocapsa* coccoliths in Holocene sediments. *Mar Micropaleontol* 29: 319–350.
- Bolyen, E., Rideout, J.R., Dillon, M.R., Bokulich, N.A., Abnet, C.C., Al-Ghalith, G.A., *et al.* (2019) Reproducible, interactive, scalable and extensible microbiome data science using QIIME 2. *Nat Biotechnol* 37: 852–857.
- Bramucci, A.R., Labeeuw, L., Orata, F.D., and Ryan, E.M. (2018) The Bacterial

- Symbiont *Phaeobacter inhibens* Shapes the Life History of Its Algal Host *Emiliania huxleyi*. *5*: 1–12.
- Brown, E.R., Cepeda, M.R., Mascuch, S.J., Poulson-Ellestad, K.L., and Kubanek, J. (2019) Chemical ecology of the marine plankton. *Nat Prod Rep* 36: 1093–1116.
- Brownlee, C. and Taylor, A. (2004) Calcification in coccolithophores: a cellular perspective. In *Coccolithophores*. Springer, pp. 31–49.
- Buchan, A., LeClerc, G.R., Gulvik, C.A., and González, J.M. (2014) Master recyclers: features and functions of bacteria associated with phytoplankton blooms. *Nat Rev Microbiol* 12: 686–698.
- Burke, C., Steinberg, P., Rusch, D., Kjelleberg, S., and Thomas, T. (2011) Bacterial community assembly based on functional genes rather than species. *Proc Natl Acad Sci USA* 108: 14288–14293.
- Burke, C., Thomas, T., Lewis, M., Steinberg, P., and Kjelleberg, S. (2011) Composition, uniqueness and variability of the epiphytic bacterial community of the green alga *Ulva australis*. *ISME J* 5: 590–600.
- M.J., Han, A.W., Johnson, A.J.A., and Holmes, S.P. (2016) DADA2: High-resolution sample inference from Illumina amplicon data. *Nat Methods* 13: 581.
- Cavicchioli, R., Ostrowski, M., Fegatella, F., Goodchild, A., and Guixa-Boixereu, N. (2003) Life under nutrient limitation in oligotrophic marine environments: An eco/physiological perspective of *Sphingopyxis alaskensis* (formerly *Sphingomonas alaskensis*). *Microb Ecol* 45: 203–217.
- Chernikova, T.N., Bargiela, R., Toshchakov, S. V., Shivaraman, V., Lunev, E.A., Yakimov, M.M., *et al.* (2020) Hydrocarbon-degrading bacteria *Alcanivorax* and *Marinobacter* associated with microalgae *Pavlova lutheri* and *Nannochloropsis oculata*. *Front Microbiol* 11:.
- Cook, S.S., Whittock, L., Wright, S.W., and Hallegraeff, G.M. (2011) Photosynthetic pigment and genetic differences between two southern ocean morphotypes of *Emiliania huxleyi* (Haptophyta). *J Phycol* 47: 615–626.
- Cottrell, M.T. and Kirchman, D.L. (2016) Transcriptional control in marine copiotrophic and oligotrophic bacteria with streamlined genomes. *Appl*

## C

Callahan, B.J., McMurdie, P.J., Rosen,

- Environ Microbiol* 82: 6010–6018.
- Crenn, K., Duffieux, D., and Jeanthon, C. (2018) Bacterial epibiotic communities of ubiquitous and abundant marine diatoms are distinct in short- and long-term associations. *Front Microbiol* 9: 1–12.
- Crenn, K., Serpin, D., Lepleux, C., Overmann, J., and Jeanthon, C. (2016) *Silicimonas algicola* gen. nov., sp. nov., a novel member of the Roseobacter clade isolated from the cell surface of the marine diatom *Thalassiosira delicatula*. *Int J Syst Evol Microbiol* in press:
- Croft, M.T., Lawrence, A.D., Raux-Deery, E., Warren, M.J., and Smith, A.G. (2005) Algae acquire vitamin B12 through a symbiotic relationship with bacteria. *Nature* 438: 90–93.
- Cruz, B.N. and Neuer, S. (2019) Heterotrophic bacteria enhance the aggregation of the marine picocyanobacteria *Prochlorococcus* and *Synechococcus*. *Front Microbiol* 10: 1–11.
- D**
- Von Dassow, P., Ogata, H., Probert, I., Wincker, P., Da Silva, C., Audic, S., *et al.* (2009) Transcriptome analysis of functional differentiation between haploid and diploid cells of *Emiliana huxleyi*, a globally significant photosynthetic calcifying cell. *Genome Biol* 10:.
- Ducklow, H.W., Steinberg, D.K., and Buesseler, K.O. (2001) Upper ocean carbon export and the biological pump. *Oceanogr DC-OCEANOGRAPHY Soc* 14: 50–58.
- Durham, B.P., Dearth, S.P., Sharma, S., Amin, S.A., Smith, C.B., Campagna, S.R., *et al.* (2017) Recognition cascade and metabolite transfer in a marine bacteria-phytoplankton model system. *Environ Microbiol* 19: 3500–3513.
- Durham, B.P., Sharma, S., Luo, H., Smith, C.B., Amin, S.A., Bender, S.J., *et al.* (2015) Cryptic carbon and sulfur cycling between surface ocean plankton. *Proc Natl Acad Sci U S A* 112: 453–457.
- Dziallas, C. and Grossart, H.P. (2011) Temperature and biotic factors influence bacterial communities associated with the cyanobacterium *Microcystis* sp. *Environ Microbiol* 13: 1632–1641.
- E**
- Engel, A., Delille, B., Jacquet, S., Riebesell, U., Rochelle-Newall, E., Terbrüggen, A., and Zondervan, I. (2004) Transparent exopolymer particles and dissolved organic carbon production by *Emiliana huxleyi* exposed to different CO<sub>2</sub> concentrations: A

- mesocosm experiment. *Aquat Microb Ecol* 34: 93–104.
- Engelen, S., Hingamp, P., Sieracki, M., Vargas, C., Audic, S., Henry, N., *et al.* (2015) Eukaryotic plankton diversity in the sunlit ocean. *Science (80- )* 348: 1261605–1/11.
- Escudié, F., Auer, L., Bernard, M., Mariadassou, M., Cauquil, L., Vidal, K., *et al.* (2018) FROGS: find, rapidly, OTUs with galaxy solution. *Bioinformatics* 34: 1287–1294.
- F**
- Falkowski, P.G., Fenchel, T., and Delong, E.F. (2008) The microbial engines that drive earth’s biogeochemical cycles. *Science (80- )* 320: 1034–1039.
- Falkowski, P.G., Katz, M.E., Knoll, A.H., Quigg, A., Raven, J.A., Schofield, O., and Taylor, F.J.R. (2004) The evolution of modern eukaryotic phytoplankton. *Science (80- )* 305: 354–360.
- Falkowski, P.G. and Raven, J.A. (1997) Aquatic Photosynthesis. *Blackwell Sci Oxford* 375.
- Fan, L., Reynolds, D., Liu, M., Stark, M., Kjelleberg, S., Webster, N.S., and Thomas, T. (2012) Functional equivalence and evolutionary convergence in complex communities of microbial sponge symbionts. *Proc Natl Acad Sci U S A* 109:.
- Faust, K. and Raes, J. (2012) Microbial interactions: From networks to models. *Nat Rev Microbiol* 10: 538–550.
- Fei, C., Ochsenkühn, M.A., Shibl, A.A., Isaac, A., Wang, C., and Amin, S.A. (2020) Quorum sensing regulates ‘swim-or-stick’ lifestyle in the phycosphere. *Environ Microbiol* 22: 4761–4778.
- Field, C.B., Behrenfeld, M.J., Randerson, J.T., and Falkowski, P. (1998) Primary Production of the Biosphere: Integrating Terrestrial and Oceanic Components. *Science (80- )* 281: 237 LP – 240.
- Foster, R.A., Kuypers, M.M.M., Vagner, T., Paerl, R.W., Musat, N., and Zehr, J.P. (2011) Nitrogen fixation and transfer in open ocean diatom-cyanobacterial symbioses. *ISME J* 5: 1484–1493.
- Frada, M., Probert, I., Allen, M.J., Wilson, W.H., and de Vargas, C. (2008) The “Cheshire Cat” escape strategy of the coccolithophore *Emiliana huxleyi* in response to viral infection. *Proc Natl Acad Sci U S A* 105: 15944–15949.
- Frada, M.J., Bidle, K.D., Probert, I., and de Vargas, C. (2012) In situ survey of life cycle phases of the coccolithophore *Emiliana huxleyi* (Haptophyta). *Environ Microbiol* 14: 1558–1569.
- Frada, M.J., Rosenwasser, S., Ben-Dor, S.,

- Shemi, A., Sabanay, H., and Vardi, A. (2017) Morphological switch to a resistant subpopulation in response to viral infection in the bloom-forming coccolithophore *Emiliana huxleyi*. *PLoS Pathog* 13: 1–17.
- Fu, H., Uchimiya, M., Gore, J., and Moran, M.A. (2020) Ecological drivers of bacterial community assembly in synthetic phycospheres. *Proc Natl Acad Sci U S A* 117: 3656–3662.
- Fuqua, W.C., Winans, S.C., and Greenberg, E.P. (1994) Quorum sensing in bacteria: The LuxR-LuxI family of cell density- responsive transcriptional regulators. *J Bacteriol* 176: 269–275.
- ## G
- Garcia-Pichel, F., Belnap, J., Neuer, S., and Schanz, F. (2009) Estimates of global cyanobacterial biomass and its distribution. *Arch Hydrobiol Suppl Algal Stud* 109: 213–227.
- Garcia-Pichel, F., Zehr, J.P., Bhattacharya, D., and Pakrasi, H.B. (2020) What's in a name? The case of cyanobacteria. *J Phycol* 56: 1–5.
- Gärdes, A., Iversen, M.H., Grossart, H.P., Passow, U., and Ullrich, M.S. (2011) Diatom-associated bacteria are required for aggregation of *Thalassiosira weissflogii*. *ISME J* 5: 436–445.
- Gärdes, A., Ramaye, Y., Grossart, H.-P., Passow, U., and Ullrich, M.S. (2012) Effects of *Marinobacter adhaerens* HP15 on polymer exudation by *Thalassiosira weissflogii* at different N: P ratios. *Mar Ecol Prog Ser* 461: 1–14.
- Geng, H., Sale, K.L., Tran-Gyamfi, M.B., Lane, T.W., and Yu, E.T. (2016) Longitudinal Analysis of Microbiota in Microalga *Nannochloropsis salina* Cultures. *Microb Ecol* 72: 14–24.
- Giovannoni, S.J. (2017) SAR11 bacteria: the most abundant plankton in the oceans. *Ann Rev Mar Sci* 9: 231–255.
- Giovannoni, S.J., Cameron Thrash, J., and Temperton, B. (2014) Implications of streamlining theory for microbial ecology. *ISME J* 8: 1553–1565.
- Giovannoni, S.J., Hayakawa, D.H., Tripp, H.J., Stingl, U., Givan, S.A., Cho, J.C., et al. (2008) The small genome of an abundant coastal ocean methylotroph. *Environ Microbiol* 10: 1771–1782.
- Giovannoni, S J, Tripp, H James, Givan, S., Podar, M., Kevin, L., Baptista, D., et al. (2005) Genome Streamlining in a Cosmopolitan Oceanic Bacterium. *Science (80- )* 309: 1242–1245.
- Giovannoni, S.J., Tripp, H J, Givan, S., Podar, M., Vergin, K.L., Baptista, D., et al. (2005) Cultivation and Growth Characteristics of a Diverse Group of Oligotrophic Marine Gammaproteobacteria. *Science (80- )*

- 309:.
- Giovannoni, Stephen J, Tripp, H James, Givan, S., Podar, M., Vergin, K.L., Baptista, D., *et al.* (2005) Genome streamlining in a cosmopolitan oceanic bacterium. *Science* (80- ) 309: 1242–1245.
- Gomez, F. (2012) A quantitative review of the lifestyle, habitat and trophic diversity of dinoflagellates (Dinoflagellata, Alveolata). *Syst Biodivers* 10: 267–275.
- Gonzalez, J.M., Simó, R., Massana, R., Covert, J.S., Casamayor, E.O., Pedrós-Alió, C., and Moran, M.A. (2000) Bacterial community structure associated with a dimethylsulfoniopropionate-producing North Atlantic algal bloom. *Appl Environ Microbiol* 66: 4237–4246.
- Green, D.H., Echavarri-Bravo, V., Brennan, D., and Hart, M.C. (2015) Bacterial diversity associated with the coccolithophorid algae *Emiliana huxleyi* and *Coccolithus pelagicus* f. *braarudii*. *Biomed Res Int* 2015:.
- Green, J.C., Course, P.A., and Tarran, G.A. (1996) The life-cycle of *Emiliana huxleyi*: A brief review and a study of relative ploidy levels analysed by flow cytometry. *J Mar Syst* 9: 33–44.
- Grossart, H.P., Czub, G., and Simon, M. (2006) Algae-bacteria interactions and their effects on aggregation and organic matter flux in the sea. *Environ Microbiol* 8: 1074–1084.
- Grossart, H.P., Kiørboe, T., Tang, K.W., Allgaier, M., Yam, E.M., and Ploug, H. (2006) Interactions between marine snow and heterotrophic bacteria: Aggregate formation and microbial dynamics. *Aquat Microb Ecol* 42: 19–26.
- Grossart, H.P., Riemann, L., and Azam, F. (2001) Bacterial motility in the sea and its ecological implications. *Aquat Microb Ecol* 25: 247–258.
- ## H
- Haberkorn, I., Walser, J.C., Helisch, H., Böcker, L., Belz, S., Schuppler, M., *et al.* (2020) Characterization of *Chlorella vulgaris* (Trebouxiophyceae) associated microbial communities1. *J Phycol* 56: 1308–1322.
- Hackett, J.D., Su Yoon, H., Butterfield, N.J., Sanderson, M.J., and Bhattacharya, D. (2007) Plastid Endosymbiosis. Sources and Timing of the Major Events., Elsevier Inc.
- Hagino, K., Bendif, E.M., Young, J.R., Kogame, K., Probert, I., Takano, Y., *et al.* (2011) New evidence for morphological and genetic variation in the cosmopolitan coccolithophore *Emiliana huxleyi* (prymnesiophyceae)

- from the *cox1b-atp4* genes. *J Phycol* 47: 1164–1176.
- Handley, K.M. and Lloyd, J.R. (2013) Biogeochemical implications of the ubiquitous colonization of marine habitats and redox gradients by *Marinobacter* species. *Front Microbiol* 4: 1–10.
- Harvey, E.L., Deering, R.W., Rowley, D.C., Gamal, A. El, Schorn, M., Moore, B.S., *et al.* (2016) A bacterial quorum-sensing precursor induces mortality in the marine coccolithophore, *Emiliana huxleyi*. *Front Microbiol* 7:.
- Hattenrath-Lehmann, T.K. and Gobler, C.J. (2017) Identification of unique microbiomes associated with harmful algal blooms caused by *Alexandrium fundyense* and *Dinophysis acuminata*. *Harmful Algae* 68: 17–30.
- Hay, W.W., Mohler, H.P., Roth, P.H., Schmidt, R.R., and Boudreaux, J.E. (1967) Calcareous Nannoplankton Zonation of the Cenozoic of the Gulf Coast and Caribbean-Antillean Area, and Transoceanic Correlation (1).
- Hubbell, S.P. (2001) The unified neutral theory of biodiversity and biogeography (MPB-32), Princeton University Press.
- Hutchinson, G.E. (1957) Concluding remarks. *Cold Spring Harb Symp Quant Biol* 224: 415–427.
- ## J
- Jackrel, Sara L., Schmidt, K.C., Cardinale, B.J., and Denef, V.J. (2020) Microbiomes reduce their host's sensitivity to interspecific interactions. *MBio* 11: 1–11.
- Jackrel, S.L., White, J.D., Evans, J.T., Buffin, K., Hayden, K., Sarnelle, O., and Denef, V.J. (2019) Genome evolution and host-microbiome shifts correspond with intraspecific niche divergence within harmful algal bloom-forming *Microcystis aeruginosa*. *Mol Ecol* 28: 3994–4011.
- Jackrel, Sara L, Yang, J.W., Schmidt, K.C., and Denef, V.J. (2020) Host specificity of microbiome assembly and its fitness effects in phytoplankton. *ISME J*.
- Janouskovec, J., Gavelis, G.S., Burki, F., Dinh, D., Bachvaroff, T.R., Gornik, S.G., *et al.* (2017) Major transitions in dinoflagellate evolution unveiled by phylotranscriptomics. *Proc Natl Acad Sci U S A* 114: E171–E180.
- Jiao, N., Herndl, G.J., Hansell, D.A., Benner, R., Kattner, G., Wilhelm, S.W., *et al.* (2010) Microbial production of recalcitrant dissolved organic matter: Long-term carbon storage in the global ocean. *Nat Rev Microbiol* 8: 593–599.
- Johansen, J.E., Pinhassi, J., Blackburn, N., Zweifel, U.L., and Hagström, Å.

- (2002) Variability in motility characteristics among marine bacteria. *Aquat Microb Ecol* 28: 229–237.
- Johnson, W.M., Kido Soule, M.C., and Kujawinski, E.B. (2016) Evidence for quorum sensing and differential metabolite production by a marine bacterium in response to DMSP. *ISME J* 10: 2304–2316.
- Jordan, R.W. and Chamberlain, A.H.L. (1997) Biodiversity among haptophyte algae. *Biodivers Conserv* 6: 131–152.
- ### K
- Kahlke, T. (2018) Ampli-Tools (Version 1.0). *Geneva Zenodo doi* 10:.
- Kai, M., Hara, T., Aoyama, H., and Kuroda, N. (1999) A Massive Coccolithophorid Bloom Observed in Mikawa Bay, Japan. *J Oceanogr* 55: 395–406.
- Kamptner, E. (1943) Zur Revision der Coccolithineen-Spezies *Pontosphaera huxleyi* Lohm. *Anzeiger der Akad der Wissenschaften, Wien* 80: 43–49.
- Karlusich, J.J.P., Ibarbalz, F.M., and Bowler, C. (2020) Exploration of marine phytoplankton: from their historical appreciation to the omics era. *J Plankton Res* 1–18.
- Kearney, S.M., Thomas, E., Coe, A., and Chisholm, S.W. (2021) Microbial diversity of co-occurring heterotrophs in cultures of marine picocyanobacteria. *Environ Microbiomes* 16: 1–15.
- Kimbrel, J.A., Samo, T.J., Ward, C., Nilson, D., Thelen, M.P., Siccardi, A., *et al.* (2019) Host selection and stochastic effects influence bacterial community assembly on the microalgal phycosphere. *Algal Res* 40: 101489.
- Krohn-Molt, I., Alawi, M., Förstner, K.U., Wiegandt, A., Burkhardt, L., Indenbirken, D., *et al.* (2017) Insights into Microalga and bacteria interactions of selected phycosphere biofilms using metagenomic, transcriptomic, and proteomic approaches. *Front Microbiol* 8: 1–14.
- ### L
- Labeeuw, L., Khey, J., Bramucci, A.R., Atwal, H., De La Mata, A.P., Harynyuk, J., and Case, R.J. (2016) Indole-3-acetic acid is produced by *Emiliania huxleyi* coccolith-bearing cells and triggers a physiological response in bald cells. *Front Microbiol* 7:.
- Laber, C.P., Hunter, J.E., Carvalho, F., Collins, J.R., Hunter, E.J., Schieler, B.M., *et al.* (2018) Coccolithovirus facilitation of carbon export in the North Atlantic. *Nat Microbiol* 1–11.
- Landa, M., Blain, S., Christaki, U., Monchy, S., and Obernosterer, I. (2016) Shifts in bacterial community composition associated with increased

- carbon cycling in a mosaic of phytoplankton blooms. *ISME J* 10: 39–50.
- Landa, M., Burns, A.S., Roth, S.J., and Moran, M.A. (2017) Bacterial transcriptome remodeling during sequential co-culture with a marine dinoflagellate and diatom. *ISME J* 11: 2677–2690.
- Lauro, F.M., McDougald, D., Thomas, T., Williams, T.J., Egan, S., Rice, S., *et al.* (2009) The genomic basis of trophic strategy in marine bacteria. *Proc Natl Acad Sci* 106: 15527–15533.
- Lawson, C.A., Raina, J.B., Kahlke, T., Seymour, J.R., and Suggett, D.J. (2018) Defining the core microbiome of the symbiotic dinoflagellate, *Symbiodinium*. *Environ Microbiol Rep* 10: 7–11.
- Lehahn, Y., Koren, I., Schatz, D., Frada, M., Sheyn, U., Boss, E., *et al.* (2014) Decoupling physical from biological processes to assess the impact of viruses on a mesoscale algal bloom. *Curr Biol* 24: 2041–2046.
- Leliaert, F., Verbruggen, H., and Zechman, F.W. (2011) Into the deep: New discoveries at the base of the green plant phylogeny. *BioEssays* 33: 683–692.
- Li, D.X., Zhang, H., Chen, X.H., Xie, Z.X., Zhang, Y., Zhang, S.F., *et al.* (2018) Metaproteomics reveals major microbial players and their metabolic activities during the blooming period of a marine dinoflagellate *Prorocentrum donghaiense*. *Environ Microbiol* 20: 632–644.
- Litchman, E., de Tezanos Pinto, P., Edwards, K.F., Klausmeier, C.A., Kremer, C.T., and Thomas, M.K. (2015) Global biogeochemical impacts of phytoplankton: A trait-based perspective. *J Ecol* 103: 1384–1396.
- Logares, R., Deutschmann, I.M., Junger, P.C., Giner, C.R., Krabberød, A.K., Schmidt, T.S.B., *et al.* (2020) Disentangling the mechanisms shaping the surface ocean microbiota. *Microbiome* 8: 55.
- Lohmann, H. (1902) Die Coccolithophoridae: eine Monographie der Coccolithen bildenden Flagellaten, zugleich ein Beitrag zur Kenntnis des Mittelmeerauftriebs, Fischer.
- Lopes dos Santos, A., Gourvil, P., Tragin, M., Noël, M.H., Decelle, J., Romac, S., and Vaultot, D. (2017) Diversity and oceanic distribution of prasinophytes clade VII, the dominant group of green algae in oceanic waters. *ISME J* 11: 512–528.
- Lopes dos Santos, A., Pollina, T., Gourvil, P., Corre, E., Marie, D., Garrido, J.L., *et al.* (2017) Chloropicophyceae, a new class of picophytoplanktonic

- prasinophytes. *Sci Rep* 7: 1–20.
- López-Pérez, M. and Rodríguez-Valera, F. (2014) The family Alteromonadaceae. *The Prokaryotes* 69–92.
- Louca, S., Parfrey, L.W., and Doebeli, M. (2016) Decoupling function and taxonomy in the global ocean microbiome. *Science* (80-) 353: 1272–1277.
- Lovejoy, C., Bowman, J.P., and Hallegraeff, G.M. (1998) Algicidal effects of a novel marine *Pseudoalteromonas* isolate (class Proteobacteria, gamma subdivision) on harmful algal bloom species of the genera *Chattonella*, *Gymnodinium*, and *Heterosigma*. *Appl Environ Microbiol* 64: 2806–2813.
- Lupette, J., Lami, R., Krasovec, M., Grimsley, N., Moreau, H., Piganeau, G., and Sanchez-Ferandin, S. (2016) *Marinobacter* dominates the bacterial community of the *Ostreococcus tauri* phycosphere in culture. *Front Microbiol* 7:.
- M**
- Mausz, M.A. and Pohnert, G. (2015) Phenotypic diversity of diploid and haploid *Emiliania huxleyi* cells and of cells in different growth phases revealed by comparative metabolomics. *J Plant Physiol* 172: 137–148.
- Mayali, X. and Azam, F. (2004) Algicidal bacteria in the sea and their impact on algal blooms. *J Eukaryot Microbiol* 51: 139–144.
- Mayers, T.J., Bramucci, A.R., Yakimovich, K.M., and Case, R.J. (2016) A bacterial pathogen displaying temperature-enhanced virulence of the microalga *Emiliania huxleyi*. *Front Microbiol* 7:.
- Mestre, M., Ruiz-González, C., Logares, R., Duarte, C.M., Gasol, J.M., and Sala, M.M. (2018) Sinking particles promote vertical connectivity in the ocean microbiome. *Proc Natl Acad Sci U S A* 115: E6799–E6807.
- Meyer, N., Bigalke, A., Kaulfuß, A., and Pohnert, G. (2017) Strategies and ecological roles of algicidal bacteria. *FEMS Microbiol Rev* 41: 880–899.
- Mishamandani, S., Gutierrez, T., Berry, D., and Aitken, M.D. (2016) Response of the bacterial community associated with a cosmopolitan marine diatom to crude oil shows a preference for the biodegradation of aromatic hydrocarbons. *Environ Microbiol* 18: 1817–1833.
- Mönnich, J., Tebben, J., Bergemann, Case, R.J., Sylke Wohlrab, and Harder, T. (2020) Niche-based assembly of bacterial consortia on the diatom *Thalassiosira rotula* is stable and reproducible. *ISME J* 14: 1614–

1625. Van Mooy, B.A.S., Hmelo, L.R., Sofen, L.E., Campagna, S.R., May, A.L., Dyhrman, S.T., *et al.* (2012) Quorum sensing control of phosphorus acquisition in *Trichodesmium consortia*. *ISME J* 6: 422–429.
- Moran, M.A., Kujawinski, E.B., Stubbins, A., Fatland, R., Aluwihare, L.I., Buchan, A., *et al.* (2016) Deciphering ocean carbon in a changing world. *Proc Natl Acad Sci U S A* 113: 3143–3151.
- Morris, R.M., Longnecker, K., and Giovannoni, S.J. (2006) *Pirellula* and OM43 are among the dominant lineages identified in an Oregon coast diatom bloom. *Environ Microbiol* 8: 1361–1370.
- Morris, R.M., Rappé, M.S., Connon, S.A., Vergin, K.L., Siebold, W.A., Carlson, C.A., and Giovannoni, S.J. (2002) SAR11 clade dominates ocean surface bacterioplankton communities. *Nature* 420: 806–810.
- Mühlenbruch, M., Grossart, H.P., Eigemann, F., and Voss, M. (2018) Mini-review: Phytoplankton-derived polysaccharides in the marine environment and their interactions with heterotrophic bacteria. *Environ Microbiol* 20: 2671–2685.
- N**
- Nearing, J.T., Douglas, G.M., Comeau, A.M., and Langille, M.G.I. (2018) Denoising the Denoisers: an independent evaluation of microbiome sequence error-correction approaches. *PeerJ* 6: e5364.
- Nelson, D.M., Tréguer, P., Brzezinski, M.A., Leynaert, A., and Quéguiner, B. (1995) Production and dissolution of biogenic silica in the ocean: Revised global estimates, comparison with regional data and relationship to biogenic sedimentation. *Global Biogeochem Cycles* 9: 359–372.
- Neufeld, J.D., Boden, R., Moussard, H., Schäfer, H., and Murrell, J.C. (2008) Substrate-specific clades of active marine methylotrophs associated with a phytoplankton bloom in a temperate coastal environment. *Appl Environ Microbiol* 74: 7321–7328.
- Neukermans, G. and Fournier, G. (2018) Optical modeling of spectral backscattering and remote sensing reflectance from *Emiliana huxleyi* Blooms. *Front Mar Sci* 5: 1–20.
- Nissimov, J.I., Vandzura, R., Johns, C.T., Natale, F., Haramaty, L., and Bidle, K.D. (2018) Dynamics of transparent exopolymer particle production and aggregation during viral infection of the coccolithophore, *Emiliana huxleyi*. *Environ Microbiol* 20: 2880–2897.
- Not, F., Latasa, M., Marie, D., Cariou, T.,

- Vaulot, D., and Simon, N. (2004) A single species *Micromonas pusilla* (Prasinophyceae) dominates the eukaryotic picoplankton in the western English Channel. *Appl Environ Microbiol* 70: 4064–4072.
- Not, F., Siano, R., Kooistra, W.H.C.F., Simon, N., Vaulot, D., and Probert, I. (2012) Diversity and ecology of eukaryotic marine phytoplankton. In *Genomic insights gained into the Diversity, Biology and Evolution of Microbial Photosynthetic Eukaryotes*. Piganeau, G. (ed). Amsterdam: Elsevier, pp. 1–53.
- O**
- Okada, H. and McIntyre, A. (1977) Modern coccolithophores of the Pacific and North Atlantic oceans. *Micropaleontology* 1–55.
- Van Oostende, N., Moerdijk-Poortvliet, T.C.W., Boschker, H.T.S., Vyverman, W., and Sabbe, K. (2013) Release of dissolved carbohydrates by *Emiliana huxleyi* and formation of transparent exopolymer particles depend on algal life cycle and bacterial activity. *Environ Microbiol* 15: 1514–1531.
- Orata, F.D., Rosana, A.R.R., Xu, Y., Simkus, D.N., Bramucci, A.R., Boucher, Y., and Case, R.J. (2016) Polymicrobial Culture of Naked ( N-Type ) *Emiliana huxleyi*. *Genome Announc* 4: 9–10.
- P**
- Paasche, E. (2001) A review of the coccolithophorid *Emiliana huxleyi* (Prymnesiophyceae), with particular reference to growth, coccolith formation, and calcification-photosynthesis interactions. *Phycologia* 40: 503–529.
- Parada, A.E., Needham, D.M., and Fuhrman, J.A. (2016) Every base matters: Assessing small subunit rRNA primers for marine microbiomes with mock communities, time series and global field samples. *Environ Microbiol* 18: 1403–1414.
- Parke, M., Manton, I., and Clarke, B. (1955) Studies on marine flagellates II. Three new species of *Chrysochromulina*. *J Mar Biol Assoc United Kingdom* 34: 579–609.
- Patil, S.M., Mohan, R., Shetye, S.S., Gazi, S., Baumann, K.H., and Jafar, S. (2017) Biogeographic distribution of extant Coccolithophores in the Indian sector of the Southern Ocean. *Mar Micropaleontol* 137: 16–30.
- Patzelt, D., Wang, H., Buchholz, I., Rohde, M., Gröbe, L., Pradella, S., *et al.* (2013) You are what you talk: quorum sensing induces individual morphologies and cell division modes in *Dinoroseobacter shibae*. *ISME J* 7:

- 2274–2286.
- Paul, C., Mausz, M.A., and Pohnert, G. (2013) A co-culturing/metabolomics approach to investigate chemically mediated interactions of planktonic organisms reveals influence of bacteria on diatom metabolism. *Metabolomics* 9: 349–359.
- Paul, C. and Pohnert, G. (2011) Interactions of the algicidal bacterium *Kordia algicida* with diatoms: Regulated protease excretion for specific algal lysis. *PLoS One* 6:.
- Philippot, L., Raaijmakers, J.M., Lemanceau, P., and Van Der Putten, W.H. (2013) Going back to the roots: the microbial ecology of the rhizosphere. *Nat Rev Microbiol* 11: 789–799.
- Plummer, S., Taylor, A.E., Harvey, E.L., Hansel, C.M., and Diaz, J.M. (2019) Dynamic regulation of extracellular superoxide production by the coccolithophore *Emiliana huxleyi* (CCMP 374). *Front Microbiol* 10:.
- Pollock, J., Glendinning, L., Wisedchanwet, T., and Watson, M. (2018) The Madness of Microbiome: Attempting To Find Consensus “Best Practice” for 16S Microbiome Studies. *Appl Environ Microbiol* 84: e02627-17.
- Pomeroy, L., leB. Williams, P., Azam, F., and Hobbie, J. (2007) The Microbial Loop. *Oceanography* 20: 28–33.
- Poulton, A.J., Holligan, P.M., Charalampopoulou, A., and Adey, T.R. (2017) Coccolithophore ecology in the tropical and subtropical Atlantic Ocean: New perspectives from the Atlantic meridional transect (AMT) programme. *Prog Oceanogr* 158: 150–170.
- Probert, I. and Houdan, A. (2004) The Laboratory Culture of Coccolithophores BT - Coccolithophores: From Molecular Processes to Global Impact. In Thierstein, H.R. and Young, J.R. (eds). Berlin, Heidelberg: Springer Berlin Heidelberg, pp. 217–249.
- Prodan, A., Tremaroli, V., Brodin, H., Zwinderman, A.H., Nieuwdorp, M., and Levin, E. (2020) Comparing bioinformatic pipelines for microbial 16S rRNA amplicon sequencing. *PLoS One* 15: 1–19.

## R

- Raffi, I., Backman, J., Fornaciari, E., Pälke, H., Rio, D., Lourens, L., and Hilgen, F. (2006) A review of calcareous nanofossil astrobiochronology encompassing the past 25 million years. *Quat Sci Rev* 25: 3113–3137.
- Ramanan, R., Kang, Z., Kim, B.H., Cho, D.H., Jin, L., Oh, H.M., and Kim, H.S. (2015) Phycosphere bacterial diversity

- in green algae reveals an apparent similarity across habitats. *Algal Res* 8: 140–144.
- Read, B.A., Kegel, J., Klute, M.J., Kuo, A., Lefebvre, S.C., Maumus, F., *et al.* (2013) Pan genome of the phytoplankton *Emiliana* underpins its global distribution. *Nature* 499: 209–213.
- Rhodes, L.L., Peake, B.M., MacKenzie, A.L., and Marwick, S. (1995) Coccolithophores *Gephyrocapsa oceanica* and *Emiliana huxleyi* (Prymnesiophyceae= Haptophyceae) in New Zealand's coastal waters: Characteristics of blooms and growth in laboratory culture. *New Zeal J Mar Freshw Res* 29: 345–357.
- Rolland, J.L., Stien, D., Sanchez-Ferandin, S., and Lami, R. (2016) Quorum Sensing and Quorum Quenching in the Phycosphere of Phytoplankton: a Case of Chemical Interactions in Ecology. *J Chem Ecol* 42: 1201–1211.
- Rosana, A.R.R., Orata, F.D., Xu, Y., Simkus, D.N., Bramucci, A.R., Boucher, Y., and Case, R.J. (2016) Draft genome sequences of seven bacterial strains isolated from a polymicrobial culture of coccolith-bearing (C-type) *Emiliana huxleyi* M217. *Genome Announc* 4:.
- Rost, B. and Riebesell, U. (2004) Coccolithophores and the biological pump: responses to environmental changes. In *Coccolithophores*. pp. 99–125.
- Roth-Rosenberg, D., Aharonovich, D., Luzzatto-Knaan, T., Vogts, A., Zoccarato, L., Eigemann, F., *et al.* (2020) *Prochlorococcus* cells rely on microbial interactions rather than on chlorotic resting stages to survive long-term nutrient starvation. *MBio* 11: 1–13.

## S

- Sale, P.F. (1979) Recruitment, loss and coexistence in a guild of territorial coral reef fishes. *Oecologia* 42: 159–177.
- Samtleben, C. (1980) Die Evolution der Coccolithophoriden-Gattung *Gephyrocapsa* nach Befunden im Atlantik. *Paläontologische Zeitschrift* 54: 91–127.
- Schloss, P.D., Westcott, S.L., Ryabin, T., Hall, J.R., Hartmann, M., Hollister, E.B., *et al.* (2009) Introducing mothur: open-source, platform-independent, community-supported software for describing and comparing microbial communities. *Appl Environ Microbiol* 75: 7537–7541.
- Segev, E., Castañeda, I.S., Sikes, E.L., Vlamakis, H., and Kolter, R. (2016) Bacterial influence on alkenones in live microalgae. *J Phycol* 52: 125–130.

- Segev, E., Wyche, T.P., Kim, K.H., Petersen, J., Ellebrandt, C., Vlamakis, H., *et al.* (2016) Dynamic metabolic exchange governs a marine algal-bacterial interaction. *Elife* 5:.
- Seyedsayamdost, M.R., Carr, G., Kolter, R., and Clardy, J. (2011) Roseobactin: Small molecule modulators of an algal-bacterial symbiosis. *J Am Chem Soc* 133: 18343–18349.
- Seyedsayamdost, M.R., Case, R.J., Kolter, R., and Clardy, J. (2011) The Jekyll-and-Hyde chemistry of *Phaeobacter gallaeciensis*. *Nat Chem* 3: 331–335.
- Seyedsayamdost, M.R., Wang, R., Kolter, R., and Clardy, J. (2014) Hybrid biosynthesis of roseobactin from algal and bacterial precursor molecules. *J Am Chem Soc* 136: 15150–15153.
- Seymour, J.R., Ahmed, T., Durham, W.M., and Stocker, R. (2010) Chemotactic response of marine bacteria to the extracellular products of *Synechococcus* and *Prochlorococcus*. *Aquat Microb Ecol* 59: 161–168.
- Seymour, J.R., Amin, S.A., Raina, J.B., and Stocker, R. (2017) Zooming in on the phycosphere: The ecological interface for phytoplankton-bacteria relationships. *Nat Microbiol* 2:.
- Shibl, A.A., Isaac, A., Ochsenkühn, M.A., Cárdenas, A., Fei, C., Behringer, G., *et al.* (2020) Diatom modulation of select bacteria through use of two unique secondary metabolites. *Proc Natl Acad Sci U S A* 117: 27445–27455.
- Shin, H., Lee, E., Shin, J., Ko, S.-R., Oh, H.-S., Ahn, C.-Y., *et al.* (2018) Elucidation of the bacterial communities associated with the harmful microalgae *Alexandrium tamarense* and *Cochlodinium polykrikoides* using nanopore sequencing. *Sci Rep* 8: 5323.
- Sievert, S.M., Kiene, R.P., and Schulz-Vogt, H.N. (2007) The sulfur cycle. *Oceanography* 20: 117–123.
- Sims, P.A., Mann, D.G., and Medlin, L.K. (2006) Evolution of the diatoms: Insights from fossil, biological and molecular data. *Phycologia* 45: 361–402.
- Slightom, R.N. and Buchan, A. (2009) Surface colonization by marine Roseobacters: Integrating genotype and phenotype. *Appl Environ Microbiol* 75: 6027–6037.
- Smriga, S., Fernandez, V.I., Mitchell, J.G., and Stocker, R. (2016) Chemotaxis toward phytoplankton drives organic matter partitioning among marine bacteria. *Proc Natl Acad Sci U S A* 113: 1576–1581.
- Sonnenschein, E.C., Syit, D.A., Grossart, H.P., and Ullrich, M.S. (2012) Chemotaxis of *Marinobacter adhaerens* and its impact on

- attachment to the diatom *Thalassiosira weissflogii*. *Appl Environ Microbiol* 78: 6900–6907.
- Sörenson, E., Bertos-Fortis, M., Farnelid, H., Kremp, A., Krüger, K., Lindehoff, E., and Legrand, C. (2019) Consistency in microbiomes in cultures of *Alexandrium* species isolated from brackish and marine waters. *Environ Microbiol Rep* 11: 425–433.
- Stocker, R. and Seymour, J.R. (2012) Ecology and Physics of Bacterial Chemotaxis in the Ocean. *Microbiol Mol Biol Rev* 76: 792–812.
- Sunagawa, S., Coelho, L.P., Chaffron, S., Kultima, J.R., Labadie, K., Salazar, G., et al. (2015) Structure and function of the global ocean microbiome. *Science* (80-) 348: 1261359–1261359.
- T**
- Taylor, F.J.R., Hoppenrath, M., and Saldarriaga, J.F. (2007) Dinoflagellate diversity and distribution. *Biodivers Conserv* 17: 407–418.
- Teeling, H., Fuchs, B.M., Becher, D., Klockow, C., Gardebrecht, A., Bennke, C.M., et al. (2012) Substrate-controlled succession of marine bacterioplankton populations induced by a phytoplankton bloom. *Science* (80-) 336: 608–611.
- Teeling, H., Fuchs, B.M., Bennke, C.M., Krüger, K., Chafee, M., Kappelmann, L., et al. (2016) Recurring patterns in bacterioplankton dynamics during coastal spring algae blooms. *Elife* 5: 1–31.
- Thompson, H.F., Summers, S., Yuceel, R., and Gutierrez, T. (2020) Hydrocarbon-degrading bacteria found tightly associated with the 50–70 µm cell-size population of eukaryotic phytoplankton in surface waters of a northeast atlantic region. *Microorganisms* 8: 1–16.
- Tipton, L., Darcy, J.L., and Hynson, N.A. (2019) A developing symbiosis: Enabling cross-talk between ecologists and microbiome scientists. *Front Microbiol* 10: 1–10.
- Tran, N.A.T., Tamburic, B., Evenhuis, C.R., and Seymour, J.R. (2020) Bacteria-mediated aggregation of the marine phytoplankton *Thalassiosira weissflogii* and *Nannochloropsis oceanica*. *J Appl Phycol* 32: 3735–3748.
- Trivedi, P., Leach, J.E., Tringe, S.G., Sa, T., and Singh, B.K. (2020) Plant–microbiome interactions: from community assembly to plant health. *Nat Rev Microbiol* 18: 607–621.
- Tyrrell, T. and Merico, A. (2004) *Emiliania huxleyi*: bloom observations and the conditions that induce them. In *Coccolithophores*. pp. 75–97.

## V

- Vardi, A., Haramaty, L., Van Mooy, B.A.S., Fredricks, H.F., Kimmance, S.A., Larsen, A., and Bidle, K.D. (2012) Host-virus dynamics and subcellular controls of cell fate in a natural coccolithophore population. *Proc Natl Acad Sci U S A* 109: 19327–19332.
- de Vargas, C., Aubry, M.P., Probert, I., and Young, J. (2007) Origin and Evolution of Coccolithophores. From Coastal Hunters to Oceanic Farmers., Elsevier Inc.
- Villar, E., Vannier, T., Vernet, C., Lescot, M., Cuenca, M., Alexandre, A., *et al.* (2018) The Ocean Gene Atlas: Exploring the biogeography of plankton genes online. *Nucleic Acids Res* 46: W289–W295.

## W

- Wadhams, G.H. and Armitage, J.P. (2004) Making sense of it all: Bacterial chemotaxis. *Nat Rev Mol Cell Biol* 5: 1024–1037.
- Wang, R., Gallant, É., and Seyedsayamdost, M.R. (2016) Investigation of the genetics and biochemistry of roseobactin production in the Roseobacter clade bacterium *Phaeobacter inhibens*. *MBio* 7: 1–10.
- Whipps, J.M., Lewis, K., and Cooke, R.C. (1988) Mycoparasitism and plant disease control. *Fungi Biol Control Syst* 161–187.
- Whitton, B.A. (2012) Ecology of cyanobacteria II: Their diversity in space and time. *Ecol Cyanobacteria II Their Divers Sp Time* 9789400738: 1–760.
- Wietz, M., Gram, L., Jørgensen, B., and Schramm, A. (2010) Latitudinal patterns in the abundance of major marine bacterioplankton groups. *Aquat Microb Ecol* 61: 179–189.
- Worden, A.Z., Follows, M.J., Giovannoni, S.J., Wilken, S., Zimmerman, A.E., and Keeling, P.J. (2015) Rethinking the marine carbon cycle: factoring in the multifarious lifestyles of microbes. *Science (80- )* 347:.

## Y

- Yakimov, M.M., Timmis, K.N., and Golyshin, P.N. (2007) Obligate oil-degrading marine bacteria. *Curr Opin Biotechnol* 18: 257–266.
- Young, J.R., Geisen, M., Cros, L., Kleijne, a, Sprengel, C., Probert, I., and Østergaard, J. (2003) A guide to extant coccolithophore taxonomy . *J Nannoplankt Res* 125.
- Young, Jeremy R. and Westbroek, P. (1991) Genotypic variation in the coccolithophorid species *Emiliania huxleyi*. *Mar Micropaleontol* 18: 5–23.

**Z**

- Zheng, Q., Wang, Y., Xie, R., Lang, A.S., Liu, Y., Lu, J., *et al.* (2018) Dynamics of heterotrophic bacterial assemblages within *Synechococcus* cultures. *Appl Environ Microbiol* 84: e01517-17.
- Zhou, J., Chen, G.F., Ying, K.Z., Jin, H., Song, J.T., and Cai, Z.H. (2019) Phycosphere microbial succession patterns and assembly mechanisms in a marine dinoflagellate bloom. *Appl Environ Microbiol* 85: 1–17.
- Zhou, J., Richlen, M.L., Sehein, T.R., Kulis, D.M., Anderson, D.M., and Cai, Z. (2018) Microbial Community Structure and Associations During a Marine Dinoflagellate Bloom.
- Zubkov, M. V., Fuchs, B.M., Archer, S.D., Kiene, R.P., Amann, R., and Burkill, P.H. (2001) Linking the composition of bacterioplankton to rapid turnover of dissolved dimethylsulphoniopropionate in an algal bloom in the North Sea. *Environ Microbiol* 3: 304–311.





## Annexes

### Annex 1

#### Collaboration

#### **Coccolith morphometrics partially delineate morphotypes in worldwide isolates of *Gephyrocapsa huxleyi***

El Mahdi Bendif<sup>1</sup>, Mariana Câmara dos Reis<sup>2</sup>, Odysseus Archontikis<sup>1</sup>, Cecilia Balestreri<sup>3</sup>, Jeremy Young<sup>4</sup>, Pierre Helaouet<sup>5</sup>, Glenn Harper<sup>6</sup>, Ian Probert<sup>7</sup>, Colin Brownlee<sup>5</sup>, Declan Schroeder<sup>3,8</sup>, Peter von Dassow<sup>9,10,11</sup>, Myriam Valero<sup>11</sup>, Colomban de Vargas<sup>2,12</sup>, Ros Rickaby<sup>1</sup>, Christian Jeanthon<sup>2</sup>

<sup>1</sup> Department of Earth sciences, University of Oxford, Oxford, UK

<sup>2</sup> Sorbonne Université, CNRS, UMR7144, Adaptation et Diversité en Milieu Marin, Station Biologique de Roscoff, Roscoff, France

<sup>3</sup> Department of Veterinary Population Medicine, University of Minnesota, Minneapolis, USA

<sup>4</sup> Department of Earth Sciences, University College of London, London, UK

<sup>5</sup> The Marine Biological Association of the United Kingdom, Plymouth, UK,

<sup>6</sup> University of Plymouth, Plymouth, UK

<sup>7</sup> Sorbonne Université, CNRS, Roscoff Culture Collection, FR2424, Station Biologique de Roscoff, Roscoff, France

<sup>8</sup> School of Biological Sciences, University of Reading, Reading, UK

<sup>9</sup> Millennium Institute of Oceanography, Universidad de Concepción, Concepción, Chile

<sup>10</sup> Department of Ecology, Pontificia Universidad Católica de Chile, Santiago, Chile

<sup>11</sup> UMI3614 Evolutionary Biology and Ecology of Algae, CNRS-UPMC Sorbonne Universités, PUCCh, UACH, Station Biologique de Roscoff, Roscoff, France

<sup>12</sup> CNRS Research Federation for the study of Global Ocean Systems Ecology and Evolution, FR2022/Tara Oceans GOSEE, Paris, France

**Coccolith morphometrics partially delineate morphotypes in worldwide isolates of  
*Gephyrocapsa huxleyi***

*In preparation*

**Abstract**

The haptophyte *Gephyrocapsa huxleyi* is by far the most widespread and abundant coccolithophore in modern ocean. It plays a fundamental role in the marine ecosystem since it produces calcium carbonate coccoliths responsible of around 30% of carbonate precipitation in the global ocean. *Gephyrocapsa huxleyi* is also well recognized for its wide phenotypic variability, mainly with morphological variants distinguished by fine morphometric variations in the coccoliths, coined as morphotypes. Although, this morphometric variability has been usually assessed in the environment, sometimes on cultured strains from a locality but rarely at a wide scale on cultured strains. In here, we measured coccolith variability in a worldwide set of 120 cultured strains of *G. huxleyi* in order to test whether this variability relates to the environmental context of isolation. We collected coccoliths of cultured strains from North Atlantic, Indian Ocean and coastal Chile growing under similar conditions, and for which we acquired scanning electron micrographs to measure morphometric features. We found significant differences between each population associated with different patterns of distribution for each measured parameter and a partial concordance between morphotypes and clusters inferred from measurements. Moreover, a significant positive correlation was found between the latitude of isolation and the width of elements forming the shield of the coccoliths, while a correlation between sea surface temperature and the length of the coccoliths was significantly negative. These preliminary results demonstrated a wide phenotypic diversity with potential sign of endemism, suggesting extending further morphometric investigations in this ecologically relevant species.

## Annex 2

### Functional assignation of abundant taxa

In order to get insights into the functional diversity found in microbiomes of *E. huxleyi* in cultures (**chapters 1 and 3**), ASVs accounting to more than 1% of relative abundance at each sample were selected (**Chapter 1**: 180 and **Chapter 3**: 32). Functional assignment was performed using FAPROTAX database (v1.2.4, 2020) (Louca *et al.*, 2016). This database maps prokaryotic clades (*e.g.* genera or species) to established metabolic or ecologically relevant functions using the published data on cultured strains (Louca *et al.*, 2016). Functional contribution was normalized by the number of reads of assigned ASVs. Functional plots were produced in R version 4.0.2 using ggplot2 (Wickham, 2016; R Core Team, 2017).

## Annex 3

### Methods of co-culture experiments

#### *Heterotrophic bacteria isolation and maintenance*

Heterotrophic bacteria were isolated from coccolithophore cultures by serial dilution or by plating using two different media prepared with aged seawater collected at SOMLIT-Astan observatory site (48°46'18''N-3°58' 6''W) (Brittany, France) and stored in the dark. A low-nutrient heterotrophic medium (LNHM) sterilized by filtration using 0.1µm pore size PES membrane filter units (Nalgene™ Rapid-Flow™) was amended with NH<sub>4</sub>Cl (10 µM), K<sub>2</sub>HPO<sub>4</sub> (1 µM), the mixture of carbon compounds used in (Rappé *et al.*, 2002) (1/10 strength), a mixture of the 20 aminoacids (1 µM each), the trace metal and vitamin solutions used in (Carini *et al.*, 2013) and DMSP (100 nM). In the second medium (YEP), the mixture of carbon compounds was replaced by yeast extract (100 mg/L) and peptone (500 mg/L). For serial dilutions, the coccolithophores cultures were diluted into the media to obtain 1 to 2 cells ml<sup>-1</sup> and 350 µl were dispensed into several 96-well deepwell microplates (Nunc). Diluted aliquots of the coccolithophore cultures were also plated on LNHM medium solidified with Phytigel (0.7 g/L) and on YEP medium solidified with agar (15g/L). Cultures were incubated at 20°C in the dark for 4-6weeks and microbial growth in liquid media was screened by flow cytometry. Purification of positive liquid cultures and colonies was achieved by streaking on the solidified media. Bacteria were maintained in solidified BD Difco marine broth medium (1/10 strength)

at 18°C on a 12:12 light:dark cycle under a white light irradiance (Philips Master TL\_D 18W/865) of about 80  $\mu\text{mol photons m}^{-2} \text{ s}^{-1}$ .

### ***Axenization and culture maintenance***

*E. huxleyi* strain RCC1212 was isolated from the Atlantic Ocean near to South Africa (Latitude: -34.47, Longitude: 17.30) on September 1st, 2000. This strain was axenized using the protocol described at the **Chapter 3**. Cultures were kept in K/2 medium prepared (Keller *et al.*, 1987; Probert, 2019) with reconstituted red sea water (<https://www.redseafish.com/red-sea-salts/red-sea-salt/>) and filter-sterilized at 0.1  $\mu\text{m}$  and were regularly checked for bacterial contamination by flow cytometry as above mentioned. Axenization of cultures used for the experiments was confirmed by fixing 5 mL of culture with glutaraldehyde 25% (0.25% final concentration), staining with SYBR green (1/10,000 final concentration) and filtering in 0.2  $\mu\text{m}$  polycarbonate black membrane (Millipore Isopore) for observation by epifluorescence microscopy. Axenic cultures were grown in 50 mL vented tissue culture flasks at the same light and temperature conditions as the bacterial isolates.

### ***Experimental set-up***

Prior to experiments, axenic cultures were daily diluted by inoculating the same volume of fresh media. This allowed to quickly increase the volume of culture while keeping them in exponential growth. For bacteria, four days before the experiment unique colonies of each targeted bacterium were streaked in fresh solid medium. At the day of the experiment single colonies were diluted in axenic K/2 medium.

For each test, I inoculated axenic *E. huxleyi* at a cell concentration of  $\sim 5 \times 10^4$  cells/mL with a bacterium partner at the cell concentration of  $\sim 1 \times 10^6$  cells/mL. All the bacterial treatments were performed in triplicates and axenic controls in 4 replicates. Cultures were kept at the same light and temperature conditions as for maintenance.

### ***Sampling and flow cytometry analysis***

For 11 days 490  $\mu\text{L}$  of each culture was fixed with glutaraldehyde 25% (0.25% final concentration) and Polaxamer 188 solution 10% (Sigma-Aldrich) (0.1% final concentration) incubated for 20 min in the dark, flash frozen in liquid nitrogen and stored at -80°C for flow

cytometry analysis (FCM). Samples were analyzed in a Guava easyCyte flow cytometer (Millipore) equipped with a 488 and a 633 nm lasers and the standard filter setup.

## References

- Carini, P., Steindler, L., Beszteri, S., and Giovannoni, S.J. (2013) Nutrient requirements for growth of the extreme oligotroph ‘Candidatus Pelagibacter ubique’ HTCC1062 on a defined medium. *ISME J* 7: 592–602.
- Keller, M.D., Selvin, R.C., Claus, W., and Guillard, R.R.L. (1987) Media for the culture of oceanic ultraphytoplankton. *J Phycol* 23: 633–638.
- Louca, S., Parfrey, L.W., and Doebeli, M. (2016) Decoupling function and taxonomy in the global ocean microbiome. *Science* (80- ) 353: 1272–1277.
- Probert, I. (2019) K/2 Ian / K-ET. protocols.io.
- R Core Team (2017) R: A language and environment for statistical computing. R Foundation for Statistical Computing, Vienna, Austria. URL <https://www.R-project.org/>.
- Rappé, M.S., Connon, S. a, Vergin, K.L., and Giovannoni, S.J. (2002) Cultivation of the ubiquitous SAR11 marine bacterioplankton clade. *Nature* 418: 630–633.
- Wickham, H. (2016) ggplot2: Elegant Graphics for Data Analysis. Springer-Verlag New York ISBN 978-3:

## Annex 4

First page of master's thesis paper published during my PhD.



## RESEARCH ARTICLE

## Spatial heterogeneity and hydrological fluctuations drive bacterioplankton community composition in an Amazon floodplain system

Mariana Câmara dos Reis<sup>1,2\*</sup>, Inessa Lacativa Bagatini<sup>3</sup>, Luciana de Oliveira Vidal<sup>4</sup>, Marie-Paule Bonnet<sup>5,6</sup>, David da Motta Marques<sup>7</sup>, Hugo Sarmento<sup>1</sup>

**1** Laboratory of Microbial Processes and Biodiversity, Departamento de Hidrobiologia, Universidade Federal de São Carlos, São Carlos, SP, Brazil, **2** Programa de Pós-graduação em Ecologia e Recursos Naturais, Universidade Federal de São Carlos, São Carlos, SP, Brazil, **3** Laboratório de Ficologia, Departamento de Botânica, Universidade Federal de São Carlos, São Carlos, SP, Brazil, **4** Laboratório de Ciências Ambientais, Centro de Biociências e Biotecnologia, Universidade Estadual do Norte Fluminense, Campos dos Goytacazes, RJ, Brazil, **5** UMR 228 Espace DEV, Institute of Research for Development, Montpellier, France, **6** International Joint Laboratory, LMI OCE, Institute of Research for Development/Universidade de Brasília, Brasília, Brazil, **7** Institute of Hydraulic Research, Universidade Federal do Rio Grande do Sul, Porto Alegre, RS, Brazil

\* Current address: Sorbonne Université/Centre National de la Recherche Scientifique, UMR 7144, Adaptation et Diversité en Milieu Marin, Station Biologique de Roscoff, Place Georges Teissier, Roscoff, France.

\* [maricamarareis@gmail.com](mailto:maricamarareis@gmail.com)



## OPEN ACCESS

**Citation:** Câmara dos Reis M, Lacativa Bagatini I, de Oliveira Vidal L, Bonnet M-P, da Motta Marques D, Sarmento H (2019) Spatial heterogeneity and hydrological fluctuations drive bacterioplankton community composition in an Amazon floodplain system. PLoS ONE 14(8): e0220695. <https://doi.org/10.1371/journal.pone.0220695>

**Editor:** Raffaella Casotti, Stazione Zoologica Anton Dohrn, ITALY

**Received:** March 8, 2019

**Accepted:** July 22, 2019

**Published:** August 9, 2019

**Copyright:** © 2019 Câmara dos Reis et al. This is an open access article distributed under the terms of the [Creative Commons Attribution License](https://creativecommons.org/licenses/by/4.0/), which permits unrestricted use, distribution, and reproduction in any medium, provided the original author and source are credited.

**Data Availability Statement:** The SRA database of the data reported are available in the GenBank under the accession number SRP127556. The BioSample accession data are also available in GenBank under the accession numbers from SAMN08239888 to SAMN08239899.

**Funding:** MCDR received a grant from Conselho nacional de desenvolvimento científico e tecnológico (grant process 132749/2015-7). ILB received a grant from Fundação de Amparo à

## Abstract

Amazonian floodplains form complex hydrological networks that play relevant roles in global biogeochemical cycles, and bacterial degradation of the organic matter in these systems is key for regional carbon budget. The Amazon undergoes extreme seasonal variations in water level, which produces changes in landscape and diversifies sources of organic inputs into floodplain systems. Although these changes should affect bacterioplankton community composition (BCC), little is known about which factors drive spatial and temporal patterns of bacterioplankton in these Amazonian floodplains. We used high-throughput sequencing (Illumina MiSeq) of the V3-V4 region of the 16S rRNA gene to investigate spatial and temporal patterns of BCC of two size fractions, and their correlation with environmental variables in an Amazon floodplain lake (Lago Grande do Curuai). We found a high degree of novelty in bacterioplankton, as more than half of operational taxonomic units (OTUs) could not be classified at genus level. Spatial habitat heterogeneity and the flood pulse were the main factors shaping free-living (FL) BCC. The gradient of organic matter from transition zone-lake-Amazon River was the main driver for particle-attached (PA) BCC. The BCC reflected the complexity of the system, with more variation in space than in time, although both factors were important drivers of the BCC in this Amazon floodplain system.

## Résumé

### Structure et assemblage des microbiomes bactériens dans la phycosphère d'*Emiliana huxleyi*

Les interactions entre le phytoplancton marin et les bactéries sont une symbiose fondamentale dans les océans, affectant les cycles du carbone et des nutriments. Au cours de la dernière décennie, l'introduction de nouveaux outils de séquençage environnemental à haut débit a dévoilé une diversité inattendue de bactéries associées au phytoplancton dans l'océan ou en culture. Cependant, les modèles et les processus de sélection et d'assemblage du microbiome dans la phycosphère, c'est-à-dire la région environnant la cellule phytoplanctonique, restent mal connus. Dans cette thèse, *Emiliana huxleyi*, un phytoplancton-clé pour le cycle global du carbone et l'une des microalgues les plus étudiées de nos jours, a été sélectionnée comme espèce modèle.

La première partie du travail visait à étudier la diversité microbiologique associée à 73 souches d'*E. huxleyi* et de son taxon frère *Gephyrocapsa oceanica*, isolées des océans mondiaux entre 1959 et 2015. Leurs microbiomes étaient dominés par des Gammaprotéobactéries du genre *Marinobacter*, indépendamment de la variation inter et intra-espèce de l'hôte, du lieu d'isolement et de l'âge des cultures. L'abondance et la distribution des principaux taxons bactériens associés aux cultures d'*Emiliana/Gephyrocapsa* dans les jeux de données de métabarcodes d'ADNr 16S issus des océans du monde, ont montré qu'ils sont préférentiellement associés à des fractions planctoniques de grande taille et enrichis dans les couches bathypélagiques, attirant l'attention sur le rôle potentiellement important des bactéries associées au phytoplancton dans le flux des agrégats organiques et du plancton de grande taille vers la couche océanique profonde.

La deuxième partie était consacrée à l'étude des moteurs de la sélection et de l'assemblage du microbiome dans les cultures. Les microbiomes de souches appartenant à 7 phyla de phytoplancton et résultant de millions d'années d'évolution, isolées des mêmes échantillons d'eau de mer lors de campagnes océanographiques ont été comparés. Nos résultats indiquent que la diversité des microbiomes dans les phycosphères cultivées est régie par des processus déterministes à plusieurs échelles, dont le lieu d'isolement et le milieu de culture.

Dans la troisième et dernière partie de ce travail, nous avons étudié les facteurs de sélection du microbiome par *E. huxleyi*. Des échantillons d'eau de mer collectés à l'intérieur et à l'extérieur d'une efflorescence d'*E. huxleyi* au large de la Bretagne (2019) ont servi d'inoculum à une culture axénique d'*E. huxleyi* et les microbiomes assemblés ont été suivis pendant un an. Nous avons observé que les microbiomes assemblés étaient dépendants de la composition de la communauté bactérienne initiale et résistants aux perturbations. Dans l'ensemble, les résultats des trois parties mettent en évidence la stabilité des microbiomes du phytoplancton dans le temps et sa résilience aux changements d'état de santé de l'hôte. Dans son ensemble, ce travail fournit une ressource de base originale sur la diversité bactérienne des cultures de microalgues et une collection d'isolats bactériens qui peuvent être utilisés dans de futures études des interactions phytoplancton-bactéries.

Mots-clés: *Emiliana huxleyi*, phycosphère, bactéries, diversité du microbiome, processus de sélection, métabarcoding.

## Abstract

### Structure and assembly of bacterial microbiomes in the *Emiliana huxleyi* phycosphere

Interactions between marine phytoplankton and bacteria are a critical symbiosis in the oceans, affecting carbon and nutrient cycles. Over the last decade, the introduction of novel tools for high-throughput environmental sequencing has unveiled an unexpected diversity of bacteria associated with phytoplankton in the ocean or in culture. However, the drivers of microbiome assembly in the phycosphere, *i.e.* the surrounding region of the phytoplankton cell, remain poorly known. In this thesis, *Emiliana huxleyi*, a key phytoplankton for global carbon cycle and one of the most studied microalgae, was selected, as a model species.

The first part of the work aimed at studying the microbiome diversity associated with 73 cultured strains of *E. huxleyi* and its sister taxon *Gephyrocapsa oceanica*, isolated from the world ocean between 1959 and 2015. Their microbiomes were consistently dominated by members of the gammaproteobacterial genus *Marinobacter*, independent of the inter- and intra-specific variation of the host, the place of isolation, and the age of the cultures. Abundance and distribution of the main bacterial taxa associated with *Emiliana/Gephyrocapsa* cultured strains in existing 16S rDNA metabarcoding datasets from the world ocean, provided evidence that they are preferentially associated with large plankton size fractions and enriched in the bathy-pelagic waters. These results call attention to the putative crucial role of phytoplankton-associated bacteria in the flux organic aggregates and of larger plankton to deeper ocean layer.

The second part of this thesis was dedicated to the investigation of the drivers of microbiome assembly in cultures. Microbiomes of strains belonging to 7 phytoplankton phyla resulting from millions of years of evolution and isolated from the same seawater samples during oceanographic expeditions were compared. Our results indicate that the diversity of the microbiomes in cultured phycospheres is driven by deterministic processes at multiple scales, including the location of isolation and the cultivation medium.

In the third and final part of this work, we investigated drivers of the microbiome selection by *E. huxleyi*. Filtered seawater samples collected inside and outside an *E. huxleyi* bloom offshore Brittany (2019) served as inocula into axenic *E. huxleyi*, and the resulting microbiomes were followed over one year. We observed that the resulting microbiomes were dependent on the composition of the initial bacterioplankton community, as well as resilient to disturbance.

Altogether, the results from the three parts highlight the stability of phytoplankton microbiomes over time and its resilience to changes in the health status of the host. Ultimately, this work provides a new baseline resource of bacterial diversity from microalgal cultures and a collection of bacterial isolates which can be used in future studies to investigate phytoplankton-bacteria interactions.

Key-words: *Emiliana huxleyi*, phycosphere, bacteria, microbiome diversity, selection processes, metabarcoding.